The University of Adelaide

Department of Geology and Geophysics

Interpretation of Gravity Data Over Central Jawa, Indonesia

Indra Budiman

June 1991

A thesis submitted to the University of Adelaide

in fulfilment of the requirements for the degree of

Master of Science.

Contents

List of Figures

Appendix A

List of Tables

Statement

This thesis contains no material which has been accepted for any other degree or diploma in any university and, to the best of my knowledge, no material previously published or written by another person, except where due reference is made in the text.

I consent to the thesis being made available for photocopying and loan where applicable if accepted for the award of the degree.

Indra Budiman

June, 1991

Acknowledgements

There are many people who should be thanked for their helpful contributions throughout this research. Professor David Boyd who supervised the work from start to finish and for the benefit of his geophysical insight, experience and particularly phylosophical way of thinking. Dr. John Paine and Mr Andy Mitchell are gratefully acknowledged for access to their excellent software programs on the computer. I would like to thank my colleagues, Dr. Shanti Rajagopalan, Robert O'Dowd, Andrew Lewis, Zhiqun Shi, Shaohua Zhou and Nasir Syarif for their discussion and help on many occasions, especially on computer related matters, and for permission to use many of their programs. Also Dr. John Fodden, Hamdan Z. Abidin,   Ukat Sukamta and M. Syah Arifin for their helpful disscusion on geological related matters.

Other people from the department that should be thanked are Dr. Bill Stuart, the Director of the National Centre for Petroleum Geology and Geophysics for the opportunity to attend the 1988 courses. John Willoughby, Phil McDuie and Rick Barret for their technical assistance of the computer facilities.

Numerous people from outside the Department of Geology and Geophysics were also involved, these include Dr. Mohamad Untung former Director of the Geological Research and Development Centre, Indonesia who encourage the author to take this subject, Dr. Rab. Sukamto the Director of the Geological Research and Development Centre, Indonesia for giving me leave of absence from my duty at that institute for the whole period of this study, and in permiting me to use the central Jawa gravity data for this research. Mrs Janice Laurie from Advisory Centre for University Education. The Australian International Development Assistance Bureau for granting me a research scholarship.

Most of all, I am very grateful to my wive and my children for their sacrifice, great understanding and being patient during my study time in Adelaide.

Abstract

Central Jawa, Indonesia, is a complex region resulting from the collision of the south eastern margin of Eurasia and the northward drift of the Australian continent, together with the westward drift of the Pacific plate.

The Bouguer anomaly contour map used in this study is the most detailed gravity map of central Jawa yet to be interpreted. This contour map was produced on the basis of the Bouguer reduction density value of 2.67 gr/cm^3. However, the result of the Parasnis straight line method for Bouguer reduction density of the northern part of Purwokerto indicates that the density value of 2.25 gr/cm^3 is more suitable. The interpretation of this gravity study is restricted by certain limitations, for example, the actual gravity observations were not available and there was very limited geophysical control from other methods. However, the results provide the starting point for further gravity study over central Jawa.

The gravity map shows a major boundary which strikes in a roughly east-west direction; in the Kebumen (Karangsambung) area this boundary coincides with the outcrop of a major fault which separates the Eocene basement in the south from younger sediment in the north. This boundary is displaced by a north-west trending structure.

The major volcanoes in central Jawa such as the Slamet, Merbabu, Merapi, Ungaran and Rogojembangan volcanoes are along an east-west line which is parallel to the major fault described in the above paragraph but displaced 30 km north of it.

The map shows that there are two types of major volcanoes, those which produce a strong gravity anomaly and those which do not. At the Ungaran volcano, a circular feature gravity anomaly with positive values reflect a dense body whose density contrast is 0.5 gr/cm^3 higher than surrounding rocks. This body has a diameter of 7 km and extends for a depth of 2 km to 10 km.

On the basis of the results of computer processing, modelling and analysis of gravity data, the effective interpretation of those anomalies provide us with better understanding of the major structural elements of island arcs.

Chapter 1

Introduction

1-1. The Location of the Study Area.

The investigation area, that is, central Jawa, is located between the latitude $06^{o}00'00''$ and $08^{o}30'00''$ south and the longitude $109^{o}00'00''$ and $111^{o}00'00''$ east (figure 1-1). Roughly speaking, this research covers an area of 30000 km^2.

Jawa, which is located between the Jawa Sea and the Indian Ocean, is only one among the 13000 islands which spread out over the complex region called Indonesia. It is a geologically complex region because it is the meeting place of three great tectonic plates. The first plate is the Eurasia plate in the northwest, the second plate is the Pacific plate in the northeast and the third plate is the Indian-Australian plate in the south - southeast. The Pacific plate is moving west - northwestward in relation to the Eurasia plate, and the Indian-Australian plate is heading toward the north (figure 1-2); it has collided with the Pacific Plate in the east and formed the Irian Jaya mountains, and in the west at Jawa, the Indian Ocean lithosphere is subducted below Jawa.

1-2. Potential for Research.

The study area has a strong potential to be used as a geophysical research project, because several significant geological problems such as mountain building processes, evolution of orogenic belts, earthquake, and subduction zone can be found in this region. However, the result of this research project is really influenced by the availability of
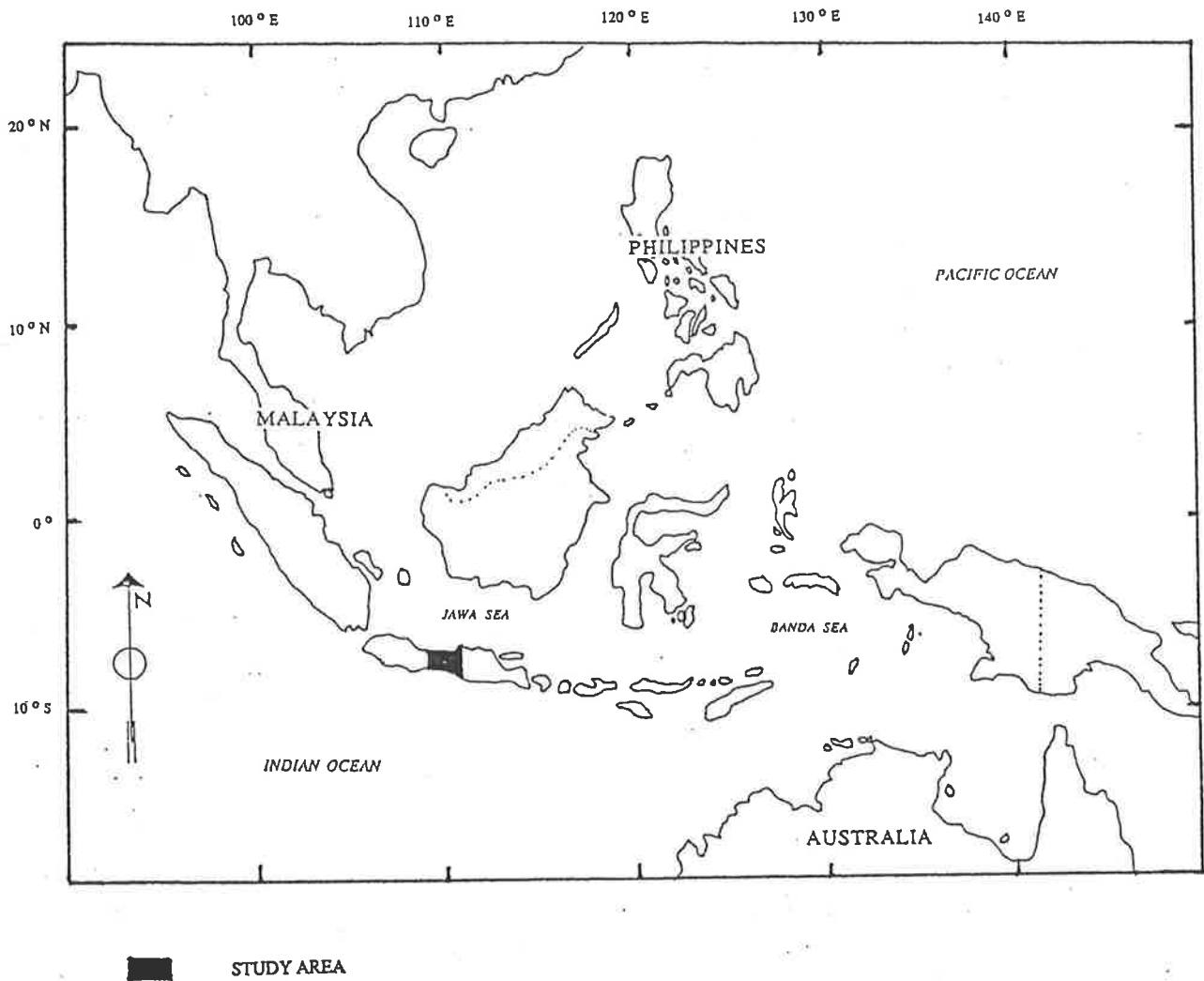
Figure 1-1. The location of the study area.
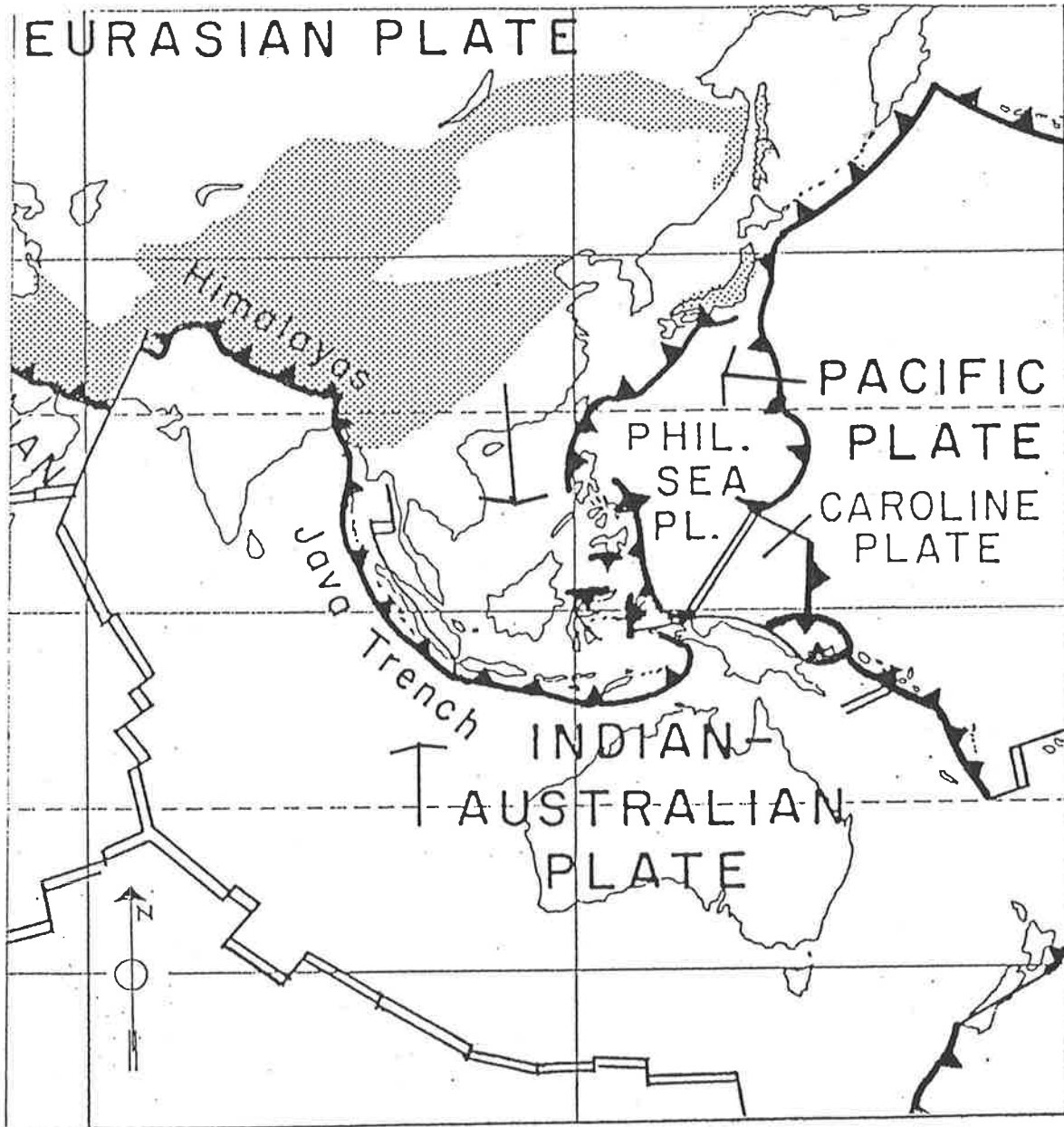
Figure 1-2. The complex movements of the three great plates of the Indonesian region (modified from Hamilton, 1979).

data, the procedures which were used during the collecting of the data and also by the facilities which are available for interpreting the data.

During the last twenty years, the island of Jawa has been covered by a semi-regional gravity survey. The study area, in this case central Jawa, has been covered by the above survey with a station density of about 1 station per 10 sq km. The total number of gravity stations in this area is almost 2900. These numerous gravity data which were collected during that period, however, have not been systematically interpreted.

It is immediately evident from an initial inspection of the 1 : 100000 scale Bouguer anomaly contour map that there are two separate though related problem for which the gravity data may provide new information :

1. The structure of the volcanoes.

The gravity anomalies over major volcanoes differ considerably and this is almost certainly due to differences in the internal structure, composition and history of the volcanoes. Alternative gravity models of the volcanoes can be produced by computer modelling and matching these with the observed anomalies should help us at least to have a clearer picture of the internal structure of the volcanoes.

2. The structure of the underlying rocks through which the volcanoes have been intruded.

It appears that the longer wave length anomalies are due to structures deep in the earth crust. The interpretation of these anomalies, based on the results of computer processing and analysis of gravity data, should provide us with a better understanding of the major structural elements of island arcs.

Before the aims of this research can be adequately defined, the following limitations must first be taken into consideration :

1. The special problems of data over big volcanoes.

Due to the restricted access to the big volcanic areas, several of these are still uncovered by gravity stations. In other words, the density distribution of gravity stations is slightly decreased in these specific areas.

2. Special problems related to the availability of the geophysical information.

The main problem is due to the fact that the raw gravity data over the study area are poorly documented. For certain reasons, it has also not been freely available during the research. Therefore no gravity observed and elevation station values can be used for this study. This research is based entirely on the Bouguer anomaly values calculated using density reduction of 2.67 gr / cm^3. It is clear that this lack of density reduction values might influence the flexibility of the interpretation stage.

There have been no crustal seismic sections and only very limited access to magnetics data available during this research, because the magnetic survey of the study area is still restricted.

3. To the best of the author's knowledge, this is the first research on a semi-detailed gravity interpretation of Indonesia. Consequently, only a small number of gravity study references can be used for this research.

1-3. Aims of the Research.

On the basis of all the above facts and considerations, the aims of this research may be divided into the four following categories :

1. Since the study area has not yet been interpreted systematically, this research may give some new ideas or at least give more evidence by which to judge the recent concepts.

2. This research will attempt to establish the correlation between gravity data and volcanic structure.

3. Since the gravity map indicates a major boundary which separates the Eocene sediment in the south from the younger sediment in the north, this research may give more evidence about the above relationship.

4. Last but not least, hopefully the result of this research may give a better understanding of the major structural elements of island arcs.

1-4. The Previous Work.

The first gravity measurements in Indonesia were undertaken in the early 1920's by Vening Meinesz. Some of this work was done in the Indian Ocean south of Jawa. In this work, Vening Meinesz discovered for the first time belts of positive and negative gravity anomalies for some 100 to 200 km width (fig. 1-3). In spite of the fact that the initial crustal model which was constructed on the basis of these results is considered to be a misleading model, this information greatly influenced tectonic theories for the next fifty years. The next era of gravity surveys, especially those on land, was done by oil companies , in this case, primarily by the Dutch oil company, Bataafsche Petroleum Maatschappy. Despite the fact that large amounts of data were collected, only a few values could be taken from those gravity surveys, because their acquisition has never been undertaken systematically and also the detailed maps were never published. Publications of this era include the gravity map of Southeast Asia by De Bruyn (1951), a compilation of Vening Meinesz data and those of oil companies. Also some gravity sections through Sumatra and Jawa were interpreted by Collete (1954).

As the value of gravity surveys in understanding regional tectonics became more widely appreciated, large scale and systematic surveys of Indonesia were planned in 1965 by a section of the Geological Survey of Indonesia (nowadays known as the Geological Research and Development Centre) and are still in progress. Until 1975, total 1212 gravity stations, 903 of which were observed jointly by the Institute of Geological Sciences, London and the Geological Survey of Indonesia were established throughout the whole island of Jawa. The average station density was 1 station every 100 sq km. The results were compiled in the form of 1 : 500000 scale Bouguer anomaly map which is published in a reduced scale 1 : 1000000.

From 1973 until 1977, a joint research project between the Geological Survey of Indonesia and the Geological Survey of Japan was undertaken. The gravity stations which
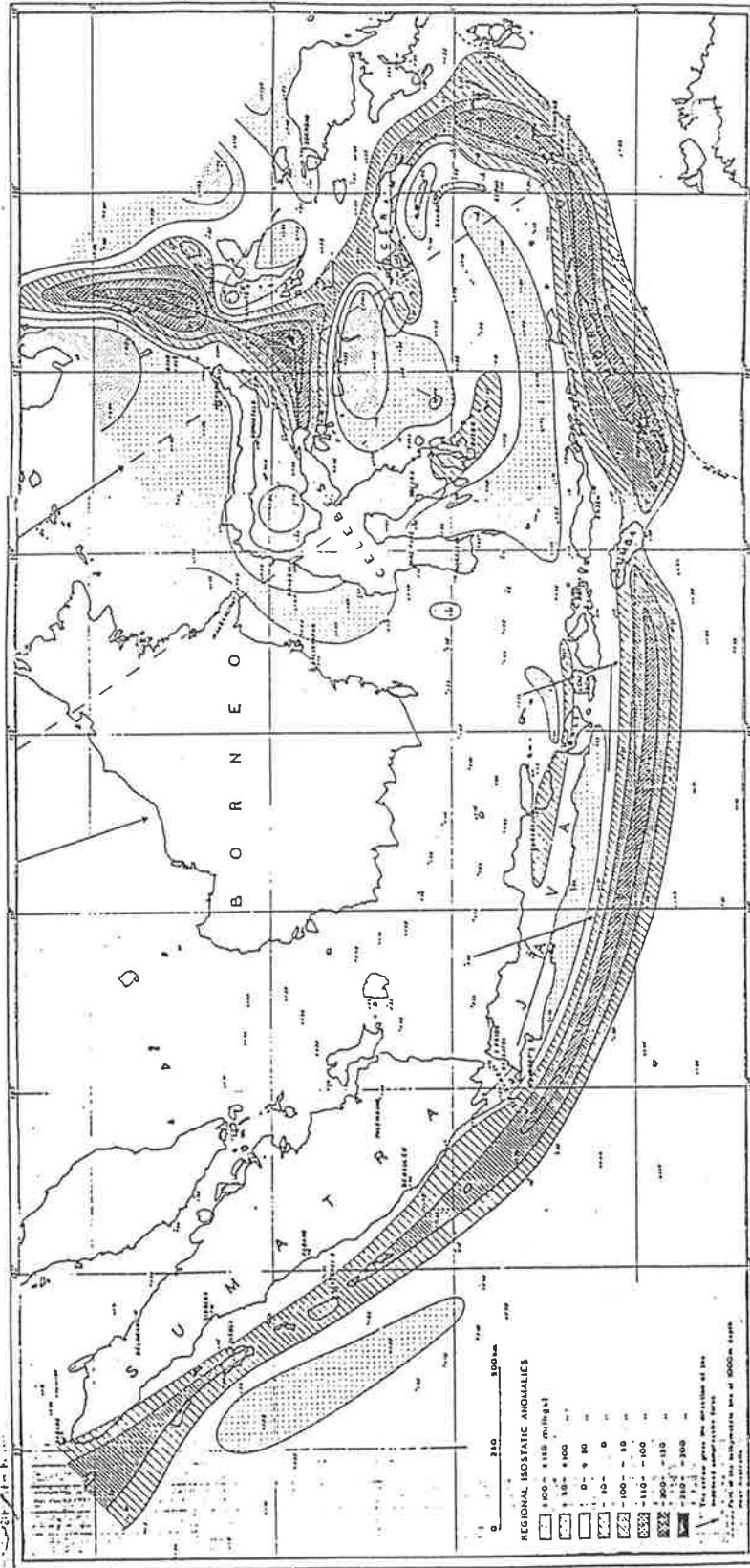
Figure 1-3. The regional isostatic anomalies of Indonesian archipelago (van Bemellen, 1949).

are established during this joint research were located at about five kilometres interval along the main road in a north-south direction. Then on the basis of the result of this gravity survey which is compiled with the result from the previous work, Untung and Hasegawa (1978) produced the gravity interpretation over the whole Jawa and Madura islands. It is clear that this work shows only the main features of the islands.

1-5. The Organisation of the Research Work.

This research work will be undertaken in several different stages which the author wishes to classify into the three following types :

1. Review of the literature.

This type of work consists of collecting both geological and geophysical information, mainly based on the textbooks, scientific journals and GRDC maps & reports both published and unpublished.

2. The computer process.

Almost all of this type of work such as digitizing, contouring, greyimage and filtering is executed with the computer facilities, both hardware and software, available at the Geology and Geophysics Department and the Computer Centre in the University of Adelaide.

3. Interpretation.

The combination of the results from the literature and the computer process which are analysed together provides the main idea and raw material for this type of work.

This includes the modelling process which consumes a lot of computer time.

The relationship between the three above aspects of the research is described on the flow chart in fig. 1-4.

```
┌ ─ ─ ─ ─ ─ ─ ─ ─ ─ ─ ─ ─ ─ ─ ─ ─ ─ ─ ─ ─ ─ ─ ┐
│  Gravity survey and gravity data reduction  + correction  │
└ ─ ─ ─ ─ ─ ─ ─ ─ ─ ─ ┬ ─ ─ ─ ─ ─ ─ ─ ─ ─ ─ ┘
```

```
┌ ─ ─ ─ ─ ─ ─ ─ ─ ─ ─ ─ ─ ┐
│   Bouguer anomaly contour map  │
│   1:100000 scale (hand contouring)  │
└ ─ ─ ─ ─ ─ ─ ─ ─ ─ ─ ─ ─ ┘
```

| Geological information |

| Geophysical information |

| Initial inspection |

| Digitizing processes |

| Grid file |

| Contour | Image | Shaded relief | Upward continuation | Trend surface residual | Spectral analysis |

| Qualitative interpretation | | Quantitative interpretation | | Modelling |

| Interpretation completed |

| Thesis |

Note :

⌐ ─ ⌐ *The previous works which have been done by the Geological Research and Development Centre.*

Figure 1-4. Flow chart diagram of the organisation of the research work.

1-6. Outcome of the Research.

Since this is the first central Jawa semi detailed gravity data interpretation, it may raise as many problems as it solves. Therefore, as an outcome of this research, the two following aspects may be noted at this stage :

1. It indicates the major fault in the geology of Jawa.

2. It is a guide to what needs to be done to get a better interpretation in the future which is discussed in the conclusion section.

Chapter 2

Geological Information

2-1. Introduction.

The gravity survey of Jawa was undertaken in order to help to solve some of the geological problems identified by geologists. On the basis of this relationship, the gravity survey over the whole island is undertaken.

Geological information is one of the fundamental requirements which must be fulfilled before attempting the interpretation of a geophysical survey, in this case the gravity survey or gravity interpretation. The geological information should be taken into consideration when the gravity survey is planned. Without this information in the early stages, the gravity survey would constitute a survey with no aim. Therefore such information can be regarded as the reference framework and a guide to the purpose of the gravity survey. When an interpretation is in progress, the geological information suggest models for calculation and may show that some solutions are not right.

The geological information about the study area which is used in this research is mainly based on the geological compilation from van Bemmelen (1949). The GRDC geological maps of the 1 : 100000 from certain areas which have been published are also used for this research. Information and idea about the tectonic evolution of Jawa and Indonesia are largely obtained from Hamilton (1979). In addition, the structures and tectonic developments within some parts of central Jawa discussed by Tjia (1966), Asikin (1974) are also taken as information. The latest information about both geological &

tectonic features of the study area is taken from the Jawa-Kalimantan transect of Gafoer et al. in Untung, (in prep.).

The geological map of the study area can be seen in figure 2-1.

2-2. Tectonic and Geological Information on the Jawa Region.

Historically, the earliest information about the geology of Jawa was reported by F Junghuhn (1854). This account was followed by the publication of Verbeek and Fennema (1896). Later on, the monumental geological study of Indonesia was compiled by van Bemmelen (1949) in The Geology of Indonesia. Nowadays,in this era of plate tectonic theory, the long account by Hamilton in the USGS Professional Paper report on The Tectonics of the Indonesian Region can be considered as the most recent comprehensive publication on geological work in Indonesia (Hamilton, 1978).

As already mentioned in the previous chapter, that Indonesian region has been the site of three great plate movements, viz: the Eurasia plate, the western Pacific plate and the Indian Australian plate. Due to a complexity of the region, numerous studies have been made in Indonesia by several geoscientists. However, a lot of problems remain insoluble or at least still remain as controversial phenomena. As has been stated by Milsom (1982), the Sunda Arc now tends to be viewed as an active continental margin rather than a normal arc, whereas the Banda arc in which the process is more complicated is still an area of geological debate and heated controversy.

In Jawa, the basement is composed of a melange of late Cretaceous or very early Tertiary age (Hamilton, 1979). There are only two areas in which pre-Eocene complexes are exposed in Jawa. The melange is well exposed in the southwest and in the central part of Jawa (Asikin, 1974; Hamilton, 1979).
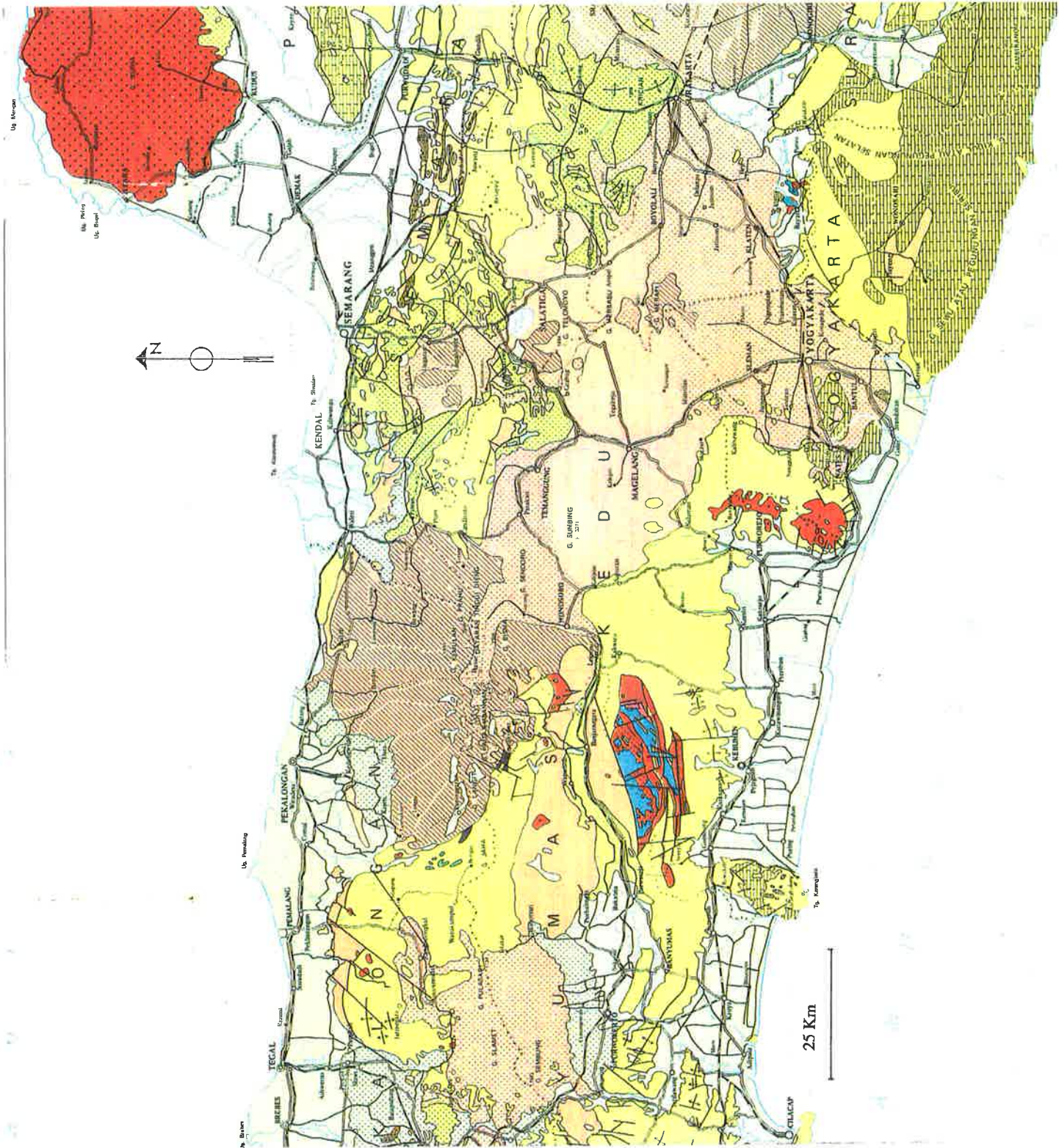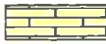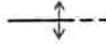
Figure 2-1. The geological map of central Jawa (Geological Survey of Indonesia, 1977).

Aluvium
Alluvium

Aluvium, fasies gunungapi
Alluvium, volcanic facies

} *Holosen*
Holocene

Plistosen, fasies sedimen
Pleistocene, sedimentary facies

Plistosen, fasies batugamping
Pleistocene, limestone facies

Plistosen, fasies gunungapi
Pleistocene, volcanic facies

} *Plistosen*
Pleistocene

Pliosen, fasies sedimen
Pliocene, sedimentary facies

Pliosen, fasies batugamping
Pliocene, limestone facies

Pliosen, fasies gunungapi
Pliocene, volcanic facies

} *Pliosen*
Pliocene

Miosen, fasies sedimen
Miocene, sedimentary facies

Miosen, fasies batugamping
Miocene, limestone facies

} *Miosen*
Miocene

Oligosen
Oligocene

Eosen
Eocene

} *Paleogen*
Palaeogene

Pratersier sedimen . . . . *Pratersier*
Pretertiary sediments . . . . . *Pretertiary*

Sekis kristalin
Crystalline schists

Granit (G), Granodiorit (Gd), Diorit (D)
Granite (G), Granodiorite (Gd), Diorite (D)

Gabro (Gb), Peridotit (P), Serpentin (S)
Gabbro (Gb), Peridotite (P), Serpentine (S)

Hasil gunungapi tak teruraikan
Undifferentiated volcanic products

Hasil gunungapi Kwarter muda
Young Quaternary volcanic products

Hasil gunungapi Kwarter tua
Old Quaternary volcanic products

} *Kwarter*
Quaternary

Andesit (A), Basal (B), Diabas (Di)
Andesite (A), Basalt (B), Diabase (Di)

Liparit (L), Dasit (Da)
Liparite (L), Dacite (Da)

Batuan mengandung leusit
Leucite bearing rocks

Antiklin
Anticline

Sesar
Fault

Sesar sungkup
Overthrust fault

2-3. Geological Information on Central Jawa.

The geological information on the study area can be subdivided into physiography, stratigraphy and tectonic setting.

2-3.1. Physiography.

Physiographically, from south to north, central Jawa can be divided into the four following zones (van Bemellen, 1949), (see figures 2-2 and 2-3) :

1. The southern coastal plain.

The coastal plain is about 10 - 25 km wide and lies not more than 10 m above sea level. There are three shore bars running parallel to the coast which is interrupted in the middle by the Karangbolong Mountains (475 m). These Southern Mountains have subsided below sea level between Nusa Kambangan and the mouth of the Opak river. This coastal plain is mainly covered by rice fields with no outcrop.

2. The South Serayu Mountains.

This area consists of western and eastern regions. The western region (360 metres) might be described as a new structural element belonging to central Jawa or alternatively as an elevation in the Bandung depression zone of west Jawa. The eastern region is distinguished from the western one by a simple narrow anticline starting near Adjibarang and transversely cut by the Serayu River. In the eastern part of Banyumas this anticline develops into an anticlinorium of some 30 km in width cropping out in the Luk Ulo area. Then it is terminated by the independent dome of the West Progo Mountains (1022 metres).

3. The North Serayu Range.

This area with a width of 30 - 50 km, might be described as a belt of marine sediments which is crowned by volcanoes. Its western end is capped by the Slamet

100 Km

Quarternary volcanoes.

Alluvial plains of northern Jawa.

Rembang-Madura anticlinorium.

Bogor-, North Serayu-, and Kendeng-anticlinorium.

Domes and ridges in the central depression zone.

Central depression zone of Jawa, and Randublatung zone.

Southern Mountains.
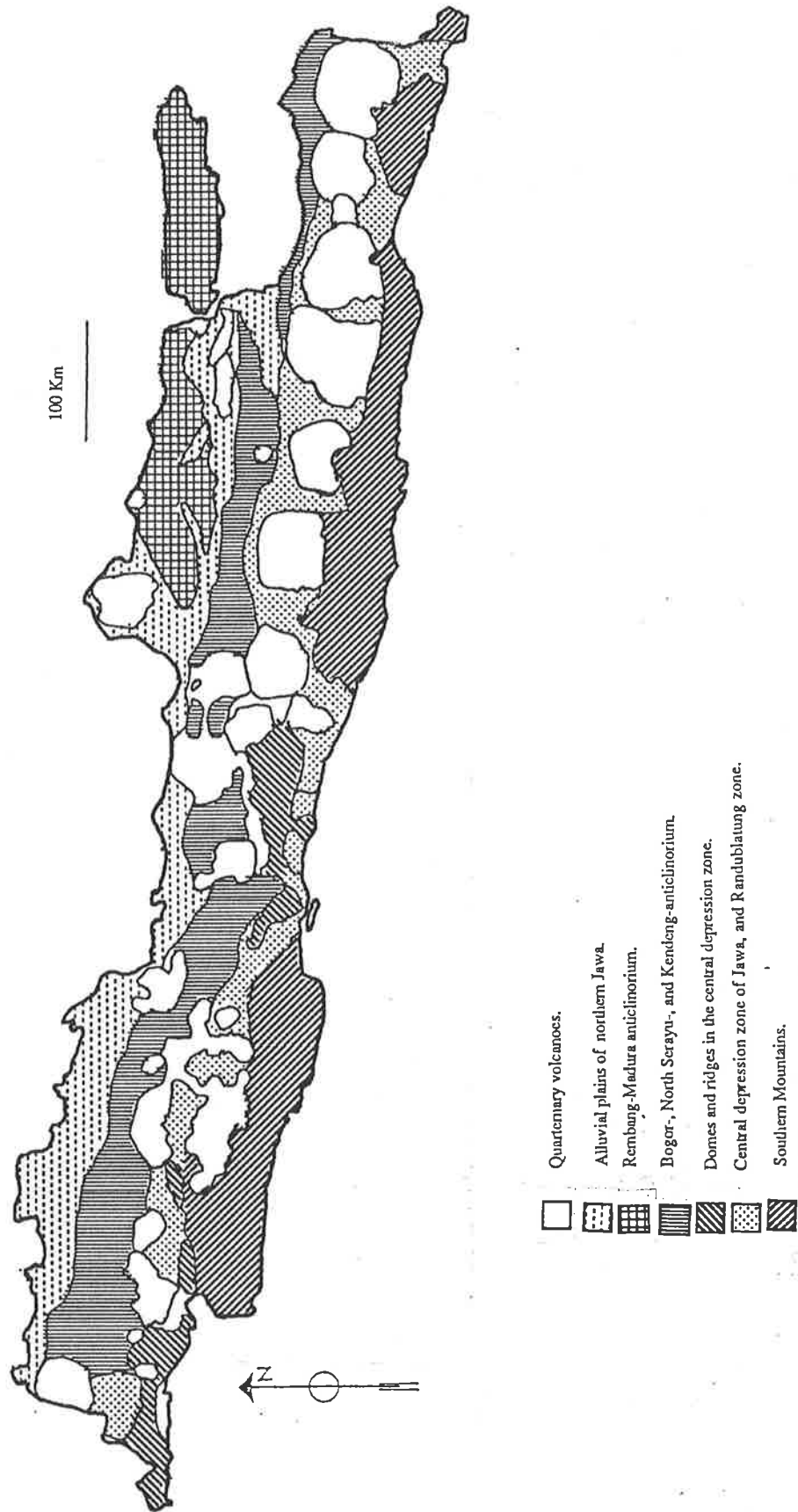
Figure 2-2. The physiographical map of the Jawa (simplified from van Bemellen, 1949).
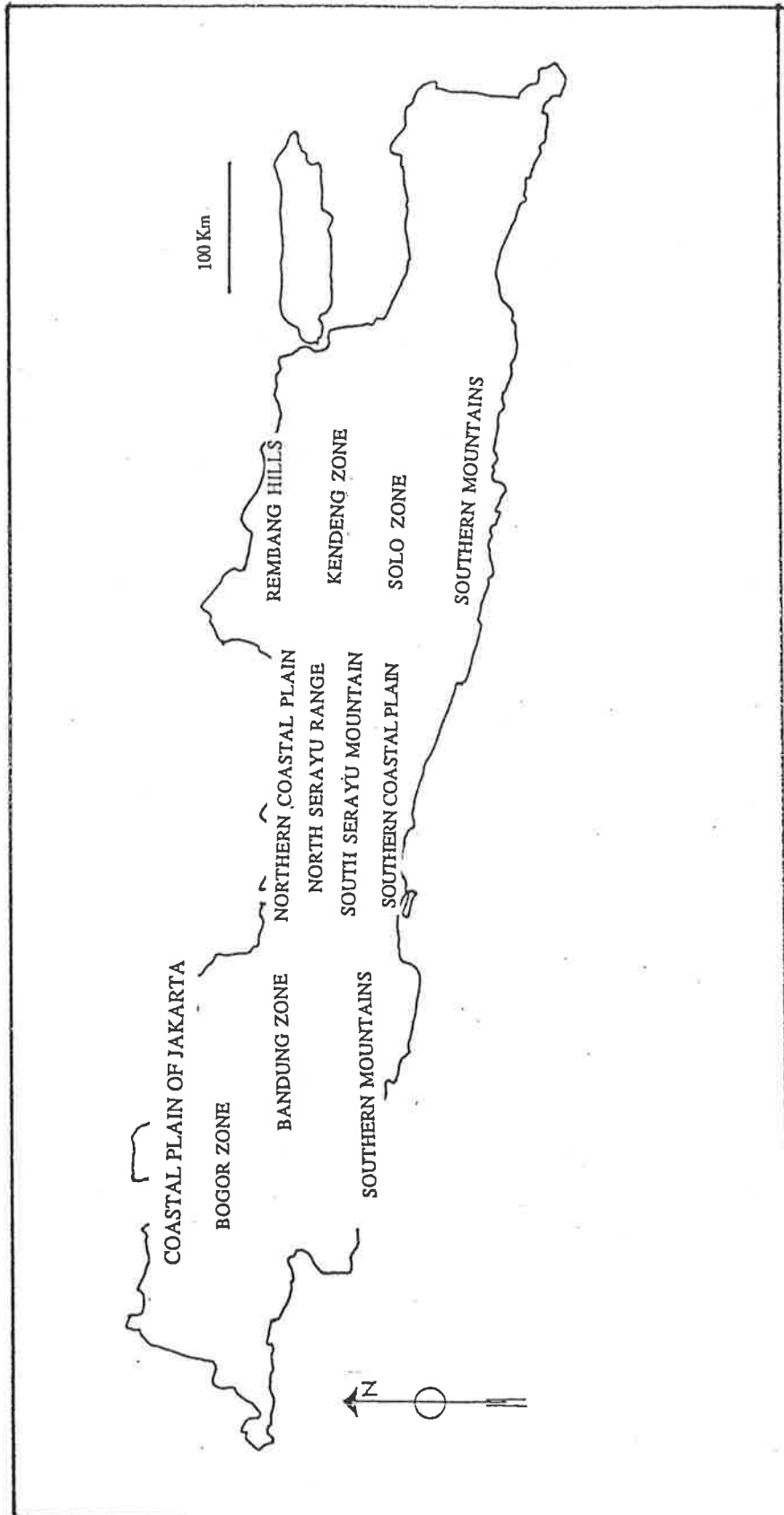
Figure 2-3. The zone division of the physiographical map of the Jawa (simplified from van Bemellen, 1949).

volcano (3428 metres) and its eastern part is covered by the young volcanic products of the Rogojembangan Mountains (2177 metres), the Dieng complex (2565 metres) and the Ungaran volcano (2050 metres).

4. The northern coastal plain.

This coastal plain forms the connecting link between West Jawa and East Jawa and has its maximum width (40 km) south of Brebes. South of Tegal and Pekalongan it narrows to about 20 km and disappears in the eastern part of Pekalongan where the headland of the mountains reaches the coast (van Bemellen, 1949).

Like the southern coastal plain, the area is mainly covered by rice fields with no outcrop. There is one abandoned oil field which can be found at Tjipluk area.

The rocks in this area, from south to north, are gradually becoming younger, with Paleogene and Miocene sediments in the south, Quarternary volcanoes in the middle and Neogene sediments in the north.

The southern physiographic zone is characterized by rather stable sedimentation and less deformed rocks which lie on top of a basement compound of schists, phyllites and quartzites which are intruded by ultra basic rocks. The basement is overlaid by coarse-grained clastic rocks of Eocene and Oligocene consisting of mostly carbonate and pyroclastic rocks and showing a transgressive phase from the south. Pyroclastic materials, an indication of volcanic activity, become more abundant towards the north of this area (van Bemmelen 1949).

Most active volcanoes in Jawa are of the stratovolcanic type arrayed along a medial zone of the island and they mask the underlying geology (Hamilton, 1979). The dominant rock types of the main volcanic belt are pyroxene andesite and high-alumina basalt (Neumann van Padang, 1951; Nicholls and Whitford, 1976; Whitford and Nicholls, 1976). In the northern part of Jawa, young but inactive volcanoes consist mainly of potassic alkalic rocks (Klompe, 1954).

Melange in this area is exposed beneath a folded cover of shallow-water and continental sediments, dated possibly within the Eocene (Hamilton 1979).

2-3.2. Stratigraphy.

The geology of central Jawa is a complex feature (see fig. 2-4).

The oldest rocks cropped in central Jawa are exposed at the Karangsambung and in the eastern part of Jogjakarta (see figure 2-1). These rocks can be grouped into late Cretaceous - Plaeocene melange known as Luk Ulo melange (Asikin, 1974). The volcanic and intrusive rocks found in wells, both onshore and offshore, exposed at the northern part of central Jawa, are presumed to be Paleocene to early Oligocene and late Cretaceous respectively. Some sedimentary rocks in the different wells are dated as late Cretaceous to early Oligocene.

In the northern part of Kebumen, sediments of Eocene to Oligocene age are also found. These sediments, called Olistostromes, are deposited in trench slope to arc trench gap, while the base is in fault contact with Luk Ulo melange.

The southernmost part of central Jawa is occupied by late Oligocene to early Miocene volcanics. The volcanics are interfingering with contemporaneous trench and back arc sediments. In the southern part of this area, dacitic to andesitic bodies intruded the pre-existing rocks during the late to early Miocene.

In the northern part of the region, the middle Miocene sediments are conformably overlying the older rocks. In contrast, in the southern part, the stratigraphic unit is unconformable. Within a basin in the northern part of Kebumen, however, middle Miocene turbidites are found conformably over early Miocene marine sediments. Also this sequence is intruded by acid to basic rocks of late to middle Miocene.

The stratigraphy of the area is set out in more detail in table 2-1.

2-3.3. Tectonic Setting.

The northward subduction of the Indian Ocean plate underneath the Sunda Land during late Cretaceous to early Tertiary time is considered to be responsible for the formation of the Luk Ulo melange (Asikin, 1974). At the same time, the magmatism which
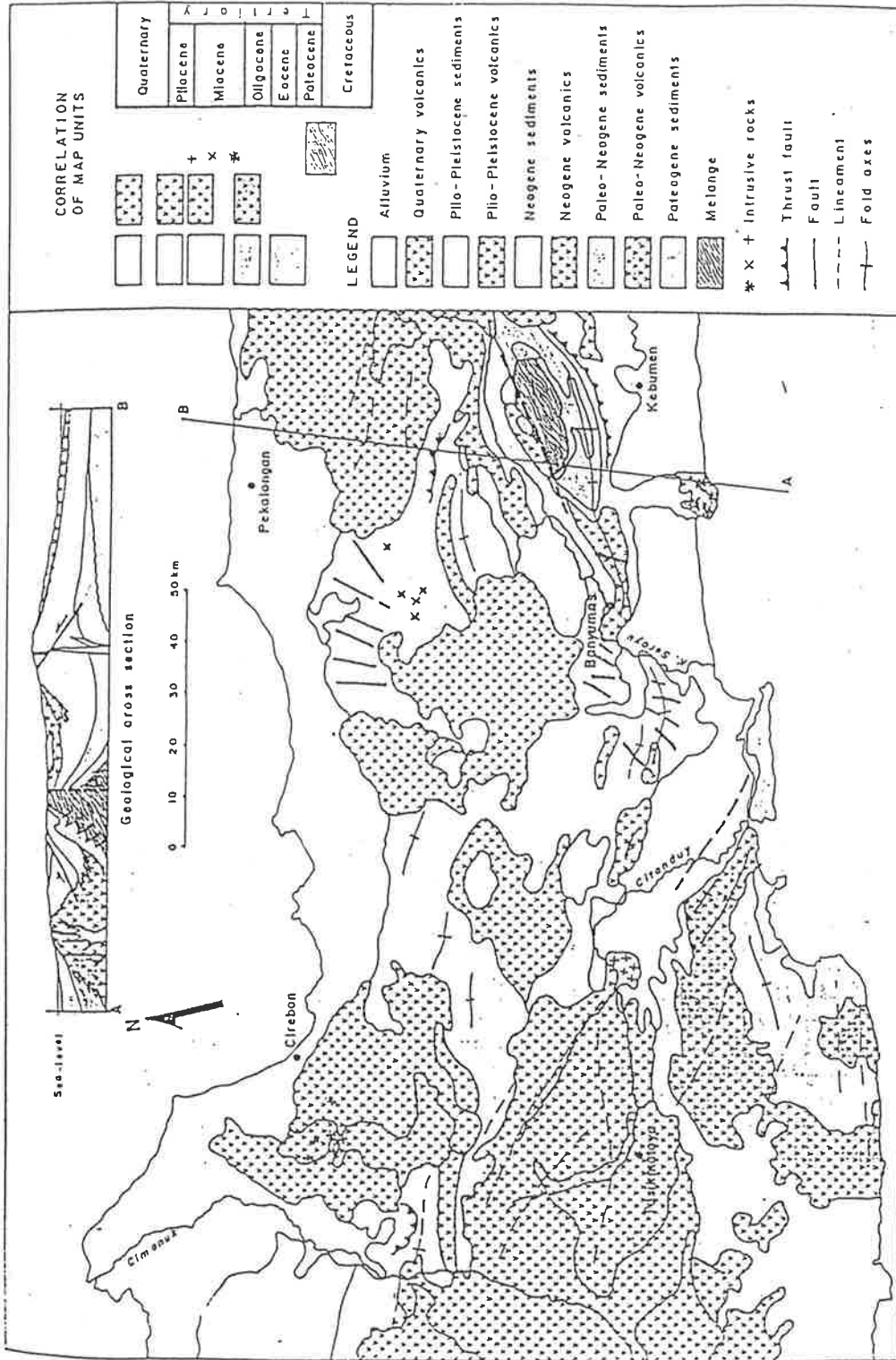
Figure 2-4. The cross section of the Lukulo area includes the simplified geological map of the area (Gafoer et al., in prep.).

Age				Symbol of Units	L i t o l o g y	Volc./ Plut. act.	Remark
Quaternary	Holocene			Qa	Clays, silts, sands; granules, pebble and cobble	v v v v	Continental sediments, exeption In Jawa sea and Indian Ocean.
				Qhv	Volcanic breccias, tuff and lavas of andesitic and basaltic compositions.	v v v v	
	Pleistocene			QTs	Tuffaceous claystone, siltstone, sandstone, conglomerate and breccia, plant remains.	v v v v	
				QTv	Volcanic breccia, tuff and lavas of andesitic-basaltic compositions, locally pumiceous	v v v v	
Tertiary	Pliocene			Tps	Sandstone, claystone, conglomerate, marl, limestone and molluscs, locally tuff. Sandstone intercalations	+ + + v v v v	Shallow marine or shelf sediments, partly slope or deep sea sediments
	Miocene	Late		Tmps	Tuff sandstone, clay, marl, limestone, tuff, conglomerate and lignite. Locally turbidites with interbeds of breccia.	v v v v	
				Tmpv	Volcanic breccias (andesitic-basaltic), tuffs, lavas, and pumiceous breccia.	v v v v	
		Middle		Tmms	Calcareous sandstone, claystone, shale, marl, and limestone. Locally turbidites.	+ + +	Shallow marine
		Early		Toms	Sandstone, volcanic breccia, Intercalations of claystone, tuff and calcareous sandstone Locally turbidites.	+ + + v v v v	(23.5±1.2 2) my Back - arc, fore - arc and volcanic arc sediments
				Tomv	Andesitic breccia, lava and tuff. Locally dacitic; Intercalations of tuffaceous/calcareous sandstone, marl and limestone. Altered.	v v v v	
	Oligocene			Tpov	Teos: Chaotic rocks with fragments of limestone, conglomerate, sandstone, claystone, basalt, breccia, matrix of scaly clay or shale.	v v v v	Olisostrome of trench slope area.
	Eocene		Teos		Tpov: Welded tuff, andesitic-basaltic lavas and agglomerate, with Interbeds of sandstone, siltstone, coal and limestone.	v v v v	Jatibarang volcanic Back - arc basins - sediments
	Paleocene		TKmc		TKs: Shale, siltstone and sandstone with intercalations of limestone and lignite.	v v v v	
Cretaceous				TKs	TKmc: Chaotic rocks with blocks of schist, phyllite, serpentinite, gabbro, basalt, chert and matrix of scaly clay or shale.	v v v v + + +	Melange (65.1±3.9) my
Jurassic				KTb	Silty argillite, coarse clastics, mainly slightly metamorphosed sandstones. Locally intrusive rocks or metamorphic rocks (undifferentiated)	?	Subsurface information
Triassic							
pre Triassic					Pre-Tertiary consisting mainly of metamorphic rocks (undifferentiated)	?	Subsurface information

Table 2-1. The stratigraphy of the central Jawa compiled from surface and subsurface information (Gafoer et al. in Untung, in prep.).

occurred in the north coast of central Jawa resulted in early tertiary volcanisms along more or less west southwest - east northeast directions.

During the subduction of late Cretaceous to Paleocene, sedimentation of Eocene-Oligocene Olistostromes in trench-slope areas took place. In the back arc, block faulting developed and controlled the Tertiary basin formation. As a result of downthrown blocks, for example, the Belitung and Jawa basins were formed in this period, while the upthrown blocks in between became the Karimunjawa arc.

In the late Oligocene, uplifted blocks became highs in the Luk Ulo area and the development of basins was affected by downthrown blocks. The volcanic arc was located more to the south during this period. It is suggested that the movement of the southeast Asian continent towards the Indian Ocean caused the southward migration of the subduction zone (Asikin, 1974).

A basin in the northern part of Kebumen was located in a trench slope during the Paleocene which later during the Eocene-Oligocene became a trench-fill basin. Then during the late Oligocene to early Miocene it was in a back arc and since the middle Miocene in an arc-trench gap (Gafoer et. al., 1987).

. The tectonic activity during the middle Miocene seems to be weaker than the activity in the previous periods. In the middle part of the area, magmatic activity is found and manifested in the form of dykes, whereas local unconformity occurred in the southern part of the region. The volcanic arcs in this period were shifted more to the north. Relatively, the regions have remained in fixed position since the Miocene (Sunoto and Wahyono, 1987).

During the late Miocene to Pliocene, the vertical movements in the arc-trench gap resulted in local unconformities and rapid subsidence. An increase of volcanic activity occurred during this period of time and also turbidites were formed in many places.

In the early Plio-Pleistocene, regional uplift occurred over nearly the whole area of Jawa, including the study area. This was followed by folding, faulting and volcanism along the longitudinal axis of the area.

The folding took place when lateral forces advanced from the south while at the same time there was northward movement of the Indian-Ocean plate. Therefore, regional trends run

approximately in a west-east direction. During this time, thrust fault developed parallel to the fold axis; meanwhile, strike slip faults and normal faults are found crossing the direction of the fold axes. Furthermore, it can be noticed that magmatic activity in this period has continued until the present time.

The probable schematic cross section of all of the above evolution can be seen on figure 2-5.

2-4. Geological Information on Four Areas of Interest.

Because of the association of gravity anomalies and the known geology, the four following areas have been chosen for use in the gravity modelling process in chapter 7. They are Luk Ulo, West Progo Mountains, Ungaran volcano and Merapi volcano areas (see figure 2-6).

The choice of those areas is based on the two following considerations :
Firstly, they have relatively more available geological information than other areas. Secondly, the Luk Ulo area in which a major fault exists, is considered to represent the boundary between the younger sediment in the north and the older one in the south. Furthermore, the West Progo Mountains and the Ungaran volcano represent the inactive volcanoes, whereas the Merapi volcano represents the active ones.

In order to provide more geological information for the modelling process of the gravity interpretation , those areas of interest will be discussed in more detail.

2-4.1 Lukulo Area.

This area which is located in the Karangsambung region is the broadest and highest part of the South Serayu geanticline. Harloff (1929, 1933), classified the crystalline basement complex which is exposed in this area into the three following categories :

1. Real crystalline schists (ortho and para-gneises, glaucophane rocks).
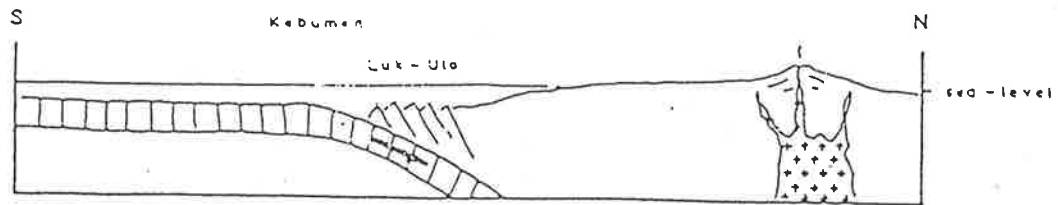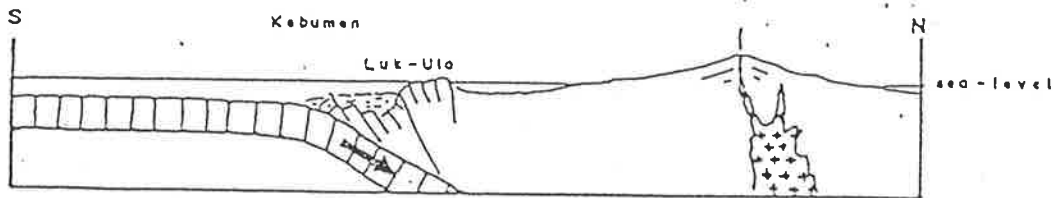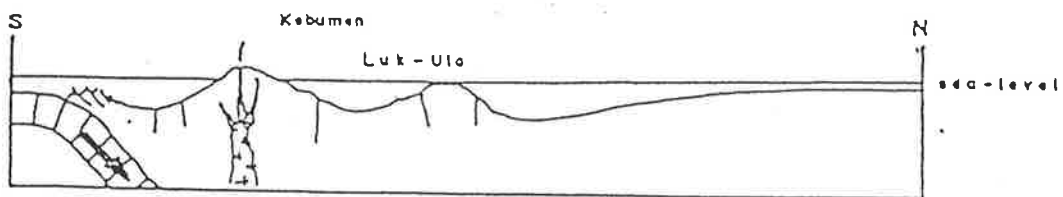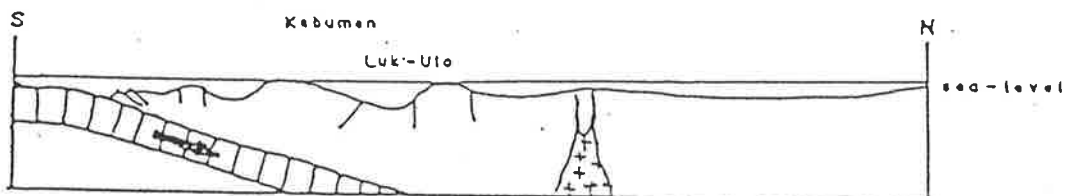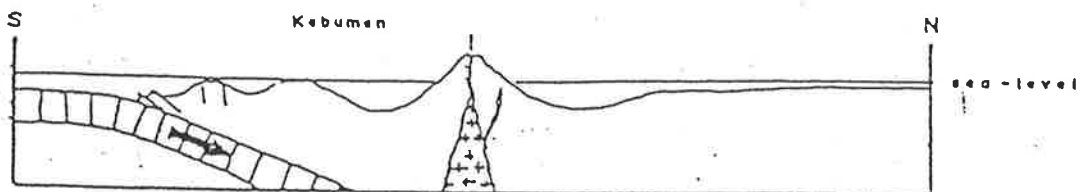
Figure 2-5. The schematic migrations of subduction zone during Tertiary (Gafoer et al., in prep.).
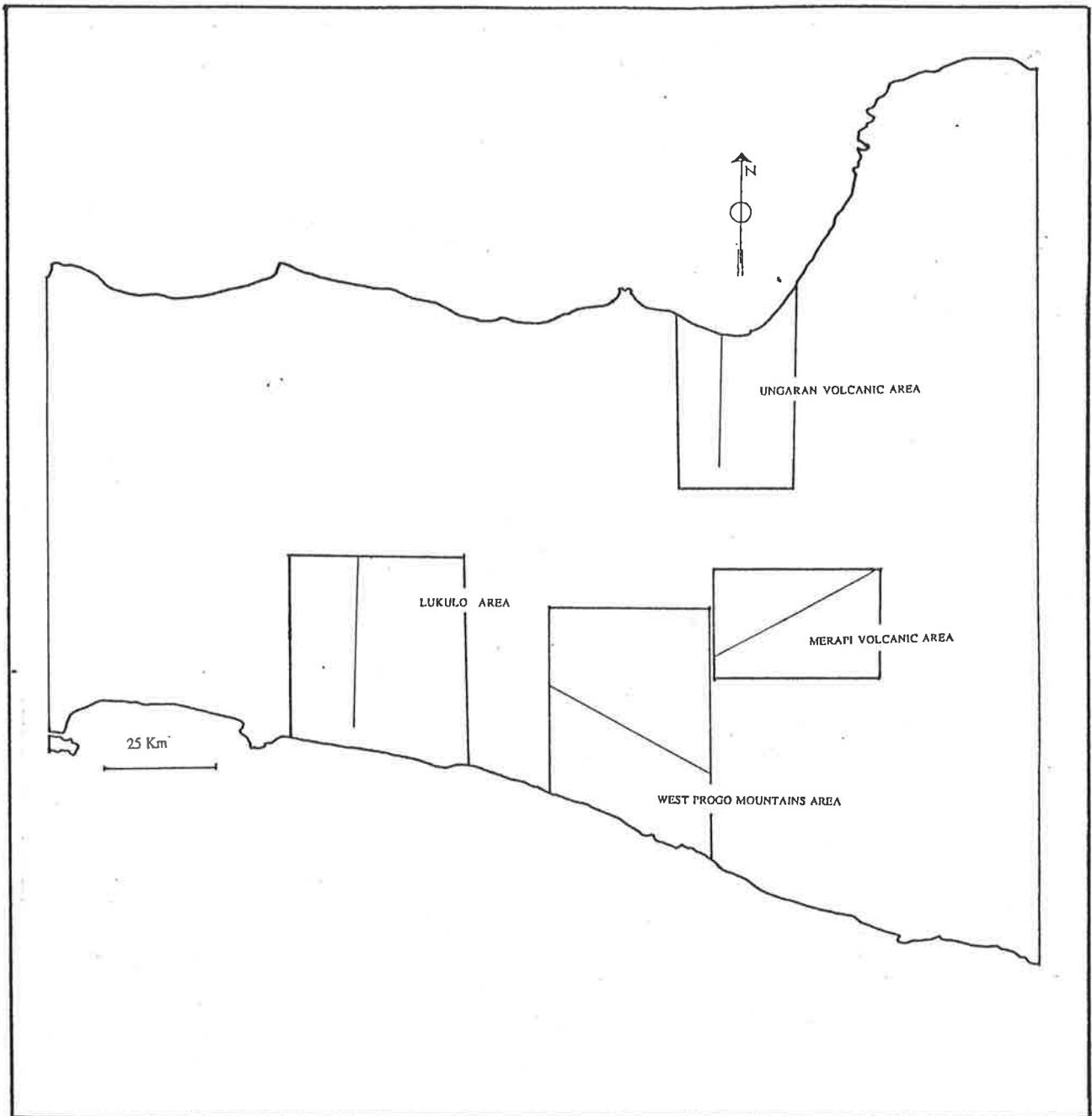
Figure 2-6. The location of the four areas of interest include their cross sections.

2. A series of shales, phyllites, quartzites, and graywackes or tuffites (with detritus of basic and acid volcanic rocks); light red limestones with streaks of chert, containing radiolaria, and partly marmorized limestones. The age of this part is estimated as lower Mesozoic.

3. Three small occurrences of clay shales with lenses of limestone, containing Orbitolina estimated as Cretaceous.

The pre-Tertiary complex is unconformably covered by Eocene sediments. Since this Eocene stratum has served as lubricant between basement complex and the overlying Neogene, a normal section could not be observed (van Bemellen, 1949).

One cross section of this area which includes the simplified geological map of some parts of the study area can be seen in figure 2-4.

The Lukulo area contains features of special interest because the oldest rocks in Jawa are exposed and cropped out in this region. These are assumed to be "the basement" rocks on all of southern central Jawa and possibly even the whole area of central Jawa.

2-4.2 West Progo Mountains Area.

This area can be described as an oblong dome. The core of this dome is occupied by three deep eroded "Old-andesit volcanoes".

1. The central part, Gajah volcano, which is the oldest one, produced basaltic augite-hypersthene andesites.

2. The southern part, Idjo volcano, was built up after the formation of Gajah volcano. It erupted materials similar to those of the Gajah volcano; however, the outer part of its mantle consists of hornblende-augite andesites. Finally dacites intruded the core.

3. The northern part is the Menoreh volcano. Its mantle consists of hornblende-augite andesitic tuffs and breccias, whereas in the deeper parts, dacitic and trachy-andesitic rocks are dominant.

All information about structure at depth in this area is based on speculation. One cross section of this area which is taken from the GRDC 1 : 100000 scale geological map can be seen in figure 2-7.

The age of this volcano is estimated as post Eocene (van Bemmelen 1949), see table 2-2.

2-4.3 Ungaran Volcano Area.

This area consists of three generations called respectively the oldest Ungaran volcano, the old Ungaran volcano and the young Ungaran volcano. The development of these volcanoes can be seen on figure 2-8.

The present concept of the structure of this area is shown in sections which are taken from van Bemellen (1949) and the GRDC 1 : 100000 scale geological map with limited depth based on the surface outcrops (figures 2-9 and 2-10, respectively).

2-4.4 Merapi Volcano Area.

This volcano is widely known as a very active volcano in central Jawa. Van Bemellen (1949) mentioned that it is located just on the intersection of two types of faults :

1. The transverse fault, which separates east Jawa from central Jawa.

2. The longitudinal fault which forms the boundary between the western Kendeng ridge and the Ngawi subzone north of Simo.

The Merapi volcano can be distinguished into older and younger zones. The older Merapi is deeply carved by erosion, and dissected by faults. It consists of olivine basalt, and also of augite-hypersthene-hornblende andesites. The younger volcano, which is still active, produces augite-hypersthene andesites with subordinate hornblende. According to van

Time	Gadjah Volcano (centre)	Idjo Volcano (South)	Menoreh Volcano (North)
Lower Miocene (T.e$_5$)	Djonggrangan limestones		
Oligocene			Trachy-andesites
		Dacites	Dacites
		Hornblende-augite andesites	Hornblende-augite andesites
	Basaltic pyroxene andesites	Basaltic pyroxene andesites	
Upper Eocene	Eocene of Nangguian		

Table 2-2. The development of the West Progo Mountains (van Bemellen, 1949).

Figure 2-7. Cross section of the West Progo Mountains area (GRDC, 1975).
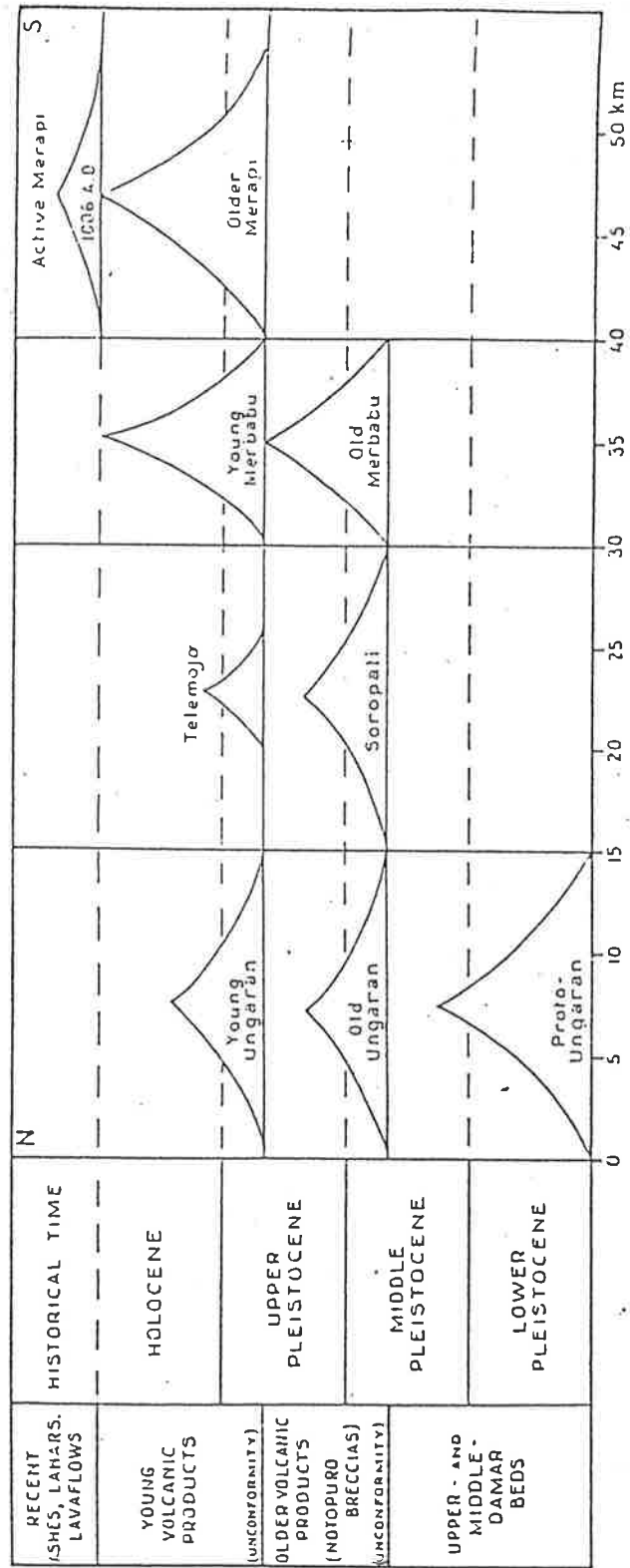
Figure 2-8. The development of volcanic structures of the transverse row Ungaran-Merapi
(van Bemellen, 1949).
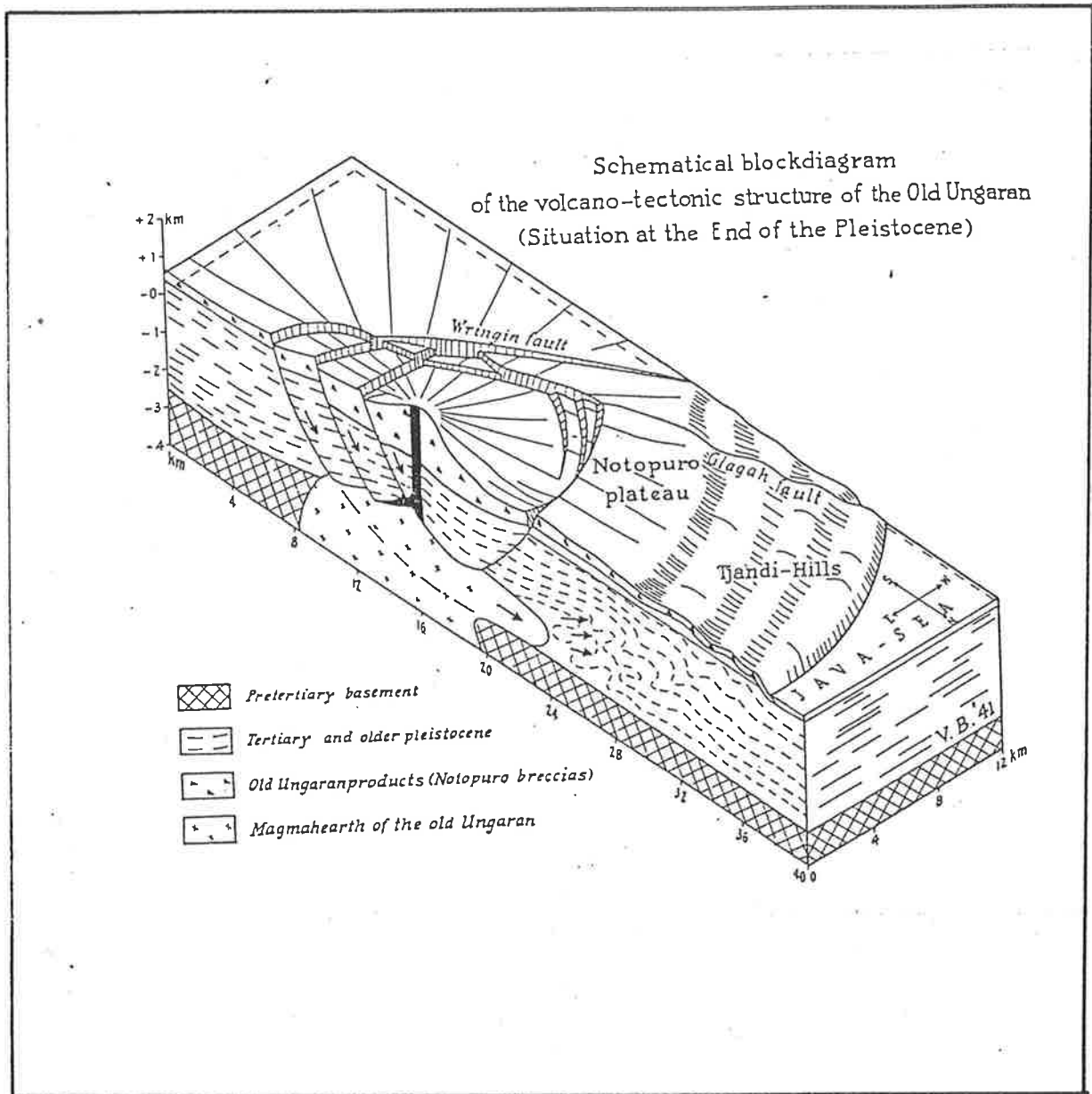
Figure 2-9. Block diagrams of the old Ungaran volcano (van Bemellen, 1949).
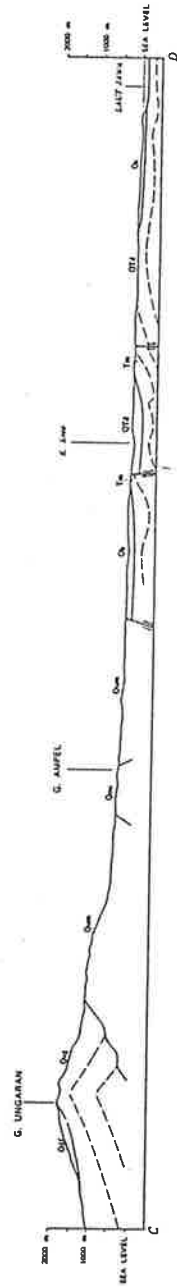
Figure 2-10. Cross section of the Ungaran volcano (GRDC, 1976).

Figure 2-11. Cross section of the Merapi volcano (van Bemellen, 1949).

Bemmelen (1949), the older Merapi is dated as upper Pleistocene with the destruction of the cone occurring in 1006 AD, or in other words, the active part of Merapi volcano was built up during the last thousand years (see figure 2-7).

The whole Merapi volcano form a relatively thin horizontal sheet on pancake of volcanic material which completely cover the underlying Tertiary sediments and volcanic rocks. One cross section of this volcano which is taken from van Bemellen (1949) can be seen on figure 2-11.

Chapter 3

Geophysical Information

3-1. Introduction.

The original research presented in this thesis is based mainly on the gravity data. However, in order to interpret the gravity data effectively, the interpretation must be consistent with all known facts including the results of other types of geophysical surveys. In other words, the interpretation of the gravity data should be supported by other geophysical data when those data are available. Therefore, the geophysical information which is used for this research is divided into only two groups of information, the gravity information and the other geophysical information.

In addition, that geophysical information which is presented in this chapter may be used as basic geophysical information for future research over this area.

The gravity information on central Jawa consists of the offshore gravity data and the onshore gravity data. The offshore gravity data were collected in the Indian Ocean by Vening Meinesz in the early 1920's. In 1932 & 1934, the results of this survey were interpreted and published with contributions by Umbgrove on the relations to geology and by Kuenen on the relations to morphology. Later marine gravity surveys were done by the Scripps Institution of Oceanography which was started by the Monsoon Expedition (1960-1961) and then completed by the Eurydice Expedition in 1975. There can also be noted some gravity traverses by ships in transit-R/V H. M. S. Cook of the Hydrographic Survey, England (Gray, 1959-1962); Pioneer of U.S.C.G.S., Oceanographer of NOAA; Vema and Robert Conrad of Lamont-Doherty Geological Observatory. The onshore gravity

information was taken mainly from the Untung and Sato report (1978) based on joint research between the Geological Survey of Indonesia and the Geological Survey of Japan.

The other geophysical information dealt with seismic information and airborne magnetic information from the study area. All of this seismic information was taken from the Hamilton report (1979) and Ben-Avraham et al., (1973). The simplified version of the aeromagnetic contour map which prepared by Pertamina, the Indonesian state-owned oil company, was taken from Buyung (in prep.). The original seismic & aeromagnetic data are not published and not available for study.

3-2. Gravity Information.

From the historical point of view, the gravity survey and research activity in Indonesia can be divided into the three following episodes :

1. Firstly, the activities which were undertaken during the Dutch Government's occupation of Indonesia. The first gravity measurements were taken in the early 1920's by Vening Meinesz, throughout the Indonesian archipelago. This remarkable gravity survey discovered for the first time the positive and negative belts along the Sunda arc in the Indian Ocean south of Jawa. This was indeed a remarkable gravity survey, because this information greatly influenced tectonic theories for the next fifty years. In the mean time also, a large number of gravity surveys were done on land by oil companies, especially by the Dutch oil company (Bataafsche Petroleum Maatschappy), evidently for the purpose of oil exploration. A large amount of data was collected in this episode. However, only a small value can be placed on those data, because their acquisition has never been undertaken systematically and also the data have never been published (Untung, 1978).

2. The second era is the period after the Dutch Government left Indonesia until 1965. Due to the very limited budget and also the lack of understanding of the importance of the gravity data, no significant result can be taken from this period.

3. The third era was the period after 1965 until recent years. As the value of gravity surveys in understanding regional tectonics became widely appreciated, large scale and systematic surveys of Indonesia were planned in 1965 by the Geological Survey of Indonesia (by the section nowadays known as the Geological Research and Development Centre) and are still in progress. This era can be noted as the period in which both quantity and quality of gravity collecting data have been increasing rapidly. In particular, since 1970, large scale and systematic surveys have been carried out relatively well.

The gravity data information which are available might be divided into two areas, offshore area and onshore area. Therefore the information will be divided into the two following sub sections :

3-2.1 The Sunda Arc Gravity Data Information.

In the early 1920's, Vening Meinesz undertook the gravity measurements along the Sunda and the Banda arcs. The gravity measurements were taken by using a pendulum apparatus on board a submarine. The most important result which should be noted from this survey is the discovery of positive and negative belts of regional isostatic anomalies for a width of some 100 to 200 km in the Indonesian archipelago (fig. 1-3). The negative anomalies of -100 to -150 mgals coincide with the submarine ridge south of Jawa, later on described as an outer arc. From this arc toward Jawa the anomalies lessen to 50 to 100 mgals in the inner deep (Untung, 1978). These belts of large negative anomalies usually

coincide with islands where the geology shows strong folding and overthrusting (Vening Meinesz 1954). On the basis of all those gravity features, concepts of the process of mountain building and the formation of island arc systems were formed by many earth scientists.

3-2.2 Jawa Gravity Data Information.

The earliest source of onshore gravity data information which is used for this research is taken mainly from the Untung and Sato report in 1978. This information is based on the 1 : 500000 scale simplified Bouguer anomaly contour map of Jawa and Madura islands with a station density of about 1 per 100 sq km. This map was based on the result of the gravity reduction of the 1930 International Gravity Formula with a density value of 2.50 gr/cm^3.

Since central Jawa is only one part of Jawa island, it is prudent to examine, although only in general terms, the gravity information of the whole island first. At least, the general trend of the gravity information over Jawa island can be used as the first approximation for deeper analysis of the gravity features in central Jawa.

Generally speaking the trend of the anomalies over the whole island is in an east-west direction. Since Jawa can be divided into three provinces, west Jawa, central Jawa and east Jawa, the anomaly orientation of Jawa may be grouped into more specific orientations. Based on 1 : 500000 scale Bouguer anomaly contour map, the trend in west Jawa is in a northwest-southeast direction, whereas in central Jawa and east Jawa, the trend is more east west rather than in a northwest-southeast direction (fig 3-1).

According to Untung (1978), the gravity anomalies over the whole island may be divided into the three following categories :

1. The southernmost belt with anomalies between 90 to 170 mgals which are matched with the southern mountains area.

Figure 3-1. The simplified Bouguer anomaly contour map of jawa and Madure islands (Untung et al., 1975).
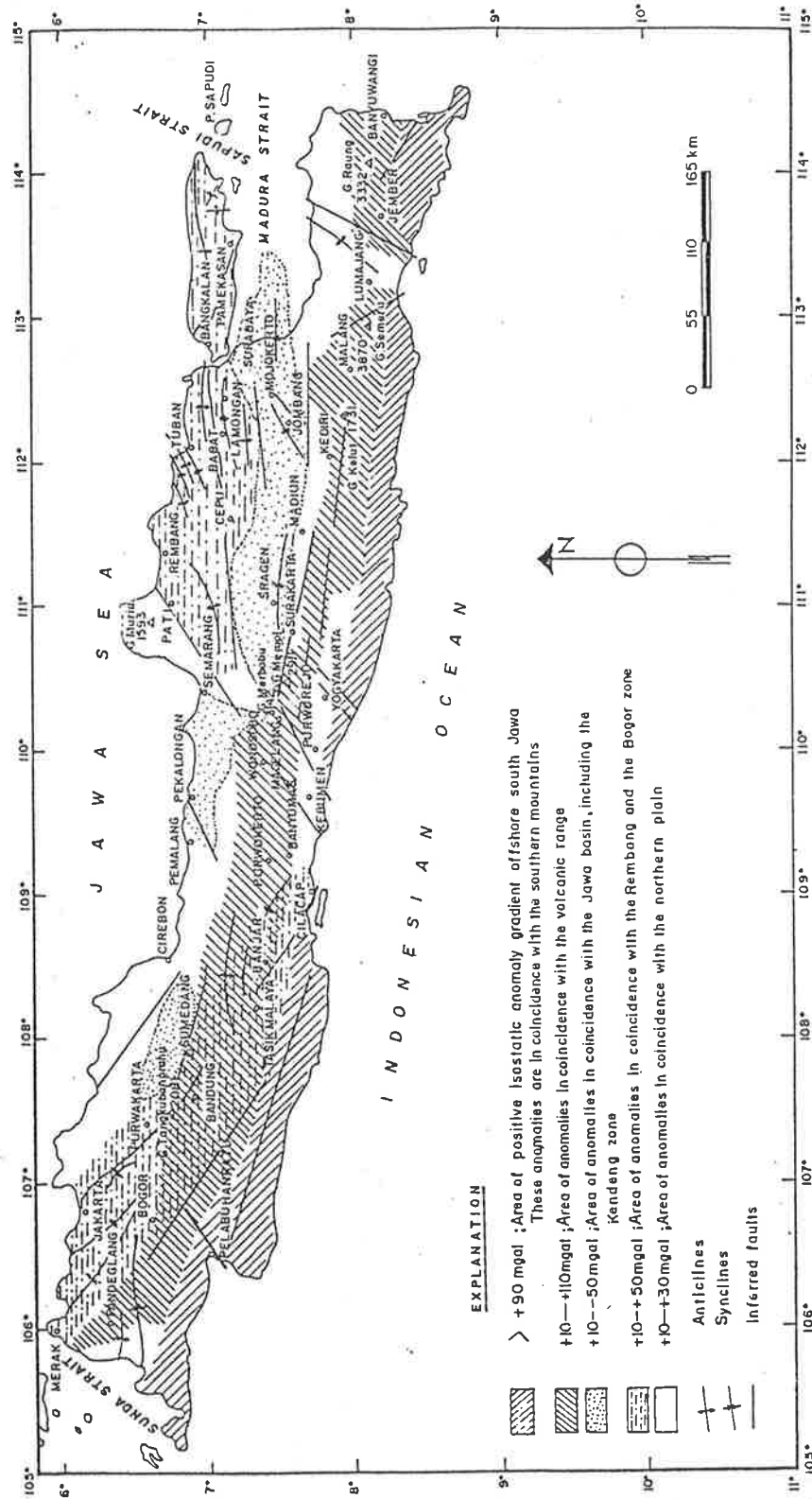
Figure 3-2. The general structure pattern map of Jawa and Madura Islands as interpreted on the basis of the Bouguer anomaly map (Untung et al., 1975).

2. The centre belt with anomalies between 10 to 110 mgals which coincide with the volcanic arrays.

3. The last belt is the northern belt with anomalies ranging from 10 to 50 mgals; it follows the zone of the folded sediments of the northern part of Jawa.

Figures 3-1 and 3-2 show the simplified Bouguer anomaly map of Jawa and Madura and their general structural pattern map as interpreted qualitatively from the gravity data respectively.

High anomalies of 180 to 212 mgals have been detected in the southwestern corner of Jawa. This coincide with the outcrops of basic and ultra basic rocks such as gabbro, peridotite, and serpentinite exposed in the Ciletuh area in west Jawa. Furthermore, something anomalous is found in the Luk Ulo area and in the Lumajang depression in east Jawa whereas negative anomalies up to -60 mgals can be observed along the Kendeng zone of east Jawa (Untung, 1978). In addition, this negative anomaly can be followed to Madura Strait where values of -50 mgals are detected (de Bruyn, 1951).

3-2.2.1 Central Jawa Gravity Data Information.

Generally, as has been mentioned previously, the trend of the anomalies over central Jawa is to an approximately east-west orientation. As can be seen clearly from figure 3-1, the maximum gravity value reaches 140 mgals at the West Progo mountains on the south coast, whereas the minimum gravity value reaches -55 mgals at the Kendeng zone in the eastern part of the area. The gravity values decrease rapidly from 140 mgals on the south coast to around 0 mgal or 10 mgal in the north coast area. The gravity anomaly values might be classified into the three categories which have been described in the previous section.

3-3. Other Geophysical Information.

There is no significant geophysical data available except the gravity data itself which can be used for this research. However, several sections from seismic surveys in the Indian Ocean area and an aeromagnetic contour map along the western part of the study area may be considered and used as supporting data for the above gravity data.

3-3.1. Seismic Data Information.

The seismic information used for this research is taken from Ben-Avraham et al., 1973. This seismic information illustrates the seismic velocities of crustal and uppermost mantle elements across the Jawa trench subduction system (fig 3-3). Actually this is a seismic-refraction study which was done by R. W. Raitt (unpublished) and then cited by Ben-Avraham (1973). The two following features are suggested by Raitt (1967) :

1. The crust in the nothern part of Jawa trench is much thicker than that in the southern part of it. Also the unconsolidated and semiconsolidated sediments are much thicker in the north rather than in the south of the trench.

2. The oceanic crustal layer (with velocity 6.9-7.2 km/sec) extends across the trench to within 50 km of Jawa.

On the basis of this seismic study, Hamilton (1978) suggested that the outer-arc basin is filled by low-velocity sedimentary rocks which also compose the upper part of the melange wedge beneath the crust of the outer arc ridge. It seems that velocities increase downward in the melange wedge.

Hoshino and Sunoto (1978) also assumed on the basis of the Raitt study that the order of structural zones from south to north in Jawa may be divided into the three following zones (figure 3-4) :

Figure 3-3. The seismic velocities of crustal and uppermost mantle elements across the Jawa trench subduction system (Ben-Avraham et al., 1973).
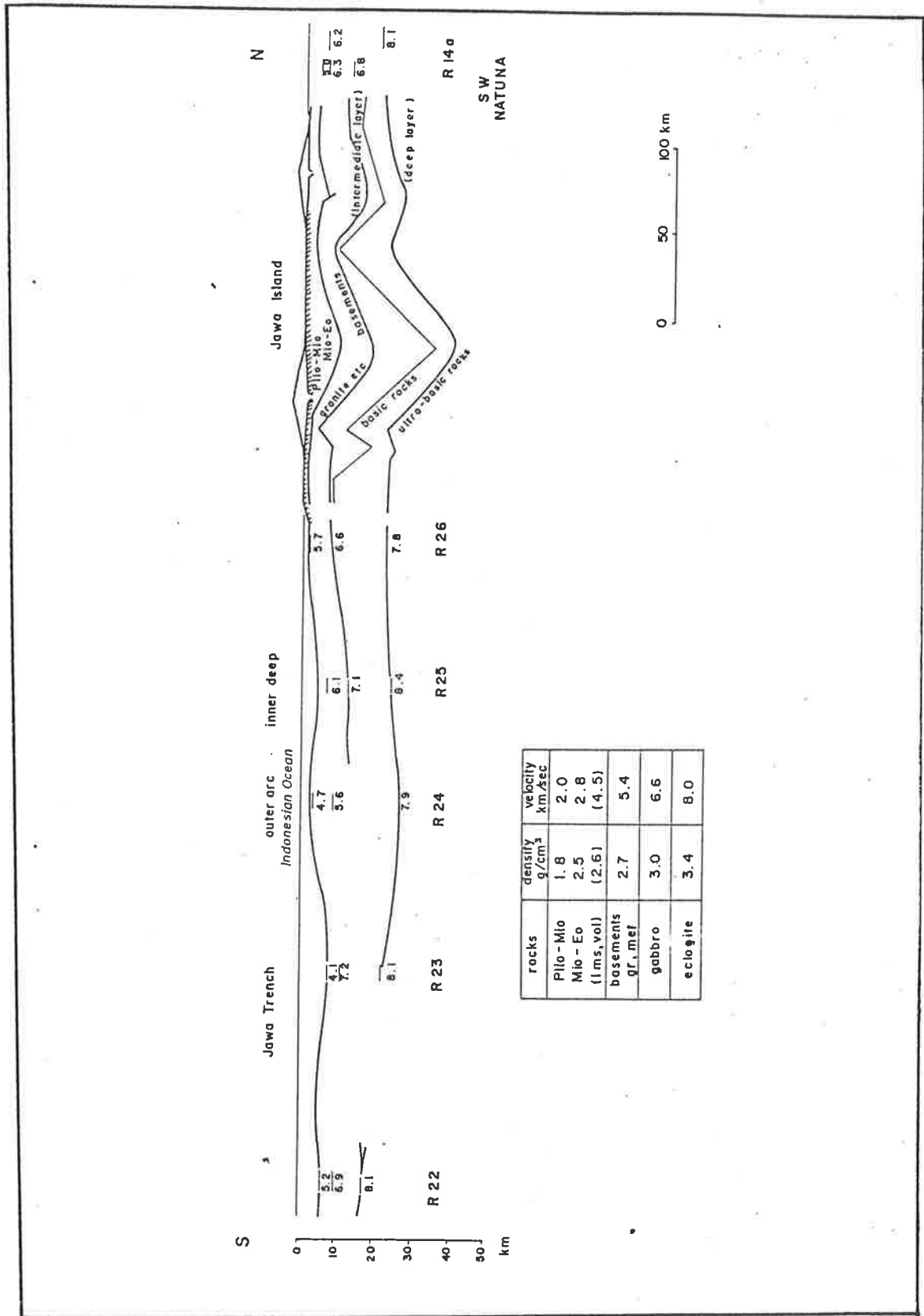
Figure 3-4. Section from the Jawa trench crossing Jawa (Hoshino and Sunoto, 1978).

1. Zone of stable shelf characterized by shallow magmatism. This indicates an area of uplift.

2. Zone of depression or graben bordered by steep faults. This is a site of volcanic activity.

3. Zone of geosyncline or basin with sedimentation which began in early Paleogene. (Hoshino and Sunoto, 1978).

There has been no seismic profile found on the land area during the period of this research.

3-3.2. Airborne Magnetic Data Information.

The airborne magnetic data information which is used for this research are taken from Buyung (in prep.). That simplified version of the aeromagnetic contour map was prepared by Pertamina, the Indonesian state-owned oil company (figure 3-5).

Only very limited information can be taken from this kind of contour map, because the high ground areas, such as volcanoes, were not covered by the above aeromagnetic survey. The range of residual aeromagnetic values is between 2800 nT and 3400 nT. However, the above aeromagnetic map was drawn by taking the contour value of 3400 nT as 0.0 nT.

According to Buyung (in prep.), the anomaly trend is generally in an east-west direction, which changes to the northwest at longitude 108°30' E in the western part of the area.

On the basis of that aeromagnetic contour map, the three following patterns should be noticed :

1. It seems that the anomaly values increase along the south coast of Jawa. Three high anomaly values have been recorded in the south coast area. The first one is 250 nT at coordinates 110°00' E and 7°45' S. The second value is 300 nT at coordinates
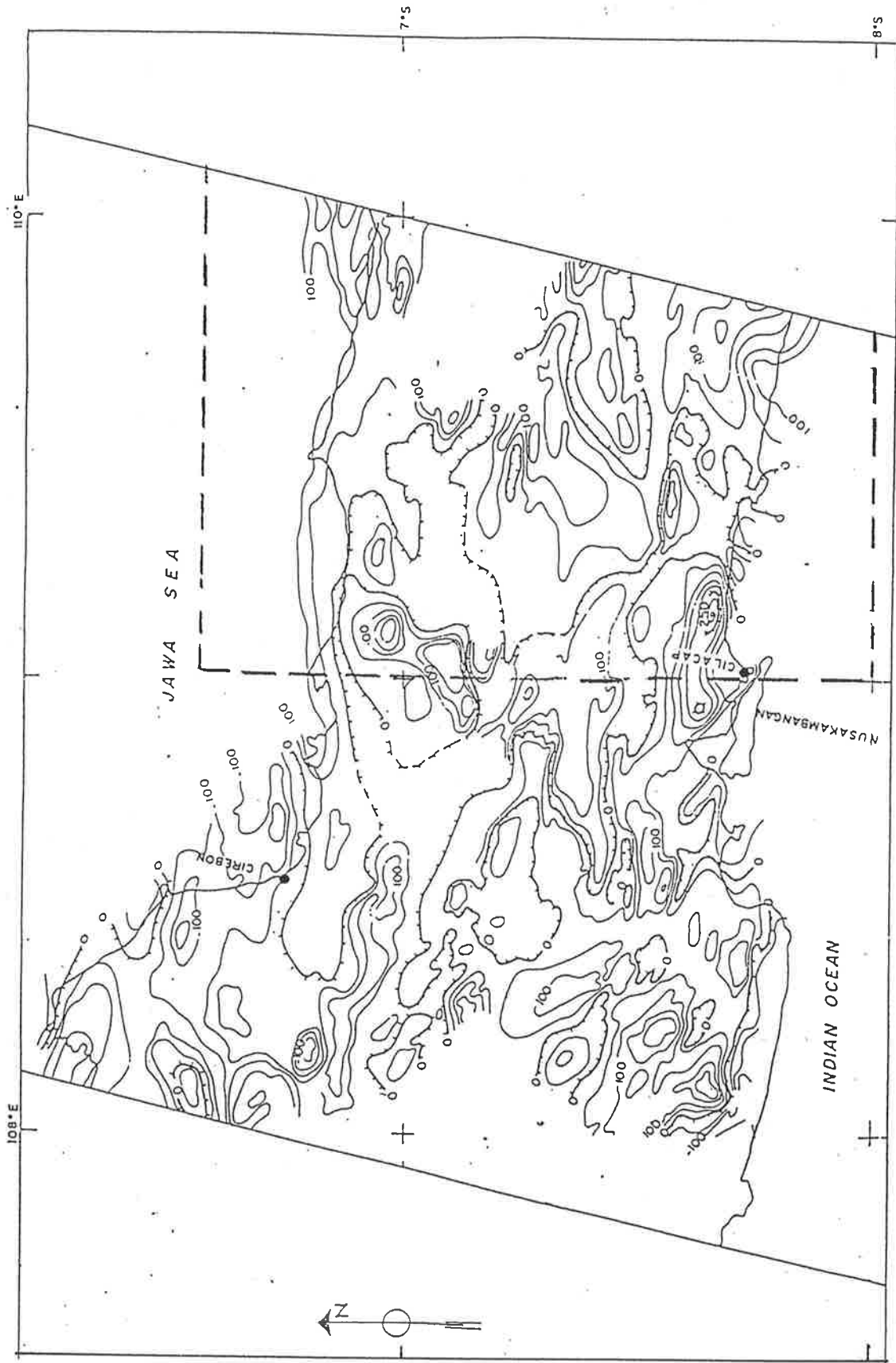
Figure 3-5. The simplified aeromagnetic contour map of the Jawa transect area (Buyung, in preparation).

Map scale 1:2,000,000   Contour interval 50 gammas

108°15' E and 7°37' S. The third and the highest value is 400 nT at coordinates 109°00' E and 7°40' S .

2. Low magnetic anomalies are present in the middle part of the area in which the minimum value of - 250 nT is reached.

3. The north coast of central Jawa is occupied by an anomaly of around 50 nT with east-west orientation running parallel to the coast (Buyung, in prep.).

Chapter 4

Physical Property of the Rock

4-1. Introduction.

The gravity anomalies which are obtained from gravity measurement, after appropriate reductions, are essentially dependent only upon lateral changes in the density distribution of the earth material. Without this density variation of the rocks, no gravity anomalies will occur. Therefore, the information about density of the subsurface rock constitutes an essential element in gravity interpretation study, especially in quantitative interpretation.

In addition, the standard correction for elevation includes a density factor, so in regions where there are large variations in elevation the appearence of the contour map may be strongly influenced by errors in the assumed density of the rock.

This kind of information which is known as physical property of the rock will be disscused in this chapter.

4-2. Procedure.

Theoretically, to obtain the physical property of the rock is just a simple procedure. The rock samples are collected directly from study area then their density determined by the measurement on the basis of the Archimedes' law. However, practically this often constitutes a difficult process. It is common to find that for the purpose of both gravity and

47

magnetic surveys, in areas of poor out crop or deep weathering, the rock samples from the survey area are not readily available. To overcome this problem several density determination methods are discussed and provided for this purpose.

4-3. Density of the Rock.

The determination of density of the subsurface rocks constitute an important element in the gravity interpretation study. It is important to know as far as possible the density of the rocks from the study area, because with the knowledge of the density contrast, which causes the gravity anomaly, the range of acceptable solutions in the quantitative interpretation might be limited.

In the absence of rock samples, a table of typical densities of the rocks which represent the regions where gravity surveys are made may have to be used. One table of average densities were obtained from a large number of laboratory measurements on core and subsurface samples provided by J. W. Peters from Mobil Oil Company (Dobrin, 1988). However, the range of density of the rock type is often quite wide, and there is overlap between the type of rocks.

To overcome this problem, it is highly desirable to collect rock samples directly from the study area and then measure their density in the laboratory. One of the density measurements commonly made is the measurement based on Archimedes' law. With this simple calculation, the density of the rock sample is obtained by obtaining the weight of the rock in the air and comparing this value with the differences between the weight of the rock in the water and the weight in the air. It must be remembered, however, that it is really difficult to obtain a rock sample which truly represents the type of the rock. It is not always easy to obtain density values because of the difficulty of finding fresh, unweathered rock samples. It is also common to find that when rock samples which are collected by

geologists in different surveys with different aims, available, they are not from typical rock which are actually required for this purpose.

Several pieces of research and studies have been done to examine and analyze this problem. The effect of the depth on the density value of the sediment was examined by Nettleton (1934) and also by Hedberg (1936).

· Other approaches to density determination in which the correlation of the observed gravity value and the elevation are compared have been offered by Nettleton (1939), Hammer (1950), Cook and Thirlaway (1952), Parasnis (1952), Domzalski (1955), Vajk (1956), Whetton et al. (1957), Grant and Elsaharty (1962).

On the basis of the above research and studies, two methods which have been suggested for the purpose are in principle the same :

1. The profile method.

The Bouguer anomaly along a line is calculated using a range of assumed values of density. Then the shape of the anomaly curve is compared with the topography along the profile. The density curve which shows the least correlation with the topographical curve is chosen as the representative density.

· 2. The straight line method.

The Bouguer anomaly at the stations is assumed to be zero. Consequently, the formula for the reduction of the Bouguer anomaly becomes :

$$0 = g_o - gN + (0.3086 - 0.0419\ \rho)\ h$$

or $g_o - gN = 0.0419\ h\ \rho - 0.3086\ h$

This formula can be simplified into :

$$y = \rho\ x + c$$

where :

$$y = g_o - gN$$

$$x = 0.0419\ h$$

$$c = -0.3086\ h$$

· This is the equation of a straight line whose slope is proportional to ρ (Parasnis, 1970).

All information, both the results of the measurement of the density of rock samples and the bulk density derived from the gravity results is considered in choosing the density contrast which will be used in quantitative interpretation or, in this case, for the modelling process.

4-4. Density of the Rock in Jawa and Madura Islands.

In this study interpretation, however, there has been no direct access to the rock samples of the study area. Consequently, the density of the rock types should be taken from certain available tables of rock density.

In correlation with the joint cooperation in gravity and geological studies in Jawa between the Geological Survey of Indonesia and the Geological Survey of Japan in 1978, density measurements were taken on that project. All density measurements were made on the basis of Archimedes' law. Their results are tabulated in table (4-1) and the location from which the rock samples were taken can be seen on fig.4-1.

On the basis of this table, the average density of the rock samples which are collected from Karangsambung area is about 2.62 gr/cm^3. This may be assumed as the density of the basement rock in that particular area. The sandstones belonging to the Eocene to Oligocene show values of 2.57 gr/cm^3 to 2.65 gr/cm^3 in wet condition and 2.50 gr/cm^3 to 2.62 gr/cm^3 in dry condition. Therefore an average density of 2.60 gr/cm^3 may be applied for Miocene to Eocene sandstones. The results from volcanic rocks, andesitic and basaltic lavas, give the densities of 2.58 gr/cm^3 to 2.77 gr/cm^3 in wet condition and 2.47 gr/cm^3 to 2.73 gr/cm^3 in dry condition.

This kind of information may be considered sufficient since it can be used to control the suitable density contrast which is taken for the modelling process in chapter 7.

EXPLANATION

JC1 — JC43   Samples in Central Jawa, collected in 1974
JW1 — JW39   Samples in West Jawa, collected in 1974
301 — 356   Samples in East Jawa, collected in 1975
401 — 488   Samples in Central Jawa, collected in 1975

JAWA SEA

INDONESIAN OCEAN

DJAKARTA
DPURWAKARTA
CIREBON
PEKALONGAN
SEMARANG
BANDUNG
CIAMIS
PURWOKERTO
BANJARNEGARA
YOGYAKARTA
WONOGIRI
PACITAN
SUKABUMI
TUBAN
SURABAYA
SAMPANG
JOMBANG
NGAWI
MALANG
BANYUWANGI

ROUTE C
ROUTE D

0   25   50   75   100 Km

Figure 4-1. Location map of the rock samples which were collected from Jawa and Madura islands (Hoshino, Sunoto and Inami, 1978).

No.	Sample No.	Laboratorium Name	Lithology	Age or Formation	Density ρn	ρd	ρw	Porosity ϕ	Velocity (km/sec) P	S
1.	JW— 1		Limestone	Late Miocene	2.15	1.92	2.20	28.5		
2.	4		Limestone	(Oligo–Mio) Rajamandala fm	2.74	2.75	2.76	0.8		
3.	7	JWJ	Mudstone	Oligocene	2.63	2.61	2.64	3.4	3.80	2.25
4.	8	JMO	Sandstone	(Oligo–Eo) Walat fm	2.41	2.40	2.56	15.6	2.99	2.24
5.	10		Peridotite	Pre-Tert.	2.51	2.42	2.53	11.9	2.69	1.38
6.	11		Gabbro	Pre-Tert.	2.83	2.81	2.86	4.9		
7.	12	JWE	Sandstone	(Eo) Ciletuh fm	2.51	2.50	2.53	3.1	4.64	2.57
8.	13		Tuffaceous ss.	(Plio–Mio) Bentang fm	1.78	1.40	1.93	53.3		
9.	14		Mudstone	Miocene				1.33		
10.	158		Andesite	Quaternary	2.56	2.51	2.58	7.5		
11.	16		Andesite	Quaternary	2.47	2.47	2.58	11.5		
12.	17	JWA	Mudstone	Miocene	2.45	2.43	2.55	11.7	2.99	1.87
13.	18		Sandstone	Oligo (Early-Mio)	2.54	2.51	2.59	7.3	1.83	1.27
14.	22		Limestone	Mio (Cimandiri fm)	2.69	2.69	2.75	5.7	4.59	
15.	23		Mudstone	Miocene	2.07	1.93	2.14	20.4	1.96	
16.	25		Limestone	Miocene	2.68	2.65	2.69	4.2	4.64	
17.	28		Mudstone	Early—Mio		2.24			2.55	
18.	31	JW8	Sandstone	Early—Mio	2.34	2.32	2.48	15.7	2.07	1.42
19.	32		Mudstone	Miocene					2.64	
20.	34		Limestone	Miocene	2.71	2.70	2.72	2.4	4.78	
21.	35		Mudstone	Miocene		2.37			1.13	
22.	37		Andesite	Quaternary	2.76	2.73	2.77	3.3	5.24	
23	38		Andesite	G. Salak (Quaternary)	2.68	2.67	2.73	5.6		
24.	39		Andesite	Quaternary	2.70	2.70	2.78	8.1		
25.	36		Mudstone	Miocene	1.70	1.68	1.78	10.4		
26.	402	JMC	Shale	Late Miocene	1.32	1.24	1.76	52.4	1.46	0.86
27.	404		Volcanic	Pleistocene	2.12	1.89	2.55	67.6		
28.	405A		Tuff	Quaternary	2.67	2.65	2.70	4.5		
29.	405B		Diorite	Quaternary	2.74	2.69	2.75	6.1		
30.	406	JML	Sandstone	Eocene, Bajat fm	2.28	2.28	2.41	13.1	3.71	2.86
31.	407A		Diorite	Pre-Tert.	2.71	2.67	2.72	4.1		
32.	407B		Diorite	Pre-Tert.	2.85	2.83	2.85	2.2		
33.	410A		Talc Schist	Palaeogene	2.69	2.60	2.77	16.4		
34.	410B		Talc Schist	Palaeogene	2.50	2.43	2.53	10.3		
35.	411		Nummulitic Limestone	Holocene	2.71	2.70	2.71	0.8		
36.	412A		Limestone	Holocene	2.50	2.45	2.57	12.4		
37.	412B		Schist	Holocene	2.58	2.49	2.61	10.9		
38.	413	JME	Sandstone	Early Miocene	2.63	2.63	2.66	3.2	4.24	2.85
39.	415A	JMG	Diorite	Miocene	2.80	2.80	2.81	1.1	4.68	2.50
40.	415B		Diorite	Miocene	2.78	2.76	2.79	2.2		
41.	419		Limestone	Oligo—Mio	2.59	2.55	2.64	9.0	4.00	2.00
42.	421A	JML	Tuff Sandstone	Pliocene	1.64	1.61	2.00	39.7	1.40	0.69
43.	421B		Sandstone	Holocene	2.08	1.81	2.21	40.2		
44.	423		Gabbro	Miocene	2.75	2.73	2.75	1.9	5.00	2.85
45.	425	JMN	Volcanic S.S.	Oligocene	2.16	2.15	2.40	25.1	0.87	0.46
46.	426		Basalt	Miocene	2.80	2.75	2.75	5.3	5.00	2.50
47.	428A		Marl	Miocene					4.40	2.20
48.	428B		Limestone	Miocene	2.65	2.62	2.66	3.6		

Table 4-1. The result of the density measurement of the rock samples which were collected from Jawa and Madura islands (Hoshino, Sunoto and Inami, 1978).

No.	Sample No.	Laboratorium Name	Lithology	Age or Formation	Density			Porosity	Velocity (km/sec)	
					ρn	ρd	ρw	ϕ	P	S
49.	434		Limestone	Miocene	2.64	2.61	2.67	6.8		
50.	438		Shale	Palaeogene	2.72	2.70	2.73	2.7		
51.	443	JMN	Fine Mudstone	Miocene	2.28	2.25	2.43	17.3	3.56	2.73
52.	444		Basalt	Holocene	2.64	2.55	2.66	10.4		
53.	445	JMO	Shale(Mudstone)	Mio–Plio	1.52	1.48	1.88	39.7	2.45	1.60
54.	446		Calcareous tuff	Miocene	2.02	1.89	2.45	56.0		
55.	446		Calcareous tuff	Miocene	1.93	1.74	1.24	50.2		
56.	447	JMQ	Shale	Late Mio–Plio	2.05	2.05	2.34	29.0	2.26	1.10
57.	449	JMR	Sandstone	Miocene	1.97	1.97	2.24	27.3	2.02	1.00
58.	451		Andesite	Miocene	2.66	2.60	2.68	7.5		
59.	452		Tuffbreccia	Pleistocene	2.04	1.69	2.17	47.4		
60.	453		Andesite	Quaternary	2.49	2.41	2.55	13.5		
61.	454		Andesite	Quaternary	2.67	2.63	2.72	7.8		
62.	455		Diorite	Holocene	2.78	2.76	2.81	4.6		
63.	456		Hornfels	Holocene	2.65	2.62	2.67	5.0		
64.	457		Diorite	Holocene	2.07	1.80	2.19	39.7		
65.	458		Basalt	Quaternary	2.80	2.76	2.81	4.3		
66.	460		Andesite	Quaternary	2.50	2.49	2.57	7.8		
67.	461		Basalt	Quaternary	2.60	2.58	2.65	6.4		
68.	462		Breccia	Quaternary	1.96	1.61	2.05	44.4		
69.	464		Tuff(andesite)	Quaternary	2.58	2.57	2.63	4.5	1.80	1.00
70.	465		Coarse tuff	Quaternary	2.56	2.53	2.59	5.9	3.30	2.00
71.	466A		Tuff	Quaternary	2.43	2.42	2.49	7.6	1.50	1.00
72.	467		Basalt	Palaeogene	2.61	2.55	2.66	10.5	4.00	2.20
73.	468		Phyllite	Palaeogene	2.78	2.76	2.79	2.2	5.70	2.50
74.	470		Dolerite	Miocene	2.71	2.67	2.73	5.9	3.60	1.80
75.	471		Serpentine Schist	Pre-Tert.	2.41	2.28	2.49	14.3		
76.	473A		Andesite	Quaternary	2.79	2.78	2.82	4.1		
77.	473B		Andesite	Quaternary	2.74	2.70	2.79	8.2		
78.	475		Diorite	Pleistocene	2.70	2.61	2.72	11.3		
79.	482	JMT	Mudstone	Late Miocene	1.31	1.31	1.84	53.3	1.96	1.16
80.	422		Limestone	Eocene	2.70	2.69	2.71	2.0		
81.	JC– 1		Sandstone	Pliocene					2.97	
82.	2		Andesite	Lava (Quaternary)	2.83	2.82	2.86	3.6	4.20	
83.	3		Volc. Tuff	Quaternary	2.44	2.43	2.51	8.4	4.25	1.74
84.	4		Fine Tuff	Quaternary	2.02	1.80	2.41	61.1	2.33	
85.	5		Limestone	Miocene	2.44	2.43	2.48	5.1	4.92	2.16
86.	6		Limestone	Pliocene (Early–Mio)	2.44	2.43	2.50	7.3	4.40	2.13
87.	7		Andesite Basalt	Oligocene	2.33	1.38	3.02	82.6	1.55	
88.	8		Andesite	Miocene	2.75	2.72	2.76	4.5	4.59	2.18
89.	9		Limestone	Miocene	2.50	2.49	2.56	6.2	4.59	2.18
90.	10		Volcanic Breccia	Mio–Plio	2.51	2.39	2.70	32.1	2.34	1.03
91.	12		Tuff	Late Miocene	2.39	2.28	2.47	18.2	3.66	2.37
92.	16		Limestone	Miocene (Early–Mio)	2.55	2.53	2.59	5.9	4.49	2.84
93.	18		Limestone	Late Oligo–Early–Mio	2.69	2.66	2.72	5.7	5.39	1.99
94.	19		Mudstone	Oligocene	2.68	2.67	2.71	4.2		
95.	19B	JCB	Sandstone	Late Miocene	2.57	2.56	2.60	39.3	1.63	0.88
96.	22		Marl	Pliocene					2.06	
97.	24		Mudstone	Pliocene	1.62	1.55	1.93	38.1	1.50	0.86
98.	25		Sandstone	Miocene					5.21	
99.	26		Limestone	Early Miocene	2.56	2.56	2.59	3.3	4.88	2.64
100.	30		Andesite Basalt	Miocene	2.87	2.86	2.89	6.3	5.51	3.12
101.	32		Diorite	Miocene	2.94	2.93	2.94	1.6	5.61	2.13
102.	36		Marlstone	Pliocene					1.58	
103.	40		Limestone	Late Eocene	2.58	2.58	2.63	5.2	4.62	

Chapter 5

The Evaluation of Gravity Data, Reduction and Correction

5-1. Introduction.

The gravity reading which is obtained during the survey without some form of processing is rarely suitable for interpretation. This conversion process in the observed gravity value is described as the gravity data reduction.

The first step is to convert the gravity instrument observation which consists of numbers read in an instrument into mgal unit by using some calibration factor. Then several corrections should be made in order to achieve the Bouguer anomaly value. The four following corrections are usually used in this process :

1. Latitude correction.

2. Elevation correction.

3. Bouguer correction.

4. Topographical correction, often known as Terrain correction.

Since this research had available the Bouguer gravity plotted on a contour map as the starting point, this chapter.deals only with the evaluation of the gravity data, reduction and correction which have been obtained previously by the Geological Research and Development Centre.
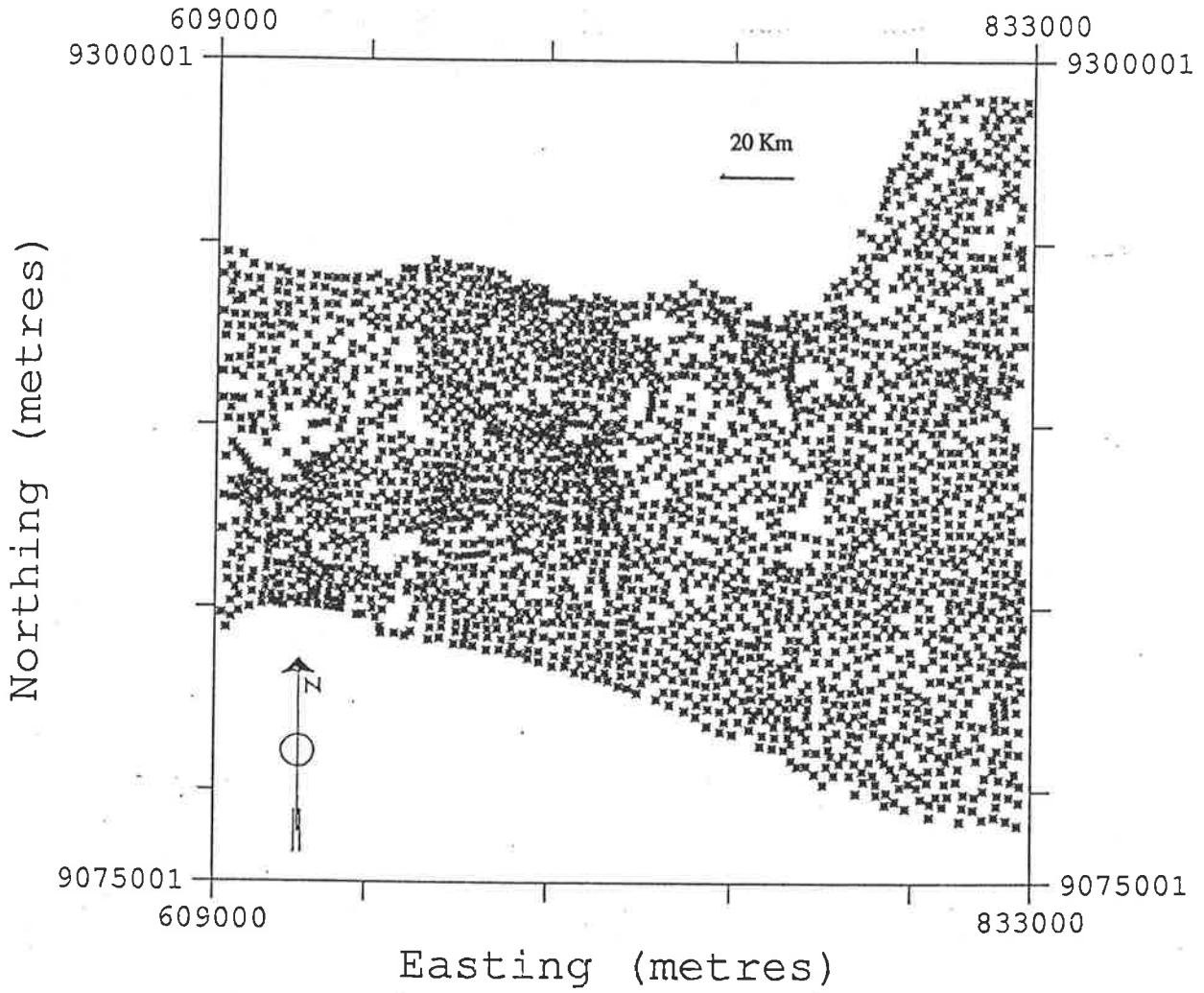
Figure 5-1. The gravity station positions over central Jawa.

5-2. The Central Jawa Gravity Data.

Based on the original 1 : 100000 scale Bouguer anomaly contour map which is available for this research, the total number of gravity stations which cover the whole study area is almost 2900. The station density of this gravity data is about 1 station per 10 sq km (fig. 5-1). All of the gravity surveys which cover the study area use the base station DG.0 which is located in the main hall of the GRDC headquarter as the reference station. This base station has a Postdam value of 977991.05 mgals which is determined gravimetrically by tying it to the London pendulum station.

For several reasons which have been mentioned in chapter 1, the raw gravity data from those 2900 stations can not be used for this research. Therefore the gravity station positions and their Bouguer anomaly value are assumed as the "gravity data" itself which will be used in chapter 6.

The reduction and correction of those numerous gravity data have been taken by the GRDC and will be evaluated in the following section :

5-3. Gravity Data Reduction and Corrections.

Although this research was not involved in the gravity data reduction and correction process, it might be wise to trace and evaluate how the gravity data reduction and correction were done and what kind of formula were used for those purposes.

Firstly, on the basis of several Bouguer anomaly maps which were published, all the gravity readings were reduced to Bouguer anomaly values by using the density of 2.67 gr / cm3. The gravity reduction processes were carried out on the basis of the 1930 International Gravity Formula whose normal gravity value is described as follows :

$$gN = 978.049(1+0.0052884 \sin^2 Q - 0.0000059 \sin^2 2Q)$$

where :

   gN = normal gravity at latitude Q

Secondly, the reduction of the Bouguer anomaly was made on the basis of the following formula :

$$BA = gO - gN + (0.3086 - 0.0419 \, \rho) \, h + Tc$$

where :

   gO = observed gravity corrected for earth -

   tide effect.

   gN = theoretical gravity value using the 1930

   International Gravity Formula.

   ρ = Bouguer reduction density of 2.67 gr / cm^3.

   h = gravity station elevation in metres

   Tc = Terrain correction.

There are two main problems which should be considered and analysed before gravity data reduction and correction can be undertaken :

1. Bouguer correction problem.

As is already known, a suitable Bouguer reduction density should be chosen carefully and proportionally for the purpose of gravity data reduction.

2. Terrain correction problem.

This problem should be handled carefully, especially in a volcanic area such as Jawa, in which the elevation of the volcano sometimes may reach as high as 2000 - 3000 metres, even more.

5-3.1. Bouguer Correction.

. Basically, there are three widely used methods of determining Bouguer reduction density in order to apply the Bouguer correction :

1. The first method is to use the standard density value, that is a value of 2.67 gr / cm^3.

2. The second method is by determining a Bouguer reduction density which minimizes the correlation between a complete Bouguer gravity anomaly and topography data.

3. The third method is by directly measuring the density of representative rock samples.

In spite of the fact that the second method is more widely used than the first and the third methods, it must be considered carefully before it is used, because it also has several weaknesses. This is explained by Williams and Finn (1985) in the following ways :

First, it will fail if there is correlation between topography and geologic structures beneath the topography. An example would be a dense intrusion directly beneath a less dense volcanic cone. This failure can easily go undetected but becomes evident if the wavelength of the anomalies relating to topography is significantly different from those produced by the underlying bodies, or if the method produces a clearly unrealistic Bouguer reduction density. A second reason is more pragmatic than theoretical. If a rugged topographic feature has an average density substantially different than the selected Bouguer reduction density, the gravity anomaly associated with it will be of high amplitude and will be highly variable on the Bouguer anomaly map. It can easily obscure a much smaller but significant anomaly produced by underlying mass.

As a consequence of the above problems, it is prudent to make maps at a variety of Bouguer reduction densities. This allows the careful study of various gravity profiles with a variety of Bouguer reduction densities.

There is no raw data available, however, for this purpose, which can be used to produce a variety of gravity profiles. All of the Bouguer anomaly maps which are available for this research are based on a conventional density value of 2.67 gr / cm^3. Therefore the only method which can be used for this research is the first method which uses the above conventional density value.

In spite of the fact that this research can only use the first method, the following rough calculation may have to be taken into consideration during the interpretation stage.

On the basis of the straight line method which has been seen in chapter 4, Bouguer anomaly values of the northern part of Purwokerto are plotted against their elevation values which are taken roughly from interpolation of elevation contour value in the geological map. It can be assumed from this statistical calculation that the most appropriate Bouguer density reduction for this area is the value of 2.25 gr/cm^3. It is clear that the difference of about 0.42 gr/cm^3 between those values may affect the result of the interpretation.

5-3.2. Terrain Correction.

Terrain correction constitutes the main problem when the gravity data are collected on a rough topographic area such as in volcanic terrain in central Jawa. The correction density used in terrain correction is usually the Bouguer reduction density. As is already known an inappropriate density may create false anomalies or obscure important anomalies.

Terrain corrections which were done for this Bouguer anomaly map, according to several Bouguer anomaly maps which were published, are divided into two zones :

a. Inner zone (0 - 60) metres, computed directly by making a 2 dimensional model.

b. Outer zone (60 - 10000) metres, using Hammer chart, that is zone E to zone K.

It can be seen clearly from the above evaluation that all of the normal procedure in reduction and correction of gravity data have been undertaken. Thus the available "gravity data" can be used for further processes.

In addition, with all of these limitations it is not possible to estimate the degree of the error of reduction and correction processes.

Chapter 6

Computer Processing and Filtering Operations

6-1. Introduction.

The wide use of the computer in the last decade has revolutionised the analysis of gravity data. Nowadays the enhancement and display of gravity data as well as the filtering process are greatly dependent on the technology of the computer.

The five following computer facilities are available in the Geology & Geophysics Department in the University of Adelaide and can be used for this research :

1. Digitizer including the appropriate program.

2. Contouring program.

3. Imaging program.

4. Enhancement program for gravity and magnetic data.

5. Filtering program for gravity and magnetic data.

Almost all of those computer programs need a data file, at least a grid data file, as the basic data for further processing.

Since a raw data file has not been available during the period of research, the first priority stage which should be undertaken is to produce a *'new raw data'* file. As has already been seen, once this data file is available, further processes such as greyimage and filtering operations can be made as the occasion arises.

The computer processing in this chapter deals with digitizing gravity and magnetic data, imaging and shaded relief, whereas the filtering operations consist of trend surface residual, upward continuation and spectral analysis.

Since this research has used the computer only as a tool to analyse the limited available gravity data, during the research time the author has neither created nor developed a computer method for the purpose of this research.

6-2. Digitizing Gravity Data.

Due to the fact that during research the raw data were not available, the author decided to digitize central Jawa Bouguer anomaly maps by tracing their contour lines with intervals of 5 mgals. This was undertaken on the basis of the 1 : 100000 scale Bouguer anomaly contour map. The original map which is used as a starting point for this research consists of four map sheets (fig. 6-1).

The grid file which was produced by this method can be used for further processes. Two main problems can be detected from the contour map which was produced on the basis of this grid file.

Firstly, several strange shapes of the contour pattern can be seen on the map. Secondly, the line pattern can be traced along the boundary between every two maps (fig. 6-2). The result of the contour map is really disturbed by the above problems.

As a consequence of this problem, the grid data file was reproduced by entering the Bouguer anomaly values of the digitized gravity station positions. In a number of gravity stations in which the Bouguer anomaly values are not available, the values are taken by interpolating from the nearest contour line values. The error for this interpolation process is estimated as not more than 0.5 mgals. As a result, the Bouguer contour map which was produced on the basis of this grid file has a better shape and more reasonable pattern (fig. 6-3). Moreover, the agreement with the original hand-contoured map which is used as the starting point of this research confirms the efficiency of this gridding and contouring procedure. Therefore with this 'new data', further analysis of gravity data and the computer processes can be made.
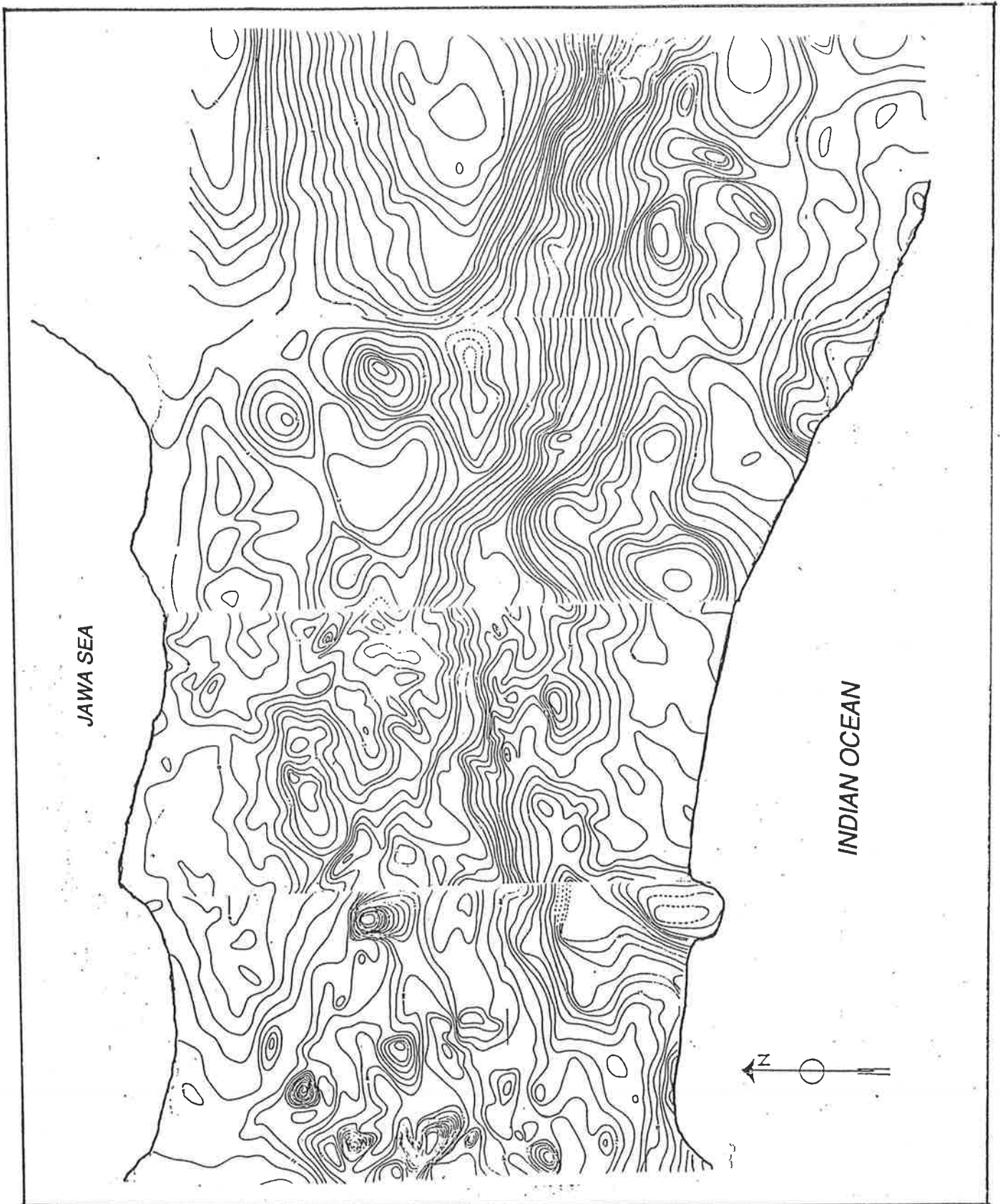
Figure 6-1. The original simplified hand contoured Bouguer anomaly map of Central Jawa which is used as a starting point of this research.

Map scale 1: 1,000,000.   Contour interval 5 milligals
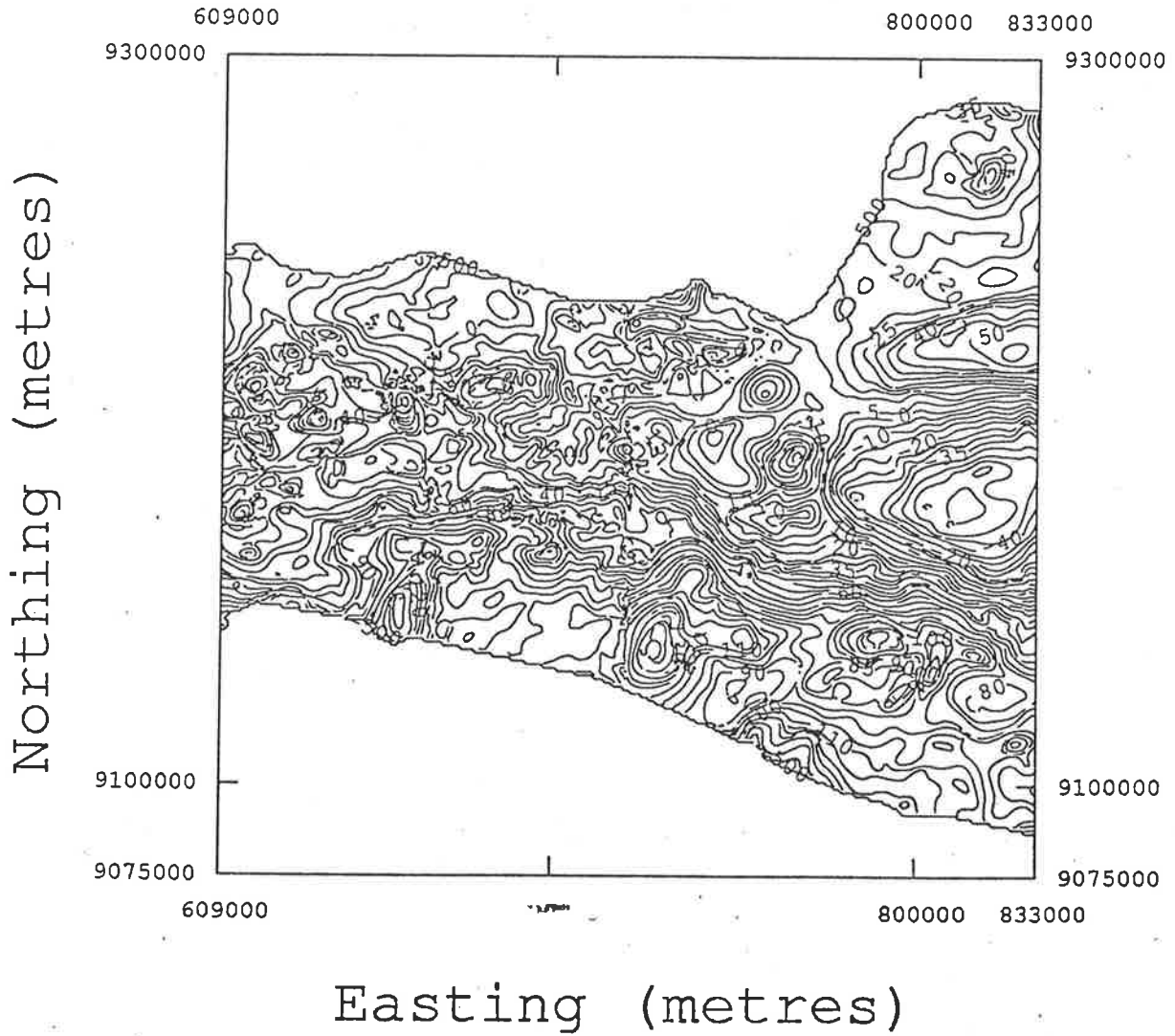
Figure 6-2. The Bouguer anomaly map constructed by digitising the hand contoured map prepared by the GRDC. The mismatch between every two maps is evident.
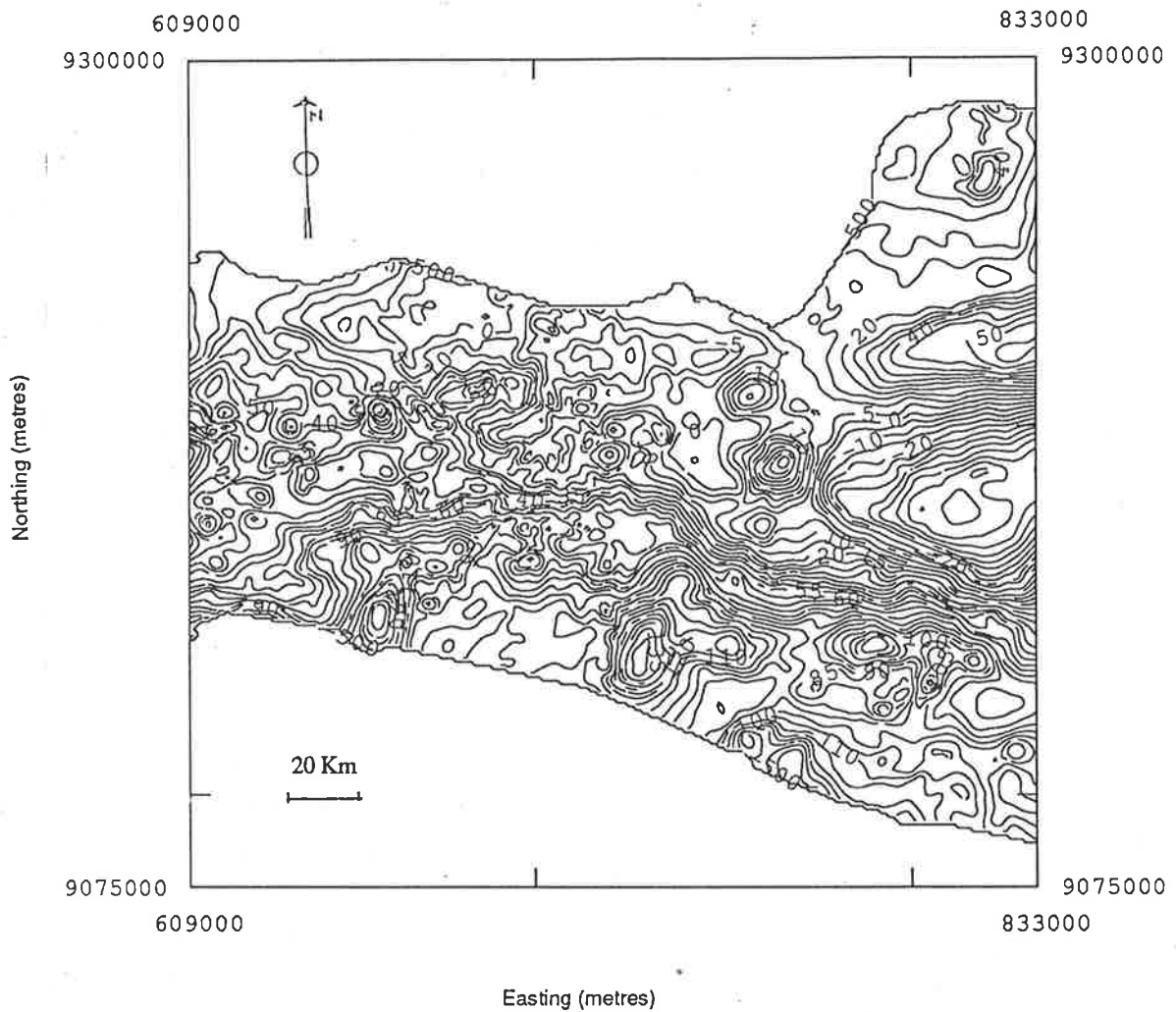
Figure 6-3. The Bouguer anomaly contour map of the study area which is produced on the basis of the 'new data file' using the individual gravity stations.

Since this gravity data file is not a normal data file, it consists of only three columns. The first and the second columns are for easting and northing, both in metres, the third column for Bouguer anomaly values. These data files can be seen in Appendix A.

6-3. Digitizing Airborne Magnetic Data.

A similar problem to the above arises in the case of airborne magnetic data. This is even worse than in the case of gravity data because the starting point for this aspect was only the simplified hand-contoured airborne magnetic map with intervals of 50 nanoteslas (Buyung in Untung, 1989, in prep.). There was no flight line position and also there was no total magnetic value available during the research. Therefore the contour lines were traced and digitised to produce a *'new data file'*.

6-4. Image.

Grey scale presentation of magnetic field intensity is one of the imaging techniques which have immeasurably improved the display and interpretation of gridded data. With this digital image processing, a wide range of data types and formats can be easily incorporated into the same image format for further analysis. Moreover, data which are collected on different scales or with different resolutions can be processed to a common map projection and scale. The most important feature is that two or more data sets can be combined or merged into only one display, so their correlation can be easily identified (Guinnes et al., 1983).

If this greyimage map is compared with the contour maps, the following advantages can be noted :
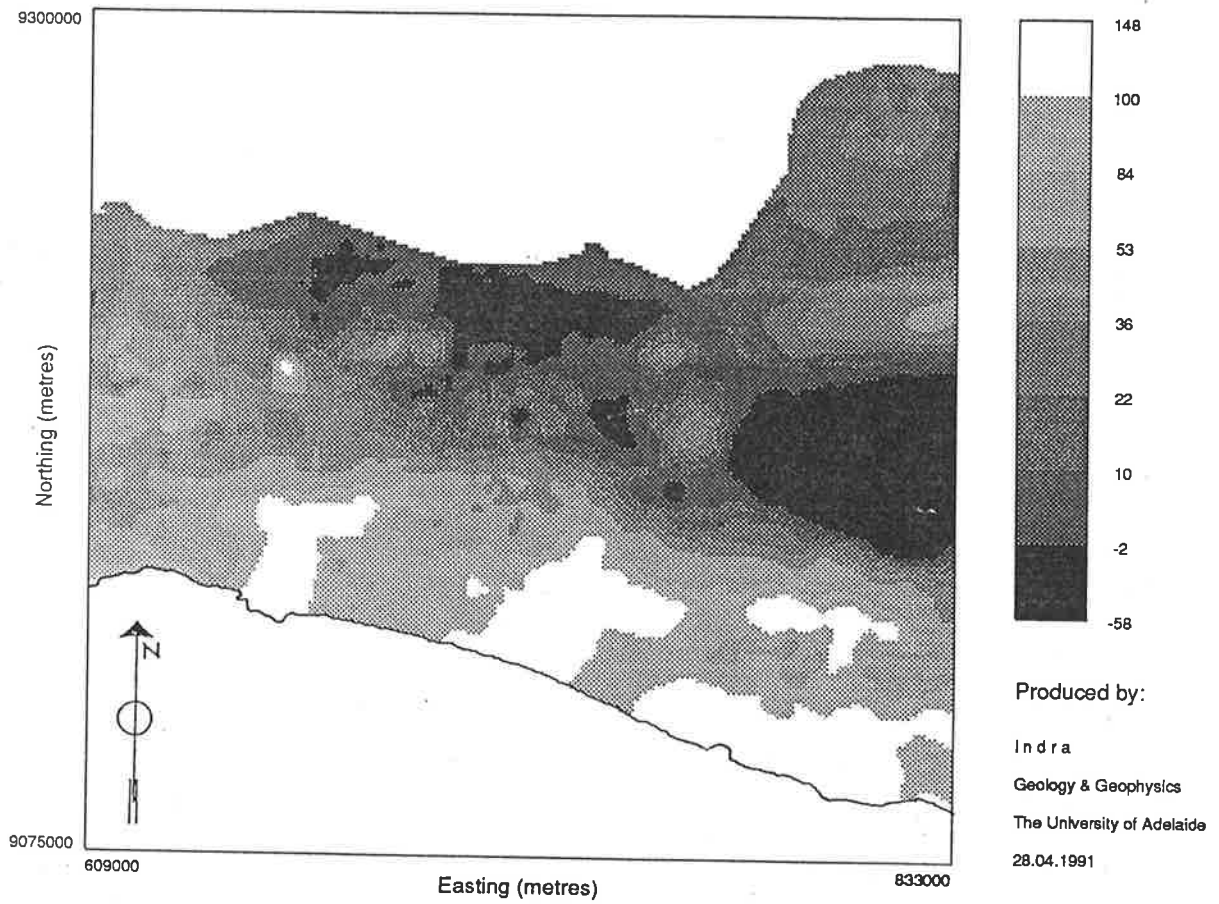
Figure 6-4. Bouguer anomaly grey-scale digital image over central Jawa.
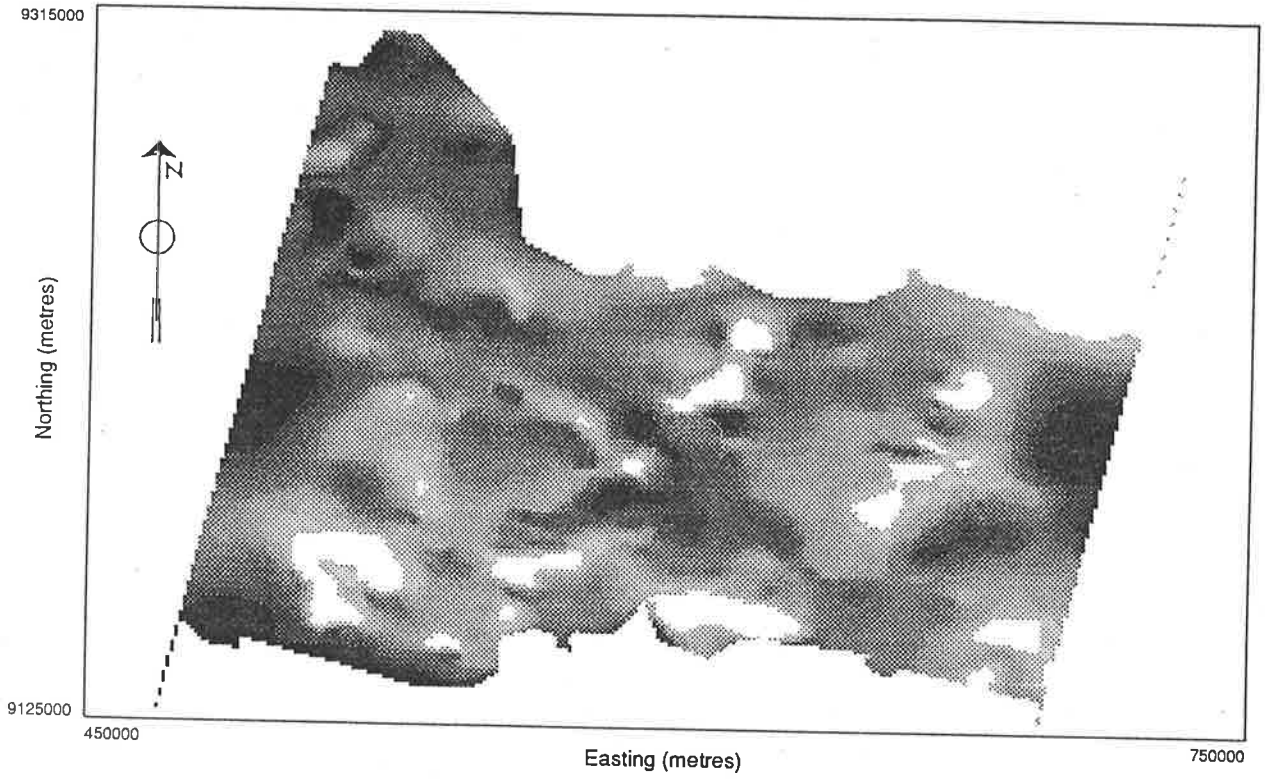
Figure 6-5. Total magnetic anomaly grey-scale digital image over Jawa transect area.

Firstly, it is suitable for almost all kind of geophysical data, such as gravity data, magnetic data, radiometric data, landsat data and so on.

Secondly, this type of map is very useful for delineating geological structures even using small scale maps.

Thirdly, from the point of view of the computer processing unit time, producing this map is relatively much faster than for a contour map of the same area. The only problem with this kind of map is that it cannot be displayed by using large scale maps, because the finite pixel size gives the map a blocky or digital appearance. Pixel size is usually controlled by the station separation and the uniformity of the stations.

With this imaging technique, the Bouguer anomaly contour map, for example, will appear more dimensionally. This is because of the effect of the tone on the grey scale. Moreover, details which are missing from the contour map can often be seen on the image of the same data.

A laser printer which has a postscript interpreter makes it possible to achieve a good quality hard copy output file from greyimage processes.

The presentation of the gravity data as digital images has been applied extensively in this research using a system developed in the Department of Geology and Geophysics in the University of Adelaide by S. Rajagopalan.

The result of this process for Bouguer anomaly and total magnetic anomaly maps can be seen in figure 6-4 and figure 6-5 respectively.

6-5. Artificial Illumination (Shaded Relief).

One of the basic activities that constitute digital image processing is image enhancement which includes increasing or decreasing the contrast, edge sharpening or smoothing, or more simply, altering the image in some respect that facilitates the interpretation of its information content (Hord, 1982).
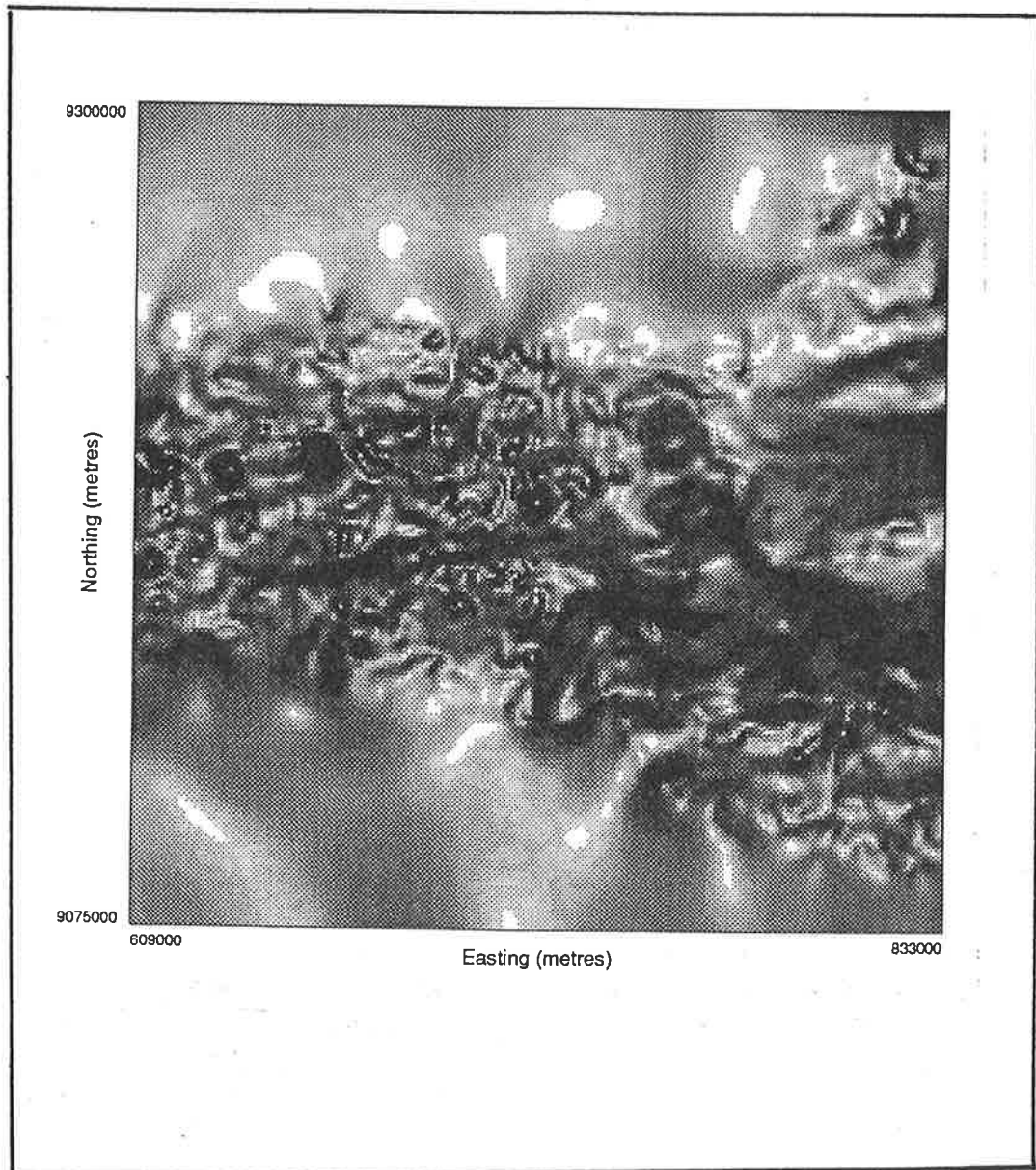
Figure 6-6. Shaded relief grey-scale digital image over central Jawa with elevation angle 90o and azimuth 0o.
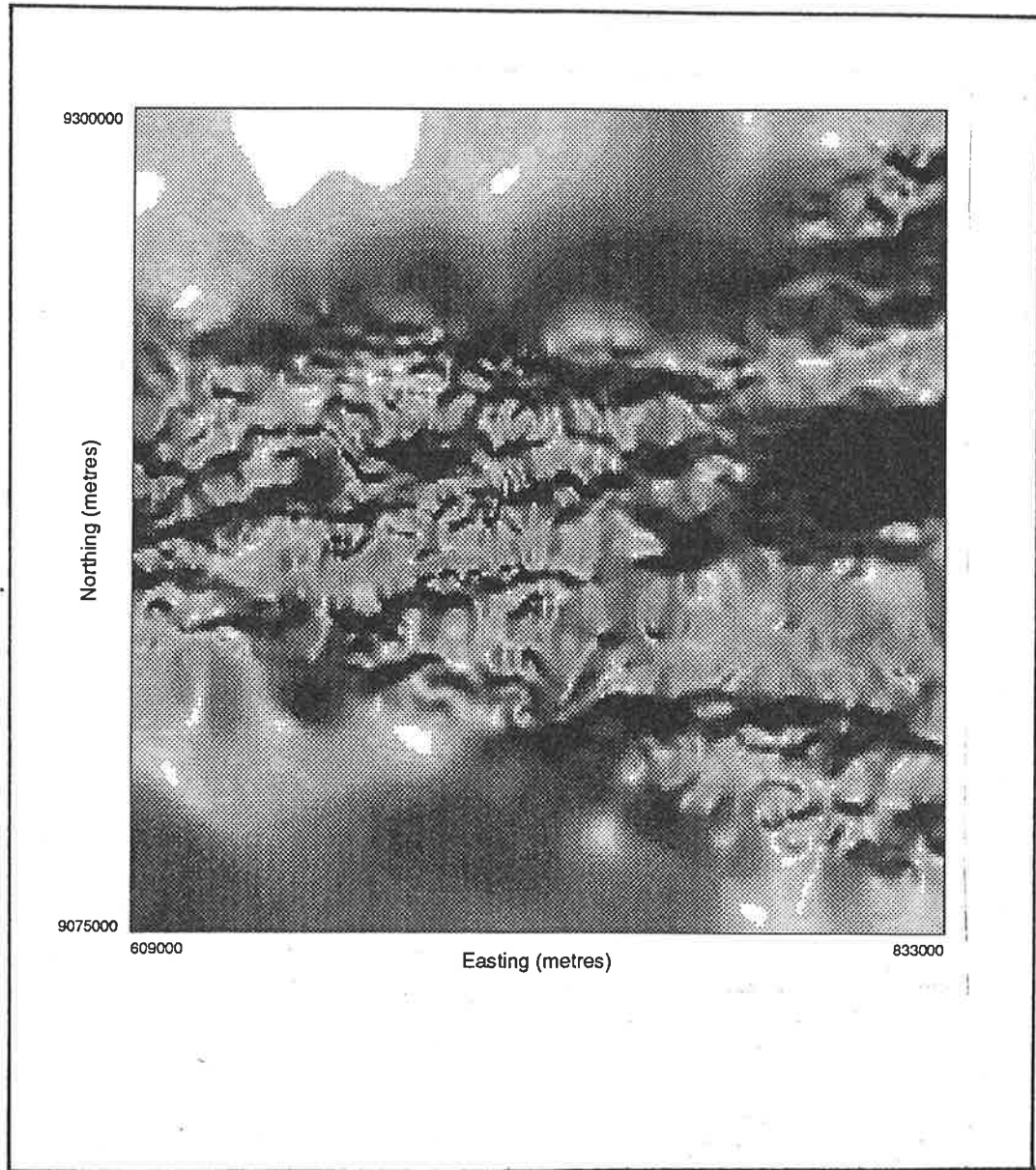
Figure 6-7. Shaded relief grey-scale digital image over central Jawa with elevation angle 45º and azimuth 0º.
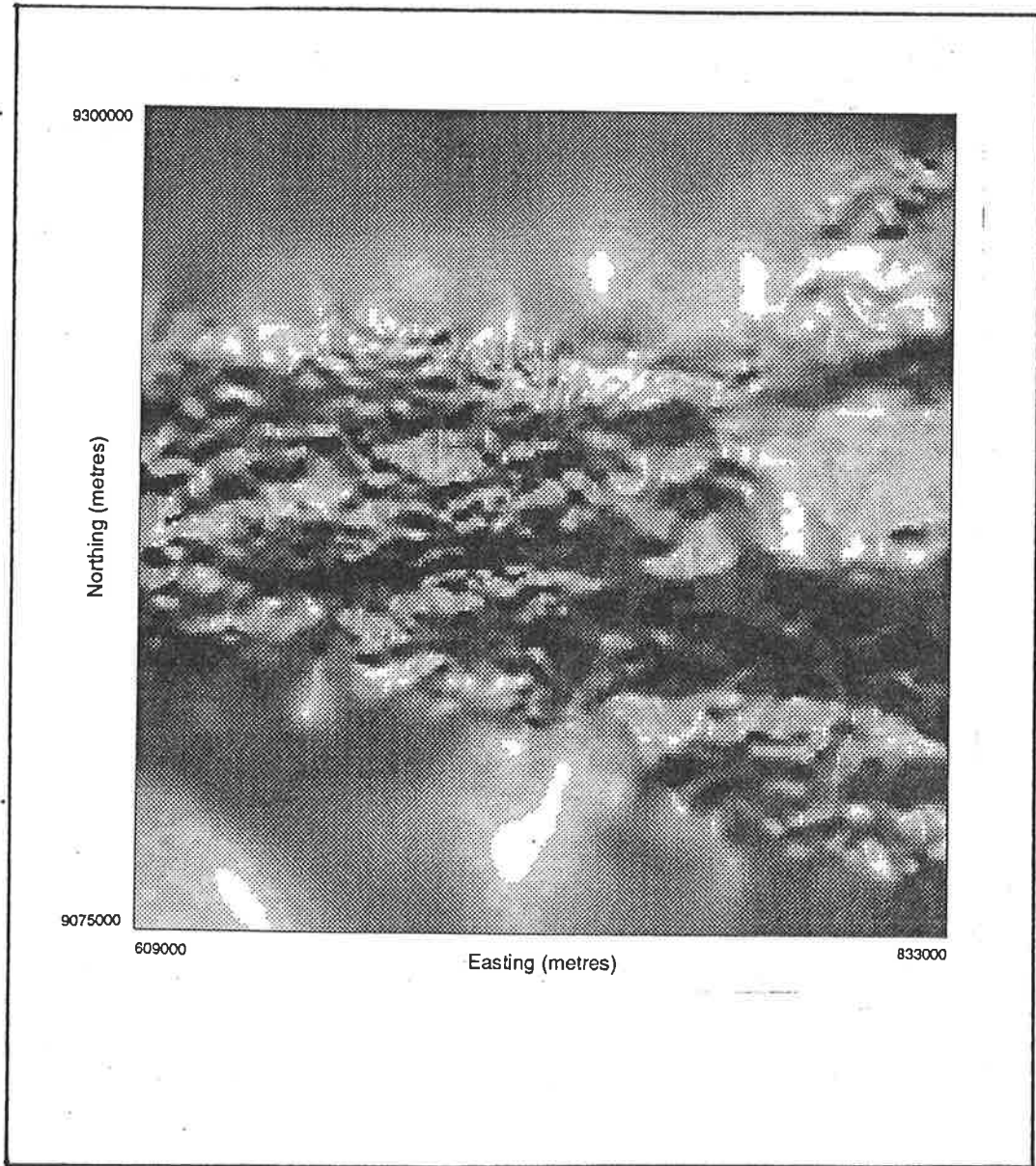
Figure 6-8. Shaded relief grey-scale digital image over central Jawa with elevation angle 45o and azimuth 180o.
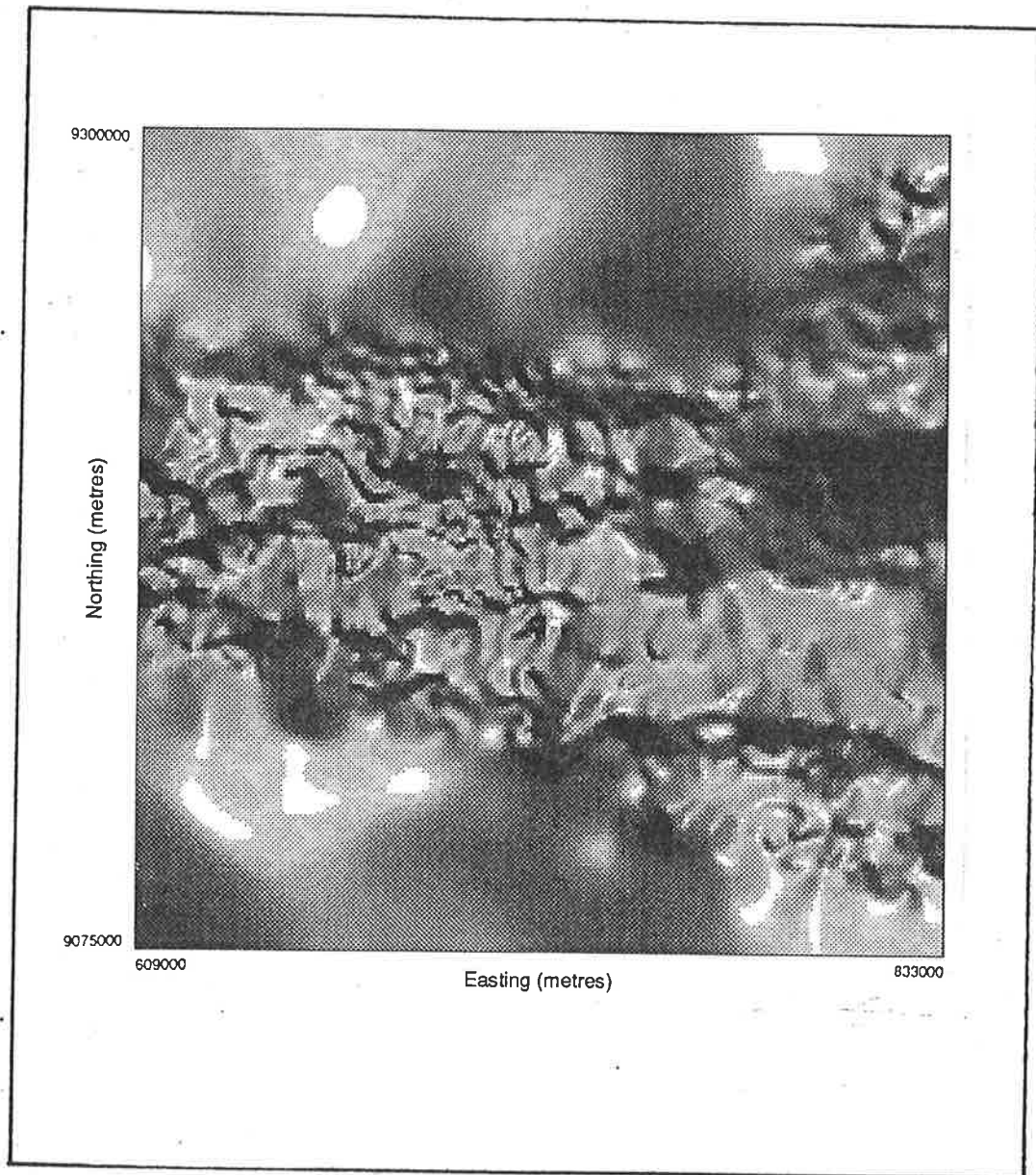
Figure 6-9. Shaded relief grey-scale digital image over central Jawa with elevation angle 45º and azimuth 30º.

The image enhancement technique which is used for this research is the artificial illumination technique. Articial illumination, also known as Shaded Relief, is actually a simple and effective enhancement technique that creates the appearance of a topographic surface illuminated from a given direction. For each element of the illuminated image, the brightness is proportional to the cosine of the angle between the normal surface and the direction of the illumination source (W. S. Kowalik and W. E. Glenn, 1987).

Essentially, by using this technique, the Bouguer anomaly contour map may be regarded as a topographical contour map illuminated from different directions. The variables which are used in a shaded relief process are the azimuth and elevation of the illuminating source. The azimuth value of 0° is assumed to be the source from the north. The azimuth value increases with a clockwise direction. Thus the azimuth value of 90° is assumed to be the source from the east.

The shaded relief program which is used for this enhancement technique has been developed in the Department of Geology and Geophysics in the University of Adelaide by Z. Shi.

Several results of this shaded relief process with a variety of combinations of elevation angle and azimuth can be seen in figure 6-6 - figure 6-9.

6-6. Filtering Operations.

One of the aims of the filtering operation is to detect information which is concerned with any specified structure and also to make clear the geological structure.

It is widely known that filtering techniques can be used in both spatial and frequency domains. However, the frequency domain process needs more complicated numerical computation than the spatial domain process. Nowadays by using a Fast Fourier Transform

algorithm in computer processing the difficulties of data processing of gravity anomalies in the frequency domain can be reduced significantly.

In this research, the spatial domain processes consist of trend surface residuals and upward continuation, whereas the frequency domain deals only with spectral analysis.

6-6.1. Upward Continuation.

Essentially, this is the method in which the gravity data are projected mathematically upward to level surfaces above the original datum plane. As the surfaces are in field free space, the result of the upward continuation process will be smoother than the anomalies obtained at ground surface. Therefore, a deep and broad geological structure may be emphasized by this method.

The upward continuation program which is used for this kind of filtering operation has been developed in the Department of Geology and Geophysics in the University of Adelaide by Z. Shi.

The results of this upward continuation process for elevations of 500, 1000, 5000 and 10000 metres can be seen in figure 6-10 to figure 6-13 respectively.

6-6.2. Trend Surface Residual.

Often, in order to seek the hidden anomalies, the separation of anomalies between the regional gravity anomaly with longer wavelength and the residual one with narrower wavelength should be made. There are several ways to effect this separation, both graphically and analytically. One of the most flexible of the analytical techniques is the use of polynomial fitting.
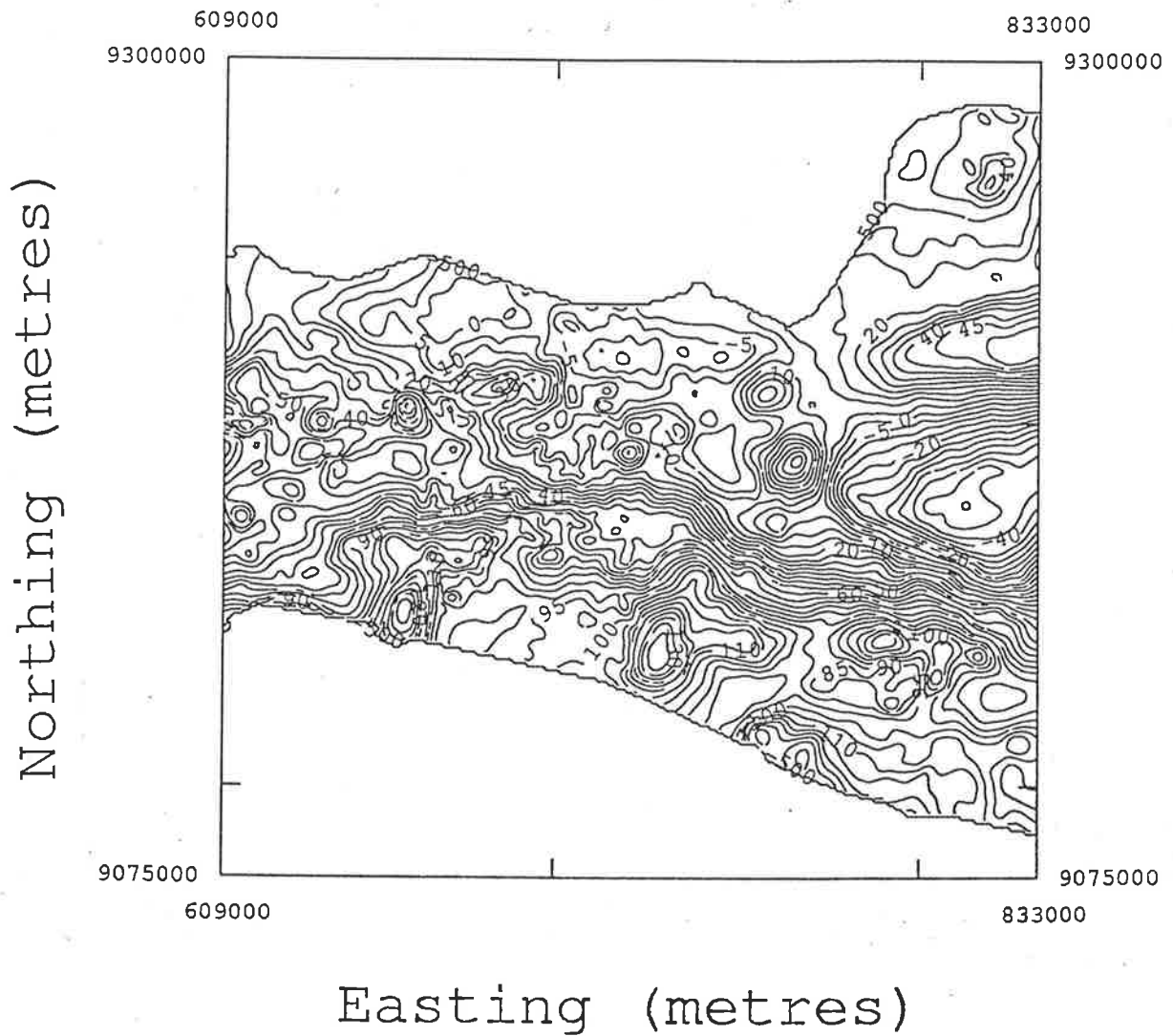
Figure 6-10. Central Jawa upward continuation with elevation of 500 metres.
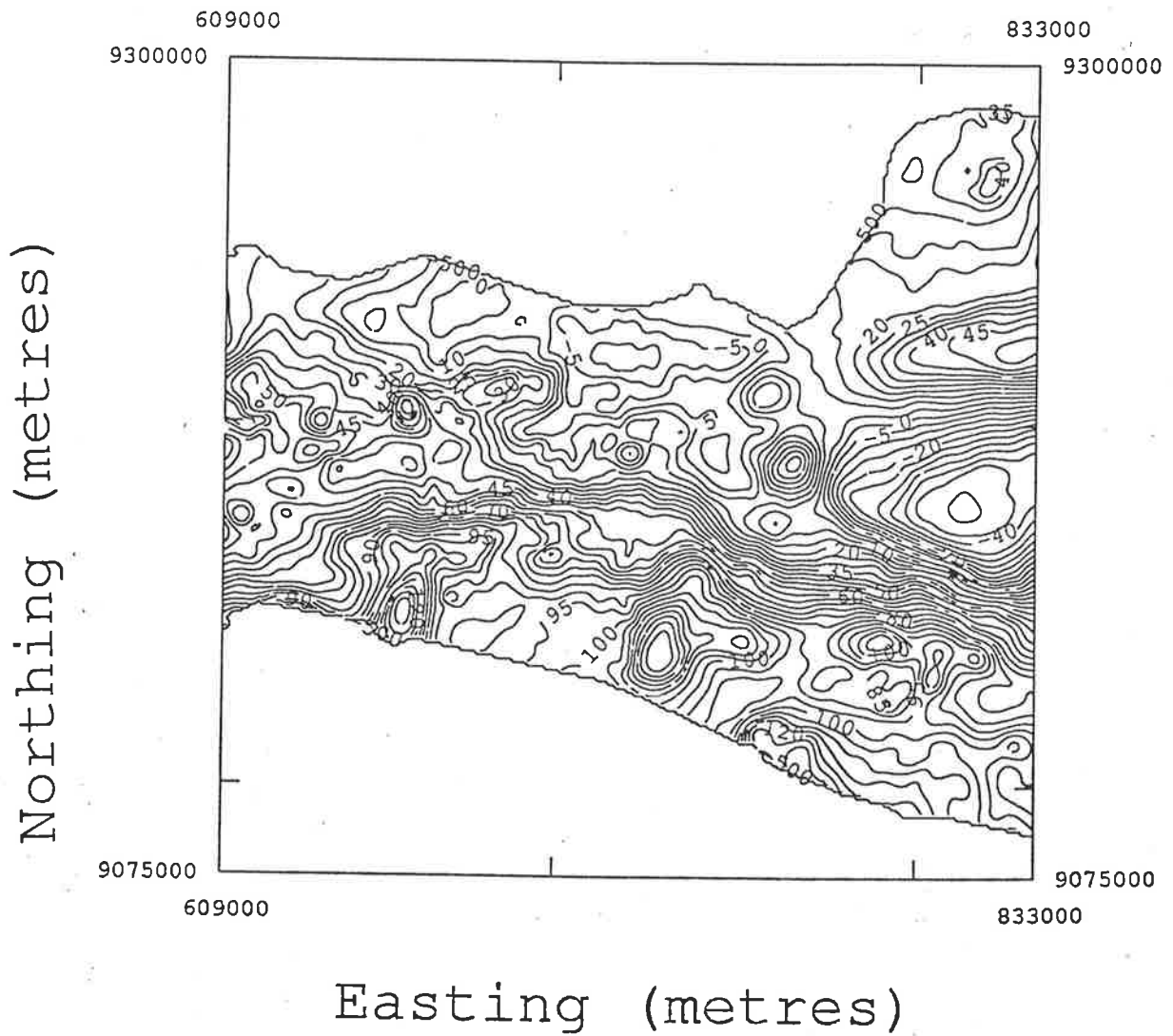
Figure 6-11. Central Jawa upward continuation with elevation of 1000 metres.
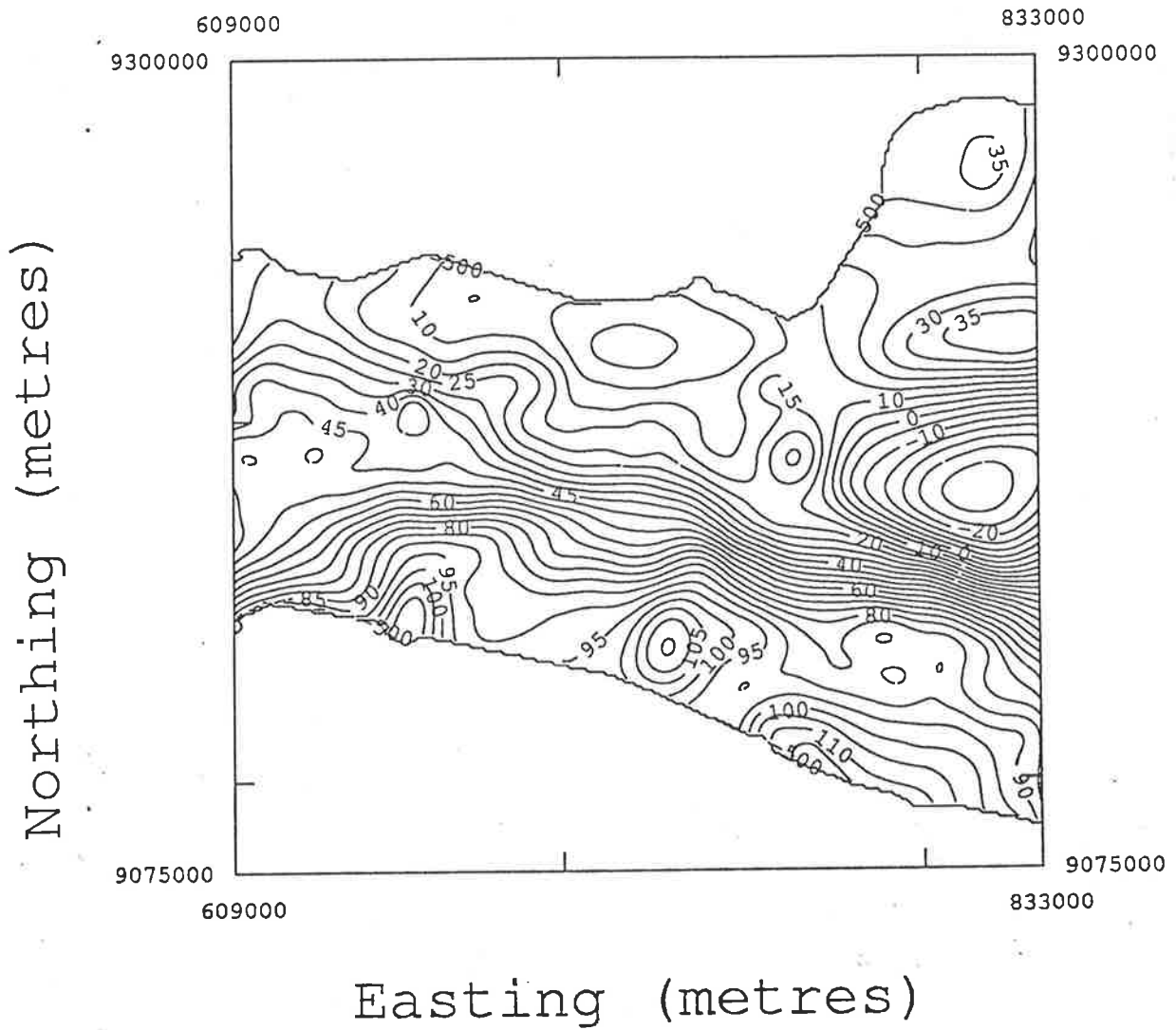
Figure 6-12. Central Jawa upward continuation with elevation of 5000 metres.
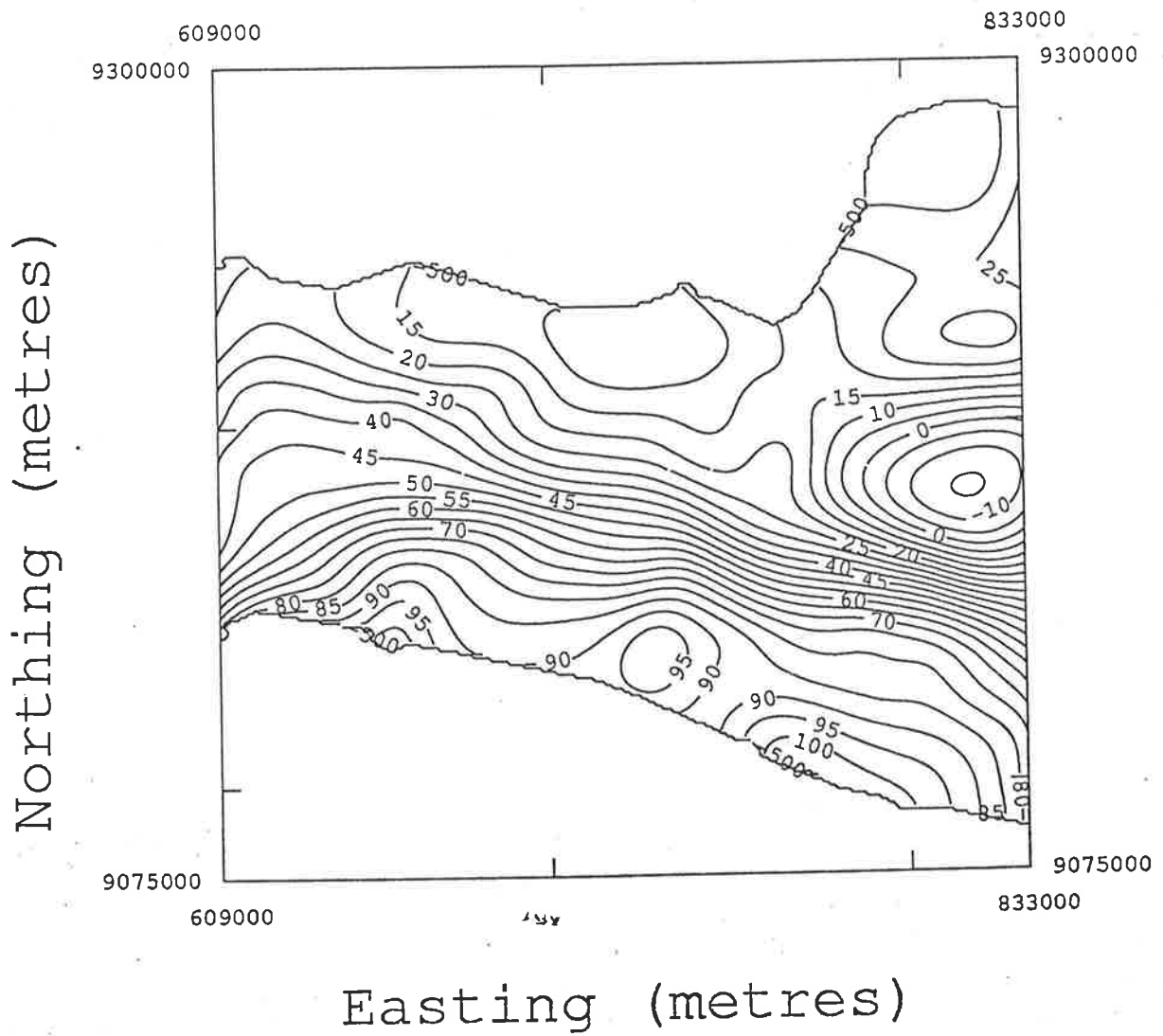
Figure 6-13. Central Jawa upward continuation with elevation of 10000 metres.
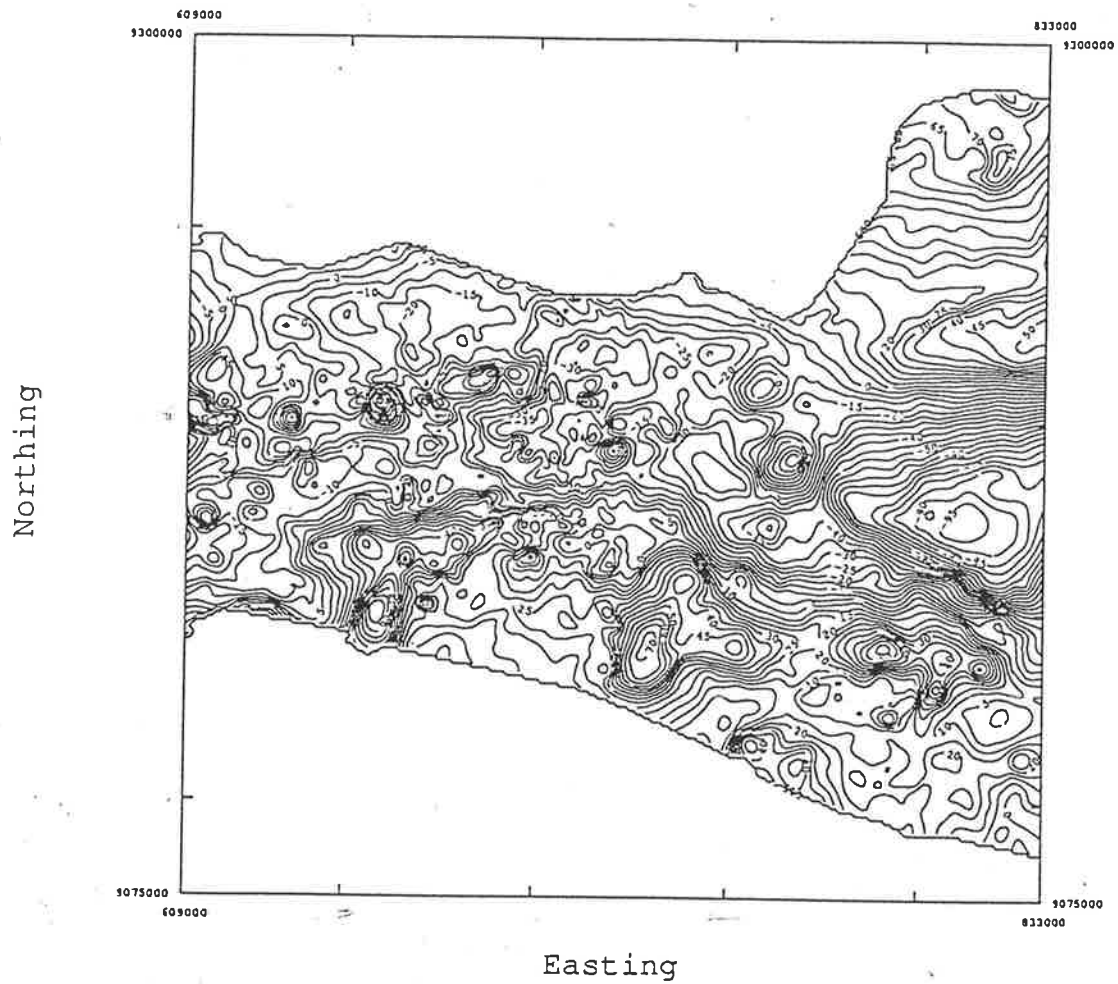
Figure 6-14. Central Jawa trend surface residual 1st orde.
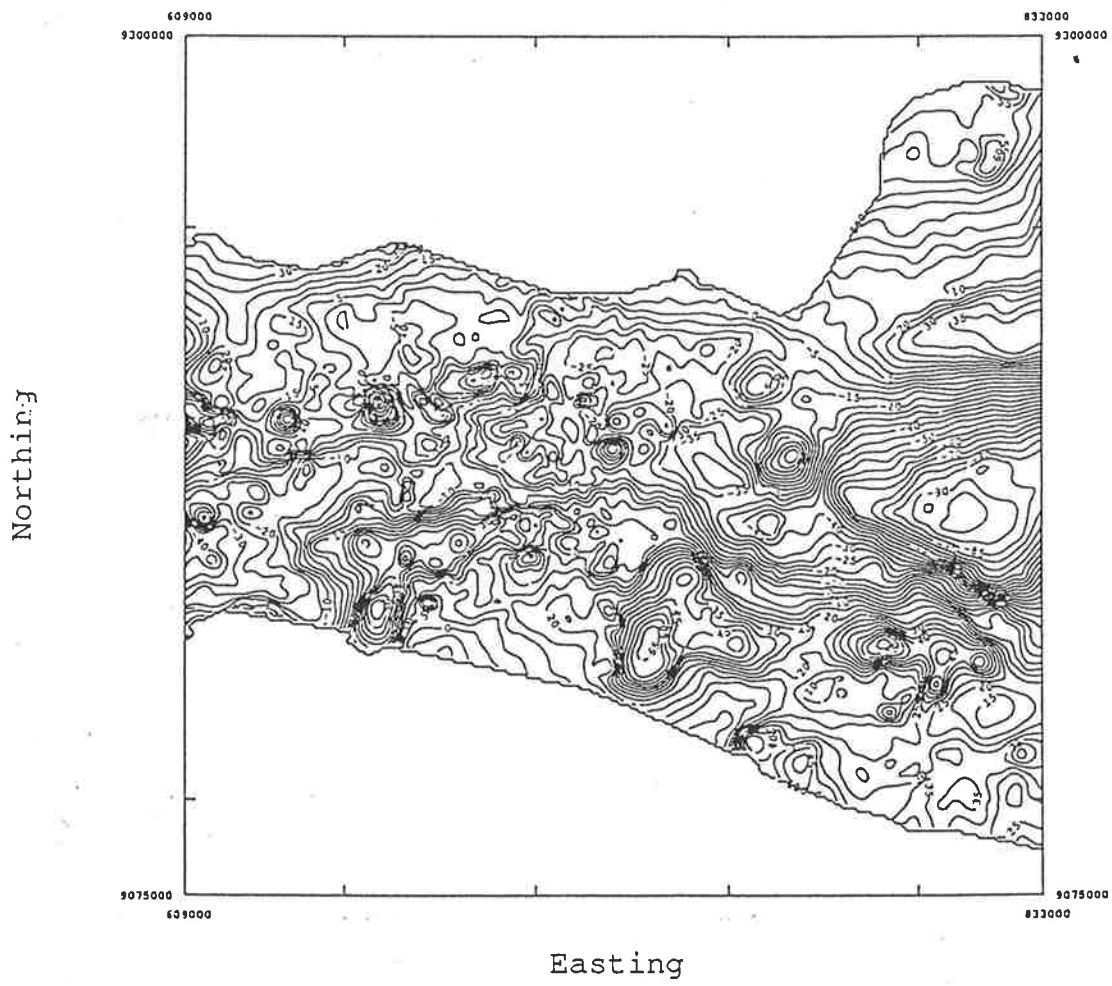
Figure 6-15. Central Jawa trend surface residual 2nd orde.
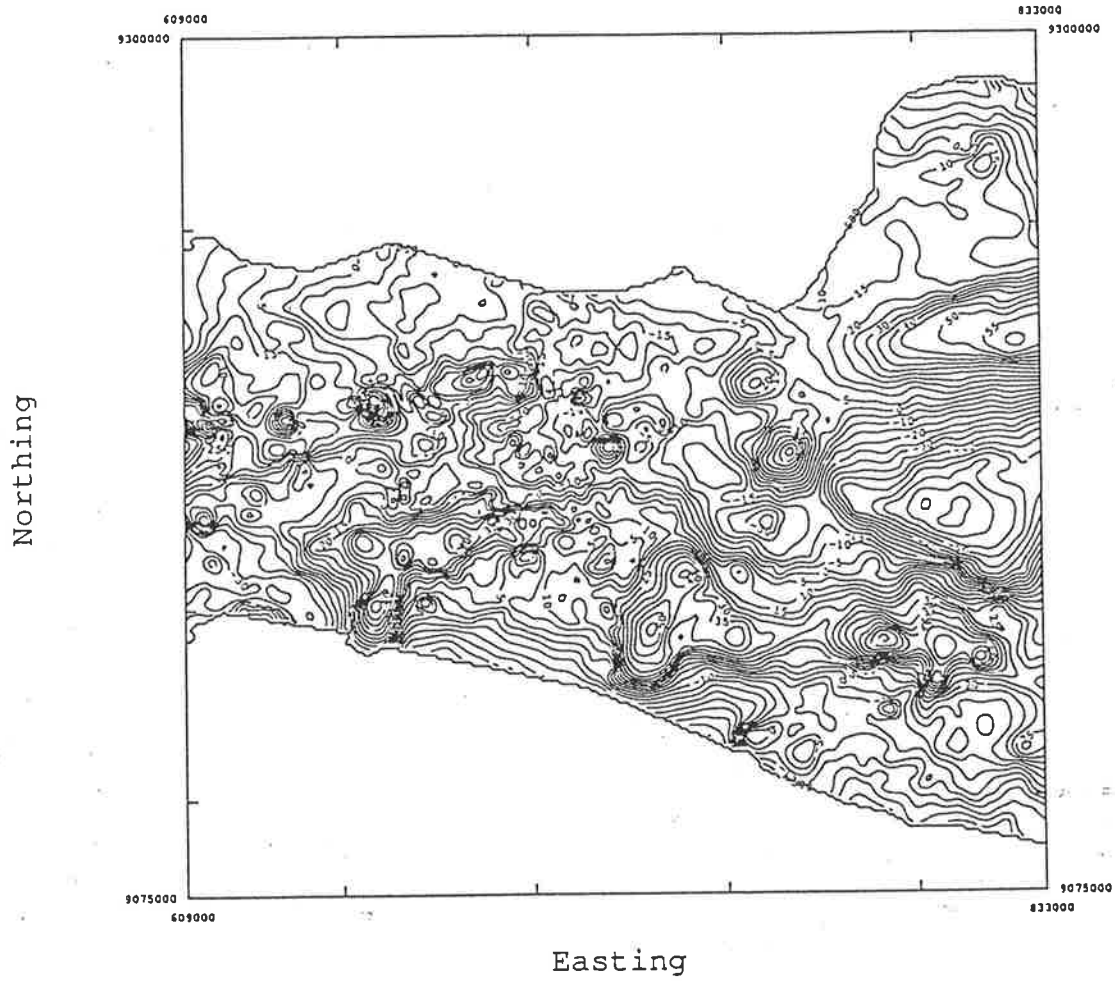
Figure 6-16. Central Jawa trend surface residual 3rd orde.
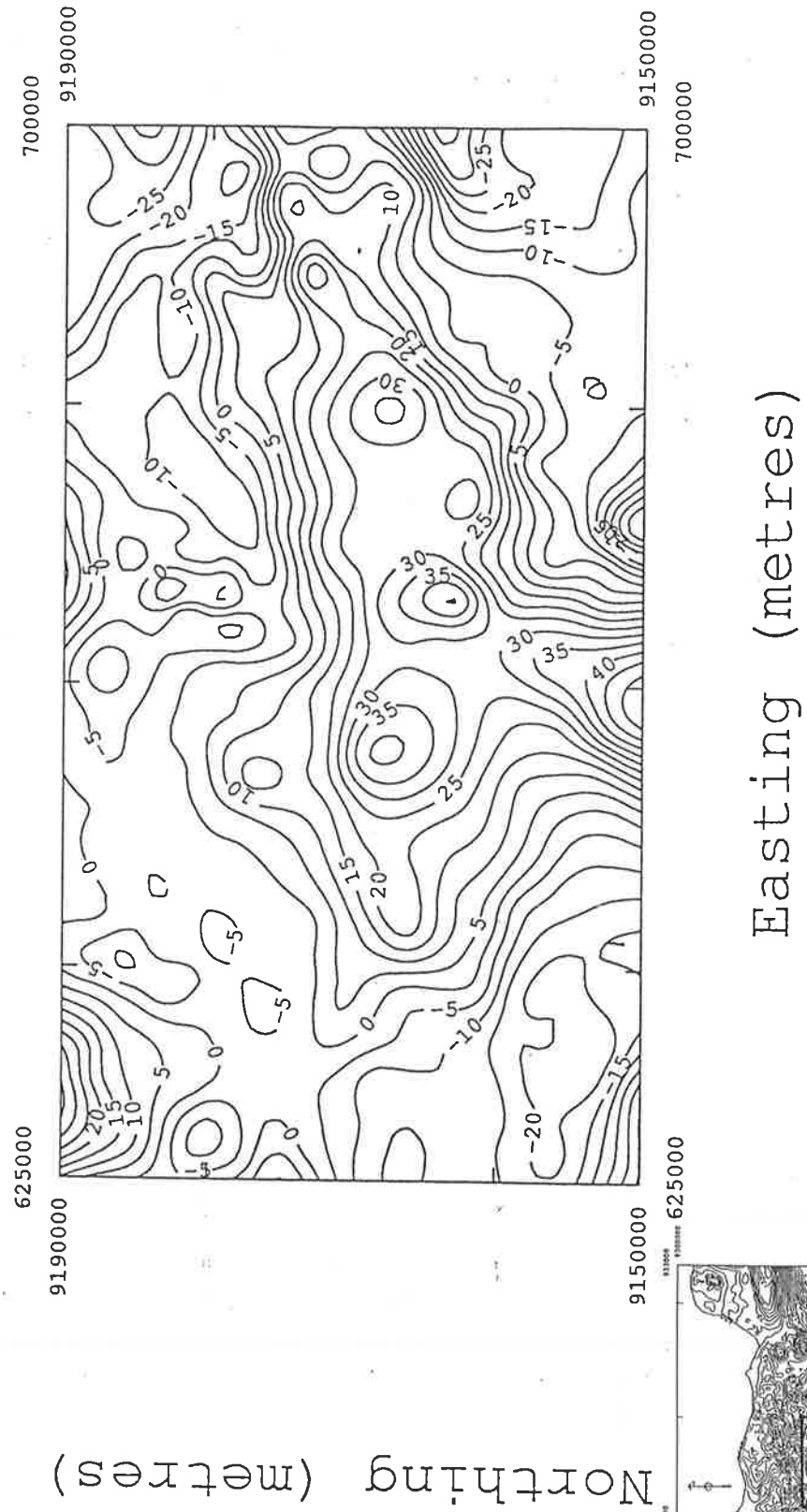
Figure 6-17. Western central Jawa trend surface residual 1st orde.
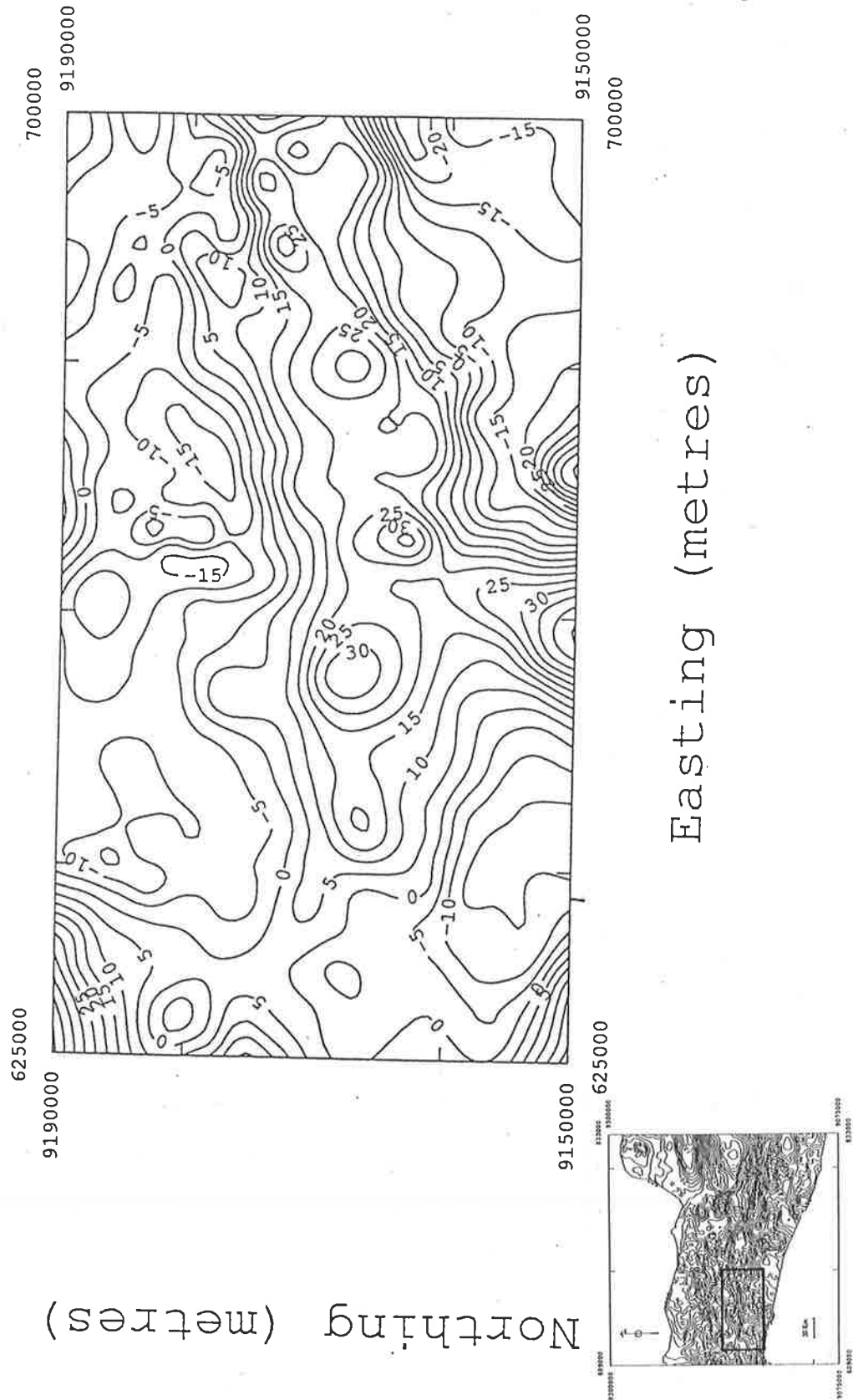
Figure 6-18. Western central Jawa trend surface residual 2nd orde

Figure 6-19. Western central Jawa trend surface residual 3rd orde.
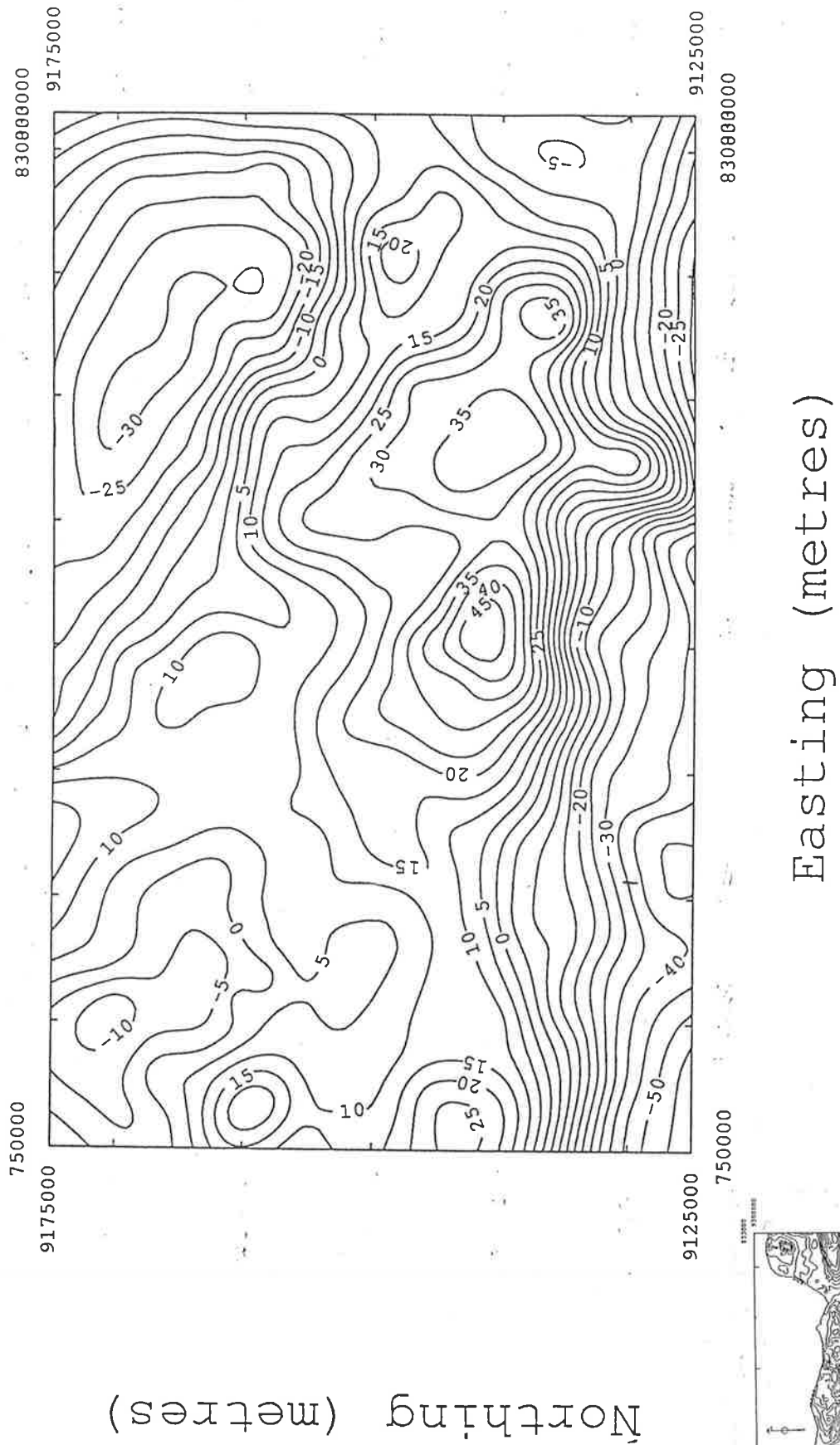
Figure 6-20. Eastern central Jawa trend surface residual 1st orde.
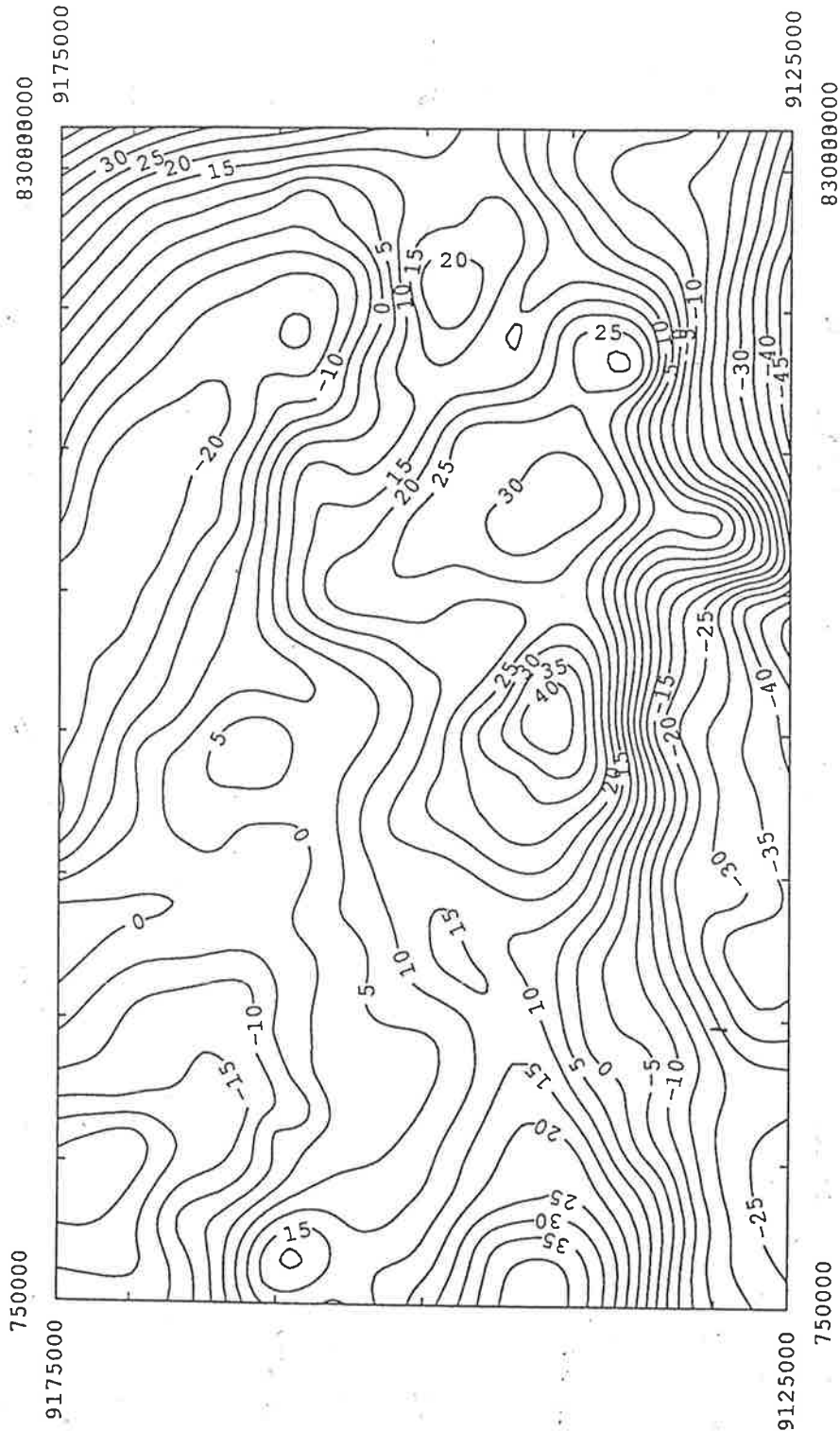
Figure 6-21. Eastern central jawa trend surface residual 2nd orde.
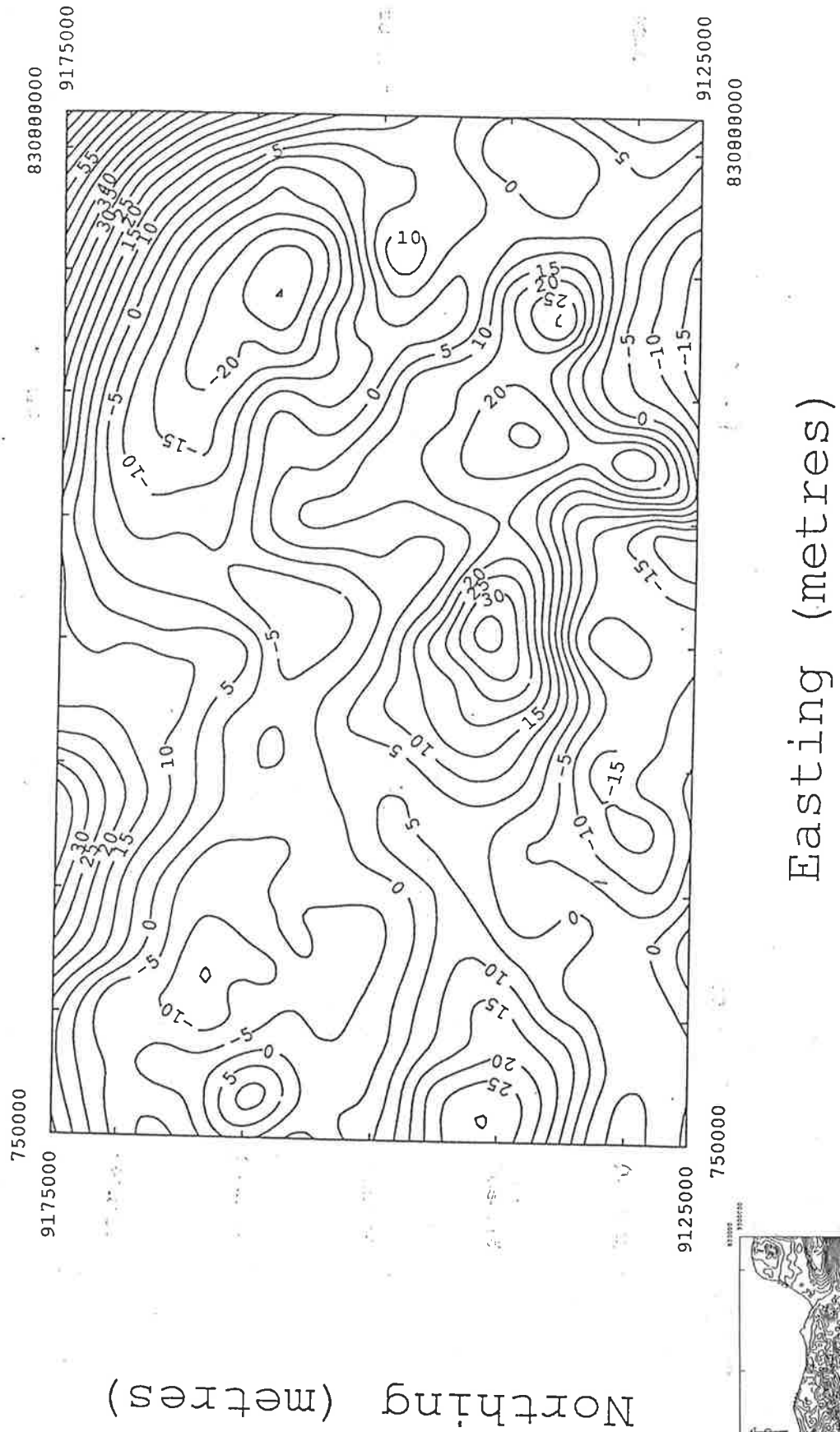
Figure 6-22. Eastern central Jawa trend surface residual 3rd orde.

Basically, trend surface residual by fitting of polynomials is a technique which assigns polynomials to the regional anomaly by using the method of least square. Then, in order to obtain the residual anomalies, this regional anomaly is subtracted from the original anomaly.

Three kinds of polynomials were fitted to the regional anomaly surface in this research :

Firstly, the polynomial represents a first degree polynomial involving three unknown factors.

Secondly, the polynomial represents a second degree polynomial involving six unknown factors.

Thirdly, the polynomial represents a third degree polynomial involving ten unknown factors.

There are two types of areas which have been chosen for this process. The first type is taken from the whole study area and the second type is the two areas whose steep gradient is very strong. The result of this process can be seen in figure 6-14 to figure 6-22, respectively.

6-6.3 Spectral Analysis.

This spectral analysis process can be determined as one part of harmonic analysis which is used for analyzing and synthesizing oscillatory phenomena in nature. Essentially, the objective of this process is to obtain the spectral distribution of oscillatory phenomena and also to reveal their statistical characteristics. In simple language, the aim of this process is to determine the mean depth of density discontinuity.

The spectral analysis program which is used for this kind of filtering operation has been developed in the Department of Geology and Geophysics in the University of Adelaide by Z. Shi.

Figure 6-23 shows the result of this process. The mean depth of the deep effect is estimated as about 11000 metres, whereas that for the shallow effect is estimated as about 2500 metres.
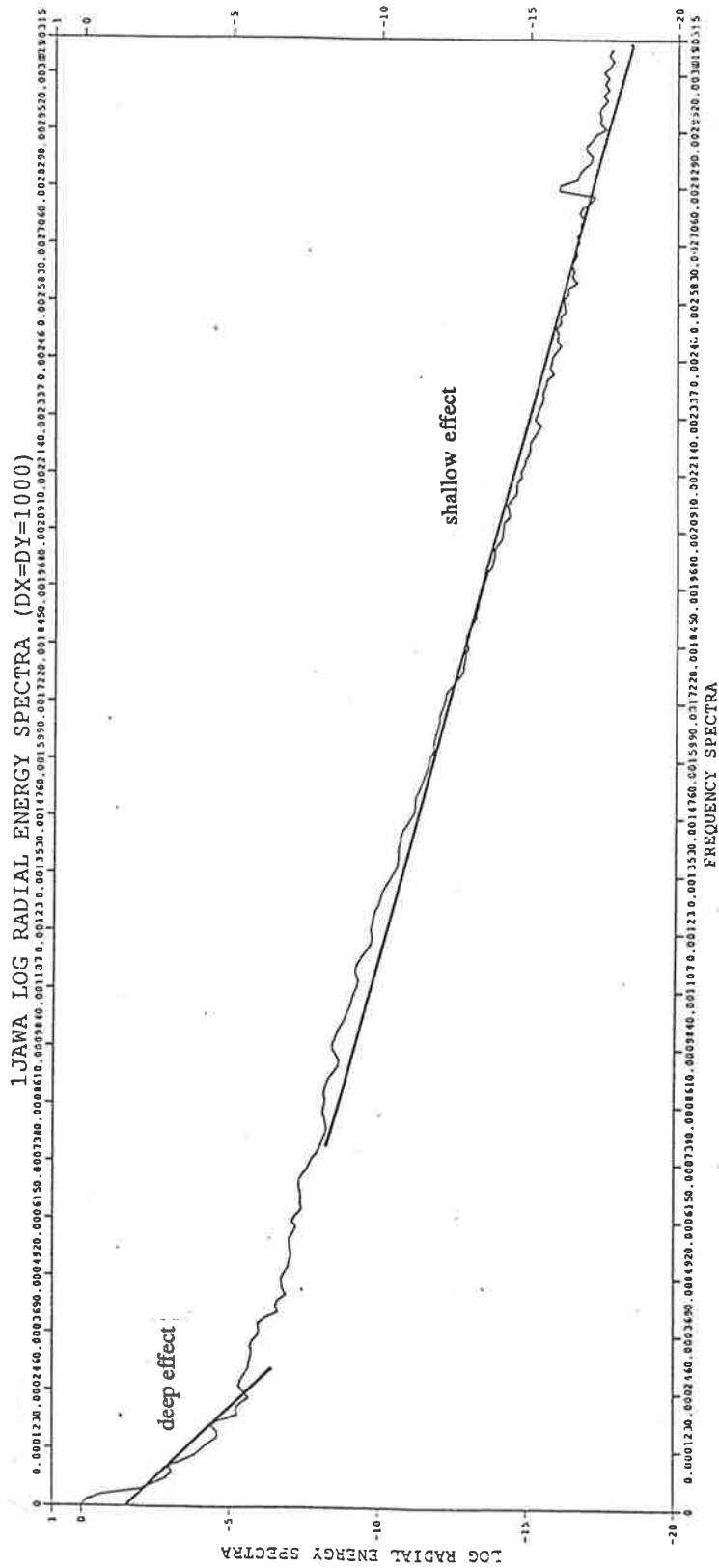
Figure 6-23. Central Jawa mean depth continuation with deep effect 11000 metres and shallow effect 2500 metres.

Chapter 7

Interpretation

7-1. Introduction.

The geological interpretation of gravity data, as in other geophysical methods, might be considered as the "final" step in a long process beginning when the survey was planned. The results from all of the previous steps such as survey planning, field measurement, gravity reduction & correction, filtering, contouring and imaging are combined together with geological and other geophysical information to be interpreted at this stage. Then it should be possible to translate the result of this process and reflect the meaning of the contour map, image and profile of the gravity data in terms of geology. On the basis of the result of this "final" step, some new action might be suggested and undertaken in order to achieve the main aim of the survey. Therefore, this step might be considered as the most important and difficult part of the whole process.

Unlike the interpretation of seismic records, the interpretation of gravity data cannot be accessed as directly as subsurface structure. Therefore, it is important always to keep in mind during the interpretation process that the gravity data contours naturally reflect a potential field rather than a visual subsurface structure. Strictly speaking, the geological interpretation of gravity data involves more uncertainties than the interpretation of seismic data.

It has already been seen that the interpretation process is built up on the basis of a combination of scientific knowledge and a sense of art. Even Dobrin (1989) stated that the

interpretation is more art than science. Therefore this stage constitutes the most interesting and challenging part of the whole process.

There are two types of interpretation to be done at this stage, qualitative and quantitative interpretations.

1. The qualitative interpretation of this gravity data deals with the analysis of anomalous features of the Bouguer anomaly maps. The possible cause of the anomalies and their relationship to the subsurface structure are described briefly.

. Several results and items of information which are taken from the previous chapter, such as the results from Upward continuation, Trend surface, Greyimage and Shaded relief are used proportionally.

2. The quantitative interpretation which deals with the modelling processes will be described in the second part of this chapter. Some information about density of the rock and the result of the spectral analysis process are combined to control this type of interpretation.

7-2. The Qualitative Interpretation.

The interpretation of gravity data in this chapter is presented on the basis of the 1 : 500000 scale Bouguer anomaly contour map. For certain areas, it is presented on the basis of the 1 : 100000 scale map. The scale of 1 : 100000 and 1 : 500000 are chosen because those are the scales of the geological maps for the region and it is essential for good interpretation to make a precise comparison of the two types of data.

The qualitative interpretations are presented and analyzed on the basis of the trend of the anomaly, the amplitude and lastly on the coincidences between anomaly features of Bouguer anomaly maps and geological information about the area.

Firstly, the Bouguer anomaly contour map of the study area may be examined according to its trend direction. Generally speaking, the trend of the anomalies over central

Jawa is in an east-west direction (figure 7-1). This trend is consistent with the information which is taken from the result of the previous work in chapter 3 (Untung, 1978).

Secondly, on the basis of their Bouguer anomaly values, the whole area may be simplified and divided into the four following groups of anomalies (fig.7-2) :

1. The very high area group with Bouguer anomaly values higher than 100 mgals, which occur along the south coast of Jawa, described as group one.

2. The second group is a high anomaly group with Bouguer anomaly values between 50 to 100 mgals, described as group two. This group includes group one as a small part of the group.

3. The low anomaly group with values between 0 to 50 mgals, described as group three.

4. Lastly, there is a very low anomaly group with values smaller than 0 mgal, described as group four.

Thirdly, on the basis of their coincidences with the geological information, the four following points may be noted at this stage :

1. A strong gradient anomaly feature can be traced along the boundary between group three and group two with a trend in an east-west direction. This pattern is interrupted slightly into a north west-south east direction just before the Merbabu and Merapi volcanoes and then goes back to the previous pattern (fig.7-3) This feature coincides with one major fault in the Karangsambung area (see figure 2-2).

2. The very high Bouguer anomaly group coincides mainly with the southern mountains area (fig.7-4)

3. There is a conspicuous very low anomaly (-55 mgal) coinciding with the Kendeng zone area which has a thickness sequence of Tertiary sedimentary rocks which reaches several thousand metres (De Genevraye and Samuel, 1972), (fig.7-5).

4. The position of active volcanoes which lie just along the northern part of the above strong gradient anomaly features of group two and group three (fig.7-6)
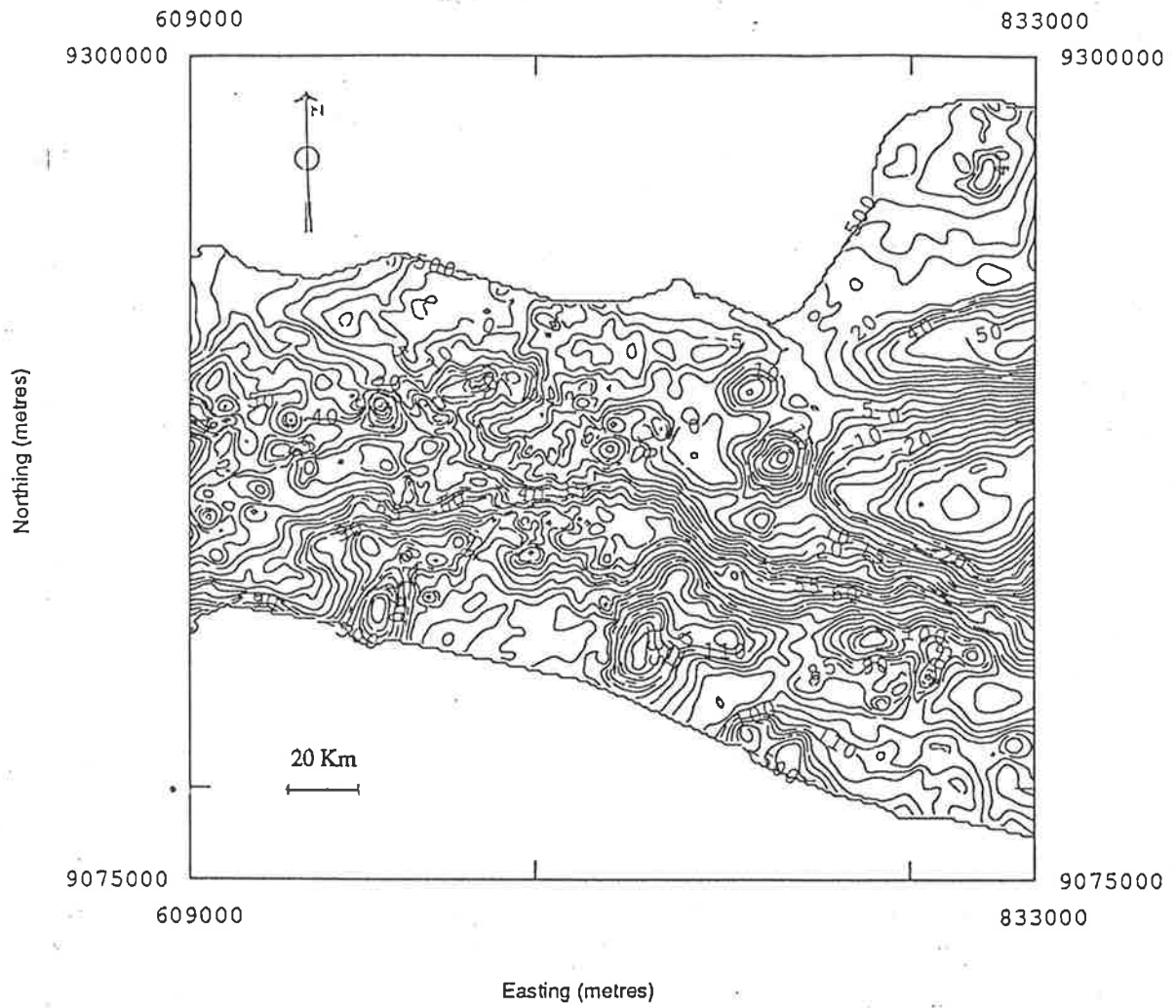
Figure 7-1. The central Jawa Bouguer anomaly contour map with trend east-west direction.
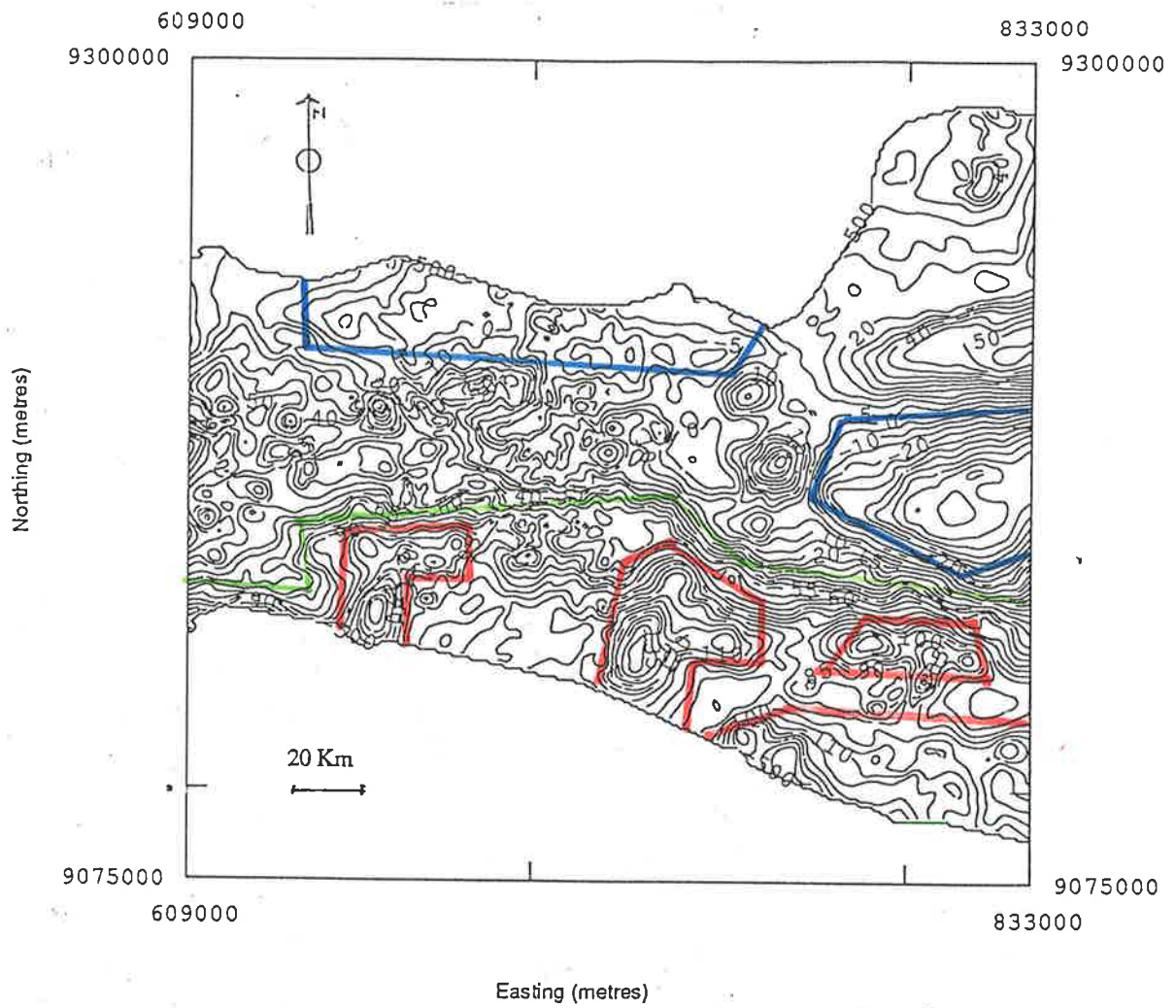
Figure 7-2. Group of anomalies as divided on the basis of the amplitude anomaly values.
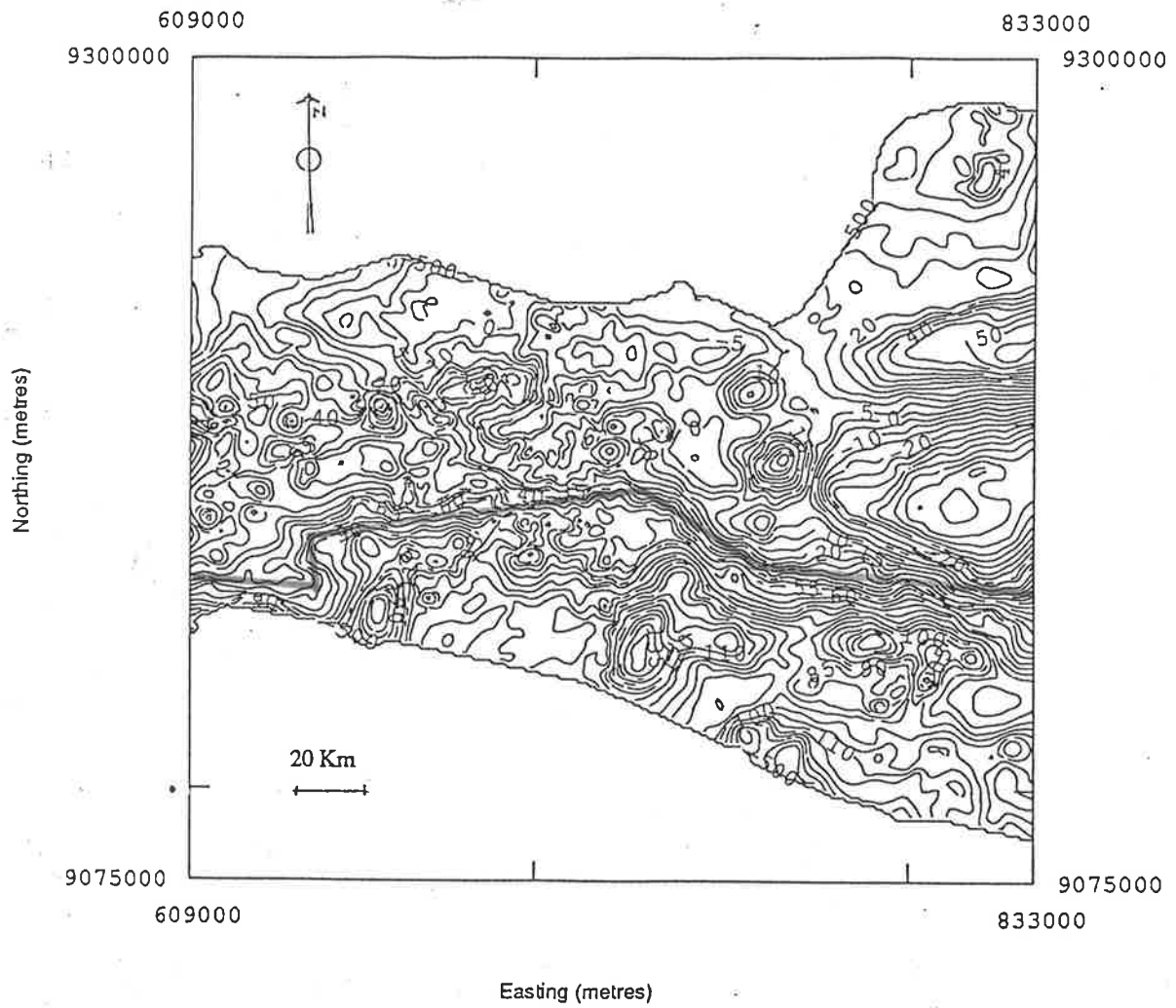
Figure 7-3. A strong steep gradient anomaly feature along the major boundary.
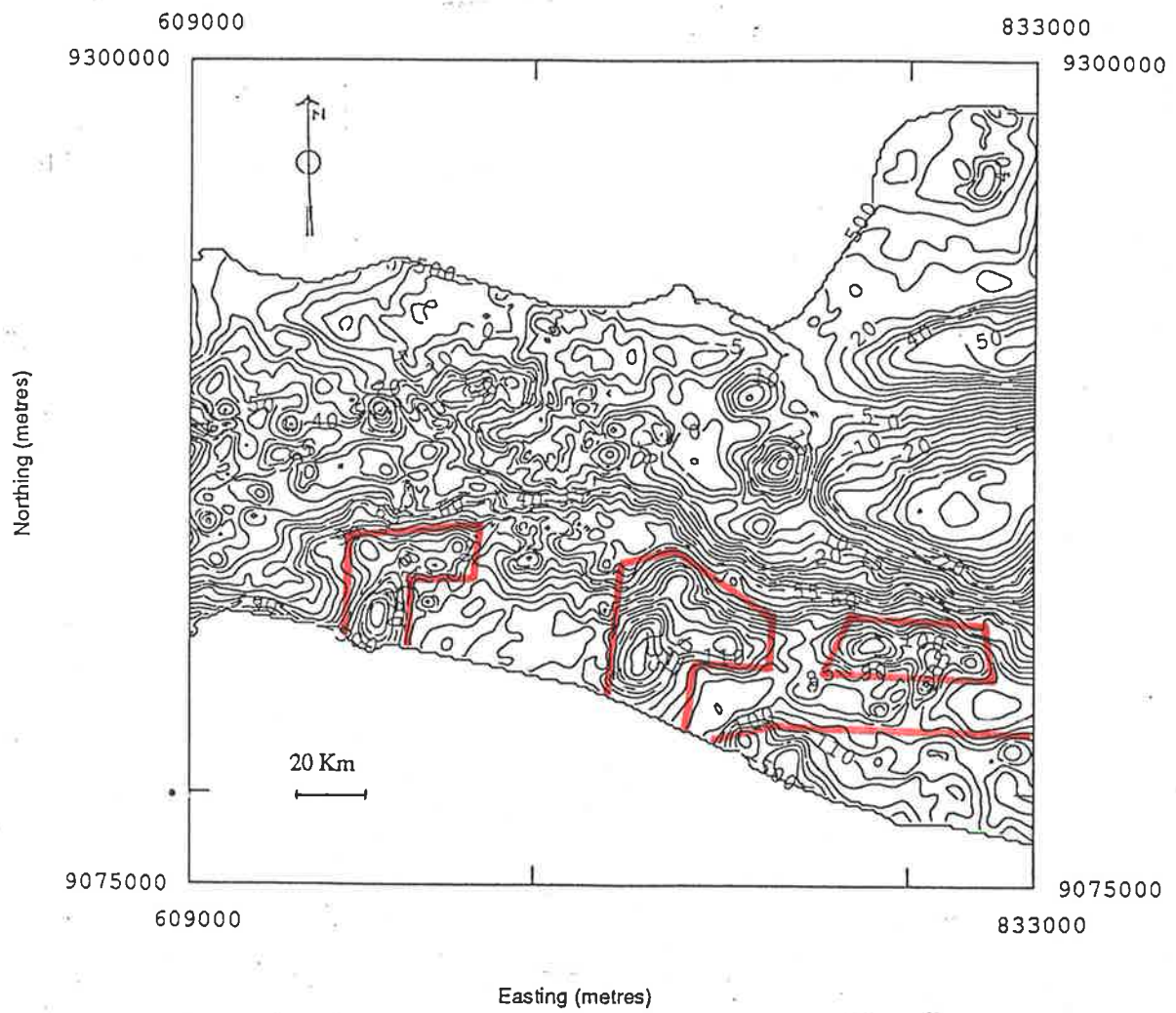
Figure 7-4. The very high Bouguer anomaly group which coincides with southern mountains area.
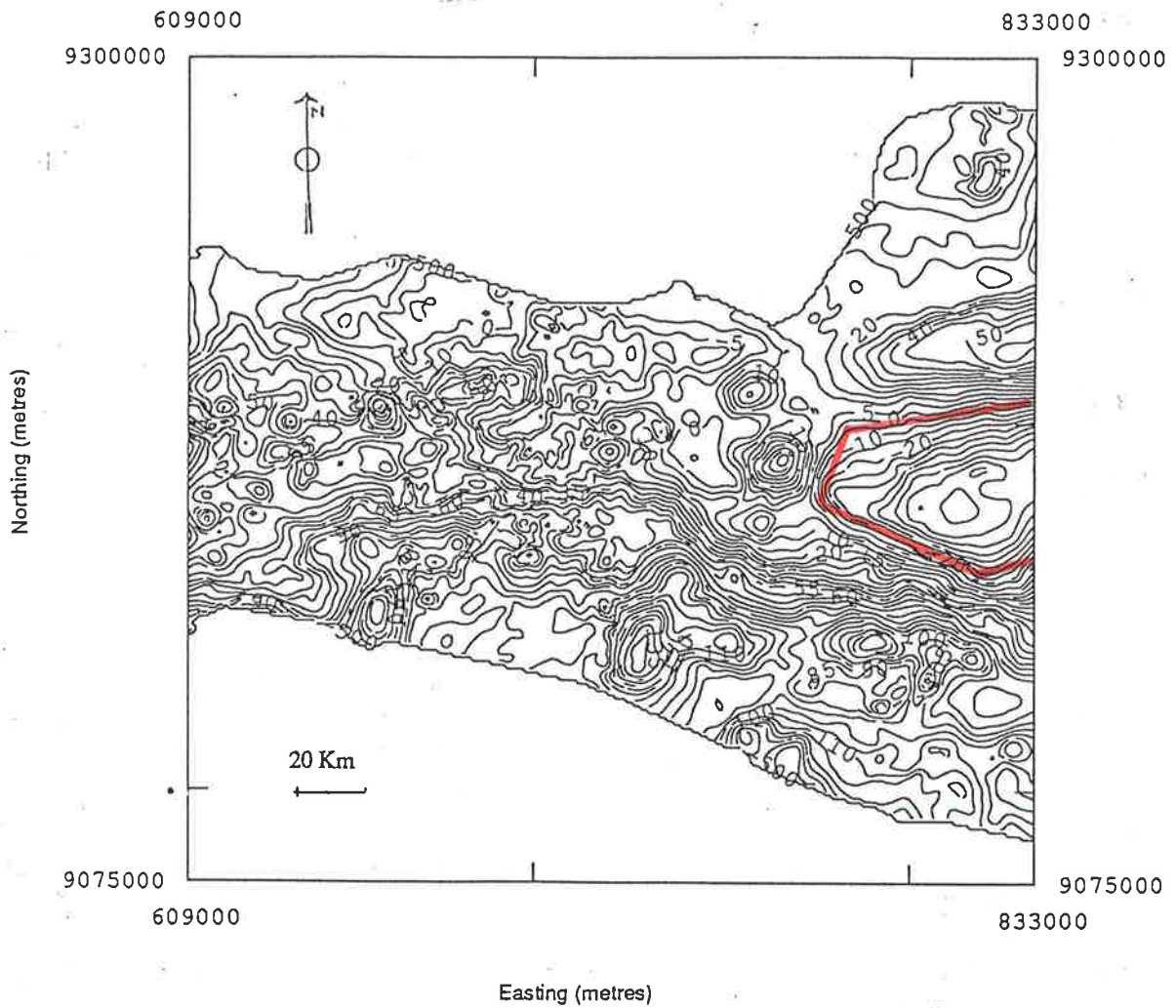
Figure 7-5. The very low Bouguer anomaly group which coincide with the Kendeng zone.
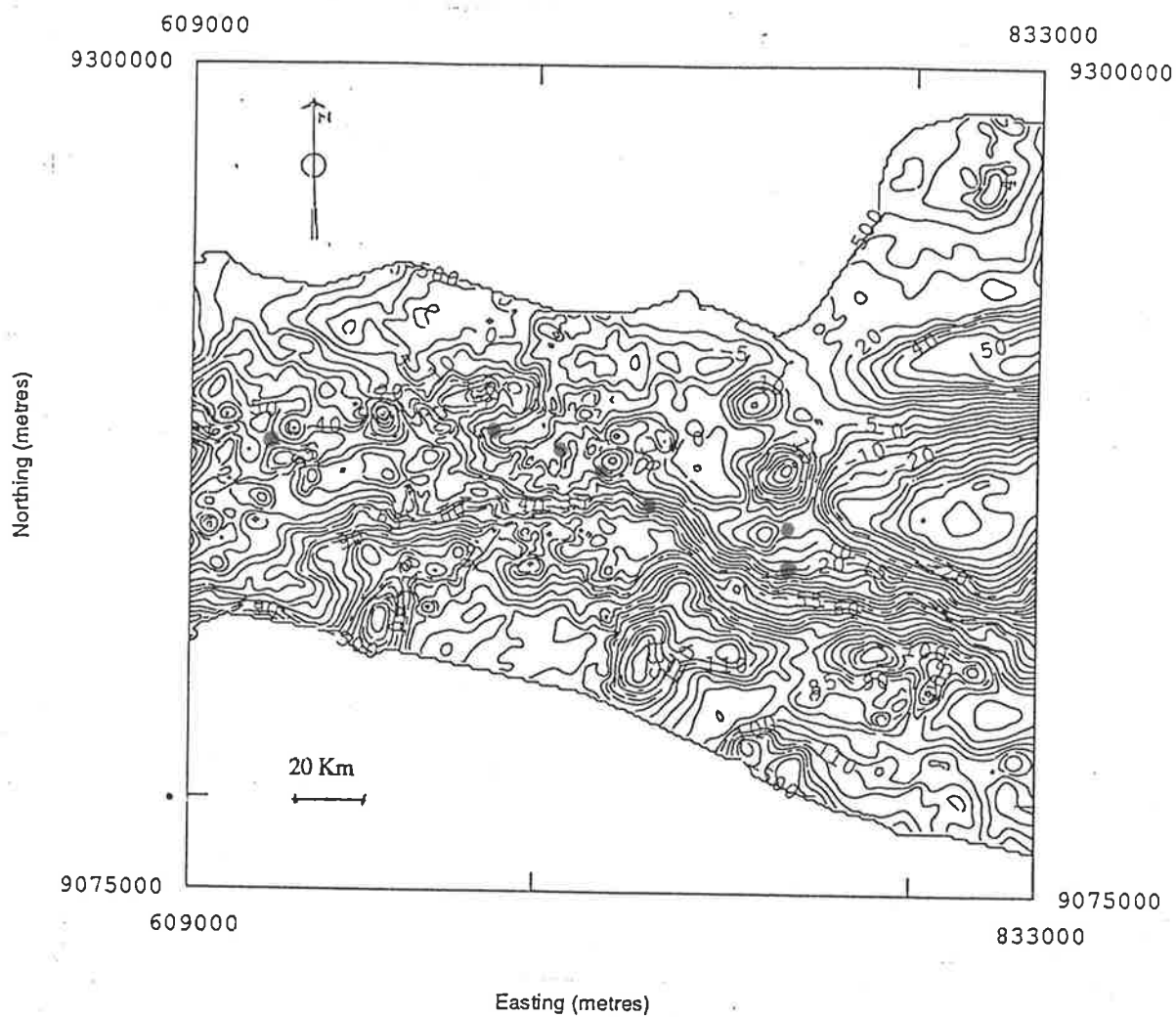
Figure 7-6. The position of active volcanoes in central Jawa.

In order to make it simple, but not simpler, on the basis of all previous evidence, the author wishes to divide the whole area into two large groups separated by a strong gradient anomaly feature (fig.7-7) :

1. The A group which is located at the northern part of strong gradient anomaly features, mainly occupied by alluvium, old and young Quaternary volcanic products. Locally, Miocene and Pliocene sedimentary facies, Pleistocene volcanic and sedimentary facies exist at some areas.

2. The B group which is located at the southern part of the strong gradient anomaly features, occupied by young Quaternary volcanic products, alluvium and Miocene sedimentary facies with Miocene limestone facies exist in certain areas. Eocene and pre-Tertiary sediments are exposed in the Karangsambung area.

There is one important point which should be noted at this stage. The boundary between A group and B group which lies in the Karangsambung area may be assumed as the boundary between the younger rock in the north and the older rock in the south. This is supported by the following information taken from the geological information in chapter 2.

1. The A group mainly occupied by alluvial sedimentary especially on the northern coastal plain of the area.

2. The B group occupied by Eocene sediment. In the Karangsambung large exposure of the pre-Tertiary rock exists. Also this rock can be found in the Jiwo hill, eastern part of Jogyakarta.

There are several interesting features in each of the above major groups in which some gravity profiles for the modelling phase are taken from those areas. Therefore, these two major groups may be divided into the following subgroups (fig.7-8) :

. 1. The A group.

A1 with Bouguer anomaly values between 0 to 50 mgals occupied dominantly by the active volcanoes.

A2 with Bouguer anomaly values between -5 to 20 mgals coinciding with the northern plan alluvial sediment.
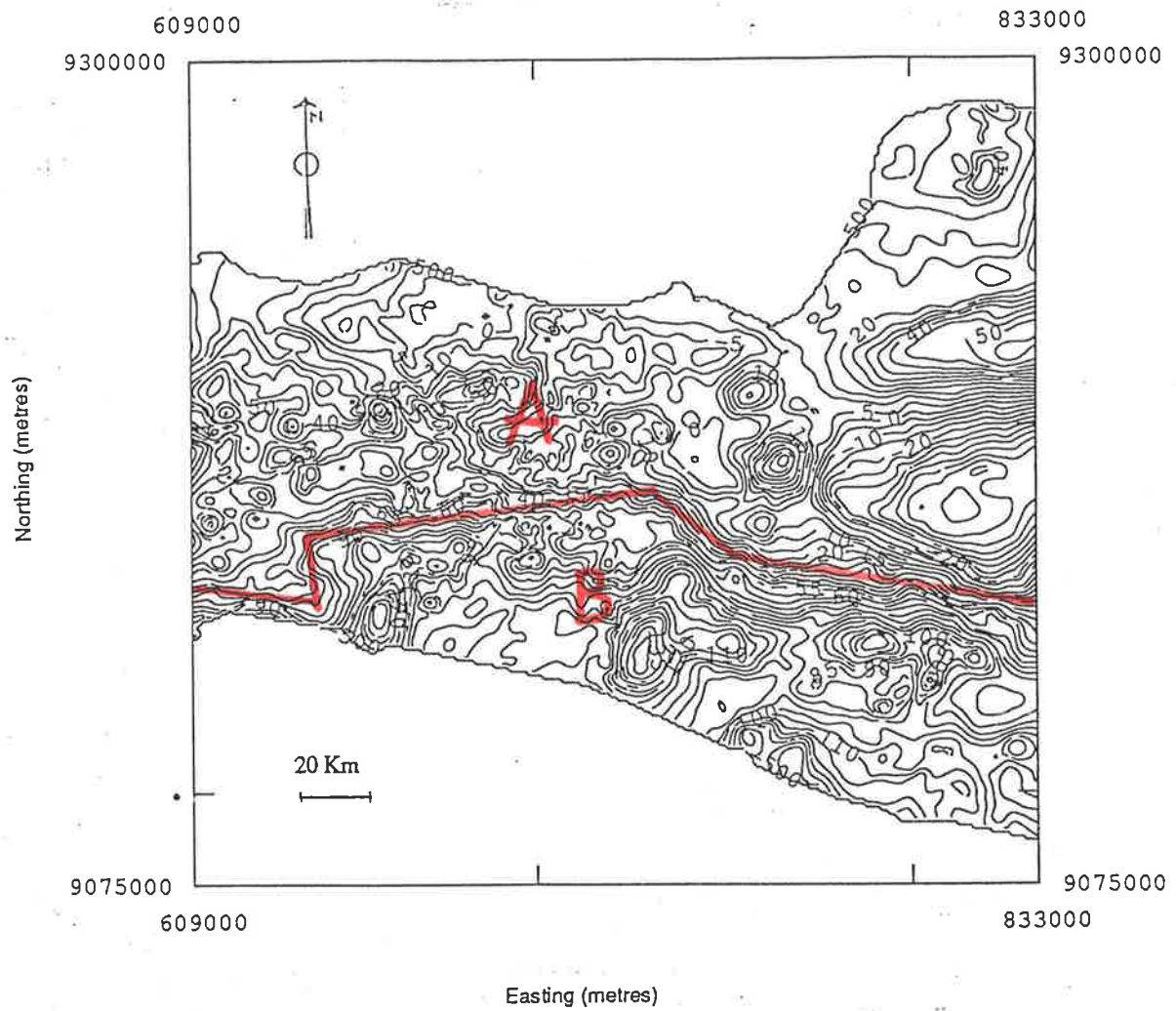
Figure 7-7. The A group occupies northern part of the strong steep gradient and the B group
at the southern part of that.
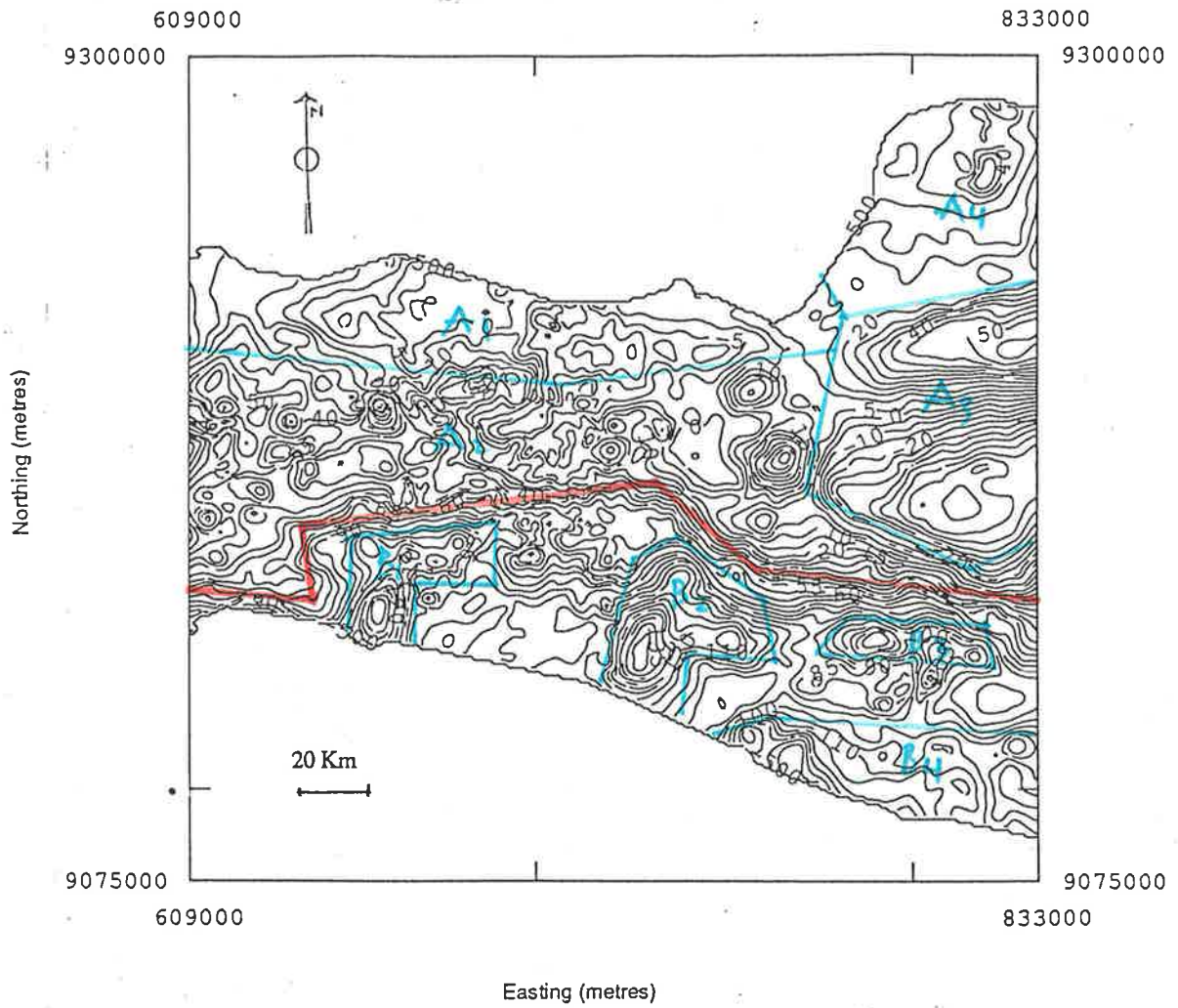
Figure 7-8. The A and B groups with their subgroups.

A3 with Bouguer anomaly values between -50 to 55 mgals in which two contrasting circular patterns exist. The first one is a large negative circular pattern which coincides with the Kendeng depression zone. The second circular pattern is a positive circular pattern which is occupied by limestone sediment.

A4 with Bouguer anomaly values between 15 to 50 mgals coincides with the northern alluvial sediment and Muria volcano respectively.

2. The B group.

B1 is a circular pattern with maximum anomaly of 140 mgals coinciding with the Karangbolong Mountain.

B2 is a circular pattern with maximum anomaly of 140 mgals coinciding with the West Progo Mountains.

B3 is a rectangular pattern with anomaly of between 100 to 120 mgals coinciding with unknown geological features, but it may be correlated to the pre-Tertiary rock which is present in the Jiwo hills, eastern part of Jogjakarta (see figure 2-2).

B4 with anomaly values of between 100 to 130 mgals which coincide with the Seribu Mountains.

Four areas have been chosen as the areas in which the gravity profiles for quantitative interpretation will be taken and then used in the modelling phase. To construct a good gravity model of the areas, the information from qualitative interpretation should be considered carefully. Therefore, the following sub-sections will describe the gravity features of the areas in more specifically:

7-2.1. Lukulo Area.

This area is occupied by a very strong steep gradient gravity feature (figure 7-9). The trend of this feature is running in an approximately east-west direction. The range of
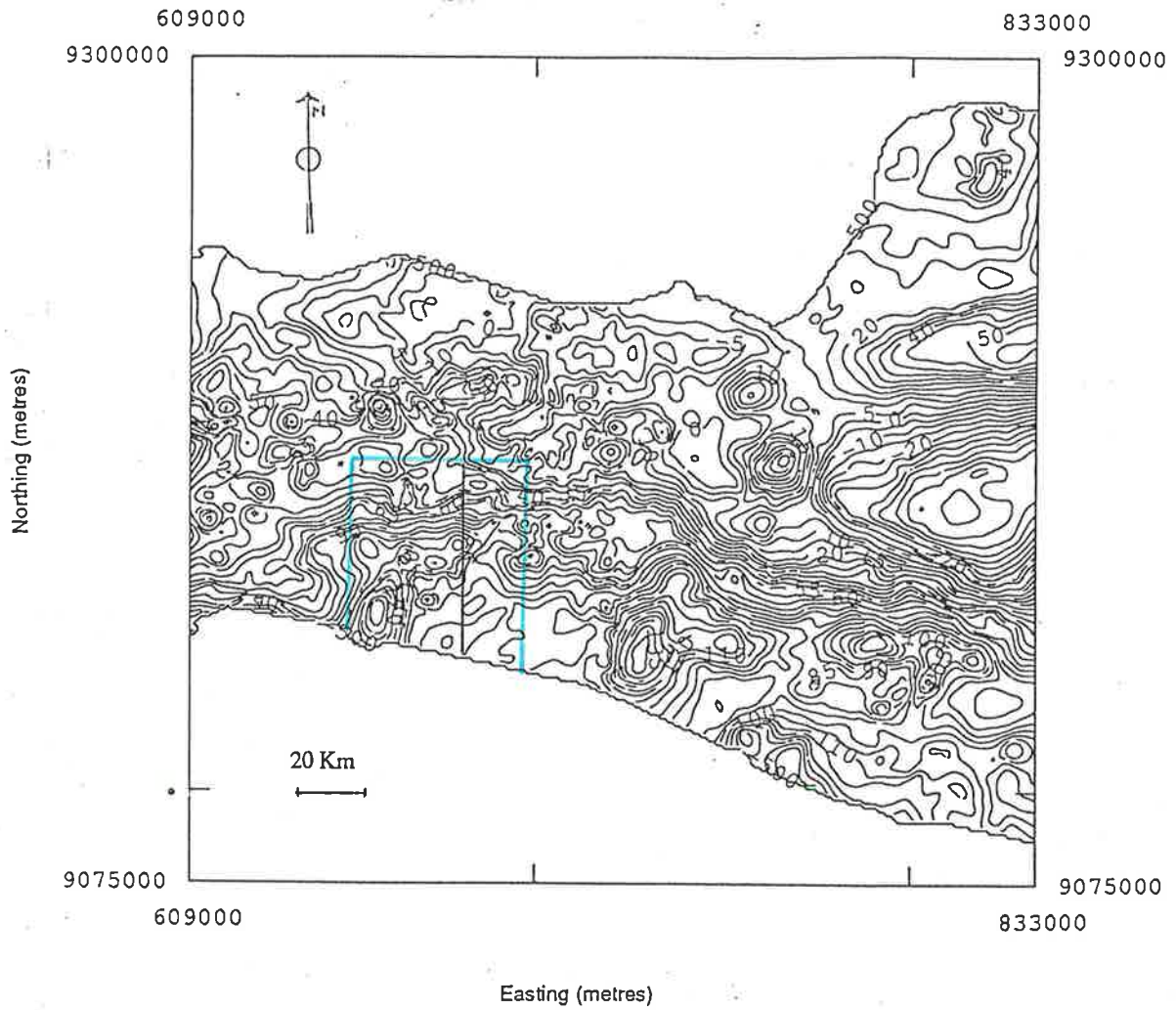
Figure 7-9. The Lukulo Bouguer anomaly contour map with profile line.
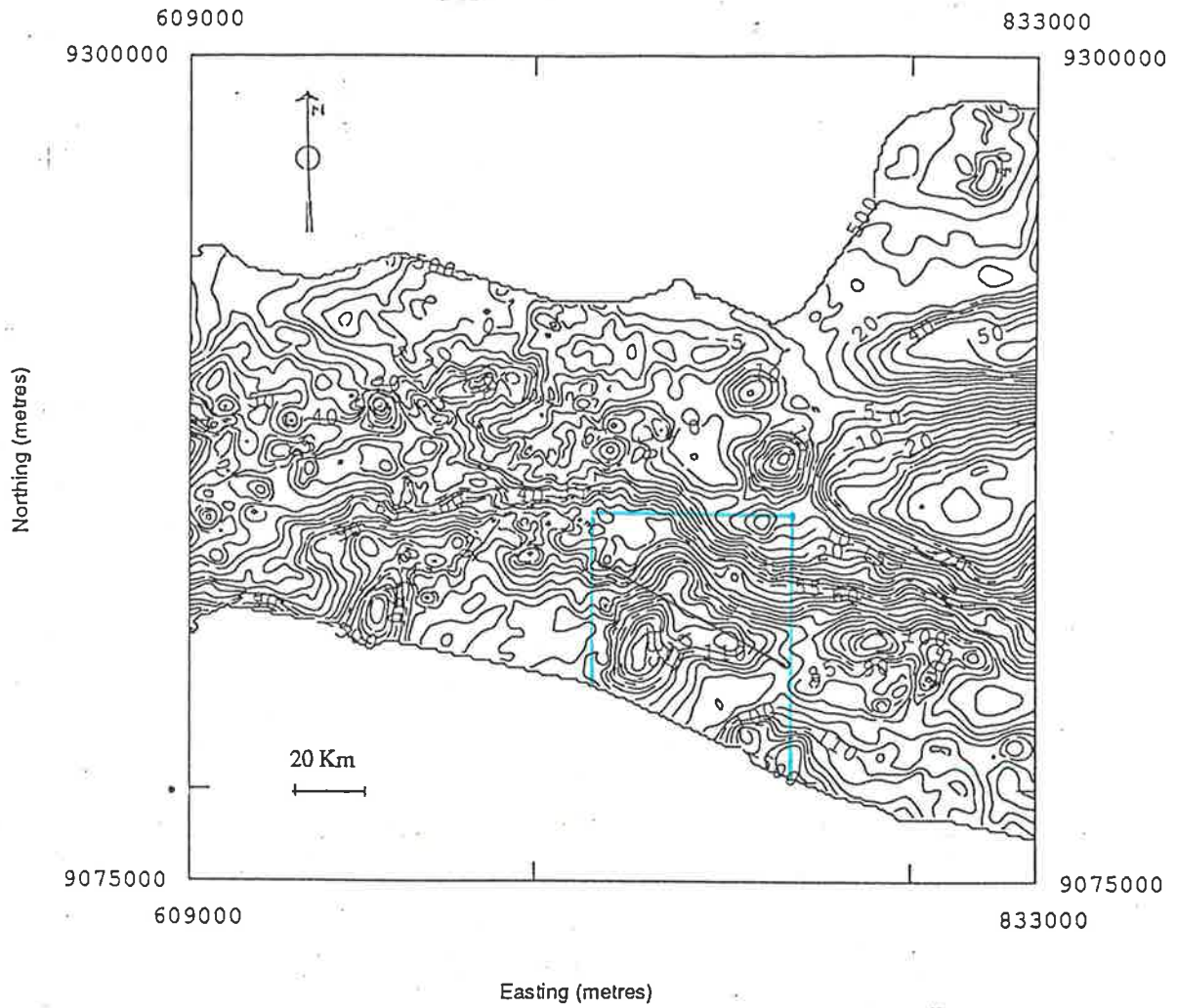
Figure 7-10. The West Progo Mountains Bouguer anomaly contour map with profile line.

the anomalies is between 45 mgals to 95 mgals. According to the geological information, this feature coincides with one major fault which exists in the Karangsambung area. (see figures 2-2).

7-2.2. West Progo Mountains Area.

This area is marked by group one of the Bouguer anomaly contour (figure 7-10). Almost all of this area is occupied by a strong circular anomaly feature with a maximum anomaly of about 145 mgals. The range of the Bouguer anomaly values is between 95 mgals to 145 mgals. This circular feature coincides with an oblong dome with a north northeast-south southwest diameter of 32 km and a west northwest-east southeast length of 15-20 km. The core of this dome consists of three old andesite volcanoes.

7-2.3. Ungaran Volcano Area.

There are two circular gravity anomaly features occupying this area (fig 7-11). The young Ungaran volcano is located just between two of these circular features. The northern part has an anomaly amplitude of 18 mgals and the southern one an anomaly amplitude of about 40 mgals. The circular gravity anomaly in the northern part coincides with the old and the oldest Ungaran volcanoes.

7-2.4. Merapi Volcano Area.

.The Merapi volcanic area, based on the regional gravity map, is mainly covered by group three of the Bouguer anomaly contour with values ranging between 10 mgals to 80 mgals (figure 7-12). This steep gradient anomaly feature runs in an approximately northwest-southeast direction. There is no indication that circular features, as on other volcanoes, exist. This very active volcano which is subject to an extensive research program is occupied mainly by the young and old Quaternary volcanic products.
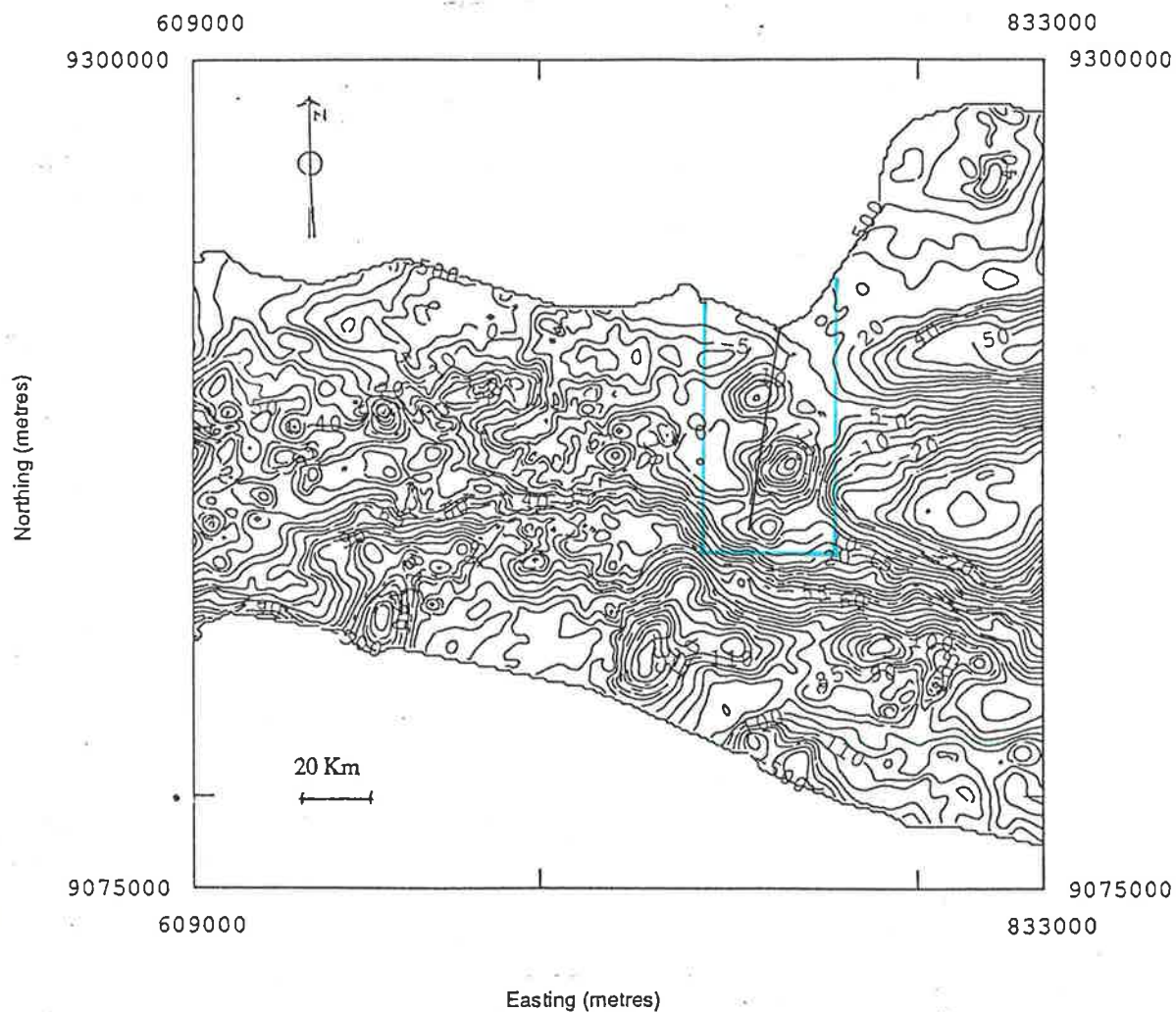
Figure 7-11. The Ungaran volcano Bouguer anomaly contour map with profile line.
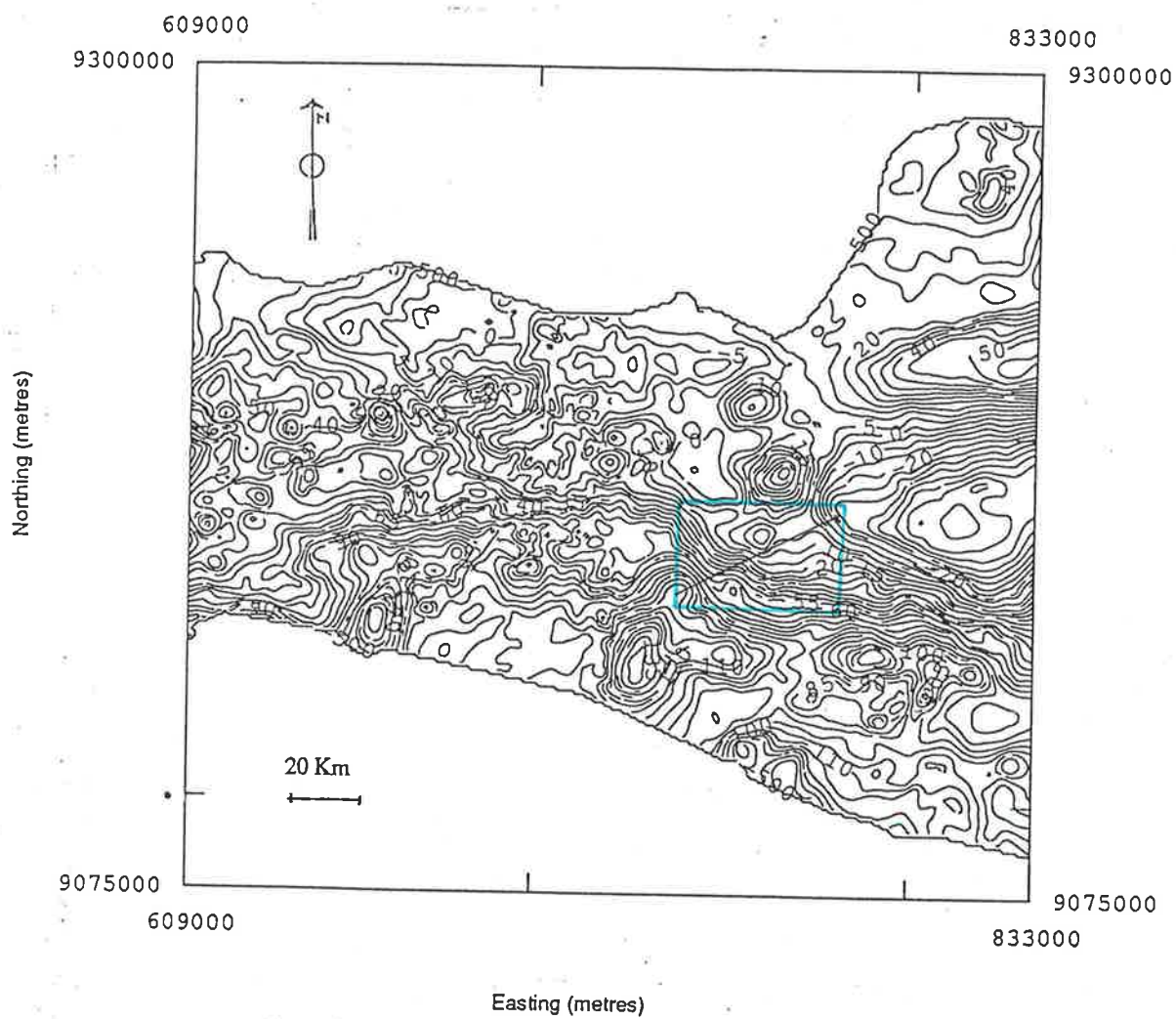
Figure 7-12. The Merapi volcano Bouguer anomaly contour map with profile line.

7-3. The Quantitative Interpretation.

The application of Newton's law or the differentiation of its potential field makes possible the determination process of a body's attractive force at any desired point in space. On the basis of this application, the comparison between the gravity effect of a burial body having different geometrical shapes and depths and the gravitational acceleration actually observed along one profile can be made. This comparison in gravity interpretation is known as the gravity modelling process.

Essentially, without geological and other geophysical information as a control, the gravity modelling process constitutes a determination of geometrical shape only. Thus determination of the position, the shape and the density contrast of the causative body is the main purpose of this gravity modelling process. Due to the fact that this type of interpretation emphasizes quantity rather than quality, it is classified as quantitative interpretation.

This subchapter deals entirely with gravity modelling of geological structures from the observed anomalies. The geological information about the region explained in chapter 2 and the density of rock samples described in chapter 4 will be used as the basic information for the construction of models.

The gravity models that are being used and described in this chapter are merely presented on the basis of the author's geological understanding and also on the judgment of the geology of the area. Strictly speaking, different models could be made from the existing anomalies. However, on the basis of the geological information which is combined with other geophysical information, the models presented would constitute a plausible and reasonable result.

7-4. Computer Gravity Modelling.

One of the most valuable methods which is used to analyze gravity data is a technique of modelling. Essentially, this technique consists of four different stages :

Firstly, assuming a shape of the subsurface body model which causes the anomaly.

Secondly, predicting the gravity effect from it at the surface by determining position and density contrast.

Thirdly, comparing these gravity effects with the observed values.

Fourthly, modifying the model by iterative procedures to minimize as far as possible the differences between the observed and the computed effects which are initially observed (Dobrin, 1989).

In order to assume the shape of the body model, the geological feature which causes the anomaly is usually approximated or simplified first by a simple geometrical form. There are five geometrical forms widely used for this purpose. They are sphere, horizontal cylinder, horizontal sheet, vertical sheet and vertical circular cylinder forms. The gravity effect of those geometrical forms can be computed mathematically. For geological features which are difficult to approach by those geometrical forms, polygons are used as an alternative. However, the mathematical computation for this geometrical form is a complicated one. The development of the computer in the last decade allows the complicated mathematical computation to be made more accurately and also in a short time.

Nowadays, there are several modelling programs available which can be used for quantitative gravity data interpretation. Fundamentally, most of all those modelling programs are designed on the basis of the Talwani and Ewing (1960) or Cady (1980) programs.

7-5. GRIN Program.

The modelling program named GRIN, which is used for this research, was created and developed by R. A. Almond during a period when he was involved in joint research in gravity mapping in Kalimantan, Indonesia, between the Geological Research and Development Centre of the Indonesian Government and the Bureau of Mineral Resources of the Australian Government.

The GRIN program is an interactive gravity modelling program that allows the user to compare the gravitational effect of a model with a set of gravity observations by gravity curve matching. The algorithm of this program is designed mainly on the basis of Cady's paper (1980) in which the body of the model is approached by the 2.5 dimension method. With this method, the convenience and speed of the 2-D approach is combined with much of the generality of the 3-D approach.

This program was designed for use on computer HP 1000 which was installed in the Geological Research and Development Centre in Bandung, Indonesia. Later it was modified for use on Personal Computer (PC). The only instruction operation book available for this research is the instruction operation for the GRIN program in HP 1000 (R. A. Almond, unpublished). Therefore, in order to use that GRIN program on the PC, the author created one instruction operation specially for the IBM PC, which is mainly based on the original instruction operation (see Appendix B).

7-6 Curve Matching and Ambiguity Problems.

Curve matching itself which is used in this modelling program is a trial and error process. Often this process consumes a lot of processing time because several parameters such as density contrast, depth and / or width of body etc, should be combined in a variety

of ways. In order to minimize the range of these combinations, the first approximation may be undertaken.

As the first approach, the thickness of a body which causes a given change in Bouguer anomaly is roughly estimated by a simple *'Bouguer slab'* calculation using the following formula :

$$dg = 0.0419 \, d\rho \, t$$

where :

    dg = bouguer anomaly amplitude in mgal

    $d\rho$ = density contrast in gr / cm^3

    t = thickness of a body in metres

Certainly, the above quick calculation is used only as an approximation value. In other words, this value is only used as the first guide for data input in the GRIN program. Once those parameters are available for input data, the GRIN program can be used for further action.

It has already been seen that a common problem in the gravity modelling process is the ambiguity of the model. This aspect should be handled very carefully before the reasonable and plausible body model can be accepted.

In order to avoid or at least to minimize this problem, other controls may be used to support the body model which is created by the modelling program. Ideally, several other geophysical data, such as magnetic, seismic, drill-hole data should be combined with gravity data to control the body model.

However, an ideal situation such as that cannot always exist in reality. Often the gravity data are collected in areas with no other geophysical information available or at least, not available yet. In such cases, a combination of gravity data model and geological information may be used to interpret the gravity data. In other words, the geological information may help to control the gravity model. Consequently, a number of plausible

gravity body models should be created before the reasonable gravity model, both geologically and geophysically, can be accepted.

In a situation almost similar to the above, this research uses mainly geological information to control the gravity modelling process.

7-7. Central Jawa Gravity Modelling.

Consistent with the four areas of interest which are discussed in chapter 2, four profiles which are taken from the same areas are used as input data for the gravity modelling process of this research. The direction of the profile is taken in accordance with the available geological cross section. The four profiles are taken subsequently from the Lukulo, West Progo Mountain, Ungaran and Merapi volcanic areas. Therefore the results of the modelling process will be presented and divided into four subsections :

7-7.1 Lukulo Area.

The profile which is taken from the Lukulo area is the profile with a north-south direction. The gravity model of this area consists of two bodies (figure 7-13). The type of those bodies is the 2 D polygonal prism. The density contrast of the bodies is taken 0.4 gr / cm3 higher than the surrounding area. Three relationships between two bodies were tried, the normal fault, the reverse fault and the vertical fault. However, the result of those two previous relationship were less perfect then the later one. Therefore the relationship between those bodies is assumed as a vertical fault. The depth of the second body is about 2 km increasing to about 8 km in the southern part, while for the first body it is about 14 km. The thickness of the first body is about 2 km and that of the second body is about 14 km.

Compared with the location of the major fault on the geological map (see figure 2-4), this vertical fault is at approximately the same location. Therefore this vertical fault may be assumed as the reflection of the major fault which exists in the Karangsambung area.

7-7.2 West Progo Mountains Area.

The profile is taken with a north west - south east direction. The geological cross-section is taken from the GSI of 1 : 1000000 scale geological map (Rahardjo, W., et al., 1977) (see figure 2-7). The model consists of five bodies of 3-D polygonal prism type (figure 7-14). Body number 1 with 2 km depth, 4 km thickness and strike length about 5 km, has a density of 0.5 gr/cm^3 higher than country rock. This body is surrounded by four less dense bodies where density is about 0.1800 to 0.2000 gr/cm^3 higher than country rock.

Compared with the geological section, body number 1 which has a dominant effect on the amplitude of the gravity profile may be correlated with some dense material covered by andesit.

7-7.3 Ungaran Volcano Area.

The profile is taken in an approximately north-south direction. The geological cross-section is taken from the geological map of the GSI of 1 : 100000 scale geological map (Thaden, R. E., et al., 1975) (see figure 2-10). In addition, one block diagram of old Ungaran taken from van Bemellen (1949) (see figure 2-9) is also used to control this gravity modelling process. The model consists of four bodies with body number 1 using the 3-D polygonal prism type, while the others are types of 2-D polygonal prisms (figure 7-15). The density of body number 1 is 0.5 gr/cm^3 higher than surrounding rock, with depth about 2 km, thickness 9 km and strike length about 5 km. Bodies number 2 and 3 have a density of about 0.1 gr/cm^3 lower than surrounding rock, while body number 4 has a density of 0.2

gr/cm^3 higher than country rock. The location of body number 1 almost coincides with the location of the old Ungaran. Compared with the block diagram of old Ungaran (figure 2-9), from the point of view of shape and position, body number 1 may be correlated to the magma hearth of this volcano.

7-7.4 Merapi Volcano Area.

The profile which is taken from the Merapi volcanic area is the profile with a southwest-northeast direction. The geological cross-section is taken from van Bemellen (1949), (see figure 2-11). The body model consists of 5 bodies of 2-D polygonal prism type (figure 7-16). The western part of the profile is occupied by two bodies whose relationship is assumed to be the normal fault. Their density is about 0.5 gr/cm^3 higher than surrounding rocks. Body number 3 lies on the top of body number 2 with a density of 0.07 gr/cm^3 lower than country rock. Body number 4 has a density of about 0.1 gr/cm^3 higher than surrounding rock and body number 5 is about 0.07 gr/cm^3 lower than that.

Compared with the geological section, body number 1 coincides with the buried bodies of the Menoreh volcano (eastern part of west Progo mountains).
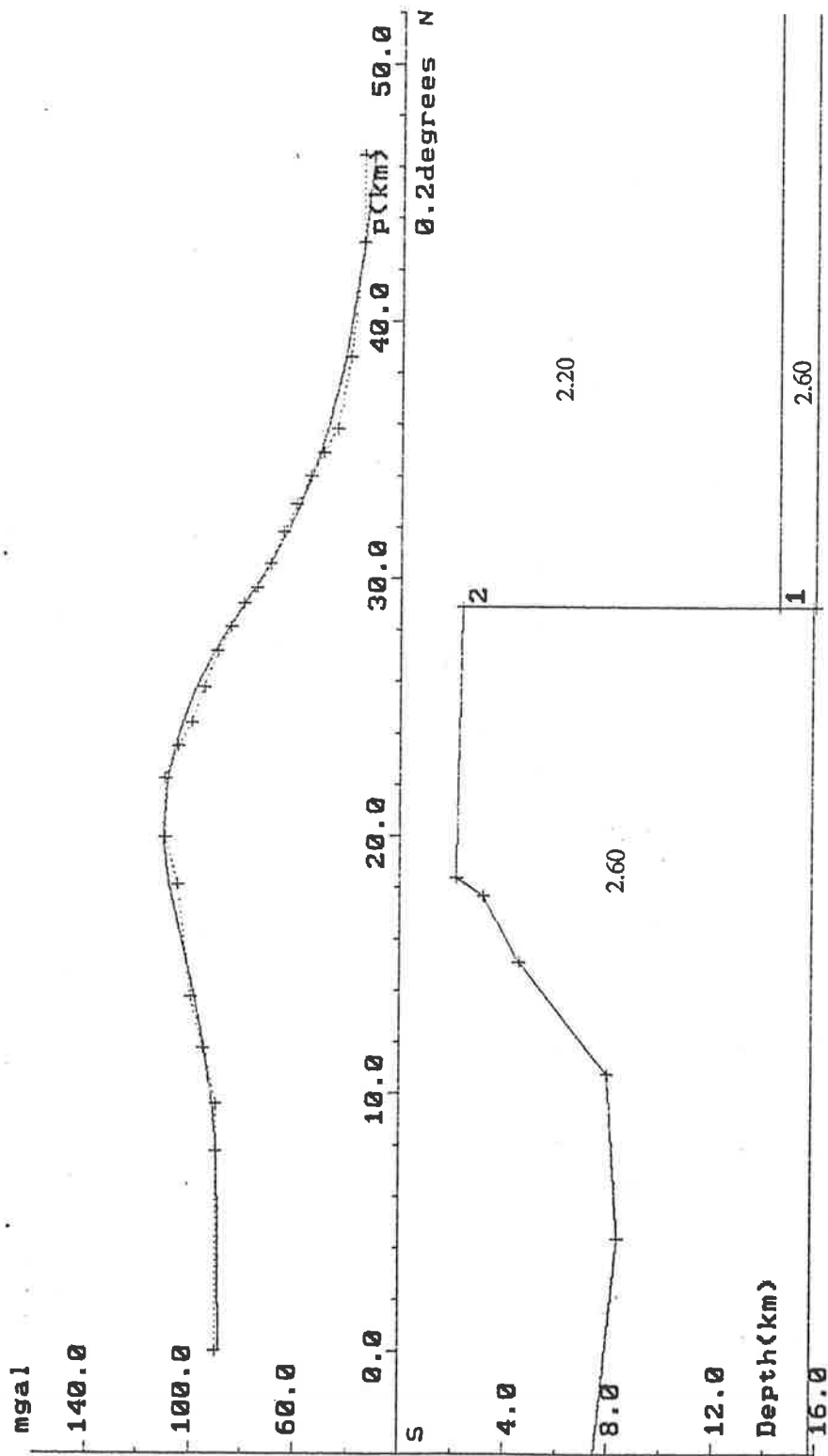
Figure 7-13. The Lukulo gravity model.
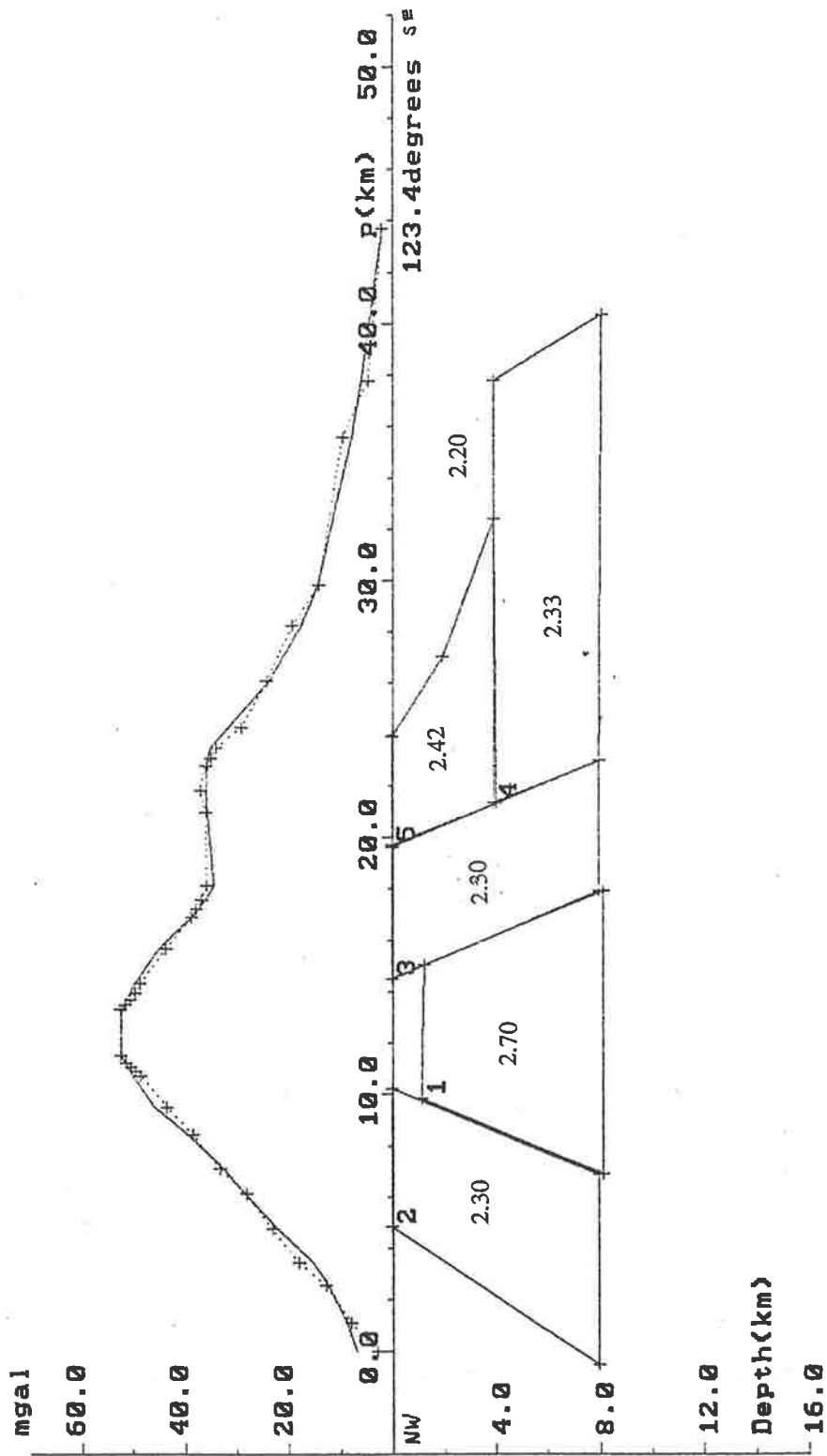
Figure 7-14. The West Progo Mountains gravity model.
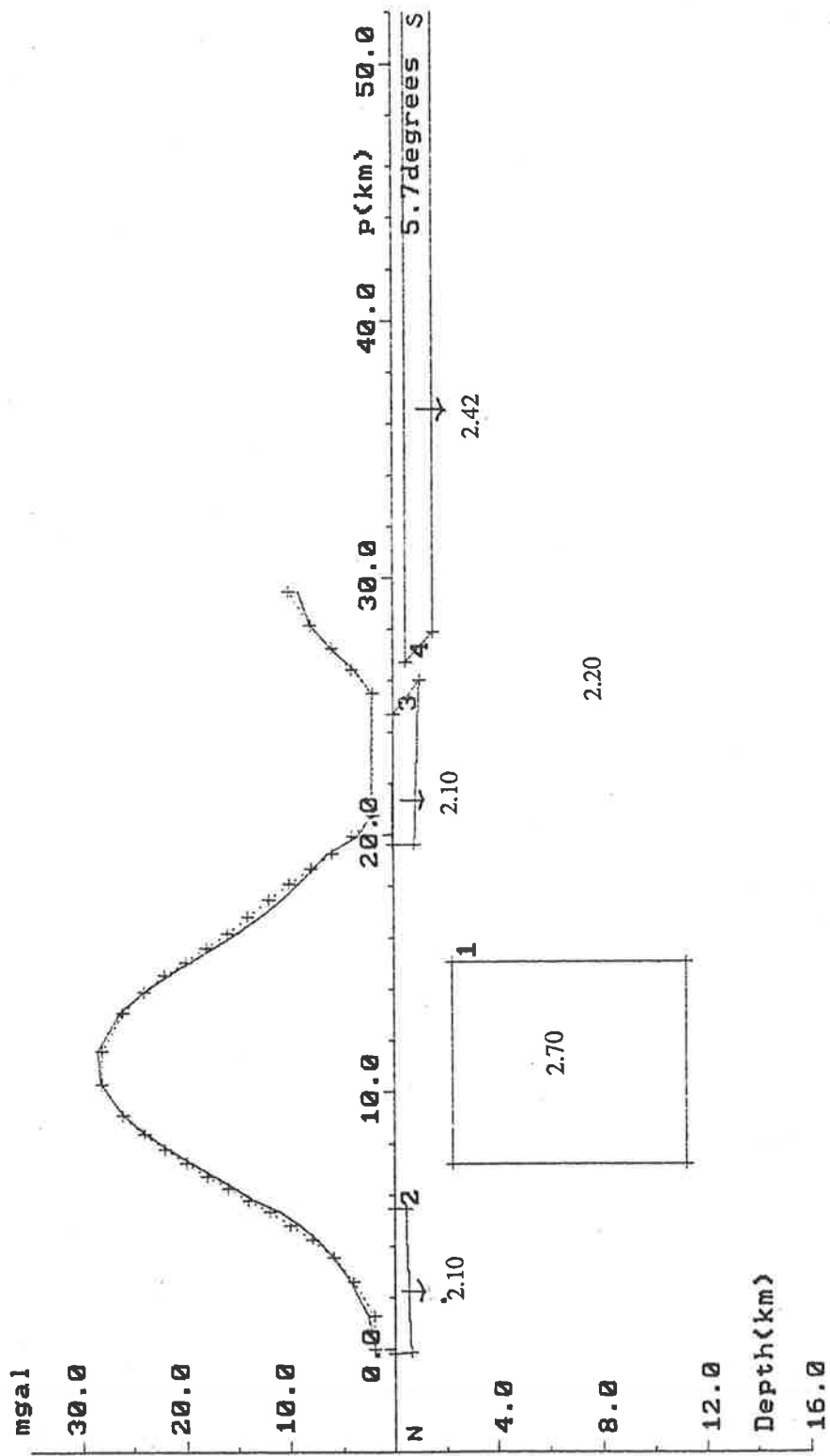
Figure 7-15. The Ungaran volcano gravity model.
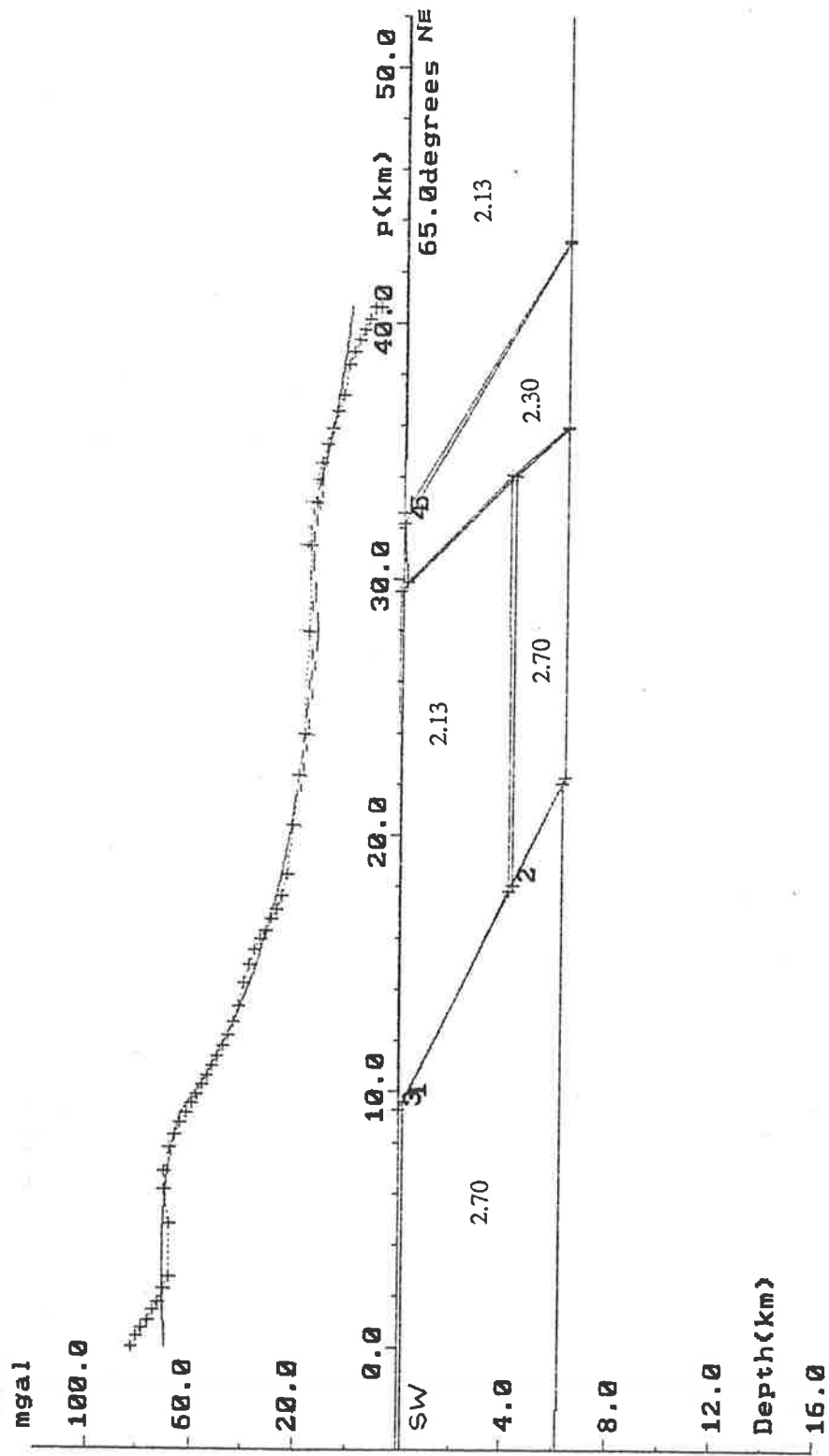
Figure 7-16. The Merapi volcano gravity model.

Chapter 8

Discussion and Concluding Remarks

8-1. Introduction.

There are a number of theories about the development of this broad complex region based on the plate tectonic theory which have previously been suggested. The proof for the various models however, is still accepted with difficulty by some geoscientists because they have their own theories or opinions. There are three groups of scientists still arguing about this complex region. The first group is based on the publications of Hamilton (1979, 1989). The second group is based on Carter et al, 1976, and Audley-Charles et al, 1979. The third group is based on Chamelaun and Grady, 1978. The first group argues that thick belts of chaotic melange are produced by scraping off material from downgoing plate in a subduction zone and acreting it to the opposite side of the zone. The second group assumes a more limited role for the chaotic deposits and sees the geology of the outer arc islands as dominated by the emplacement of large and coherent thrust sheets followed, in the Quaternary, by a phase of intensive block faulting. The third group regard thrusting as of minor importance and normal faulting as paramount. So far, conclusive arguments are rare and some of the basic field relationships are still in doubt (Milsom et al., 1983).

The study area is only a small part of this broad region. Therefore, discussion in this chapter may not be directly correlated to the above problems. However, an effort is made to harmonize the ideas of the author presented in previous chapters and the application of plate tectonic theory to these features.

In the previous chapters, the gravity response and structural interpretation were presented. On the basis of the research that has been carried out for this thesis, different models are reviewed using geophysical and geological facts. In some cases, geophysical interpretation may not directly contribute to the solution of geological problems. However, in some other cases there are a number of coincidences between geophysical interpretation and geological facts and information may be correlated as the result of this research.

Two significant results are discussed in this chapter. The first result is about the existence of the major boundary which separate the younger sediment in the northern part and the Eocene basement in the southern part of central Jawa. The second result is about the correlation between gravity data and volcanic structure influenced by the internal structure, composition and history of the volcanoes.

Therefore, this chapter presents an overview of the significant results which have come out on the basis of the interpretation of the geophysical data with geological information used as the main control. Following this, concluding remarks will be presented in this chapter as the final part of this thesis.

8-2. Regional Gravity Anomaly Pattern.

It can be clearly seen from the Bouguer anomaly contour map and also from greyimage scale, both Bouguer anomaly and shaded relief maps, that the whole study area is covered mainly by three types of anomaly patterns :

The first pattern shows steep gradient anomaly features. This pattern mainly occupies the middle part of the area with the trend running in an approximately east-west direction.

The second pattern shows circular anomaly features that lie in almost all volcanic areas, except in the Merbabu and Merapi volcanic areas.

The third pattern is the uncertain pattern. This pattern occupies the northern coastal plain and the middle part of southern coastal plain.

On the basis of this evidence, the author wishes to discuss the above patterns under the three following subsections :

8-2.1. The Major Boundary.

There is one remarkable sign which has been seen clearly in chapter 7 and which can be correlated to the major boundary in the study area. The gradient anomaly features which lie along the middle part of the area may reflect the major boundary between younger sediment in the north and the Eocene sediment in the southern part. A part of this feature has a strong coincidence with the major fault in the Karangsambung area which separates the Eocene sediment in the south from younger sediment in the north. This coincidence is strongly supported by the three following pieces of evidence :

1. The result of the modelling process in which the vertical fault is detected in Karangsambung area. (see fig. 7-13). This coincidence can be traced from Bouguer anomaly contour and from Bouguer anomaly shaded relief maps (see figures 6-3 and 6-6 to 6-9 respectively).

2. It can also be seen from the total magnetic contour and greyimage maps that something anomalous exists along this area (see figures 3-5 and 6-5 respectively). The result of upward continuation and trend surface residual shows that after filtering operations this feature still exists in the study area (see figures 6-10 - 6-22).

3. On the basis of the spectral analysis result, this strong gradient feature may be caused by the deep effect in which 11000 metres depth is detected.

Following this evidence, one assumption may be put forward at this stage. The boundary in central Jawa between the younger sediment in the north and the older one in the south runs along this major fault with continuation to the west as far as the northern part of Cilacap and to the east as far as the southern part of the Kendeng depression. This boundary is interrupted by a slight displacement at the western part of Karangbolong
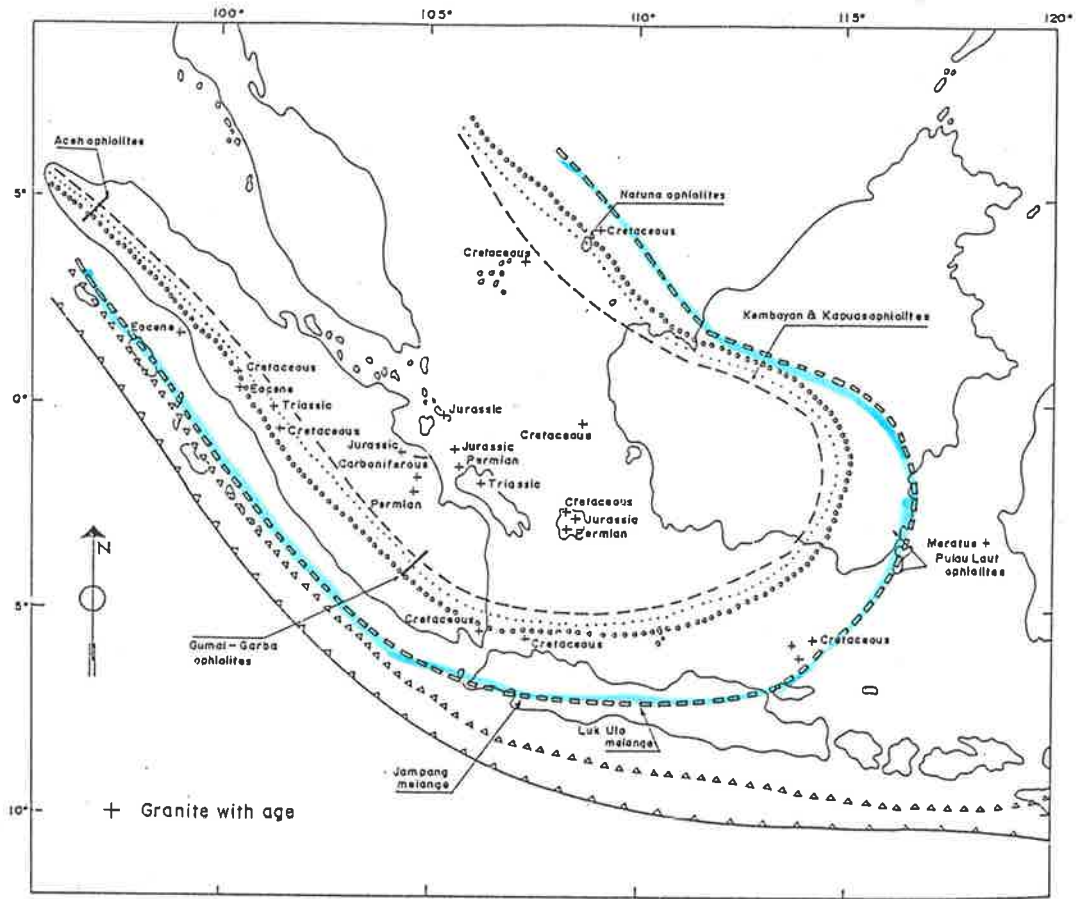
Figure 8-1. The lineament subduction line during the Cretaceous time (Katili and Hartono, 1981).

Mountain in the west and at Merbabu and Merapi volcanic sites in the east (figure 7-7).

On the basis of the modelling result in the Lukulo area which is combined with the estimated Bouguer density reduction value for the northern part of the Purwokerto area (see chapter 5), two bodies with a density of 0.4 gr/cm3 higher than country rocks may be assumed to be Miocene to Eocene sandstones. This is consistent with the result in chapter 4 where the density of 2.60 gr/cm3 is applied for those types of rocks.

The pre-Tertiary rock which is exposed in the Karangsambung area consists of metamorphosed sediments with ultramafic-mafic rocks described as Ophiolite in chapter 2. This body is presumed to be uplifted blocks of melange-Ophiolite accreted at the Cretaceous to early Tertiary. Katili and Hartono (1983) suggested that the lineament of subduction zones during the Cretaceous to the early Tertiary is located just along this boundary (see figure 8-1).

Even though further evidence both to the west and to the east of Jawa should still be provided, one speculation may be offered at this stage so that these coincidences can be related to each other. In other words, the lineament of the subduction zone during the Cretaceous to the early Tertiary may be reflected on this major boundary.

8-2.2. Typical Gravity Features Over the Central Jawa Volcanic Region.

The gravity values around the volcano not only show a characteristic distribution of the enormous underlying masses, but may also reflect the migration of material from the depths to the surface (Tsuboi, 1983). The volcanic pile is built up by accretion on an existing land surface, therefore it is common to assume that the base area is underformed or at most regionally bowed under the superimposed load of volcanic rock. Consequently, any change in crustal structure in association with volcanism would be assumed to come from crustal flexure or probably formation of an anti-root due to melting and extrusion of former basalt crustal material. Thus the interpretation of gravity data over the volcanic regions may

be considered as a critical solution because no solution is unique (Malahoff, 1969). Strictly speaking, all volcanoes are different in detail. One typical characteristic of those volcanoes which can be generalised is that they bring molten rock-magma-close to the surface (Rymer, 1991). Williams and Finn (1985), on the basis of analysis over a wide variety of volcanoes, assumed that a bulk density for the volcanic rock of the edifice to be 2.2 gr/cm^3. Therefore, during the study of gravity data over volcanic regions all of those limitation should be taken into consideration.

It is clear that the gravity data over the volcanic region in central Jawa, except in the Merbabu and Merapi volcanoes, is characterized by circular anomaly features. On the basis of the gravity values themselves, positive anomalies are dominant in all of the volcanoes in the region. This is consistent with the study of the volcanoes based on their gravity values in which the volcanoes are classified into three categories, positive, zero and negative Bouguer anomaly values (Yokoyama, 1963; Malahoff, 1969).

One gravity survey over the Semarang, Magelang and Jogjakarta regions was taken in 1968. However, since the aim of the survey was not for the purpose of a gravity study over the volcanic region, there is no specific conclusion about the relationship between gravity data and volcanic structure which can be made on the basis of this survey (Yokoyama, Suryo and Buyung, 1970).

The circular pattern which is not apparent in the Merapi volcanic area probably points to either the transverse and longitudinal faults which exists in this area or to the high density reduction value of 2.67 gr/cm^3.

8-2.3 The Causative Body Over Central Jawa Volcanic Regions.

The results of the modelling process indicate that the causative body which is responsible for the gravity anomaly over volcanic regions, both in the West Progo

Mountains and in the Ungaran volcano, has a density of 0.5 gr/cm^3 higher than the surrounding rocks. There is one result from the Ungaran volcano which should be noticed at this stage. The causative body whose depth from the surface is about 4 km may be correlated directly with the block diagram of old Ungaran which is taken from van Bemellen (1949). On the basis of these modelling result and geological information, body number 1 may be assumed to be the magma hearth of the old Ungaran. This correlation was realised just after the body model was contructed in the modelling process. In other words, the body model which was created was not biased by that geological information in the early stage. This also can be seen in the West Progo Mountains area in which the thickness of the causative body reaches almost 8 km.

In the Merapi volcano a body with a density of about 0.5 gr/cm^3 higher than the country rock is also detected. However, unlike the two previous volcanoes whose causative bodies may be connected directly with their volcanic materials, the body in the southwestern part of the summit of the Merapi volcano may be considered as the continuation of the West Progo Mountains (see fig. 7-6). In the case of Merapi, the result of the modelling process is the body with a density of about 0.1 gr/cm^3 higher than the surrounding rocks which is located just beneath the eastern part of the recent summit of the volcano. Since the Merapi volcano is still active, this body may be correlated with the volcanic material and lava flow which fill the vent of the volcano. Alternatively, this body, which is comparable with the case of the Ungaran volcano, may be correlated with the old Merapi volcanic material. This body is surrounded by less dense bodies, both in the western and eastern parts. Those bodies, whose density is about 0.07 gr/cm^3 lower than country rock, may be assumed to be the volcanic material which was constructed in the previous erruptions.

It has been seen that the density of the main causative bodies over three volcanoes is about 0.5 gr/cm^3 higher than country rock. The assumed density of andesitic and basaltic lava ranges between 2.52 gr/cm^3 and 2.75 gr/cm^3 (see table 4-1). With the density of the country rock around 2.25 gr/cm^3 (see chapter 5), the causative bodies over those volcanoes may consist of this type of volcanic rock.

It can be clearly seen from the interpretation of data about those three volcanoes that the degree of the ambiguity may be narrowed by the amount of geological information used as the control for the modelling process.

8-3. The Deep Structure Over Central Jawa.

It has already been seen that the mean depth of the deep effect is estimated as about 11000 metres. This result is consistent with the value of 10000 metres which is suggested by Hasegawa and Untung (1978). Hoshino and Sunoto (1978) constructed the relationship of the structural setting under the island of Jawa (see figure 3-4).

In comparison, on the basis of seismic refraction and gravity studies, Ewing and Worzel (1954) suggested that the Mohorovicic discontinuity lies about 9000 metres below sea level under the ocean basin, 12000 metres under the Caribbean Sea, at about 16000 metres under the trench and at slightly shallower depth under Puerto Rico. On the basis of gravity investigations over various island arc systems, Worzel (1976) concluded that the relative depression of the Moho discontinuity in the transition zone between trench and island arc is common to all systems.

On the basis of the structural setting model of Jawa which was created by Hoshino and Sunoto, 1978 (see figure 2-4) one structural gravity model of central Jawa is constructed and can be seen in figure 8-2. This structural gravity model consists of 4 layers, Pliocene-Miocene rocks (density value of 1.80 gr/cm^3), Miocene-Eocene rocks (density value of 2.50 gr/cm^3), granite/basement rocks (density value of 2.70-2.80 gr/cm^3) and gabbro/basic rocks (density value of 3.00 gr/cm^3). There is one less dense body with a density value of 1.60 gr/cm^3 in the middle of the first layer. This is assumed to be the thick Tertiary sedimentary rocks in the Kendeng zone. Since this model uses the profile which is taken from the most eastern part of the study area as the observed gravity data, minor
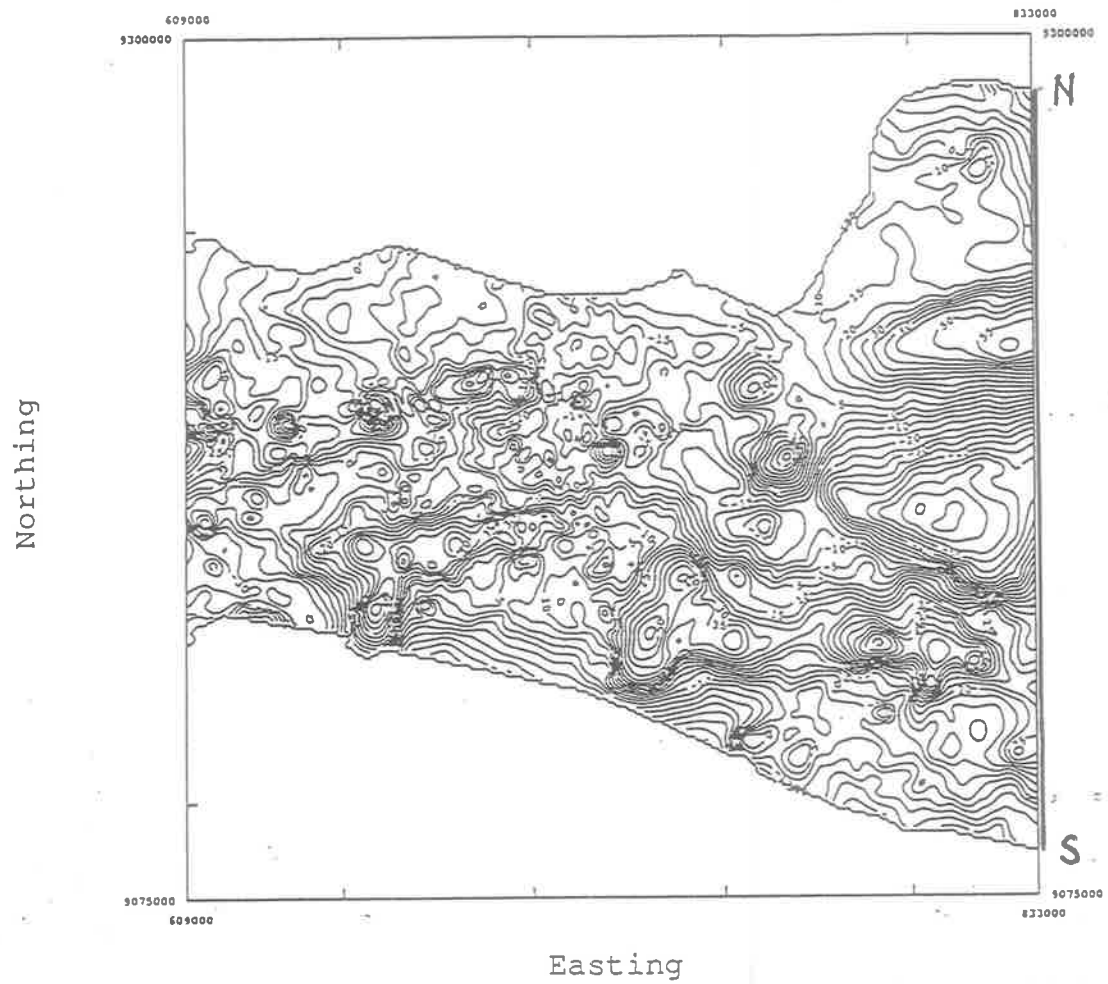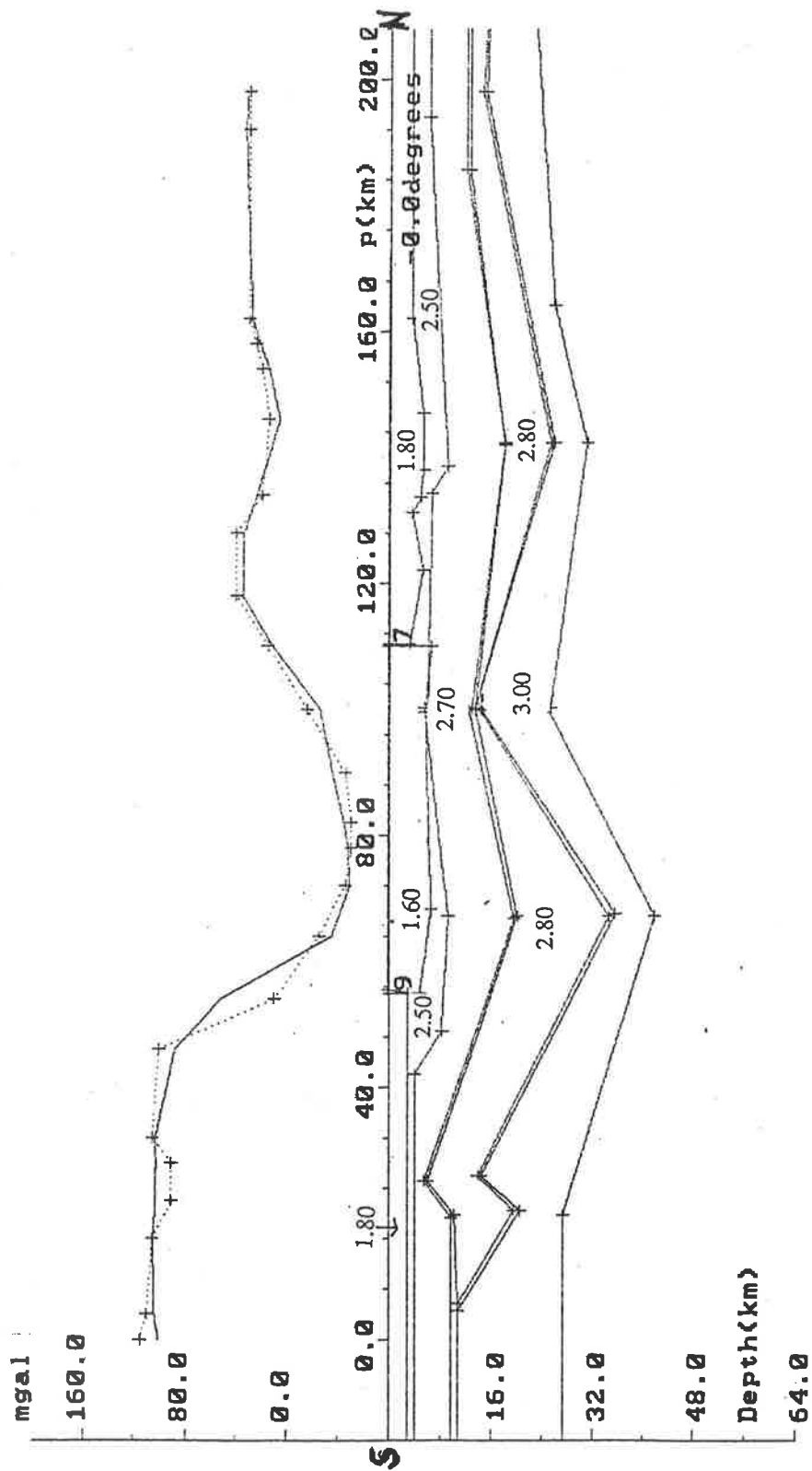
Figure 8-2. The structural gravity model over the most eastern part of the study area.

modification in the composition of the first layer should be given for another area.

8-4. Concluding Remarks.

This study has shown that the flexibility of the interpretation of gravity data is greatly dependent on the availability of raw gravity data, geological and geophysical information and the physical property of the representative rocks. In regard to the available data and information used, only a limited interpretation can be made on the basis of this research.

The convenient facility of extensive computer processing, however, has been used to solve some parts of the problem. It must be pointed out that the digitizer facility may be regarded as the main basic computer facility which should be provided in order to solve similar problems in the future. It also should be noted that the imaging process and enhancement technique, especially shaded relief, are an effective instrument for emphasizing a particular broad scale structure of interest.

The two following significant results may be stated as the important result of this gravity study over central Jawa :

1. One major fault in the geology of central Jawa is considered to be the boundary between the younger sediment in the northern part and the Eocene basement in the southern part.

2. A circular feature gravity anomaly with positive values may be regarded as the typical gravity data concerning central Jawa volcanoes. At the Ungaran volcano, this feature reflect a dense body whose density contrast 0.5 gr/cm^3 higher than surrounding rocks. This body has a diameter 7 km and extends for a depth of 2 km to 10 km. By using a modelling program, the structure of a volcano may be approached with a strong control from a geological cross section or block diagram.

As it has been mentioned in chapter 1 that this research may be used as a guide to what should be done to obtain a better interpretation in the future, it is hoped that the three following suggestions can be implemented :

1. Due to the fact that the gravity data over Jawa were collected during the period when computer data storage was not available, it is highly recomended that all available raw gravity data be stored on the computer. In the case where raw gravity data are not available any more, the digitizing procedure which has been successfully used in this research, can be undertaken.

2. Strictly speaking, each volcano is different in detail. Therefore, in order to gain a better interpretation of the volcanic region, a more detailed gravity survey of each volcanic area of interest may be considered.

3. Further studies and measurements both analytical and in the laboratory (see chapter 4) of the density of the representative rocks are highly desirable.

Eventually, the author wishes to point out that the interpretation which has been described and discussed in this thesis is only a relative interpretation of the gravity data. Nothing created by human beings is absolute in the interpretation of nature. Even the essence of gravity itself still remains in a mystery. Indeed only the Creator knows the essence of the truth.

APPENDIX A

Chapter I

Introduction

GRIN is an interactive gravity modelling program that allows the user to compare the gravitational effect of a model with a set of observations by curve matching. The curve matching is done by adjusting various parameters until the calculated gravity is sufficiently similar to the observed gravity. The parameter adjustment is done by the user and the curve matching is a trial and error process. Parameters may be adjusted directly by altering their values as they are displayed in data form, or indirectly by using the graphical capabilities of the terminal. Facilities are provided for saving models and edited observations at disc file for further use.

Originally, GRIN program was installed on Hewlett Packard 1000 in the Geophysical Division, Geological Research and Development Centre, Bandung, Indonesia. Due to the fact that the number of users of this program increased rapidly, and as only 2 graphic computer terminals which can be used for this program were available at GRDC, it was considered really important to produce the GRIN program which can be done on a Personal Computer. Consequently, several adjustments should be made for that purpose.

In 1987, there was GRIN program for Personal Computer available in Geology & Geophysics Department, the University of Adelaide. There was no special operating instructions book for this program, however, except the original operating instructions for the GRIN program which is only suitable for the Hewlet Packard 1000 computer.In relation to the above problem, these operation instructions for the GRIN program are based mainly on the original operation instructions which were written by the author of GRIN program, R A Almond (unpublished). Several minor modifications have been made accordingly, as several non-fundamental functions can not be used on personal computer facilities.

Chapter II
General Description

2.1 *Coordinates.*

First of all, the model and gravity stations are positioned in a 3-dimensional space defined by axes X, Y, and Z. The Z axis is directed vertically down and is the depth axis. The X and Y axes define the horizontal surface on which the stations are located. GRIN considers the +Y direction corresponds to true north, and +X is assumed to be east.

There is a third axis P in the (X,Y) plane. This axis passes through the observations and is used for displaying data in profile form.

The gravity-field axis F is directed up from the (X,Y) plane and is used for plotting observed and calculated gravity values.

The shape of a body is independent of the above coordinates. Each body's shape is defined in its own coordinate system with axes A,B and C.

All the spatial axes X, Y, Z, P, A, B and C are scaled in kilometres, while the gravity field axis F is scaled in milligals.

All of the above relationships are shown in figure 1.

2.2 *Observed data*

A special structure for observed gravity data should be created as follows:

Line 1
A title of up to 54 characters which is used to label various types of output.

Line 2
A second header record of up to 78 characters. Although this record is not used by GRIN, it is displayed when the file is read. It enables a more complete description of the file contents than is possible in the 54 characters of the title.

All subsequent lines
Each subsequent line contains easting, northing and gravity data values (X, Y, F). Default value for this format is 3E14.8 ; i.e. each of X, Y and F occupying a field of 14 columns in the record.

An example of an actual data file can be seen in table 2.

2.3 *Model*

A model consists of up to 20 discrete bodies which can be chosen from one or more of the types listed below. There are four types of body which can be used for this purpose.

> Type 1
> 2-dimensional dyke-shaped body: referred to as a 'dyke' in this document.
> · Type 2
> 2-dimensional horizontal polygonal prism: referred to as a '2-D polygonal prism' in this document.
> Type 3
> 3-dimensional rectangular prism of arbitrary orientation: referred to as a 'rectangular prism' in this document.
> Type 4
> 3-dimensional horizontal polygonal prism: referred to as a '3-D polygonal prism' in this document.

The '2-dimensional' expression has the conventional geophysical meaning that the body is infinite in one dimension.

A body may be positioned anywhere in the semi-infinite half-space defined by the X, Y and +Z axes. A body may be shifted or rotated anywhere within this half-space, though some body types have more degrees of rotational freedom than others.

2.4 *Display of data and model*

In order to achieve a complete 3-dimensional understanding of the data and model, the following two types of plot can be used in GRIN.

2.4.1 *Plan plot*

In a plan the horizontal distribution of observations is superimposed on a plan view of the bodies (fig. 2). This gives the clearest overall picture of the model and is the only way of displaying the strike of bodies.

When observations are input to the program a 'profile line' is calculated as the regression · line (Y on X, or X on Y) that passes through the station locations. This profile line is shown on the plan. It is constrained to have a bearing of greater than -45 degrees and less than or equal to +135 degrees relative to the +Y axis.

2.4.2 *Profile plot*

The profile plot displays the relationship between the model, its calculated gravitational effect and the observed gravity. It also provides facilities for graphical editing of observations and bodies.

In order to display non-linear data as a profile, GRIN projects the locations normally onto the profile line, as it is shown in figure 3. This is equivalent to the observer taking a viewpoint on the normal to the profile line and a large distance from it. This viewpoint is always positioned so that the left end of the profile is roughly south (for profiles that are more or less north-south) or west (for profiles that are more or less east-west). This is clarified in figure 4.

In a profile plot the horizontal axis is the profile line shown on the plan. This is the P axis. Distances along this axis are kilometres relative to the southern or western end of the profile line.

The vertically up axis is the gravity axis, F, and the gravity profile is plotted in the top half of the plotting area.

The vertically down axis is the depth axis Z. The bottom of half of the plotting area contains representations of the bodies comprising the model either as projections of their outlines onto the (P,Z) plane or their intersections with this plane, depending on the type of the body.

2.5 *Commands*

There are two command modes available on the GRIN program, manual and graphical.

Manual commands are entered via the terminal's function keys. The command associated with each key is displayed at the bottom of the screen. As there are many commands and only ten function keys, GRIN divides the commands among a series of menus. A menu is the set of ten commands displayed across the bottom of the screen at a particular time.

Graphical commands are permitted whenever a plan or profile is plotted on the screen. They are executed by pressing certain alphanumeric keys and obtain information from the position of the terminal's graphic cursor. Most graphical commands are merely more convenient alternatives to manual commands.

2.6 *Scheme of operation*

Briefly speaking, only three steps should be taken for GRIN program operation. First of all, input data reading operation. Second step, the modelling phase may begin. A previously defined model may be input using the READ MODEL command. Otherwise a new model may be created by using the SET/EDIT BODY command. The model is then adjusted by using either the SET/EDIT BODY command and graphical commands. The last step, save model and or plot profile operation.

Chapter III
Manual commands

Manual commands are implemented using the function keys 1 through 0 located at the top centre of the terminal keyboard. Each key is associated with the label displayed at the top of the screen. A command is executed by pressing the key corresponding to the appropriate label.

The relationship between commands and menus is shown in table 1.

3.1 READ DATA

This command is used to read observed gravity data from a disc file using the parameters indicated on the data form shown in figure 5. Data items must have been filed as one (X,Y,F) triple per record in the format specified by the format parameter. The first 54 characters of the first record in the file is listed by GRIN when the file is read and by the LIST INPUT command, but otherwise is ignored. It is available to obtain further information about the file contents if necessary.

A rectangular window on the (X,Y) surface is specified using the LOWER LIMIT and UPPER LIMIT parameters and data lying outside this window are ignored.

A sampling parameter SAMPLE INTERVAL is available to allow densely packed data to be thinned out. When a valid data item is found, the next sample interval - 1 records are skipped.

Reading continues over the whole file, or until the maximum number of 128 data items have been read in.

After the data have been read the reference values and scale factors are applied according to the scheme:

$$\text{value} = (\text{value} - \text{reference}) * \text{scale}$$

Note 1. Side effects.
All scales are reset to zero, causing automatic rescaling of axes. A fresh profile plot is generated by the next PLOT PROFILE command.

Note 2.
There is no strict requirement for the data to be ordered by X or Y values as the whole file is searched for data that lies within the window. However the record skipping facility is more meaningful for ordered data than unordered data. After the file is read the data are automatically sorted by GRIN so that plotting is always from the left side of the screen.

3.2 REGIONAL FIELD

When interpreting on a non-regional scale an anomaly of interest can be superimposed on a linear regional trend that must be removed in order to enable satisfactory scaling of the gravity axis and direct comparison with the calculated model profile. This REGIONAL FIELD command allows a gradient to be applied along the displayed profile. Regional values corresponding to this gradient are subtracted from the observed field values whenever these are used.

The data form used to input the two parameters defining the gradient is shown in figure 6. The parameters are the regional values that are to be subtracted from the observed data values at either end of the profile. Note that the scaled values on the gravity axis of the profile plot represent observed field values after removal of the regional gradient. The current regional gradient can be seen using the LIST INPUT command.

Note. Side effect.
The gravity axis scale value is set to zero, causing it to be rescaled automatically.

A fresh profile is generated by the PLOT PROFILE command.

3.3 SAVE PROFILE

The displayed profile may be saved as a disc file by using the SAVE PROFILE command. The user is prompted to enter the name of the file. If a file of the same name exists, the user is asked for permission to overwrite it.

Note.
As the data have already been windowed, scaled and had the regional field removed, the files created by SAVE PROFILE may always be input using the default parameter values of the READ DATA command, and no regional field should need to be extracted.

3.4 PROFILE TITLE

This command sets up a small data form that allows the 54 character profile titles to be altered. This title is used to label various types of output.

3.5 SET/EDIT BODY

3.5.1 *General description*

This command sets up a data form (fig. 7) that gives a summary of the model and allows selection of a body to be edited. The number and type of the body to be edited is read from the first two fields and the appropriate data form is displayed.

Subsequent fields allow the setting of INCLUDED flag for any bodies that are defined. This is an alternative to setting the flag by using the actual data form for the body and avoids the re-calculation of the body's profile which would be forced if the flag were set by reading its data form. To set a flag insert a character other than a blank into the appropriate box. GRIN will subsequently change any non-blank characters to asterisks.

3.5.2 *Definition of bodies*

The parameters that define a body may be displayed and edited using a data form invoked by the SET/EDIT BODY command. There is a unique data form for each body type (figs. 8, 10, 12 and 14). Beneath a header section which specifies the body number and description, each form is divided into sections entitled SHAPE, POSITION and PHYSICAL PROPERTIES, and also has provision for setting the INCLUDED flag.

Whenever the data form for a body is read, the time stamp appended to the model title is updated and the next PLOT PROFILE command causes the field due to the body to be re-calculated, regardless of whether or not any changes were made to parameters. Use the LIST BODY command to view body parameters without forcing recalculation.

3.5.2.1 *Body number and description*

The first two boxes of the data form contain the body number (which may be changed to create a copy of the body) and a 40 character description. The description may contain information about the body, such as its geological information, and is included in any list of the body's parameters.

3.5.2.2 *Shape*

The shape of a body is defined within its own coordinate system (A,B,C). The origin of (A,B,C) is the 'reference point' of the body, as this is the point around which the body is defined. The definition of the shape of each body is given in the appropriate section below.

Note
Any extreme differences in body geometries must be avoided. For instance if the top of a dyke were at a depth of 100 m a depth extent of 100 km should not be specified if a 'large' depth extent were required. A 10 km depth extent would be quite adequate. Odd results, particularly in the plotting, can often be traced to this sort of problem.

3.5.2.3 *Position*

The position of a body may be adjusted by translation and rotation of its (A,B,C) axes relative to the (X,Y,Z) axes. The parameters Xr, Yr and Zr in the data form define the position of the reference point of a body on the (X,Y,Z) axes and may be varied to allow translational movement.

A body may have up to three degrees of rotational freedom - strike, dip and plunge - though for most bodies only the strike may be varied. Initially strike is 0 degrees, dip is 90 degrees and plunge is 0 degrees, and the (A,B,C) axes are parallel to the (X,Y,Z) axes. A body may be rotated in one or more of the following stages :

    1. The body is rotated <u>clockwise</u> about its +C axis through the strike angle;
    2. Then the body is rotated <u>clockwise</u> about its +B axis through an angle of dip-90 degrees;
    3. Finally the body is rotated <u>anticlockwise</u> about its +A axis through the plunge angle.

If +Y is to the north and the body's strike is along the B axis, then this rotation scheme gives strike, dip and plunge angles that are similar to their conventional geological definitions.

Note
If the strike is not large, then the plunge angle defines downward plunge to the north.

3.5.2.4 *Physical property*

The only physical property appropriate to GRIN is the density contrast of the body relative to its surroundings.

Note
GRIN uses S.I. units for specifying all parameter values but as the S.I.unit of density tonnes/metre ^{3}, is numerically identical to grammes/centimetre ^{3}, the choice of units is immaterial in this case.

3.5.2.5 *Flags*

The data form for each body contains a box for setting and clearing a flag. A flag is set by putting any character other than a space in the associated box (the character will always be converted to a ' * ' by the program). The flag may be cleared by putting a space in the box.

Each body has a single INCLUDED flag (labelled as ' body is to be included in current model ' on the data forms) which signifies whether or not the body is to be included in the current model. This enables a body to be removed from the model temporarily without altering any of its parameters.

3.5.2.6 *Definition of a dyke*

A dyke is a body with infinite strike extent and a cross-section that is a parallelogram. The top surface of the dyke is parallel to the (X,Y) plane.

The reference point of a dyke is any point on the line down the centre of the top face. This line is coincident with the B axis. The shape of the dyke is defined in terms of its cross-sectional parallelogram using the width, depth extent and dip parameters (figs 8 and 9). Width is the dimension along the A axis and depth extent the dimension along the C axis. The dip is the angle the side faces of the dyke make with the (A,B) plane, measured relative to the +A axis.

Note
The dip in this case must be incorporated as one of the shape parameters as it is not simply a rotation of coordinates. Strike is the only rotation allowed.

3.5.2.7 *Definition of a 2-D polygonal prism*

A 2-D polygonal prism has an infinite strike extent and a cross-section that is a polygon with up to 10 corners. The edges of the prism are parallel to the (X,Y) plane.

The shape of the prism is defined in terms of its cross-sectional polygon (figs. 10 and 11). The reference point is on edge1, which is coincident with the B axis. The cross-sectional polygon is defined by specifying the (A,C) coordinates of the other edges {(A2,C2) and (A3,C3) in the example in figure 11}. These are relative to edge 1 as this has fixed coordinates A=0, B=0. If the polygon has less than 10 corners, those not used must have their coordinates set to zero. Edges must be defined sequentially from the edge 1 until a zero pair of coordinates is defined. The order of definition must be <u>clockwise</u> when looking in the +B direction. Strike is the only rotation allowed.

3.5.2.8 *Definition of a rectangular prism*

A rectangular prism is a 3-D body with the shape of a rectangular box.

The reference point for the prism is at the centre of the top face (figs. 12 and 13). The faces are parallel to the A, B and C axes. The shape of the prism is defined in terms of its thickness, strike length, and height, which are its dimensions along A, B and C respectively. All three rotations, strike, dip, and plunge, are allowed.

3.5.2.9 *Definition of a 3-D polygonal prism*

This is the same as the 2-D polygonal prism except that the strike length is finite (figs. 14 and 15). The reference point is at the center of edge 1.

3.6 SAVE MODEL

This command saves the current model as a disc file. The user is prompted to input the file name. If a file of the same name exists, the user is asked for permission to overwrite it.

The data saved are the model title and the description and parameters of each body that is currently INCLUDED. The flags associated with a body are not saved.

3.7 READ MODEL

When a model has been saved with the above procedure, it can be restored by the READ MODEL command. Bodies are assigned the same body numbers that they had when they were saved and so will overwrite bodies currently associated with those numbers. Only those bodies read from the file are INCLUDED at the completion of the command. The existing model title is replaced by that from the file.

3.8 MODEL TITLE

This command sets up a small data form that allows a 36 character model title to be entered. An 18 character time stamp in the form 'hour:minute date month year' is appended to the model title by the program to give a title of 54 characters total length. The title is used by several parts of the program for labelling output.

The time stamp is updated whenever any change is made to the model.

3.9 CLEAR BODY

When this command is used, GRIN prompts the user to enter a body number. If a valid body number is entered then all its parameters are reset to zero and the body becomes undefined.

3.10 PROFILE SCALES

This command allows the offsets and scales for the distance (P), gravity (F) and depth (Z) axes to be set by the user using the data form shown in figure 16.

The offsets and scales are applied according to the scheme

scaled value = (unscaled value - offset) * scale

(i.e offsets are applied before scales). A scale value of zero in any case will cause automatic calculation of that offset and scale. Automatic scaling of the depth axis consists of setting the offset to zero and the scale to that of the distance axis.

Note. Side effects
Use of the PROFILE SCALES command causes a fresh profile plot to be created when the next PLOT PROFILE command is executed.

3.11 PLAN SCALES

This command allows the offsets and scales for the plan axes to be set by the user using the data form shown in fig. 17.

The offsets and scales are applied according to the scheme

scaled value = (inscaled value - offset) * scale

(i.e. offsets are applied before scales). A scale value of zero in any case cause automatic calculation of that offset and scale.

3.12 MODEL PLAN

GRIN takes a 3-dimensional approach to the definition of data and model and so it is essential to be able to view the relative positions of observations and bodies in space. Depth relationships can be seen from the profile plot produced by PLOT PROFILE command, but the plan plot obtained by using the MODEL PLAN command is usually necessary to obtain the full picture. The command should be invoked frequently during a modelling session to check that bodies are being positioned correctly. The plan is plotted in the following stages (figs. 1 and 2).

(X,Y) axes are drawn with +Y vertical and +X to the right. If automatic scaling is used (see PLAN SCALES command) then X and Y scales are made equal.

The plot is annotated with the title associated with the input data and with the model title.

All data points are plotted as individual crosses and are roughly centred on the screen if automatic scaling has been used. The line of regression is then drawn through the points. This is the profile line on to which data points are projected for profile plotting.

The positions of bodies in the current model are indicated as follows :

The position of a dyke is indicated by drawing its two edges.

The position of a 2-D polygonal prism is indicated by drawing its two outermost edges as solid lines (i.e. the maximum horizontal width of the body is depicted) and edge 1 as a dashed line.

The corners of a rectangular prism are projected in outline on to the (X,Y) plane where they are connected to form a 'wire diagram'. The face that was at the bottom before any rotations were applied is drawn with dotted lines and the other faces with solid lines.

A 3-D polygonal prism is drawn as its projected outline on the (X,Y) plane. In addition edge 1 is drawn as a dashed line.

The reference point of a body is marked with a small cross and the body number is written slightly to the right of this.

When the plane is completed graphical editing is enabled. This is described fully in the GRAPHICAL COMMANDS chapter.

3.13 LX 80 PROFILE

This command causes a profile similar to that produced by the PLOT PROFILE command to be plotted on the LX 80 printer. If there is more than one body in the model then user may request calculated profiles for each body to be plotted individually. This is done in response to a prompt from GRIN when other plotting is completed.

The scales used are those defined previously by the PROFILE SCALES command.

3.14 LX 80 PLAN

This command causes a plan identical to that produced by the MODEL PLAN command to be plotted on the LX 80 printer. The scales used are those defined by the PLAN SCALE command.

3.15 LX 80 RESOLUTION

There are two kinds of resolution which can be used for the above ploting process. Firstly, by using low resolution, in which a standard quality of result can be achieved. Secondly, by using high resolution, in which a better quality of result is produced.

3.16 LIST BODY

When this command is invoked, the user is prompted to type in a body number. The description and parameters defining that body are then listed on the terminal. The flags associated with the body are not listed.

3.17 LIST INPUT

This command causes all the parameters used in the most recent READ DATA command to be listed on the terminal along with the profile title, the number of data points read from the file, and details of the profile line fitted to the data by the program.

The current values of the regional field parameters are also listed.

3.18 PRINT MODEL

PRINT MODEL command causes full details of the current model to be sent direct to the line printer. The printout consists of the information from the LIST INPUT command, the model title, and the information from a LIST BODY command for each body currently included in the model.

3.19 PLOT PROFILE

PLOT PROFILE initiates calculation and plotting of profiles according to the following scheme.

1. *First plotting phase*
The outline and profile for any bodies that have been altered are erased, so that the new outline and corresponding profile can be plotted after the necessary recalculations. The profile of the summed gravity field due to all bodies is erased. If a fresh plot was requested by an earlier command (for example the MODEL TITLE command) then the whole plot is erased, and replotted with the exclusion of parts that would otherwise have been erased anyway.

2. *Calculation phase*
Gravity calculations are performed for bodies that are newly defined or that have had parameters altered.

3. *Second plotting phase*
The outlines of all bodies that are included in the model but are not plotted so far are added to the plot as follows:

A dyke, a 2-D polygonal prism or a 3-D polygonal prism is represented by drawing the polygon that is its cross-section in the (P,Z) plane. (The polygon is a parallelogram in the case of a dyke.) A 3-D polygonal prism is treated as 2-D for the purpose of plotting the cross section.

The corners of a rectangular prism are projected normally on to the (P,Z) plane and are connected to form a 'wire diagram'. The face parallel to the (A,C) plane and with minimum B coordinate (refer to figure 13) is drawn with dotted lines and all the other faces with solid lines.

The profile of the summed gravity field due to all included bodies is plotted as a solid curve and the profile of observed data as a dotted curve (every second pixel turned on) with a cross at each observed value.

4. *Graphical editing phase*
This is described below in the GRAPHICAL COMMANDS chapter.

3.20 INVERT LABELS

INVERT LABELS command causes the change of colour from bright to dark and from dark to bright in all labels which are displayed at the bottom of the screen.

Note
There is no effect for the result of modelling processes by using this command except for the convenience of the user during the GRIN session.

3.21 INVERT PLOTS.

A similar effect with the previous command for all the screen except the labels space at the bottom of the screen may be obtained by using INVERT PLOTS command.

Note
There is no effect for the result of modelling processes by using this command except for the convenience of the user during the GRIN session.

3.22 SET PLOT COLOUR

At the time of writing (June 1990), nothing can be obtained by using SET PLOT COLOUR command. Hopefully, this command can be used in the future.

Chapter IV
Graphical Commands

Many of the commands used in Manual Commands may be duplicated using the graphical capability of the terminal. GRIN enables graphical commands immediately after a plot is completed on the screen. As GRIN produces two kinds of screen plot - profile and plan -, there are two groups of graphical editing commands.

Commands are executed by moving the graphics cursor and/or pressing specified alphanumeric keys. When in graphical editing mode it is not necessary to type a carriage return to complete a command. A carriage return is used only to terminate graphical editing.

To abort a multi-key command if you make a mistake, simply complete the command with an inappropriate key sequence. For example, if an R was entered as the start of an RR command, then entering an A (or any character other than R) instead of the second R will cause the command to be ignored.

Take care that these commands stay in phase. If the first character of a multi-character command is entered and for some reason the key sequence is not completed, then subsequent commands will be mis-interpreted. For example the sequence

     P   RR

where the second character of the polygon command has been omitted will be interpreted as

     PR   R
     ∧   ∧
      ∧   ∧
  completing polygon   waiting for 2nd character
    command   of regional command

If in doubt, press the RETURN key once or twice to exit graphical editing mode. It can be restarted easily with the appropriate plot command.

4.1 *Graphical commands applicable to a profile plot*

The commands available will be displayed on the terminal if a '?' is typed.

4.1.1 *Mnn (move body)*

On a profile plot the reference point of a body is marked by a small cross with the body number written slightly to the right. To move a body along the profile, set the cursor at the new position of the reference point and key M followed by the two digit body number (e.g. M02 or M 2 for body number 2). The body and profiles will be erased and re-drawn for the new position of the body.

4.1.2 *Alter polygon commands*

A 2-D or 3-D polygonal prism is drawn on a profile as its cross-sectional polygon in the plane of the profile. Each corner of the polygon is marked by a cross. The cross sectional shape of polygonal prisms may be altered by adjusting the appropriate displayed polygons.

First identify the corner that is to be adjusted by positioning the cursor over the associated cross and pressing P. The following alterations may then be made (all polygons with a corner at the cursor position will be affected):

4.1.2.1 *PM (move polygon corner)*

After pressing P, move the cursor to the new position of the corner and press M. The polygon and profiles will be erased and re-drawn for the new body shape.

4.1.2.2 *PN (insert new polygon corner)*

After pressing P at the last corner before the new corner position, move the cursor to the desired position and then press N. A new corner will be inserted after the one at which the cursor was positioned when P was pressed. The polygon and profiles will be erased and re-drawn for the new body shape.

Note
If the polygon already has 10 corners, the command will be ignored.

4.1.2.3 *PK (kill existing polygon corner)*

After pressing P, press K. The corner will be deleted. The polygon and profiles will be erased and re-drawn for the new body shape.

The first corner, which represents the edge on which the reference point lies, may not be deleted and an attempt to do so will cause the command to be ignored.

4.1.3 *K (kill observation)*

Position the cursor over the cross corresponding to an unwanted observation and press K. The observation will be deleted and the profiles adjusted accordingly.

This command compresses the data arrays in memory and reduces the recorded number of input observations by one. A deleted point can be recovered only by re-reading the data file.

Note
Even if the first or last point of a profile is deleted, the profile line will be the same length as before. If necessary, use the SAVE PROFILE command to save the edited observations as a file and read them back again with a READ DATA command

4.1.4 *RR (subtract regional gradient)*

Define a linear regional gradient and subtract it from the displayed profile. Position the cursor at any point on the gradient line and press R. Then position it at another point on the gradient line and press R again. New end values of the regional gradient (see REGIONAL FIELD command) will be calculated.

The plot will be erased and re-drawn with the regional gradient removed. The gravity axis will be re-scaled automatically.

4.1.5 *TT (toggle plan plot)*

This commmand enables the user to go to the model plan plot for a quick look during the profile plot session by pressing T key, then to go back to profile plot just simply by pressing T key again.

4.1.6 *Bnn (plot individual body profile)*

Press B followed by the two digit body number to cause the calculated profile for that body to be drawn as a dotted curve. The body number is written halfway along the curve.

4.1.7 *Cnnpp (change a single parameter)*

A body is defined by up to 30 parameters which are numbered in the order in which they are displayed on the data form (tables 3 and 4). The C command may be used to adjust a single parameter (pp) of a body (nn) directly without leaving graphical editing mode. The C command causes the body number, its description, and the current value of the nominated parameter to be listed at the top of the screen. A new parameter value may then be keyed in, followed by RETURN. For example, if body 5 were a 2-D polygonal prism the sequence C0525 would cause parameter number 25 (the density contrast in this case) to be displayed at the top of the screen. GRIN then waits for the user to key in a new value, followed by the RETURN key. To abort the command enter an illegal quantity such as an alphabetic character instead of a number.

If the body specified is not included in the model, or the parameter number is not in the range 1 to 30, command is ignored.

Note
This is a dangerous command as it circumvents the value checking that is done by GRIN when parameters are entered via a data form. Any value may be entered for any parameter so that it is possible to enter accidentally such unphysical quantities as negative widths or negative depths. Tables 3 and 4 give the legal (but not necessarily geologically sensible) ranges of parameter values.

4.1.8 *F (generate fresh plot)*

Sections of plot are often erased inadvertently due to overlapping body outlines and profiles. Pressing F causes a complete redrawing of the displayed profile plot.

4.1.9 *Unn (Un-include body nn)*

Press U key followed by the two digit body number to cause the body and its gravity effect to disappear temporarily from the profile plot without altering any of its parameters.

4.1.10 *Inn (Include body nn)*

To restore the body and its effect which has been cleared by Unn command, press I key and followed by the two digit body number.

4.2 *Graphical commands applicable to a plan plot*

The six following commands can be used for this purpose

4.2.1 *Mnn (move body)*

On the plan the reference point of a body is marked by a small cross with the body number written slightly to the right. To alter the horizontal position of the body, move the cursor to the new position of the reference point and key in M followed by the two digit body number (e.g. M02 or M 2 for body number 2). The outline of the body will be erased and re-drawn at the new location.

4.2.2 *K (kill observation)*

The position of an observation is marked on the plan by a cross. To remove an observation, position the cursor over the corresponding cross and press K.

This command compresses the data arrays in memory and reduces the recorded number of input observations by one. A deleted point can be recovered only by re-reading the data file.

Note
Even if the first or last point of a profile is deleted, the profile line will be the same length as before. If necessary use the SAVE PROFILE command to save the edited observations as a file and read them back again with a READ DATA command.

4.2.3 *TT (toggle profile plot)*

This command enables the user to go to profile plot for a quick look during the plan plot session by pressing T key. Then to go back to model plan plot just simply press T key again.

4.2.4 *Cnnpp (change a single parameter)*

A body is defined by up to 30 parameters which are numbered in the order in which they are displayed on the data form (tables 3 and 4). The C command may be used to adjust a

single parameter (pp) of a body (nn) directly without leaving graphical editing mode. The C command causes the body number, its description, and the current value of the nominated parameter to be listed at the top of the screen. A new parameter value may then be keyed in, followed by RETURN. For example, if body 5 were a 2-D polygonal prism the sequence C0525 would cause parameter number 25 (the density contrast in this case) to be displayed at the top of the screen. GRIN then waits for the user to key in a new value, followed by the RETURN key. To abort the command enter an illegal quantity such as an alphabetic character instead of a number.

If the body specified is not included in the model, or the parameter number is not in the range 1 to 30, command is ignored.

Note
This is a dangerous command as it circumvents the value checking that is done by GRIN when parameters are entered via a data form. Any value may be entered for any parameter so that it is possible to enter accidentally such unphysical quantities as negative widths or negative depths. Tables 3 and 4 give the legal (but not necessarily geologically sensible) ranges of parameter values.

4.2.5 *Unn (Un-include body nn)*

Press U key followed by the two digit body number to cause the body to disappear temporarily from the plan plot without altering its parameters.

4.2.6 *Inn (include body nn)*

To restore the body which has been cleared by Unn command, press I key followed by the two digit body number.

Chapter V
Demonstration Tutorial

This chapter gives general step by step instructions for using GRIN with an example set of data and a simple model.

5.1 *Run GRIN*
Enter GRIN, and then after a short pause the ten labels of the main menu will be displayed across the bottom of the screen.

5.2 *Data input*
As the first step we should go to main menu number 1 (DATA MENU) by pressing key 1, and then five labels of the menu which consist of READ DATA, REGIONAL FIELD, SAVE PROFILE, PROFILE TITLE and MAIN MENU will be displayed across the bottom of the screen. Again we press key number 1 since the READ DATA instruction, which is on label no 1, should be used for entering the observed gravity data. The user is prompted to input the file name including the file directory if necessary, followed by return. The key menus will be displayed again and then we go back to the main menu by pressing key number 0 (MAIN MENU).

5.3 *Plotting*
At this stage in which the input data has already been in GRIN memory, we can go to PLOT MENU session by pressing key number 3. As the key menus are displayed on the screen, we press key number 3 for MODEL PLAN and then the plan of the station distribution of the data just read from file will be drawn on the screen (fig 2). When finished with this stage, we go back to main menu.

Although the model of the body has not been created yet, the gravity data profile can be drawn by using key number 9 on the main menu. To clarify the relationship between model plan and profile plot, let us compare them.
The horizontal distance axis which is used on the plot profile is the regression line drawn through the stations on the model plan. Moreover, the left end side of the profile is the southern end of the regression line.
When finished with this stage we go back to the main menu.

5.4 *Model input*

There are two options which can be used at this stage.

5.4:1 *New model input*
Press key number 2 on main menu (MODEL MENU) and then the six labels menu will be displayed across the screen. Since we do not have a model file, we create the model file by using key number 1 (EDIT MODEL). Alternatively we can go directly to this menu by using key number 8 on the main menu (EDIT MODEL).
First of all, GRIN prompts the user to enter the body number and body type (fig 7), followed by return. Then the user is prompted to input several parameters for a model input (fig 8 or 10 or 12 or 14), followed by return. Then GRIN will automatically go back to the main menu.

5.4.2 *Old model input*

After we enter on MODEL MENU session, choose key number 3 (READ MODEL), then GRIN prompts the user to enter the existing model file name followed by return. As soon as the model file name is received, GRIN will go back automatically to the main menu.

5.5 *Copying a body*

Sometimes it is very useful to create a second body by copying it from an existing body, because it is much faster than generating it by typing its parameters into data form. First of all use EDIT MODEL menu on main menu. When GRIN prompts the user to enter the body number and type of the body, just press return. Then when GRIN prompts the user to enter the body's parameters, change body number 1 with body number 2 and then directly press return. If we go to PLOT PROFILE on the main menu, two identical bodies can be observed overlying each other. By using *Mnn (move body)* command on graphical command (see chapter 4), the body number 2 may be moved away from its current position. As an effect of the erasing and re-plotting process, body number 1 seems to disappear. To redraw body number 1, use *F (generate fresh plot)* command on graphical command and then body number 1 will be redrawn.

Note
This way can only be used for copying a body of the same type as the existing body.

5.6 *Modelling process*

To start with the modelling process, we go to MODEL PLAN session and / or go to PLOT PROFILE session (step 3 above). At this stage we frequently use graphical commands utilities (for details, see chapter 4), step 3 and 4 together, until the desired model is created.

5.7 *Save model*
Once we are satisfied with our model or models, we can save it by using SAVE MODEL command on MODEL MENU session. Again at this stage, the user is prompted to enter the model file name to be stored on a disc file.

5.8 *Hard copy*

The result of the above processes can be printed on the printer by using LX 80 PROFILE command for the plot profile copy and LX 80 PLAN command for the model plan copy. Both of those commands are available on the PLOT MENU session.
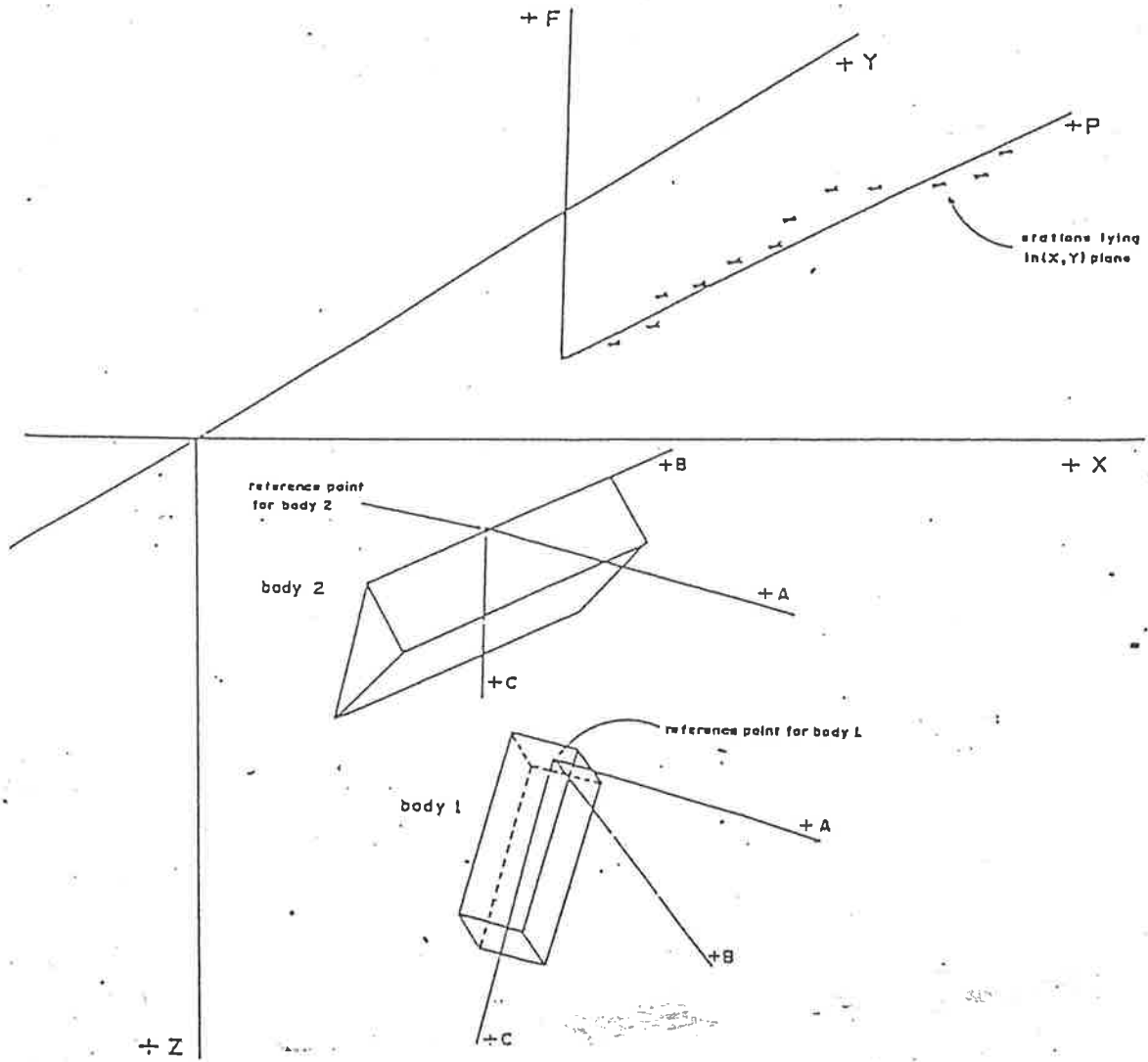
Figure 1. Axes used by GRIN.
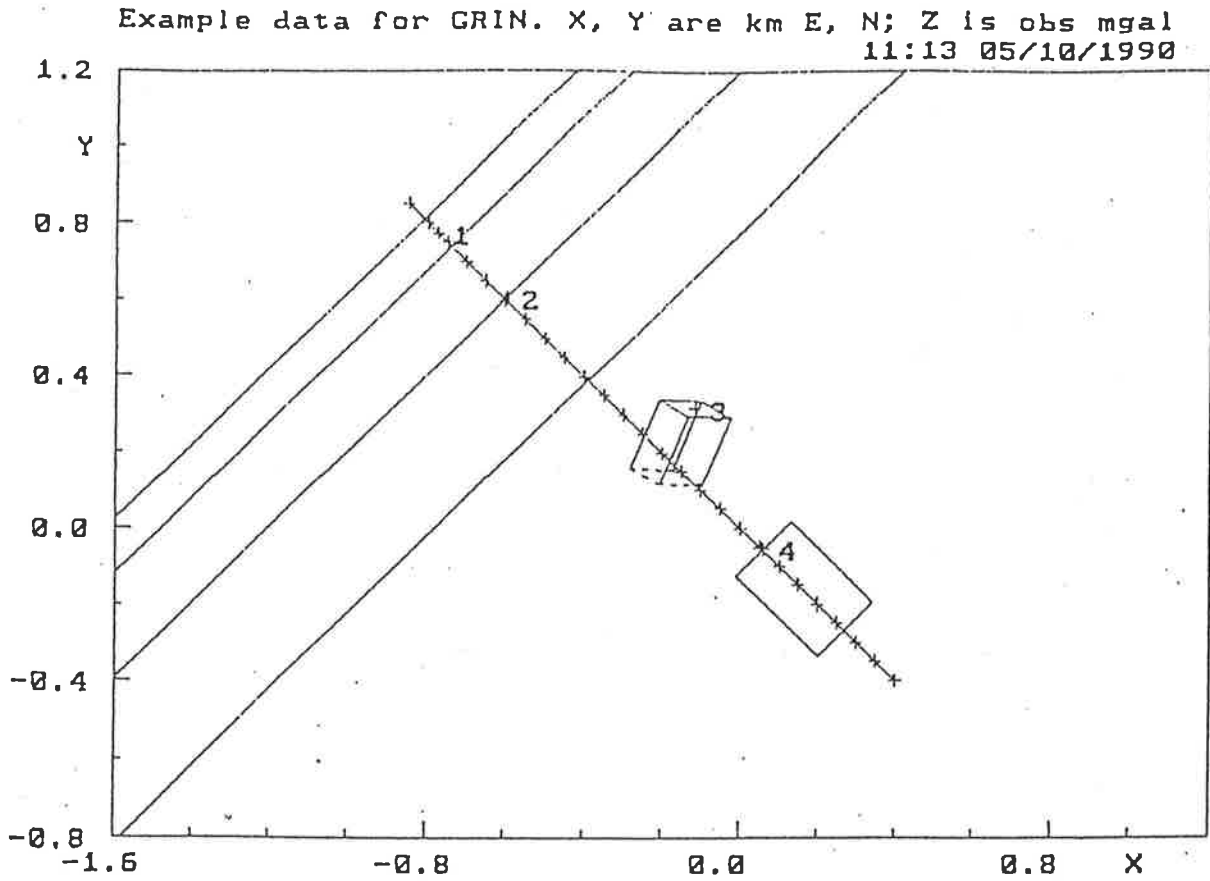
Figure 2. Typical MODEL PLAN.
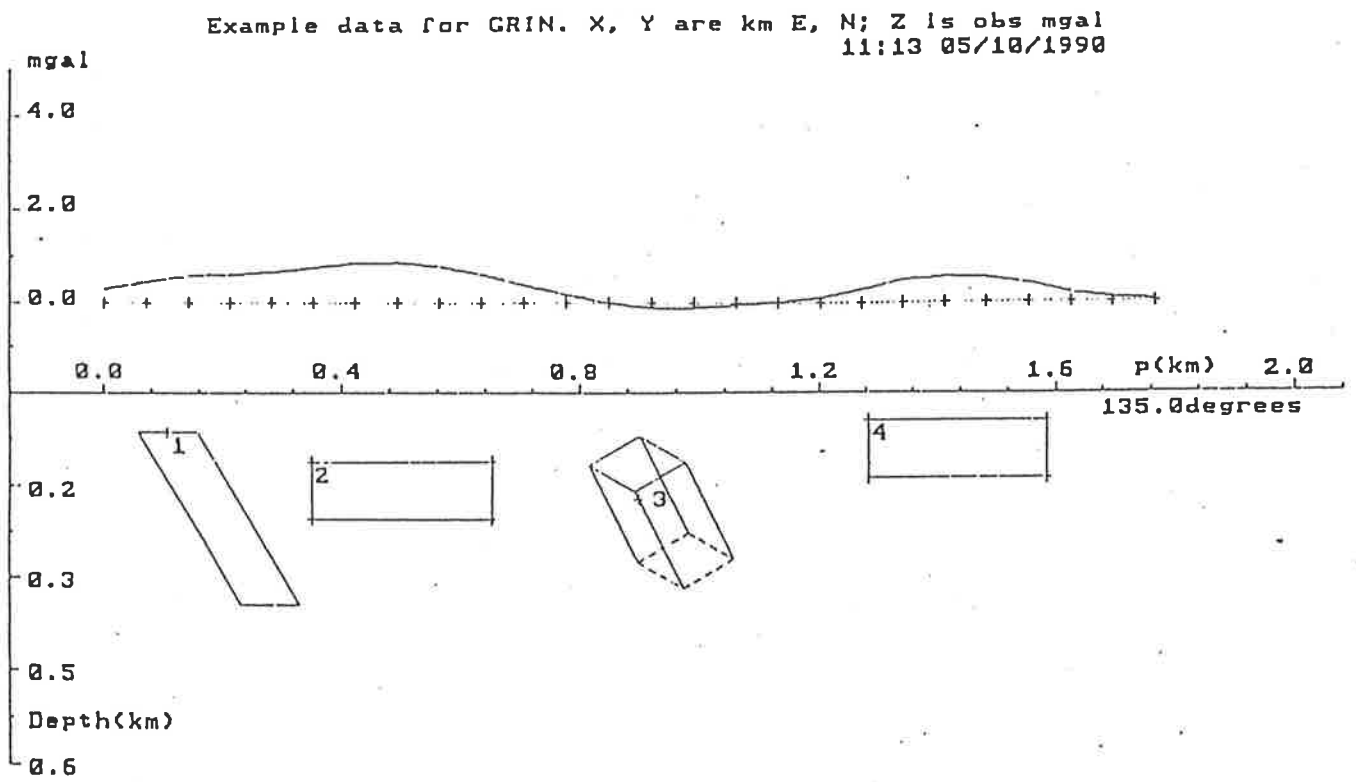
Figure 3. Typical PLOT PROFILE.
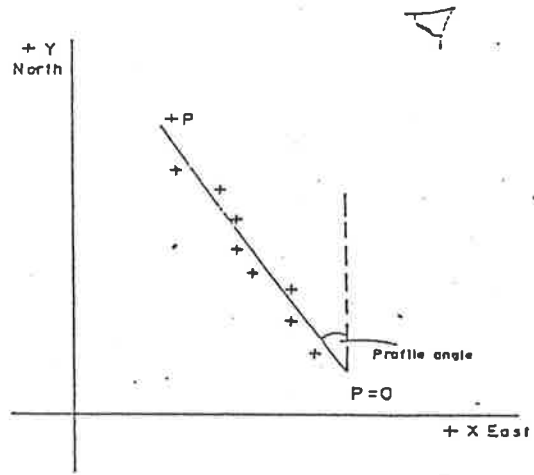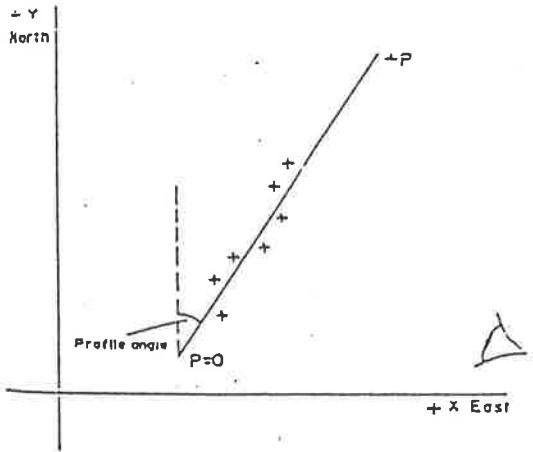
In these examples the viewpoint is in the eastern half plane, as profile angle <45^0. Therefore the southern end of the profile is at the left (P=0).
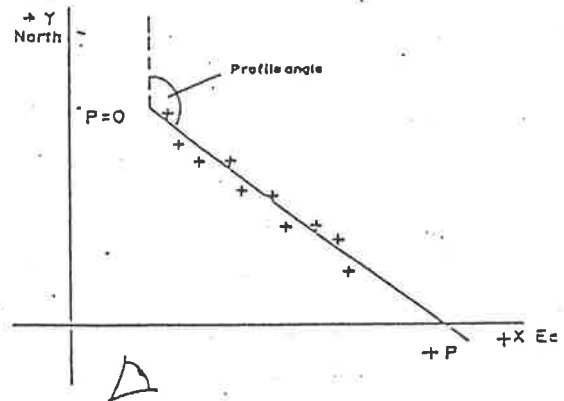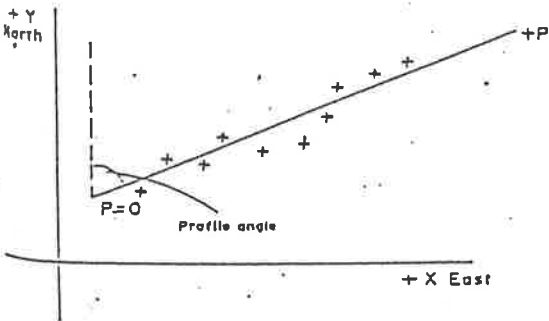
Here the viewpoint is in the southern half plane, as profile angle >45^0. Therefore the western end of the profile is to the left.

Figure 4. Viewpoints for the profile plot.

READ OBSERVATIONS FROM FILE

NAME OF INPUT FILE

      SAMPLE INTERVAL   1
      LOWER LIMIT   X -0.100000E+20   Y -0.100000E+20
      UPPER LIMIT   X -0.100000E+20   Y -0.100000E+20

REFERENCE VALUES AND SCALE FACTORS
                            X 0.00000E+00   1.00000E+00
                            Y 0.00000E+00   1.00000E+00
                            Z 0.00000E+00   1.00000E+00

Figure 5. READ DATA form.

DEFINE REGIONAL GRADIENT

Regional value at left end of profile   0.0

Regional value at right end of profile   0.0

Figure 6. REGIONAL FIELD data form.

```
              SUMMARY OF BODIES DEFINING CURRENT MODEL
Available body types are :    1 - 2-D dyke
                              2 - 2-D polygonal prism
                              3 - 3-D rectangular prism
                              4 - 3-D polygonal prism


Model title

number, type of body to be edited
BODY  TYPE  INCLUDED                    BODY   TYPE   INCLUDED
  1                                       2
  3                                       4
  5                                       6
  7                                       8
  9                                      10
 11                                      12
 13                                      14
 15                                      16
 17                                      18
 19                                      20
```

Figure 7. SET/EDIT BODY data form.

```
BODY NUMBER __TYPE 2-D DYKE    Distances must be in kilometres
Description

SHAPE
Width
Depth extent
Dip
POSITION
Reference point (any point        | Xr
on top of centreline of dyke)     | Yr
                                  | Zr

Strike re' +Y axis
PHYSICAL PROPERTIES
Density contrast (gms/cc)

Body is to be INCLUDED in current model
```

Figure 8. Data form for a 2-D dyke.
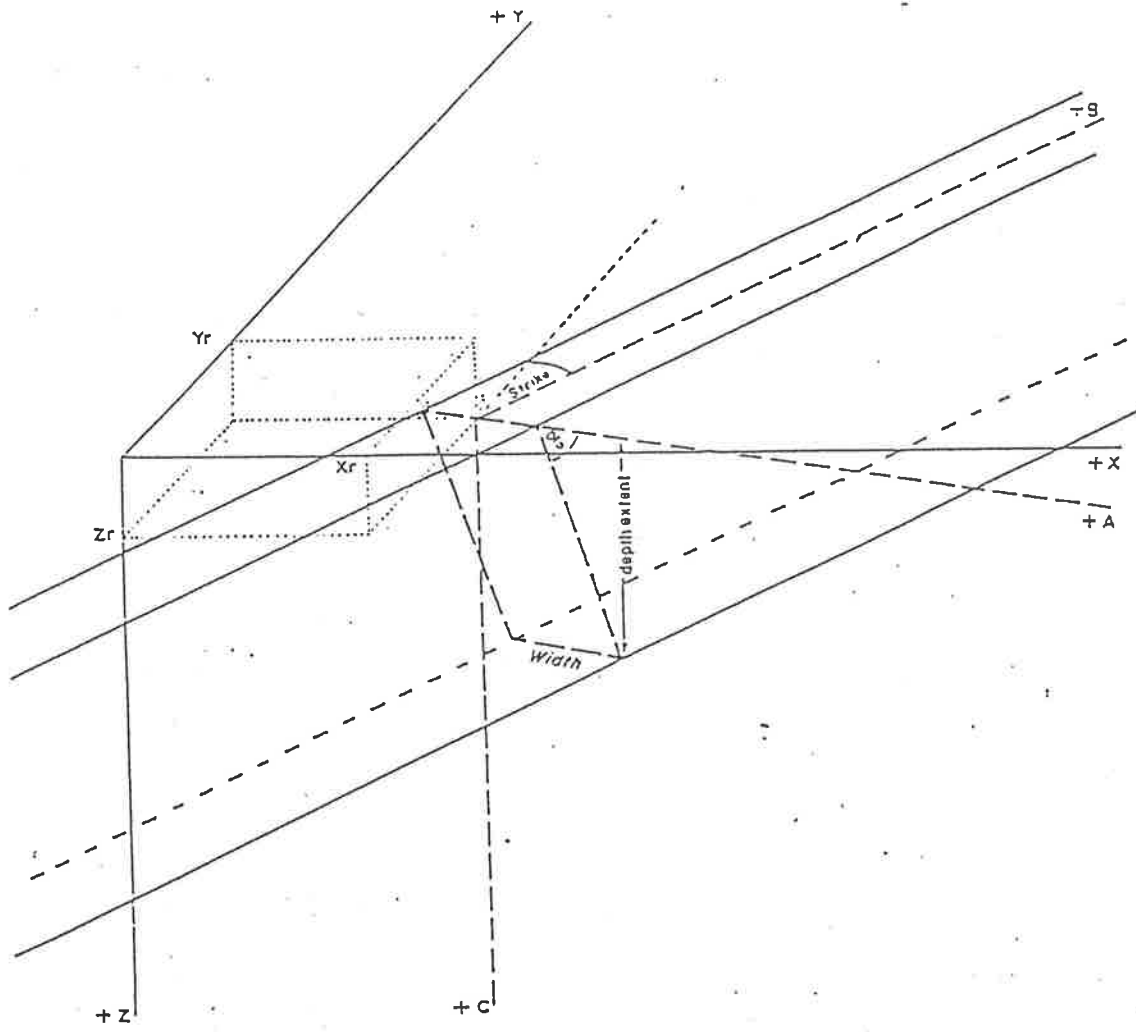
Figure 9. Definition of a 2-D dyke.

```
BODY NUMBER ___ TYPE 2-D POLYGONAL PRISM  Distances must be
                                                    in kilometres
Description

SHAPE                                       A              C
Coordinates of edges      1           0.0000         0.0000
relative to edge 1        2
in a plane normal to      3
strike                    4
                          5
                          6
                          7
                          8
                          9
                         10
POSITION
Reference point (any point          | Xr
on edge 1)                          | Yr
                                    | Zr

Strike re' +Y axis
PHYSICAL PROPERTIES
Density contrast (gms/cc)

Body is to be INCLUDED in current model
```

Figure 10. Data form for a 2-D polygonal prisms.
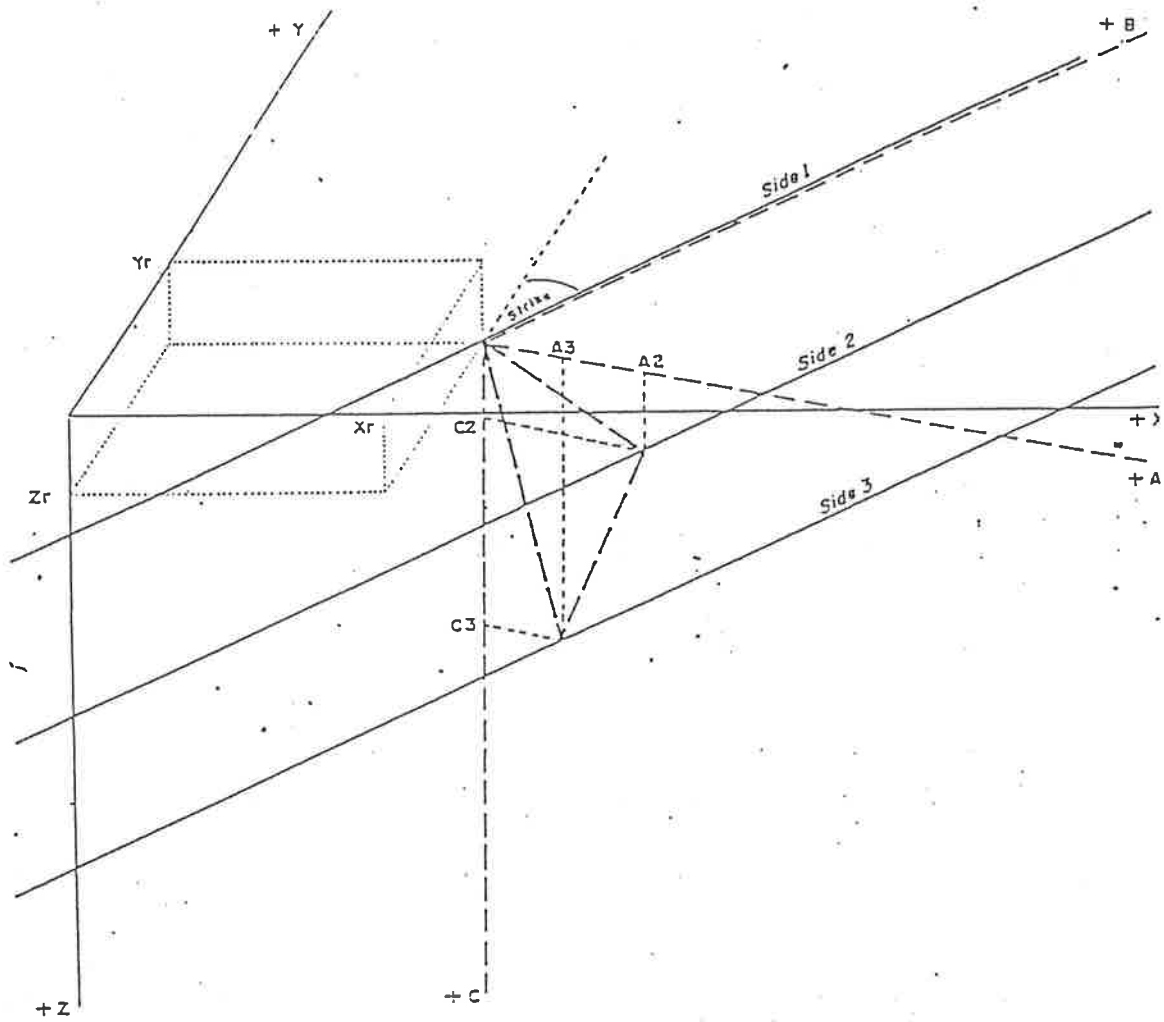
Figure 11. Definition of a 2-D polygonal prism.

```
BODY NUMBER  __  TYPE 3-D RECTANGULAR PRISM  Distances must be
                                                  in kilometres
Description

SHAPE
Thickness
Strike length
Height
POSITION
Reference point (any point          | Xr
on top of centre of prism    )      | Yr
                                    | Zr

Strike re' +Y axis
Dip to +X
Plunge to +Y
PHYSICAL PROPERTIES
Density contrast (gms/cc)

Body is to be INCLUDED in current model
```

Figure 12. Data form for a 3-D rectangular prism.
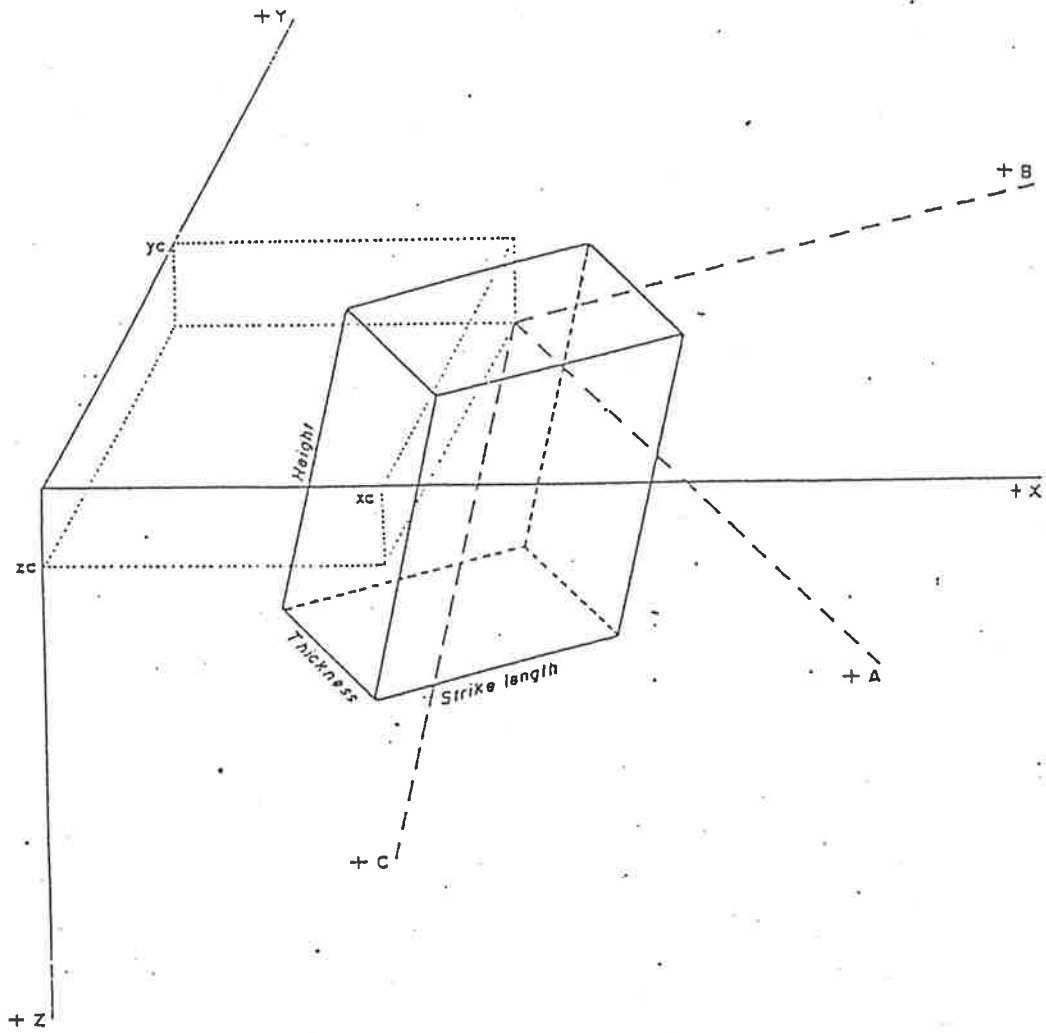
Figure 13. Definition of a 3-D rectangular prism.

```
BODY NUMBER ___ TYPE 3-D POLYGONAL PRISM  Distances must be
                                              in kilometres
Description

SHAPE                                    A              C
Coordinates of edges    1        0.0000           0.0000
relative to edge 1      2
in a plane normal to    3
strike                  4
                        5
                        6
                        7
                        8
                        9
                       10
Strike length of prism
POSITION
Reference point (any point    | Xr
on edge 1)                    | Yr
                             | Zr

Strike re' +Y axis
PHYSICAL PROPERTIES
Density contrast (gms/cc)

Body is to be INCLUDED in current model
```

Figure 14. Data form for a 3-D polygonal prism.
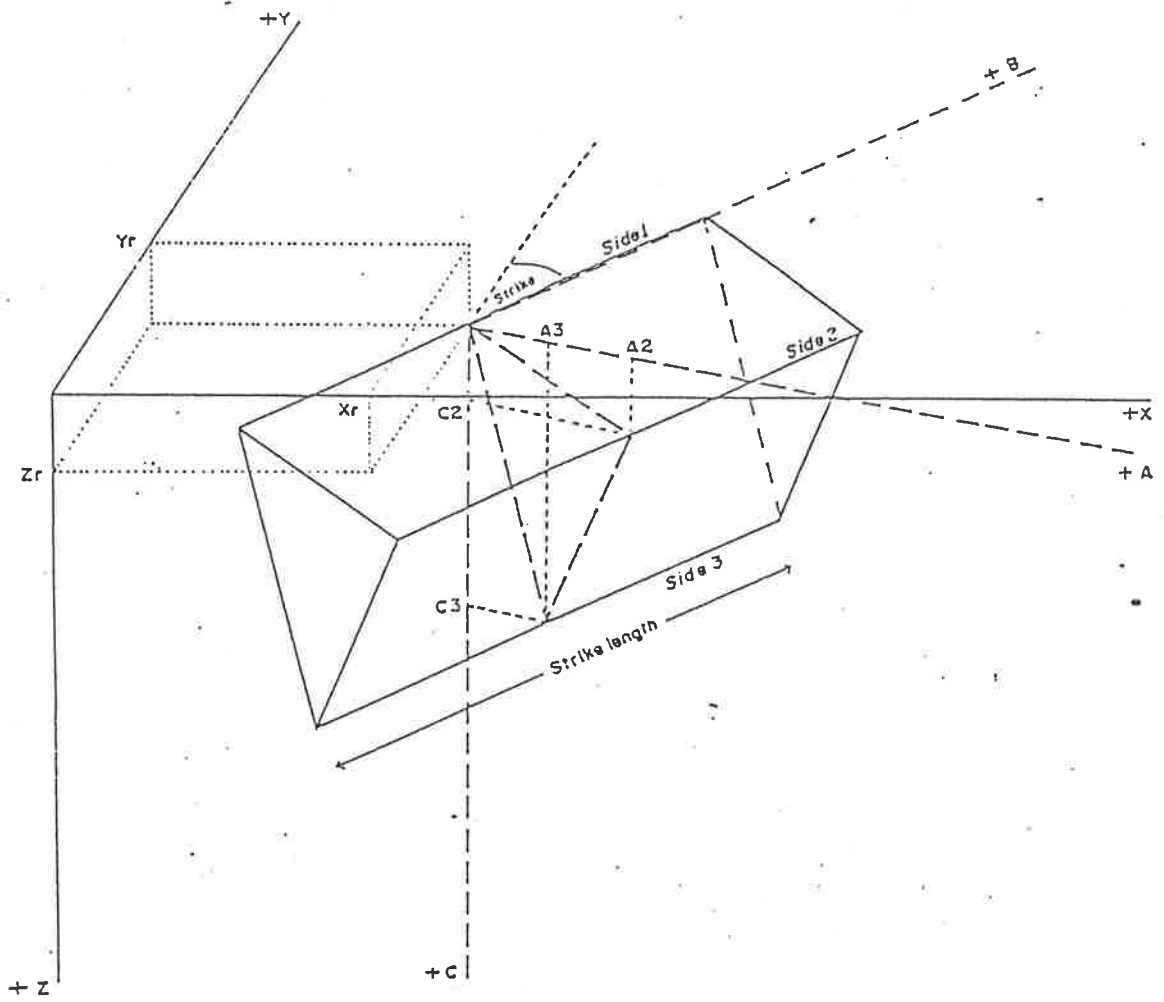
Figure 15. Definition of a 3-D polygonal prism.

DEFINE SCALES AND OFFSETS FOR PROFILE PLOT

```
scale for distance axis
offset for distance axis

scale for gravity axis
offset for gravity axis

scale for depth axis
offset for depth axis
```

Figure 16. PROFILE SCALES data form.

DEFINE SCALES AND OFFSETS FOR PLAN PLOT

```
scale for X-axis
offset for X-axis

scale for Y-axis
offset for Y-axis
```

Figure 17. PLAN SCALES data form.

CHANGE LX80 PLOTTING RESOLUTION

Set plotting resolution for LX80 to either High or Low
Plotting resolution (H or L).

Figure 18. LX80 RESOLUTION data form.

```
Data  ----------------------------------------------------------+
Menu                                                            |
                                                                |
Model  ----------------------------------------------+          |
Menu                                                 |          |
                                                     |          |
Plot  ------------------------------------+          |          |
Menu                                      |          |          |
                                          |          |          |
Inspect  ----------------------+          |          |          |
Menu                           |          |          |          |
                               |          |          |          |
Display  --------+             |          |          |          |
Menu             |             |          |          |          |
                 V             V          V          V          V
+++++++      Invert        List       Profile    Edit       Read
+++++++      Labels        Body       Scales     Model      Data

+++++++      Invert        List       Plan       Save       Regional
+++++++      Plots         Input      Scales     Model      Field

Edit         Set Plot      Print      Model      Read       Save
Model        Colour        Model      Plan       Model      Profile

Plot         +++++++       +++++      LX 80      Model      Profile
Profile      +++++++       +++++      Profile    Title      Title

Finish       +++++++       +++++      LX 80      Clear      +++++++
   |         +++++++       +++++      Plan       Body       +++++++
   |
   |         +++++++       +++++      LX 80      +++++      +++++++
   |         +++++++       +++++      Resolution +++++      +++++++
   |
   |         +++++++       +++++      ++++++     +++++      +++++++
   |         +++++++       +++++      ++++++     +++++      +++++++
   |
   |         +++++++       +++++      ++++++     +++++      +++++++
   |         +++++++       +++++      ++++++     +++++      +++++++
   |
   |         +++++++       +++++      ++++++     ++++       +++++++
   |         +++++++       +++++      ++++++     ++++       +++++++
   |
   |         Main          Main       Main       Main       Main
   |         Menu          Menu       Menu       Menu       Menu
   |          |             |          |          |          |
   |          V             V          V          V          V
   +----<------+-------<---+----<---+----<----+--<----+
```

Table 1. Key menus flow chart defined by GRIN and their inter-relationship. The ten key labels in each menu are displayed in columns. The main menu is on the left side. Undefimed labels are filled with crosses for clarify.

```
Input data gravity observed for GRIN
This data is artificial
    378.8500        9870.5420         9.10
    378.7650        9854.7890        10.56
    377.8900        9851.9087        13.75
    377.2300        9847.1009        15.45
    376.5423        9843.0007        17.90
    375.0290        9841.7000        19.00
    374.9088        9841.0076        20.54
    373.5580        9840.5690        18.79
    373.1090        9838.4500        16.90
    372.4578        9837.5000        14.50
    370.9999        9835.9078        12.00
    368.9000        9835.0229        10.97
    366.6666        9833.9090         9.78
    365.9090        9830.7878         9.00
    364.0098        9828.9890         7.90
    363.9090        9867.9055         7.53
    363.5290        9865.8790         7.02
    362.8670        9864.9800         6.90
    362.4500        9864.2100         6.20
    361.0000        9863.5600         5.10
    360.9875        9863.0099         4.20
    360.5690        9862.5689         3.10
    358.9090        9861.1005         1.95
    358.0098        9860.4957         0.35
    357.7600        9859.5700        -1.95
    357.1500        9859.2050        -2.50
```

Table 2. Example of a data file. The first and second lines are the title. The left and centre columns are easting and northing in kilometres and the right columns is the observed gravity data in milligals.

Param. no.	DYKE	(range)	RECTANGULAR PRISM	(range)
01	Width	(0 to +inf)	Width	(0 to +inf)
02	Depth extent	(0 to +inf)	Strike length	(0 to +inf)
03	Dip	(1 to 179)	Height	(0 to +inf)
04	Xr	(-inf to +inf)	Xr	(-inf to +inf)
05	Yr	(-inf to +inf)	Yr	(-inf to +inf)
06	Zr	(0 to +inf)	Zr	(0 to +inf)
07	Strike	(-90 to +90)	Strike	(-90 to +90)
08	Density contrast	(-inf to +inf)	Dip	(0 to +180)
09	+++++not defined+++++		Plunge	(-90 to +90)
10	+++++not defined+++++		Density contrast	(-inf to +inf)
11-30	+++++not defined+++++		+++++not defined+++++	

Table 3. Significance and legal ranges of parameters for dykes and rectangular prisms.

```
Param.   2-D POLYGONAL   (range)      3-D POLYGONAL (range)
 no.        PRISM                        PRISM

  01        'A' coordinate of edge 1 (must be 0)

02-10     'A' coordinates of edges 2 to 10 (-inf to +inf)

  11        'C' coordinate of edge 1 (must be 0)

12-20     'C' coordinates of edges 2 to 10 (-inf to +inf)

  21      Xr        (-inf to +inf)     Strike
                                       length      (0 to +inf)

  22      Yr        (-inf to +inf)     Xr          (-inf to +inf)

  23      Zr        (0 to +inf)        Yr          (-inf to +inf)

  24      Strike    (-90 to +90)       Zr          (0 to +inf)

  25      Density                      Strike      (-90 to +90)
          contrast  (-inf to +inf)

  26      +++++not defined+++++        Density
                                       contrast    (-inf to +inf)

27-30     +++++not defined+++++        ++++++not defined+++++
```

Table 4. Significance and legal ranges of parameters for 2-D and 3-D polygonal prisms.

APPENDIX B

Easting (metres)	Northing (metres)	Bouguer anomaly (mgals)	Easting (metres)	Northing (metres)	Bouguer anomaly (mgals)
673421.02	9225926.83	-0.96	688898.63	9208910.14	30.55
665820.11	9224490.55	-3.85	680058.73	9206759.20	35.32
668189.38	9224044.22	-3.59	678099.15	9208695.95	36.50
670717.39	9223664.24	-2.08	680720.48	9209739.57	38.94
668268.19	9221916.96	-1.32	681656.29	9211361.85	36.38
665798.77	9219004.94	-3.23	683126.79	9210763.19	45.66
668771.52	9217161.34	0.32	684640.70	9210941.99	44.29
668448.82	9219681.72	1.52	688117.78	9212825.59	45.74
666217.35	9215571.00	2.14	685666.46	9208676.23	42.26
667423.31	9214128.91	3.44	665674.02	9205339.84	25.87
671449.28	9216301.04	1.70	667590.83	9207790.94	27.79
670636.35	9219017.55	4.82	668587.59	9203639.67	32.29
670819.90	9220974.95	2.32	669319.10	9205736.87	41.26
674445.22	9222966.08	2.94	671287.35	9204195.36	45.23
676834.73	9222375.94	4.98	673977.88	9201474.32	44.78
680225.12	9224614.08	2.58	670297.32	9202001.23	36.83
682842.15	9223274.13	3.81	668603.19	9200319.42	37.27
686483.65	9223466.57	4.90	666391.46	9201758.90	37.44
690954.47	9225091.89	2.07	671264.83	9198750.51	37.32
693904.52	9225735.00	0.60	674690.22	9198970.79	41.11
696517.76	9223694.24	3.21	676742.71	9200841.73	43.08
699028.55	9218370.88	2.07	677507.17	9198538.16	31.38
701021.46	9216128.41	4.84	678627.16	9199985.37	33.44
701657.25	9212733.86	3.56	698000.67	9225512.27	-0.69
701540.53	9208891.79	1.72	700868.45	9225762.72	-6.00
701805.69	9206486.19	4.66	700983.52	9223346.07	-6.09
699566.18	9203519.15	0.19	698520.26	9222362.75	-3.81
697601.03	9203010.38	3.02	698836.07	9220668.31	-6.04
693298.71	9199796.87	2.67	701175.88	9221214.62	-6.00
690325.47	9199288.02	2.85	703071.91	9221003.31	-6.00
686918.41	9198295.19	7.50	696280.54	9220847.28	-0.04
685500.80	9199730.54	9.53	697231.50	9218614.72	-2.22
687605.62	9200587.87	9.56	700881.11	9219587.83	-4.41
694569.23	9202421.99	8.10	702881.38	9219044.54	-4.16
698544.39	9204928.02	8.24	702838.20	9216645.91	-4.21
696895.40	9215724.24	9.94	704128.84	9213905.31	-6.36
692331.70	9219704.57	8.47	703415.03	9209793.04	-9.34
694678.19	9222758.79	7.21	704079.91	9205937.51	-9.95
692821.87	9222282.81	6.90	706189.32	9205762.88	-5.57
690432.62	9223093.76	6.83	705691.85	9211734.64	-3.51
689148.59	9219144.27	8.82	711043.23	9211813.65	-4.23
687292.51	9221414.36	6.00	717828.73	9210063.11	-3.00
683931.29	9221064.85	4.25	716705.77	9213096.07	-4.75
679687.10	9222631.60	8.49	716927.66	9207675.02	-4.33
676477.10	9220182.72	8.54	717872.26	9204914.88	-1.11
672473.95	9219780.79	7.15	713414.89	9203412.97	-5.08
674174.62	9217993.76	8.26	712172.08	9205005.57	-17.32
673927.93	9214743.18	9.55	719437.99	9212547.74	-9.09
669941.07	9212783.94	9.83	714688.43	9212989.47	-7.76
667591.92	9212096.40	9.68	712519.27	9213827.17	-7.86
665795.01	9210809.83	21.66	708951.14	9212854.34	-6.04
669978.65	9210518.18	15.61	705871.11	9214567.88	-7.60
670661.07	9208404.90	16.39	707168.18	9216442.56	-9.06
672619.24	9211187.09	15.31	705165.60	9217251.04	-9.27
681184.01	9214688.67	15.58	705607.53	9219762.40	-9.83
690147.12	9215395.17	19.45	705219.78	9222802.26	-6.10
699623.39	9213054.08	18.08	707592.38	9223276.92	-6.68
676049.74	9216326.88	13.90	704086.40	9224788.90	-7.23
679350.18	9217379.45	10.15	713727.38	9225680.41	-6.93
680701.31	9220248.04	12.17	717697.66	9225075.40	-9.77
683450.67	9216965.04	13.58	720035.40	9222859.25	-12.94
683817.43	9218994.14	10.75	717390.59	9223094.85	-9.81
686499.83	9217877.12	14.79	714936.80	9222895.36	-10.19
691244.87	9217638.38	13.27	712140.17	9224005.64	-9.26
693280.16	9216165.92	13.49	710487.70	9223123.36	-11.66
695428.85	9203526.17	11.24	709591.86	9220928.43	-12.01
693197.80	9203985.60	15.17	707848.29	9219293.18	-12.31
691384.61	9202095.77	10.10	710599.86	9218555.51	-16.15
691967.84	9204879.00	14.74	712671.77	9220964.58	-18.21
683676.71	9200345.60	14.18	714393.15	9220159.22	-15.70
682974.61	9198312.23	23.60	717274.85	9220913.38	-15.89
685137.70	9202223.24	15.14	719773.79	9220399.87	-13.74
689136.27	9204523.67	17.38	716974.87	9218601.04	-18.06
681918.92	9202456.57	21.26	719772.58	9217739.39	-18.27
680036.98	9202504.57	22.77	717010.44	9216771.81	-18.00
683234.27	9203562.12	22.75	713796.67	9218012.35	-12.51
684266.83	9205032.75	23.18	711922.55	9216230.64	-11.44
686084.47	9205759.96	24.22	716005.03	9214599.84	-13.24
688255.67	9205906.40	22.52	717987.37	9215329.28	-13.06
696707.67	9213342.88	24.58	720318.87	9215381.49	-14.12
690877.62	9213450.79	22.67	709581.51	9215105.95	-13.38
690644.64	9210656.48	22.57	709378.24	9217235.75	-12.41
687168.49	9215042.44	21.74	714386.48	9211222.87	2.76
677623.89	9214770.95	21.30	713956.93	9208057.25	7.78
673421.63	9205393.87	22.30	710133.03	9208899.04	3.35
673310.59	9207942.14	27.31	707200.56	9209113.75	0.57
675222.02	9203300.98	24.13	709795.16	9205808.47	6.00
678745.77	9204078.04	27.88	707318.56	9203803.32	1.31
681366.38	9204757.15	28.41	704835.58	9203963.62	2.41
695677.13	9206484.81	29.32	704319.87	9201812.82	4.36
695341.32	9209013.61	27.29	703803.95	9199592.69	2.30
692880.96	9212319.66	33.74	706026.59	9200872.54	6.19
685072.97	9214284.88	25.49	708115.98	9200725.74	8.88
678197.46	9212814.31	28.89	709778.04	9200459.14	7.96
675142.89	9211355.92	23.09	711383.39	9199914.87	7.79
674662.07	9209837.91	28.67	712763.11	9202100.19	9.08
675155.47	9206926.93	33.93	714690.24	9199667.01	11.13
677296.26	9204920.50	30.14	715371.03	9198296.66	15.63
677323.71	9210701.91	32.64	717458.33	9198303.92	6.94

Easting (metres)	Northing (metres)	Bouguer anomaly (mgals)	Easting (metres)	Northing (metres)	Bouguer anomaly (mgals)
715871.13	9200788.12	3.92	680094.77	9175575.13	72.96
718525.86	9200657.80	10.73	682836.87	9174943.84	75.02
719800.40	9199396.32	23.34	686480.88	9174907.02	70.35
720256.94	9202130.30	12.53	685555.91	9173124.48	82.47
720077.82	9205722.73	1.14	684054.39	9172069.06	85.47
720284.51	9209067.24	1.19	692503.51	9198017.87	-4.33
695292.06	9198746.36	-5.15	696638.51	9197826.70	-2.44
698514.61	9198544.98	-2.14	699163.52	9197626.35	-0.75
697096.44	9200365.97	-2.08	700994.42	9197143.62	4.09
699951.99	9199664.50	-1.11	697849.24	9196476.23	1.46
701250.78	9199380.88	-4.88	694620.55	9196547.38	4.45
700964.83	9200864.96	-4.04	691898.15	9195799.35	2.42
702353.88	9202223.98	-4.45	689266.97	9197502.35	2.09
672537.52	9213071.18	13.99	688826.02	9194825.11	9.68
667232.35	9195322.88	41.74	700559.33	9195586.96	6.35
666488.49	9192601.71	42.70	702481.04	9196401.05	8.51
669212.23	9192245.70	47.66	703535.08	9197721.40	7.09
671183.37	9194535.53	50.14	705709.98	9195100.11	9.34
672473.55	9191817.75	52.67	703749.47	9193719.16	6.12
674470.62	9193690.61	49.10	702154.91	9194514.13	5.72
674146.83	9196579.49	33.56	699766.42	9194234.74	5.62
677497.28	9196382.67	34.97	698564.07	9191925.92	3.76
678772.64	9194402.63	35.11	697130.65	9190506.92	6.04
677990.72	9192030.77	37.77	696624.00	9194960.26	12.68
675076.50	9191314.74	42.73	691380.73	9193500.58	11.94
677509.38	9189538.24	34.77	700598.69	9190889.27	14.15
674199.17	9188820.01	41.61	702607.94	9191242.30	9.34
672395.64	9188969.65	44.45	703275.11	9188210.33	14.08
670413.98	9189060.92	45.28	702099.20	9186835.40	10.11
668740.78	9189013.62	47.88	704776.43	9187505.37	10.00
665968.83	9188959.64	46.27	704908.14	9189410.31	1.16
670105.94	9186816.20	38.12	704846.42	9192060.21	4.52
666641.84	9186348.84	39.57	707287.73	9184126.59	11.82
672188.59	9186422.95	40.34	707997.86	9186569.99	13.33
672996.29	9184444.44	40.71	706381.88	9188664.20	14.38
670293.04	9184618.64	41.09	710240.10	9187489.70	12.82
667819.39	9184821.20	41.14	710991.22	9189730.01	12.72
666465.64	9182823.27	56.25	709878.15	9189301.62	16.09
669204.40	9182275.00	44.16	707766.41	9190522.04	14.99
671292.47	9182831.12	45.63	708377.73	9192094.30	16.58
671356.14	9181474.68	45.88	710386.79	9194879.69	17.08
668625.80	9179815.83	48.69	710069.00	9196786.84	16.86
669977.49	9179425.38	46.95	708200.09	9194217.51	10.93
668607.57	9178863.38	51.95	706692.24	9192607.75	10.60
666083.69	9179206.11	59.99	710941.36	9191656.19	12.07
666962.68	9177055.70	53.12	711795.65	9193015.08	12.71
667974.42	9175889.45	53.53	712202.86	9195174.62	10.42
669592.22	9176640.12	49.81	712845.98	9197273.65	11.78
671433.37	9177508.30	44.20	713803.29	9190864.55	13.95
671521.82	9175818.54	59.11	714896.96	9192699.04	11.56
670284.40	9174504.71	68.46	716549.85	9191319.50	4.32
668249.66	9173596.35	72.51	720106.11	9192625.42	-12.79
666175.41	9172585.90	76.76	719239.57	9195902.51	12.94
670304.69	9172360.98	86.46	716700.50	9195804.42	16.42
668526.26	9170806.72	91.57	714939.86	9195992.55	21.32
673559.13	9171231.46	90.15	713629.59	9194713.94	21.57
676954.28	9171657.04	92.21	717941.46	9187135.52	14.67
678164.80	9172290.69	91.08	692488.84	9192781.11	14.51
678734.84	9174045.18	81.37	687291.13	9193786.20	16.56
676851.50	9174656.43	73.89	688694.24	9191317.67	18.56
674780.26	9174389.09	72.59	692938.90	9187192.78	19.85
672700.63	9174177.75	70.13	694468.34	9187510.20	19.01
675592.95	9176342.43	58.72	699978.94	9188288.31	19.07
674001.23	9177119.94	50.90	698757.18	9186825.09	19.82
678803.56	9177418.91	61.39	699129.42	9184782.97	15.37
677642.53	9179663.99	48.37	701971.34	9184540.60	17.04
675242.02	9179361.38	44.08	704933.74	9184263.97	19.02
673602.00	9178543.72	43.23	709614.65	9184735.47	18.99
676725.82	9180798.74	40.09	713428.96	9184808.65	19.45
672562.13	9180303.20	41.85	713315.52	9186641.07	17.51
673175.59	9182251.48	41.60	712925.80	9188059.35	16.03
679448.27	9181895.39	41.87	715245.11	9188160.10	17.37
677239.41	9185527.85	37.16	717123.54	9188375.19	15.11
676555.76	9183073.77	37.61	715529.62	9186332.23	24.44
674896.60	9185296.51	37.09	714886.51	9183847.39	21.35
674138.53	9186802.13	39.98	711059.72	9182889.26	24.94
676591.92	9187376.42	35.57	708807.75	9182524.71	25.14
679425.91	9185201.87	37.56	697196.84	9183369.79	23.27
684883.62	9197927.16	19.20	696704.33	9185838.43	21.39
686641.07	9196406.56	10.51	696874.93	9187991.65	21.81
683134.40	9195441.96	23.84	691090.47	9188086.80	22.68
684573.65	9192237.68	24.17	692532.10	9190564.00	23.20
684823.77	9190875.08	21.49	695093.43	9193249.60	23.78
682826.87	9190560.84	23.79	687435.12	9188568.01	20.97
680568.03	9192322.20	34.49	689955.53	9186658.39	27.10
679903.38	9188390.02	35.45	693333.65	9184799.82	26.11
683823.59	9187979.88	30.78	701122.48	9182457.53	25.94
685809.83	9185745.21	40.35	704789.70	9182416.28	27.12
683184.33	9185239.98	40.24	717828.02	9184259.05	28.23
681194.51	9185573.65	40.00	719766.55	9183234.67	28.86
686657.02	9184448.69	40.69	716657.61	9182724.09	29.19
682337.02	9181794.38	43.01	704794.44	9182446.93	27.12
684348.47	9181758.69	40.92	694542.58	9182269.04	32.40
686585.99	9181827.80	40.90	698463.89	9181710.93	31.13
679847.82	9179849.59	54.23	710957.15	9180965.08	32.98
681338.29	9179195.66	58.85	719589.17	9181112.36	37.50
682974.40	9179134.60	58.55	715096.63	9181605.34	35.27
685317.71	9179515.60	56.64	712464.40	9179680.38	34.90
681759.43	9175870.79	73.24	707734.24	9179749.84	36.27

Easting (metres)	Northing (metres)	Bouguer anomaly (mgals)	Easting (metres)	Northing (metres)	Bouguer anomaly (metres)
703096.30	9181291.42	35.78	637736.42	9157698.43	64.00
697451.76	9180260.93	39.48	626585.01	9155995.50	64.00
695970.77	9181443.13	36.08	626042.61	9159003.18	64.00
691978.65	9182357.09	36.60	612292.86	9157259.13	64.00
690011.72	9184796.58	37.49	631982.72	9159524.37	65.00
689565.28	9182459.72	42.81	628821.28	9158602.40	65.00
695532.68	9178183.24	40.79	632410.78	9161448.08	66.00
700607.25	9179624.19	40.70	629985.77	9160896.11	66.00
702940.18	9178967.01	41.36	624458.37	9157736.21	66.00
704441.68	9178822.21	43.28	625442.20	9155704.88	66.00
719288.70	9177258.84	47.67	633846.34	9156288.87	66.00
718857.85	9179169.54	45.67	622600.23	9155277.40	67.00
717425.08	9180001.47	45.60	629816.10	9155323.39	67.00
715106.90	9178751.17	45.68	634761.85	9154482.32	67.00
711961.12	9177498.71	48.82	636995.86	9156153.85	67.00
710283.00	9178980.35	45.47	640087.13	9155822.71	67.00
696748.28	9177176.04	44.59	635785.26	9162432.10	67.00
693398.85	9177805.57	45.68	638151.92	9166285.33	68.00
691739.91	9178496.30	49.31	638703.00	9159186.88	68.00
689601.55	9180556.92	54.04	640258.12	9158104.74	68.00
689492.05	9177837.02	53.14	636712.70	9154254.71	68.00
707624.78	9175836.94	52.55	634465.78	9152766.96	69.00
714455.08	9176587.87	51.02	639740.56	9153951.16	71.00
717719.56	9176857.09	54.28	640883.77	9170234.42	72.00
717993.64	9174809.34	57.53	637243.66	9161422.15	72.00
718808.06	9172643.01	56.02	642530.91	9155311.59	72.00
719375.75	9170820.55	50.40	636434.43	9152584.84	72.00
716237.82	9172895.41	51.75	631902.90	9152723.66	73.00
715020.94	9174298.86	51.62	618894.89	9154043.30	73.00
714683.84	9172308.00	56.39	641362.70	9151846.46	74.00
715702.81	9170794.77	45.92	624208.79	9153440.84	74.00
711213.80	9171307.63	57.81	638996.59	9160584.75	76.00
711620.13	9173250.75	49.36	644318.37	9156065.33	76.00
711288.47	9175169.72	58.23	643365.55	9153406.81	76.00
709978.65	9172290.06	62.09	639528.53	9152150.78	76.00
707771.62	9172284.11	69.53	640753.40	9168051.40	77.00
708339.26	9174397.18	57.25	643189.35	9151447.77	77.00
703711.96	9171475.92	65.22	641377.02	9149767.66	77.00
703088.28	9172789.08	63.92	621803.58	9152980.11	77.00
704329.31	9174754.32	69.75	615329.01	9153023.27	77.00
702376.61	9174618.63	71.28	614284.58	9155093.67	77.00
702697.03	9176019.54	64.96	640751.54	9160503.62	78.00
700735.30	9176204.83	59.52	644463.61	9158539.44	78.00
700440.07	9173779.62	71.16	642886.06	9149555.33	78.00
701517.56	9171062.33	73.09	639370.07	9150037.07	78.00
699843.16	9172225.19	77.56	626797.20	9153150.96	78.00
699007.95	9170736.85	74.66	645972.91	9154821.41	79.00
697248.47	9172800.85	66.61	642748.51	9168990.51	79.00
698473.63	9175417.89	68.66	636814.41	9150383.99	79.00
695478.21	9174894.97	79.19	634042.86	9150743.93	82.00
695357.09	9172255.80	75.66	642867.07	9160503.56	83.00
693295.30	9175620.43	71.38	629358.09	9152133.25	83.00
691791.96	9175923.34	60.35	613012.84	9151394.14	83.00
689093.88	9175737.87	67.49	648674.51	9169553.90	86.00
688594.02	9179385.31	61.20	641833.51	9163640.94	86.00
686882.57	9177502.11	69.14	647596.59	9156898.53	86.00
689692.51	9173187.03	95.40	618220.50	9150038.48	86.00
690683.44	9171338.85	84.90	645899.78	9160066.55	87.00
692735.05	9172764.75	82.15	648007.34	9152097.91	87.00
617058.86	9170402.13	40.00	646783.84	9168400.00	88.00
616062.97	9162946.00	40.00	644977.84	9163113.03	88.00
615182.74	9169149.92	42.00	649698.45	9155393.55	88.00
618201.95	9168869.02	44.00	621649.40	9150953.83	88.00
620297.15	9167894.32	47.00	647322.76	9147880.78	89.00
615315.51	9166247.80	47.00	631507.72	9150869.04	91.00
613358.10	9164224.20	47.00	648112.73	9159077.22	91.00
623594.98	9169540.52	48.00	642331.59	9166409.85	91.00
623628.64	9167999.33	48.00	644440.70	9167705.47	91.00
623037.34	9167129.91	48.00	615208.16	9148792.40	92.00
625400.69	9168776.74	51.00	649491.88	9167106.13	93.00
618530.67	9165218.58	51.00	646641.71	9165440.96	93.00
625274.75	9166525.70	52.00	650384.02	9158265.87	93.00
626522.41	9170088.88	53.00	648882.24	9148157.42	94.00
630682.68	9168069.38	53.00	649560.48	9164362.85	94.00
628420.95	9166607.55	53.00	610666.27	9148282.37	96.00
623284.56	9164929.96	53.00	653144.89	9158106.31	96.00
628810.37	9169739.52	54.00	649586.09	9161430.93	96.00
632256.88	9168312.90	54.00	651342.51	9152037.59	97.00
615558.34	9160049.46	54.00	652571.52	9154955.09	97.00
611974.70	9160920.37	56.00	652200.60	9160157.98	98.00
619159.81	9159414.37	57.00	631525.50	9150881.73	91.00
633312.23	9169905.89	58.00	625474.72	9151243.23	92.00
630762.94	9165328.45	58.00	624252.81	9151505.24	93.00
622963.12	9162293.07	58.00	626059.10	9150924.01	93.00
634144.35	9167028.91	62.00	627428.43	9150531.82	96.00
622778.50	9160403.81	62.00	613064.54	9147102.81	102.00
618721.10	9157366.08	62.00	655989.13	9158385.33	104.00
634058.96	9165521.89	63.00	655099.76	9156409.72	104.00
632363.56	9163980.72	63.00	651619.14	9149691.03	104.00
629725.65	9162886.37	63.00	655141.95	9169411.20	106.00
627616.01	9161471.40	63.00	611878.72	9144298.64	108.00
625591.83	9161728.10	63.00	663568.25	9164197.60	109.00
634182.88	9158279.11	63.00	660634.03	9163008.31	109.00
631760.73	9156948.95	63.00	659007.99	9161427.83	109.00
622647.71	9157222.70	63.00	658619.61	9159006.73	109.00
615714.03	9157124.21	63.00	657028.14	9155827.45	111.00
633811.25	9163679.02	64.00	654681.69	9153012.83	112.00
634407.88	9159918.29	64.00	664834.68	9158694.39	113.00
635663.12	9158946.60	64.00	664241.34	9162032.04	115.00

Easting (metres)	Northing (metres)	Bouguer anomaly (mgals)	Easting (metres)	Northing (metres)	Bouguer anomaly (metres)
652482.73	9147230.69	116.00	826090.32	9092156.85	104.06
664247.02	9155383.92	121.00	829194.85	9090678.01	104.58
664207.69	9152266.73	123.00	666101.95	9170509.93	86.94
663647.24	9149459.66	126.00	665894.94	9168295.51	102.49
661647.12	9156715.63	127.00	667646.58	9167692.19	103.24
654385.81	9149314.94	127.00	669202.68	9168013.74	100.93
662890.49	9147169.03	128.00	672541.89	9167453.76	102.43
653745.43	9144603.06	131.00	676879.59	9167531.95	104.15
662168.39	9143467.07	132.00	681946.74	9168621.65	104.24
654148.41	9143066.49	132.00	684296.56	9167541.39	99.24
661284.15	9154370.62	133.00	686998.55	9168066.16	90.84
660731.79	9142327.77	136.00	683369.48	9165120.48	94.54
656828.96	9152138.68	137.00	681135.64	9164735.88	105.50
657817.06	9142953.84	141.00	679126.74	9164365.43	107.34
777209.12	9114570.56	110.58	679578.22	9167485.52	112.12
777400.94	9111620.16	115.60	677365.44	9164353.44	107.35
777997.31	9109742.41	115.98	675284.46	9163922.00	108.05
776899.11	9107029.61	119.31	672686.39	9164171.66	109.24
775871.43	9101906.07	132.82	674538.58	9160858.75	112.76
778917.28	9104500.50	120.07	672334.90	9161657.41	113.67
780381.39	9107708.85	113.19	668720.99	9161812.06	106.86
781725.82	9109796.00	110.39	670578.38	9165067.21	106.13
782882.56	9113258.95	104.55	666010.33	9162815.03	125.93
783185.00	9104424.34	113.04	671026.55	9159831.31	102.99
784563.02	9107847.21	113.84	665696.05	9158786.28	108.17
786627.33	9105592.38	113.98	668459.50	9158699.74	98.68
786930.41	9102763.24	113.86	666494.39	9156646.39	106.19
784896.44	9099509.79	118.30	668743.15	9156414.37	91.84
785236.67	9111947.12	104.81	671941.36	9157053.43	94.67
791592.43	9112645.95	101.03	672376.28	9153986.96	87.19
794899.67	9113068.03	105.10	669968.73	9154612.39	92.97
788513.46	9108186.17	107.77	666013.25	9154744.47	110.92
789519.96	9104639.11	109.04	669048.88	9152470.15	95.23
791728.95	9109924.82	110.13	666424.54	9152455.81	106.10
792706.65	9107899.57	109.86	671236.62	9151450.33	68.56
790298.45	9102114.23	117.92	667649.67	9150209.79	99.91
790465.19	9099179.93	119.69	671012.89	9149739.02	91.84
793329.96	9099673.03	119.04	671020.47	9147041.74	92.53
792941.66	9096474.12	120.03	668028.46	9147615.26	97.35
795651.63	9097360.21	119.87	670843.71	9144710.10	91.08
798534.43	9095442.93	125.00	667641.15	9144477.67	95.96
794529.93	9106435.27	105.47	670200.00	9141823.90	90.60
797126.01	9110495.78	105.03	667240.99	9141350.23	94.35
798089.02	9107429.29	102.89	674298.87	9140126.94	86.31
796037.52	9104143.03	111.28	677038.61	9139925.40	84.16
796960.78	9101208.78	115.97	679547.02	9139556.40	86.59
799548.66	9102290.75	118.07	680201.39	9142306.26	86.81
801660.84	9101255.34	117.94	677383.07	9142176.72	85.17
802206.78	9104410.10	117.27	674816.82	9143434.13	87.86
800138.01	9105562.72	107.34	677756.64	9144188.07	87.32
805087.97	9093114.43	116.85	674970.99	9145903.24	91.37
805217.62	9096742.44	115.70	677986.88	9146202.47	91.21
802733.20	9097981.79	116.26	680605.47	9145158.98	90.27
799055.62	9114616.81	99.79	679816.17	9147835.35	93.64
802192.16	9112564.65	102.06	681900.42	9149377.64	95.79
803553.54	9109649.72	105.74	677347.78	9149506.13	93.34
804651.91	9105774.41	109.15	674859.77	9148876.03	90.99
806868.46	9098724.97	116.23	678995.15	9151537.50	92.24
808522.69	9095970.15	112.09	674629.26	9151591.65	85.00
804441.98	9102597.86	112.03	676788.65	9153284.15	89.40
809953.47	9098807.60	111.92	674858.03	9154131.85	87.47
805216.30	9111723.89	110.20	681870.39	9154494.25	87.74
810391.28	9110307.67	110.24	677651.27	9155813.65	90.16
807722.12	9109712.12	108.60	675992.41	9158331.39	90.36
808565.27	9114007.93	105.95	679550.04	9159289.75	99.84
811838.71	9113123.68	105.64	679677.94	9161347.69	99.08
809484.71	9108444.22	108.48	677185.83	9161035.29	108.36
808164.42	9105881.69	107.77	685193.97	9163311.24	83.55
809168.76	9102180.07	114.57	684643.64	9160630.93	87.71
812287.01	9102820.58	114.94	682635.52	9159186.41	86.49
813266.04	9110726.47	103.62	683092.40	9156526.75	89.64
812862.29	9106283.15	109.00	685542.73	9152744.14	95.37
814409.65	9099226.95	115.47	682914.75	9151699.43	94.48
814126.91	9095726.57	111.17	684853.54	9149554.16	95.89
813281.70	9091869.07	108.41	686084.88	9146680.18	88.53
815949.83	9111518.64	102.67	683207.13	9146765.69	93.57
819179.76	9112422.18	99.79	683460.89	9144306.07	88.57
817763.88	9108568.94	103.47	686308.78	9144302.59	88.83
817351.34	9098598.34	107.95	683741.37	9142022.39	89.00
817006.72	9095146.04	110.10	683331.00	9138489.07	90.57
819484.27	9092413.55	103.39	689661.74	9168981.11	86.93
819742.88	9100270.58	103.88	692069.34	9169476.47	88.83
820172.94	9103817.02	99.80	694121.97	9170501.20	83.41
823617.87	9111161.74	104.84	697853.91	9167823.92	81.03
822381.50	9108906.32	104.87	690897.92	9167501.28	83.50
826732.27	9113399.13	110.74	695548.37	9165426.40	80.75
826816.95	9110537.82	113.15	693152.87	9165799.97	80.64
829573.16	9110218.57	109.19	688007.33	9163991.50	83.64
825415.40	9107917.97	98.64	690713.89	9158958.39	83.45
828391.31	9104877.68	95.41	691031.13	9160343.93	80.00
822567.43	9106060.08	98.86	693252.70	9157088.38	80.41
827342.67	9102752.49	91.26	701324.89	9154983.00	84.04
829781.28	9101592.74	97.74	704854.30	9157599.70	83.50
826919.31	9098498.13	93.30	711853.22	9157667.62	84.39
824125.41	9103271.63	93.13	720056.32	9155889.03	83.50
829636.11	9097003.67	93.11	715658.79	9156099.47	78.45
823662.78	9098972.11	94.26	696920.10	9156704.96	76.59
823518.99	9096081.81	98.29	691187.66	9165411.76	78.72
822822.60	9093141.45	97.04	701202.41	9169402.75	71.34

Easting (metres)	Northing (metres)	Bouguer anomaly (mgals)	Easting (metres)	Northing (metres)	Bouguer anomaly (metres)
700918.57	9166898.99	73.50	706082.38	9147853.49	100.36
692444.40	9161609.58	73.69	707498.03	9145399.34	102.16
694258.98	9159187.00	72.71	716849.36	9140052.38	104.44
697834.97	9159471.47	72.50	714294.79	9138256.09	101.30
700908.53	9158537.42	72.66	717307.68	9137157.66	104.80
704490.97	9161647.71	74.28	719463.23	9143268.95	107.36
712318.38	9160396.16	73.22	719959.50	9139592.61	105.85
715056.31	9158048.00	73.81	719931.27	9136537.07	107.02
720370.90	9158334.68	71.14	720075.02	9134199.00	107.36
712715.67	9162847.28	68.87	716734.89	9134946.62	104.60
709697.82	9163103.53	68.20	713999.84	9135852.77	105.59
707288.69	9161830.84	69.69	720186.60	9131509.67	119.62
706384.20	9163498.84	69.27	719539.82	9128720.98	112.18
704635.27	9164437.19	69.01	716736.26	9129993.24	106.87
701331.22	9161173.15	65.12	715888.48	9132260.15	108.70
698610.06	9161960.61	59.86	713972.09	9130837.77	105.85
696621.09	9163379.49	54.99	712524.22	9133366.86	103.23
699150.01	9164488.93	49.71	710486.21	9131700.22	102.28
703888.13	9167850.22	65.00	707603.98	9132382.53	101.48
713575.20	9165229.86	60.42	704873.24	9134144.86	101.06
716008.55	9162335.11	60.01	701445.11	9134103.25	100.03
715122.03	9160169.29	59.77	801647.86	9283599.30	31.00
720351.97	9161741.78	50.74	802295.14	9286873.92	31.00
720334.19	9164812.77	51.31	807826.71	9288531.85	32.00
720566.48	9166566.08	51.14	805976.78	9286576.34	32.00
718070.19	9167344.79	58.73	802937.83	9281284.78	32.00
716509.57	9165236.09	59.92	831122.03	9286398.34	32.00
713827.57	9167903.07	54.80	811132.63	9288703.25	33.00
710538.76	9165807.48	57.02	830991.78	9289063.39	33.00
708328.09	9165329.04	57.86	813644.70	9290437.05	34.00
711162.14	9168489.39	54.08	808696.68	9285199.86	34.00
708222.16	9168812.25	52.34	807157.57	9283217.41	34.00
688097.12	9159212.53	88.27	828193.07	9281624.27	34.00
692913.61	9154058.69	85.14	819080.76	9284749.17	35.00
704086.84	9155490.73	87.58	818458.14	9292558.74	35.00
706365.27	9155462.88	85.50	829088.46	9294592.88	35.00
711314.66	9155127.79	87.33	817389.92	9289295.11	36.00
711242.15	9151088.01	89.68	813071.63	9284801.24	36.00
716225.07	9154034.06	90.15	827242.31	9288453.21	36.00
719692.72	9153359.50	91.98	822113.14	9282754.94	37.00
716993.50	9151377.05	90.68	824495.44	9289916.62	37.00
719349.09	9149531.11	84.37	825013.04	9286462.65	39.00
712094.84	9148514.24	92.97	821186.34	9289950.15	41.00
707536.10	9153264.11	94.15	826777.06	9284583.50	43.00
703621.08	9152885.98	91.91	822874.68	9284893.13	45.00
700618.80	9151484.42	91.35	820959.26	9287296.20	48.00
697585.23	9151487.04	91.81	798762.24	9269253.02	26.00
694855.45	9151383.85	94.55	799779.91	9272138.66	28.00
690734.44	9151327.30	93.78	797425.29	9274289.00	29.00
688338.52	9155871.09	90.34	796126.89	9271707.23	30.00
688356.89	9152867.25	93.31	793585.66	9270354.95	30.00
692102.58	9148993.88	88.53	792955.02	9267962.55	30.00
687731.23	9148211.18	89.60	799760.53	9280513.52	31.00
690233.45	9146908.29	88.41	798294.35	9277369.43	31.00
694372.95	9148762.75	94.97	802383.62	9274699.19	31.00
692629.69	9146727.84	94.04	800703.60	9268100.94	31.00
696309.06	9143473.30	94.97	794858.45	9264926.92	31.00
695698.18	9141245.24	94.93	795951.77	9261242.07	31.00
693284.16	9142954.76	94.62	792234.29	9265364.87	31.00
690106.97	9144473.86	90.35	792210.71	9262704.34	31.00
690861.70	9142204.32	92.13	811972.72	9258243.19	31.00
687526.89	9141260.82	91.60	805960.70	9278510.15	32.00
686925.13	9138585.57	92.00	798315.67	9266618.04	32.00
690442.64	9139618.04	94.34	809135.07	9259738.11	32.00
689699.19	9137659.72	94.63	827659.42	9265835.03	32.00
692432.58	9137566.03	95.23	805757.59	9260853.48	33.00
694787.46	9136168.22	94.97	815013.60	9258222.78	33.00
695005.77	9138642.65	96.13	820009.67	9259406.06	33.00
697731.06	9138056.62	96.44	823213.74	9260722.21	33.00
697767.48	9135285.92	97.79	825512.92	9264429.36	33.00
702045.56	9136878.86	97.87	830287.36	9272701.90	33.00
701498.17	9140935.35	96.64	830023.29	9276719.74	33.00
699139.43	9142065.65	95.94	826545.08	9279622.41	33.00
703899.61	9142648.85	99.59	809388.31	9279867.84	34.00
705797.52	9138842.59	99.20	805013.18	9274301.30	34.00
705402.11	9136000.50	99.74	802803.96	9269300.86	34.00
709077.16	9134749.31	99.35	799260.70	9263522.70	34.00
711843.81	9136818.20	98.69	803776.25	9261923.59	34.00
713927.04	9140702.59	99.80	812008.80	9261278.50	34.00
714963.86	9143072.43	97.87	819864.10	9280154.69	35.00
710728.07	9142897.74	98.60	808755.60	9276920.62	35.00
710432.73	9139943.86	98.25	812772.03	9268774.74	35.00
708701.80	9137626.88	97.89	811860.79	9270370.29	35.00
706800.51	9142451.72	99.84	803652.37	9270173.80	35.00
704276.91	9145944.66	98.69	824037.57	9263197.43	35.00
701476.42	9146159.69	98.78	827933.77	9269705.41	35.00
699231.54	9145957.11	99.61	812397.94	9272501.47	34.00
695596.66	9146575.73	96.91	814716.02	9268924.12	33.00
697715.29	9149016.66	96.40	819693.09	9275672.89	36.00
703092.91	9148084.80	97.75	810573.64	9275625.29	36.00
703172.04	9150576.65	96.47	807720.20	9262970.66	36.00
706322.23	9150334.16	98.61	823683.42	9279702.43	37.00
708614.38	9150378.09	97.38	814327.37	9278491.81	37.00
716430.76	9149044.03	97.30	809941.46	9267359.71	37.00
719649.94	9146273.00	98.89	805893.01	9265987.39	37.00
716013.86	9145584.63	100.70	808232.37	9273064.76	37.00
713886.99	9145995.51	100.18	813521.97	9262526.12	37.00
711327.19	9146270.64	101.64	827999.19	9273975.45	37.00
708744.56	9148178.95	102.04	815613.50	9275462.91	38.00

Easting (metres)	Northing (metres)	Bouguer anomaly (mgals)	Easting (metres)	Northing (metres)	Bouguer anomaly (mgals)
813112.13	9276231.94	38.00	812224.15	9243852.80	22.00
824633.92	9276965.39	38.00	821435.01	9246630.82	22.00
822176.98	9278099.57	39.00	829654.29	9248977.95	22.00
815734.85	9274239.85	39.00	827772.83	9235614.27	22.00
810412.79	9264858.34	39.00	790152.15	9249950.86	23.00
820367.45	9261673.18	39.00	791542.25	9246776.82	23.00
815910.57	9262073.84	40.00	797831.75	9243660.47	23.00
824957.81	9267021.80	40.00	801013.57	9244083.44	23.00
822759.17	9274622.58	41.00	818007.11	9246807.37	23.00
824900.33	9272213.14	42.00	825226.66	9247232.98	23.00
817226.76	9272683.36	43.00	829588.52	9248954.24	23.00
813306.45	9265047.33	43.00	810470.26	9231342.11	23.00
823990.39	9270070.69	43.00	794590.27	9228198.89	23.00
821296.75	9271762.61	50.00	792376.13	9252022.72	24.00
817774.08	9265189.82	54.00	801161.55	9247368.42	24.00
819608.91	9271351.00	51.00	802514.24	9251050.59	24.00
791252.69	9260917.50	30.00	810617.38	9247597.65	24.00
802643.07	9259231.74	30.00	815541.73	9247036.70	24.00
827674.94	9262749.89	30.00	828572.20	9248139.89	24.00
789956.18	9257764.67	29.00	815528.96	9247041.64	24.00
805367.15	9257939.11	29.00	813739.80	9251140.56	24.00
810957.93	9256150.18	29.00	811016.60	9251479.80	24.00
800048.24	9257248.59	28.00	808481.22	9248749.16	25.00
814169.81	9254543.15	28.00	802548.96	9251119.88	25.00
816856.43	9254429.58	28.00	800693.67	9249474.92	25.00
820560.74	9254483.66	28.00	825681.65	9250243.29	26.00
792846.54	9256901.05	27.00	806280.97	9250986.56	26.00
796403.37	9255814.07	27.00	804678.30	9252994.65	26.00
805405.81	9255212.35	27.00	801032.07	9252981.61	26.00
826453.74	9254128.56	27.00	798067.87	9248072.58	26.00
801758.55	9254908.08	26.00	800722.26	9227546.42	27.00
808349.09	9253578.57	26.00	794120.51	9248978.40	27.00
829568.51	9260600.15	26.00	795307.40	9251277.11	27.00
794425.15	9253857.17	25.00	824886.49	9233712.10	29.00
785179.29	9253523.55	27.00	797883.36	9225606.11	31.00
829205.10	9257515.58	27.00	831339.58	9232772.56	36.00
778411.97	9229065.81	15.00	817962.34	9231683.18	36.00
780914.92	9230653.67	15.00	821767.71	9231882.37	37.00
780403.08	9232874.55	15.00	815532.10	9230671.77	37.00
778104.03	9232324.74	15.00	813322.72	9229882.20	37.00
787176.24	9237641.68	15.00	824572.50	9229990.00	38.00
784641.82	9239587.80	15.00	821895.90	9228965.23	40.00
826100.70	9241013.11	15.00	810380.05	9228771.29	40.00
817303.72	9240046.66	15.00	806358.91	9227491.96	40.00
778213.75	9238747.78	16.00	803015.28	9225471.43	41.00
779140.79	9236225.18	16.00	818018.33	9229441.92	43.00
782324.42	9237399.06	16.00	823395.65	9226551.14	46.00
784362.89	9230999.64	16.00	816106.12	9226429.34	48.00
780820.30	9228128.21	16.00	819758.45	9226090.42	50.00
778926.52	9226826.91	16.00	827672.19	9226707.30	50.00
776593.64	9227831.91	16.00	722497.99	9197386.65	21.41
819263.06	9244125.09	16.00	724893.33	9195907.40	16.60
814625.08	9237782.22	16.00	727517.77	9196329.30	10.00
818048.37	9237610.42	16.00	729810.28	9197112.96	5.43
821652.49	9243681.43	16.00	732004.96	9194602.39	7.95
823494.13	9240121.43	14.00	734549.76	9196189.49	17.68
780509.50	9240198.32	17.00	737785.59	9197626.94	2.25
783572.03	9243198.48	17.00	735439.01	9193395.55	1.75
786757.99	9241586.78	17.00	732244.89	9191740.11	11.23
789150.02	9239855.76	17.00	731174.31	9188853.65	10.14
794216.42	9238305.85	17.00	729281.58	9192814.75	19.96
789098.56	9235458.37	17.00	727046.42	9190886.54	21.14
786312.52	9228881.06	17.00	725130.17	9188757.07	19.55
783403.07	9226851.08	17.00	721554.45	9186820.43	19.02
829562.73	9244180.92	17.00	726195.08	9185384.55	17.09
813216.11	9241331.94	17.00	733125.59	9184041.31	17.55
808038.28	9239325.22	17.00	722441.60	9184471.25	27.25
805943.52	9237500.23	17.00	723487.73	9181577.62	40.81
808832.66	9237359.66	17.00	725819.75	9178304.85	41.92
811176.01	9239011.61	17.00	722006.31	9176914.40	50.99
787096.62	9244086.05	18.00	725085.41	9175289.93	50.87
795922.50	9232172.84	18.00	722977.90	9172109.67	51.46
816504.84	9243779.46	18.00	727719.20	9172346.49	52.20
810751.90	9242475.50	18.00	728457.33	9175574.85	52.07
804676.35	9240100.22	18.00	728962.20	9178813.13	35.79
801689.94	9238436.69	18.00	732934.73	9179493.39	35.13
801147.97	9235569.98	18.00	731544.42	9172337.46	55.96
804621.51	9234210.85	18.00	732157.85	9177266.49	45.90
815666.29	9234590.19	18.00	733709.06	9174708.78	50.56
799441.03	9232970.52	18.00	736409.88	9173165.55	55.48
785544.55	9246579.49	19.00	734533.75	9177178.36	41.12
804223.03	9242662.60	19.00	736639.92	9176127.02	44.62
808385.56	9244140.83	19.00	738385.40	9174896.43	41.43
829451.71	9246720.05	19.00	740091.78	9170721.56	44.89
788735.52	9227791.03	19.00	741319.12	9174101.44	33.98
807890.64	9232538.59	19.00	741710.21	9177016.76	24.89
812477.92	9233637.79	19.00	745062.41	9174840.06	19.00
796403.22	9241582.99	20.00	738209.86	9178048.70	34.56
830357.43	9237445.50	20.00	735784.52	9179977.73	28.20
798041.91	9230129.66	20.00	738207.16	9181722.06	20.02
791876.02	9229401.96	20.00	734782.24	9182385.73	21.10
788998.71	9246962.17	21.00	729902.42	9186454.37	15.29
797922.34	9239132.54	21.00	734060.77	9186214.64	9.91
806916.53	9246213.20	21.00	738225.11	9183952.43	12.47
820978.06	9235050.61	21.00	741310.62	9181089.09	10.10
802235.96	9230365.58	21.00	736940.52	9187539.60	6.01
787888.06	9252065.59	22.00	740929.91	9184565.71	5.16
799870.52	9240905.47	22.00	743683.43	9180726.16	9.51
803949.81	9247744.73	22.00	746112.93	9178593.84	11.54

Easting (metres)	Northing (metres)	Bouguer anomaly (mgals)	Easting (metres)	Northing (metres)	Bouguer anomaly (mgals)
747792.53	9182162.08	0.68	694333.77	9232376.97	0.29
750168.95	9178152.20	13.00	696108.56	9232111.29	1.59
753044.55	9180107.97	9.00	696105.28	9229845.81	3.08
754363.92	9182230.00	1.55	695014.61	9228345.21	2.16
756851.82	9184210.38	11.99	696606.58	9226586.78	3.52
758937.00	9182020.82	18.00	697621.12	9233547.96	3.87
756339.17	9187728.10	12.30	696456.01	9235619.90	3.34
753992.43	9191454.73	12.37	696016.88	9237951.36	4.61
751382.84	9193247.33	3.82	698621.49	9235896.08	6.15
754216.11	9196006.95	4.73	698499.90	9237580.55	7.26
757199.37	9197490.02	1.62	699553.80	9234023.63	1.11
759727.18	9197393.38	5.17	701356.72	9233724.60	2.05
749126.89	9191297.93	-0.63	706259.80	9235016.34	1.82
745987.99	9190304.92	-3.83	708162.48	9231977.42	1.18
752744.46	9185915.47	-0.18	708613.19	9233957.11	5.03
750008.98	9183889.49	-1.45	710996.99	9233232.88	1.73
745360.56	9183696.91	-0.39	712667.08	9235422.73	2.51
744157.32	9187291.05	-3.52	715370.54	9234652.92	2.63
741518.25	9190142.89	-4.70	715523.94	9232188.30	1.19
737930.73	9191397.47	-1.01	717220.35	9233563.48	2.74
737615.82	9195070.74	-0.85	718092.40	9231039.38	0.05
740949.87	9194342.89	-3.31	720424.81	9233040.17	-2.29
743575.96	9193622.63	-4.46	718230.49	9228618.88	-5.69
746858.49	9193639.29	-2.53	720516.97	9228233.21	-10.08
746790.27	9196047.47	-4.26	716445.67	9226112.53	-9.08
744016.92	9197108.31	-3.34	715519.14	9229394.32	-9.45
741311.68	9197470.13	-2.06	715009.64	9227520.40	-7.06
747461.53	9195743.57	-3.00	713331.80	9232953.03	-6.88
758452.24	9193511.14	16.91	713389.22	9229252.48	-4.31
757585.95	9190914.90	20.24	711446.55	9228521.25	-1.96
759539.47	9188566.54	34.05	710751.27	9230876.19	-2.18
760820.16	9191785.04	27.33	711625.08	9226395.25	-6.81
762419.47	9195478.72	26.03	708556.83	9226015.62	-4.41
765335.42	9195974.77	27.19	708623.76	9228232.20	-4.19
765267.78	9192659.34	41.18	707149.09	9230113.99	-5.42
767442.67	9190670.28	52.26	706439.95	9229248.21	-2.67
770551.73	9196579.78	16.76	706129.76	9231861.75	-6.63
772424.26	9193121.14	20.45	704315.55	9230440.94	-5.45
774729.71	9196320.84	7.04	703691.47	9233462.23	-0.16
775271.94	9193024.68	5.52	705375.21	9226524.40	-16.43
775576.85	9190201.33	4.92	702747.32	9228399.15	-13.20
772421.88	9190035.47	18.95	700339.20	9227594.35	-10.74
774353.75	9186435.58	4.68	698261.88	9228689.22	-1.79
769804.54	9188909.30	34.69	698717.33	9231386.96	-1.55
771424.69	9184554.09	19.45	692811.50	9226877.64	-1.21
768143.13	9183972.40	28.99	692290.07	9229900.10	-1.08
764886.12	9183877.94	31.35	692255.28	9231913.22	-0.18
761109.66	9184328.86	31.16	689799.73	9232988.99	-0.67
767022.24	9181692.26	19.93	689734.31	9228104.22	-3.63
770066.05	9181529.30	16.00	689578.86	9230844.37	-1.14
769683.33	9179317.27	7.53	686991.51	9226685.73	-2.54
766783.72	9177919.70	6.86	687587.99	9229328.30	-0.17
764051.53	9180121.61	16.72	687787.73	9232484.30	-1.15
761287.53	9180733.23	11.62	687786.51	9234178.56	-2.00
763563.12	9177513.46	9.00	686045.19	9234222.20	-2.01
767044.97	9170361.34	8.11	685263.67	9236607.05	-1.61
764262.69	9170787.28	5.72	685694.46	9238506.98	-0.82
762703.21	9174103.46	-5.14	683725.95	9238128.78	-3.49
760635.45	9173111.24	-7.89	683144.85	9235342.27	-1.48
760821.44	9176736.02	1.60	684898.53	9232162.28	-3.28
757804.25	9175827.36	2.08	684940.58	9230500.84	-1.21
753510.39	9171754.94	4.16	682712.40	9228120.48	-0.40
750360.68	9174514.57	6.99	682335.12	9230206.78	-2.58
750377.91	9171241.05	11.25	682438.34	9232662.77	-3.50
747657.98	9173341.25	12.91	680558.08	9230006.29	-1.74
757344.18	9180350.13	12.42	680352.86	9227011.66	0.57
739308.97	9187972.62	1.24	678233.49	9226164.14	-1.59
752757.82	9185937.93	-0.18	679548.74	9232942.58	-3.07
668248.91	9245433.30	6.00	680222.07	9235663.85	-2.15
666087.73	9243349.04	5.58	681151.43	9237772.84	-1.06
666285.24	9241408.39	4.09	678808.87	9238523.66	-0.92
668594.91	9242834.49	3.60	677559.99	9236193.48	-1.75
671717.21	9244316.22	3.24	677293.13	9233505.37	-3.03
666287.79	9241421.21	4.09	677519.67	9230989.65	-3.71
666549.23	9239388.43	3.44	677068.67	9228321.50	-1.97
671127.73	9242156.28	1.11	675696.62	9226383.87	-1.82
675154.79	9243356.29	3.06	673821.33	9227925.25	-2.60
677556.92	9243359.08	3.07	670707.65	9226164.90	-2.60
673328.37	9241375.89	0.44	667104.58	9226128.43	-3.11
669316.65	9240074.68	0.79	670401.98	9228761.70	-5.43
676139.98	9240160.99	0.34	668072.31	9229034.03	-5.28
669236.00	9237171.08	1.35	671710.04	9230961.50	-4.28
665798.99	9236498.46	0.47	675251.68	9230778.08	-4.11
678337.67	9240395.30	0.69	667132.61	9231556.22	-5.00
680205.80	9240358.02	1.80	669753.23	9232245.35	-5.11
680741.45	9242771.53	2.28	672784.91	9233960.13	-5.29
683486.32	9242276.06	1.73	673776.02	9235725.05	-3.21
682797.26	9240085.82	0.73	671965.49	9236143.26	-2.90
688169.01	9240186.33	1.80	669095.11	9234126.66	-4.25
686665.78	9241474.23	1.63	665932.54	9233280.71	-3.50
687845.87	9236975.95	0.12	667478.59	9235165.75	-1.22
690034.24	9237403.07	1.20	671611.34	9238565.67	-0.69
691578.40	9237663.06	4.36	675114.43	9238179.36	-3.55
693208.64	9238987.09	2.42	673786.28	9235673.90	-3.21
694297.00	9236832.06	2.59	641891.81	9225060.96	14.00
692349.57	9235648.10	5.76	611117.40	9224123.75	14.00
689734.06	9235348.07	5.76	663509.07	9223179.71	3.00
692560.62	9233857.78	1.10	650597.57	9223801.35	3.00
694575.17	9234292.85	0.49	664491.96	9216462.31	6.00

Easting (metres)	Northing (metres)	Bouguer anomaly (mgals)	Easting (metres)	Northing (metres)	Bouguer anomaly (metres)
664445.97	9220600.88	6.00	641134.59	9183143.72	41.00
657172.91	9223051.24	6.00	635655.19	9210616.13	41.00
655125.94	9220025.77	11.00	626665.04	9210838.63	41.00
664138.18	9213736.36	12.00	638572.46	9200476.09	41.00
661116.11	9215073.19	13.00	648238.77	9200680.38	42.00
648132.83	9220657.03	13.00	642990.71	9201207.10	42.00
645528.80	9221960.80	13.00	638939.21	9209139.50	42.00
658155.20	9215398.88	16.00	656600.21	9184287.33	42.00
651431.82	9218438.54	16.00	625389.74	9179705.93	42.00
654400.06	9216512.28	17.00	623525.58	9180397.24	42.00
664209.63	9209376.75	18.00	622629.82	9181997.94	42.00
658526.78	9212068.14	18.00	615349.36	9201178.38	40.00
645283.86	9219389.76	18.00	665176.04	9181946.26	44.00
660382.80	9209054.72	23.00	664091.12	9178562.39	44.00
654050.77	9211327.02	23.00	656590.75	9195867.24	44.00
615197.65	9223480.25	23.00	620575.37	9183901.20	44.00
611996.49	9217718.59	23.00	614561.84	9179768.41	44.00
657752.62	9208879.85	24.00	613023.32	9179705.10	44.00
642526.08	9216666.71	24.00	620337.29	9172412.45	44.00
640838.27	9217073.49	24.00	610842.40	9171336.47	44.00
638272.56	9218773.59	24.00	624303.45	9208087.51	44.00
629684.29	9221854.28	24.00	610701.03	9207037.87	44.00
635485.73	9221187.64	25.00	618049.91	9177130.73	44.00
654946.75	9208626.25	26.00	623622.69	9206240.58	45.00
650038.72	9214945.47	26.00	620868.51	9212511.32	45.00
632679.23	9218327.39	26.00	637969.84	9178853.08	46.00
643899.40	9210482.67	25.00	631238.59	9181196.46	46.00
650990.12	9209312.85	27.00	634533.09	9184277.77	46.00
646214.73	9215017.25	27.00	620700.40	9179632.90	46.00
639592.46	9222774.82	27.00	620572.40	9178456.60	46.00
625948.32	9224240.58	27.00	647542.11	9192616.66	46.00
611957.65	9201359.29	28.00	661895.30	9195922.33	46.00
633399.46	9224450.15	28.00	637655.37	9207328.25	46.00
655027.90	9204843.32	29.00	636323.01	9205250.25	46.00
634683.77	9199689.11	23.00	653565.45	9196299.60	47.00
636239.76	9199973.42	20.00	653308.61	9199749.74	47.00
620599.89	9224122.10	31.00	648935.51	9194753.09	47.00
614934.64	9218096.65	31.00	647893.97	9180696.18	47.00
645243.24	9208152.73	32.00	639502.88	9177607.98	47.00
640883.41	9214588.77	32.00	636349.84	9178876.17	47.00
618026.89	9220842.57	32.00	634162.76	9181472.98	47.00
653558.46	9202579.90	33.00	631043.70	9177959.74	47.00
650083.10	9205408.12	33.00	632306.28	9182352.30	47.00
645952.04	9212824.76	33.00	633229.38	9185200.20	47.00
638370.60	9214751.79	33.00	617163.38	9181284.81	47.00
623351.43	9223560.14	33.00	615863.88	9180494.85	47.00
612682.75	9204303.80	34.00	616320.99	9178220.91	47.00
652178.83	9206662.83	35.00	634159.10	9206414.20	47.00
634407.33	9216891.65	35.00	613761.12	9214288.41	47.00
632324.13	9215177.08	35.00	622633.86	9194716.40	47.00
630472.27	9212847.64	35.00	661597.42	9181060.11	48.00
628731.59	9214661.93	35.00	634258.03	9177255.55	48.00
625535.89	9213580.16	35.00	634276.59	9179295.66	48.00
623712.14	9216989.99	35.00	632379.09	9179643.99	48.00
624627.61	9220025.90	35.00	634238.52	9186691.39	48.00
621185.70	9219983.29	35.00	632656.80	9186455.34	48.00
610494.69	9214365.17	35.00	629859.65	9184956.78	48.00
641002.36	9211997.34	36.00	627600.46	9184906.29	48.00
634194.57	9212913.08	37.00	621949.00	9175732.85	48.00
643801.13	9204027.03	37.00	617517.60	9172898.08	48.00
659493.81	9193653.97	37.00	644503.95	9192876.26	48.00
644935.83	9188059.23	37.00	654203.21	9181274.55	49.00
660784.93	9187475.14	27.00	636786.80	9175349.75	49.00
640513.80	9185613.27	28.00	626015.19	9177279.54	49.00
640356.76	9188720.45	29.00	617880.44	9174798.44	49.00
659384.22	9190371.58	32.00	611105.74	9180340.53	49.00
658092.93	9188636.57	32.00	632867.79	9205446.43	49.00
661620.30	9189827.57	33.00	624097.82	9204210.53	49.00
638831.99	9182877.28	33.00	618122.35	9187882.74	50.00
663525.40	9186549.98	34.00	618603.96	9179401.99	50.00
657138.08	9192539.02	34.00	621970.59	9197371.47	50.00
654071.85	9192582.66	34.00	618596.71	9197900.44	50.00
654865.91	9186607.12	34.00	620175.95	9207839.19	50.00
649148.52	9189194.26	35.00	658156.29	9181139.35	51.00
647299.08	9186788.59	36.00	647096.23	9178107.43	51.00
643165.56	9187228.71	36.00	641224.42	9176177.38	51.00
638522.66	9187501.23	36.00	622422.11	9174424.35	51.00
637946.26	9184917.51	37.00	618127.54	9183632.24	51.00
663833.37	9192416.07	38.00	647935.26	9197979.78	51.00
660204.20	9184439.25	38.00	642116.66	9198773.34	51.00
653091.13	9190354.72	38.00	617698.02	9215695.27	51.00
651763.84	9187082.65	38.00	634387.14	9175042.66	52.00
649519.78	9185525.60	38.00	628921.15	9176262.89	52.00
644239.55	9183740.32	38.00	623220.68	9171883.61	52.00
650986.39	9200840.01	38.00	614581.46	9182629.18	52.00
640103.73	9203491.55	38.00	616474.34	9183319.97	52.00
637354.04	9212498.44	38.00	645446.90	9195599.63	52.00
620592.88	9215956.48	38.00	613545.08	9206920.54	52.00
617783.62	9218403.59	38.00	651844.44	9179963.94	53.00
647344.31	9183470.58	39.00	644250.53	9175986.43	53.00
645955.01	9190167.77	39.00	639603.97	9174853.95	53.00
637929.73	9189076.49	39.00	635464.46	9189221.67	53.00
640455.86	9206126.10	39.00	642968.82	9195025.83	53.00
630592.77	9208714.03	39.00	624790.34	9198864.93	53.00
627127.38	9208567.23	39.00	618288.31	9201833.41	53.00
627147.80	9180851.51	33.00	615839.02	9206572.10	53.00
629773.59	9180188.04	38.00	659251.98	9197251.45	53.00
625250.50	9181476.77	38.00	631683.76	9173297.62	54.00
663500.01	9183966.24	41.00	615698.45	9184885.12	54.00

Easting (metres)	Northing (metres)	Bouguer anomaly (mgals)	Easting (metres)	Northing (metres)	Bouguer anomaly (mgals)
622013.18	9186383.20	54.00	797026.79	9218446.60	43.00
613041.50	9184189.36	54.00	804008.42	9216164.56	42.00
631997.79	9188111.92	54.00	811405.63	9215690.13	42.00
637632.41	9191147.13	54.00	797072.10	9221803.47	41.00
627868.52	9191994.60	54.00	798568.08	9216588.16	41.00
661024.32	9179088.71	56.00	809489.64	9215267.73	41.00
634307.97	9188599.38	56.00	794981.24	9219573.59	40.00
615853.00	9212796.70	56.00	801765.79	9215248.55	39.00
665268.06	9176062.33	57.00	815812.83	9214689.83	39.00
641488.65	9173593.56	57.00	807005.25	9214777.03	38.00
636284.29	9173263.97	57.00	798677.88	9214522.43	37.00
626833.68	9173544.70	57.00	796102.14	9214239.21	36.00
624976.67	9173565.28	57.00	814386.87	9214034.53	36.00
650417.69	9177471.83	58.00	826904.91	9213514.32	35.00
639065.94	9172999.38	58.00	790819.72	9219822.59	33.00
633001.42	9195258.53	56.00	810613.42	9213290.87	32.00
628447.04	9204479.15	55.00	791146.58	9214867.69	31.00
624203.31	9201278.62	55.00	803330.07	9212757.53	31.00
620776.43	9202384.34	55.00	816798.54	9213307.93	31.00
658039.02	9178621.66	58.00	789090.90	9217263.17	30.00
643327.71	9173067.41	59.00	792554.72	9212411.68	30.00
655789.89	9179104.68	61.00	794956.58	9211811.46	30.00
634714.64	9171935.44	61.00	819369.62	9213165.94	30.00
626037.26	9175452.82	61.00	793144.31	9223131.10	29.00
660904.59	9176014.65	62.00	800095.23	9212071.81	29.00
618370.93	9186104.25	60.00	824059.98	9212692.26	29.00
619871.53	9186939.91	60.00	806908.97	9212382.58	28.00
617211.45	9189364.07	60.00	829250.11	9212238.85	28.00
616621.23	9190438.85	60.00	786627.82	9219990.60	27.00
615453.13	9191856.71	60.00	809122.39	9212012.85	27.00
614234.06	9193150.08	60.00	814494.83	9212237.64	27.00
662784.52	9173954.00	63.00	791147.11	9210614.19	25.00
646275.12	9173557.35	63.00	789383.65	9223175.17	24.00
613221.50	9194743.22	66.00	787609.69	9214235.15	24.00
657799.47	9176009.99	67.00	787028.09	9212019.69	21.00
648995.70	9173597.63	67.00	811686.61	9210891.43	21.00
637463.09	9171271.98	67.00	818507.78	9211227.56	21.00
611512.72	9190955.36	68.00	826227.70	9210930.96	21.00
651589.00	9174331.51	71.00	783785.17	9220745.81	22.00
653031.10	9177192.01	71.00	786843.25	9223732.91	20.00
614300.26	9172908.67	71.00	782618.35	9215950.04	20.00
656876.32	9201685.10	72.00	792895.78	9208524.90	19.00
655657.09	9174323.34	73.00	805425.51	9209606.18	19.00
646210.96	9171186.99	74.00	784000.46	9224590.03	18.00
664065.90	9172056.04	76.00	782506.79	9213398.11	18.00
659763.36	9173146.51	77.00	783357.20	9210857.66	18.00
661650.97	9171380.57	82.00	780760.40	9221872.26	17.00
651756.75	9171315.82	82.00	779953.97	9218105.27	17.00
655476.04	9171853.93	84.00	781605.53	9211010.05	17.00
657799.25	9171154.97	88.00	820871.91	9210354.64	17.00
657052.20	9204901.44	97.00	823401.10	9210090.94	17.00
658473.08	9206336.63	105.00	802131.85	9208846.01	16.00
640528.62	9193097.88	61.00	814736.27	9209552.74	16.00
639086.58	9191030.05	61.00	780718.53	9225186.79	15.00
630831.67	9188937.79	61.00	779405.51	9212888.22	15.00
635531.44	9191437.07	65.00	784526.15	9208486.75	15.00
615574.15	9198180.37	18.00	796580.72	9208177.38	15.00
618893.37	9200105.67	19.00	777722.06	9224368.98	14.00
653471.53	9184287.68	43.00	777602.36	9221046.72	14.00
644989.04	9180924.36	43.00	777095.94	9216461.98	14.00
641884.42	9179899.73	43.00	812435.67	9208036.52	14.00
640071.84	9180364.55	43.00	817863.47	9209137.19	13.00
637345.41	9180999.53	43.00	780725.58	9208351.16	12.00
635947.42	9183385.80	43.00	825663.50	9208927.59	12.00
636100.15	9185886.66	43.00	785394.06	9206837.04	11.00
642650.87	9190083.32	43.00	794732.60	9205605.59	10.00
639021.63	9204671.00	43.00	776592.85	9208319.39	9.00
634904.48	9208325.61	43.00	779890.07	9206243.74	9.00
623609.71	9210549.50	43.00	782389.62	9206653.05	9.00
620689.00	9181533.47	43.00	799926.39	9207470.88	9.00
623343.21	9183956.05	43.00	805217.56	9206791.85	9.00
649143.39	9189080.11	35.00	820179.48	9208307.40	9.00
640561.13	9193074.40	61.00	777770.39	9206816.06	8.00
639006.88	9191056.35	61.00	788480.75	9205290.68	8.00
630862.17	9188887.65	61.00	809363.18	9205850.28	8.00
826510.40	9220257.58	57.00	814245.06	9207141.07	8.00
823595.95	9219592.75	56.00	777481.45	9199880.46	8.00
827906.59	9222332.05	55.00	797841.49	9205357.08	7.00
830537.17	9222414.84	55.00	779510.90	9203177.20	6.00
824629.80	9217439.18	55.00	783440.87	9203652.26	6.00
822526.30	9221789.43	54.00	786719.02	9203479.71	6.00
827645.67	9216765.59	53.00	793528.24	9203223.18	6.00
820320.57	9220241.29	53.00	811853.75	9205516.01	5.00
819730.51	9222308.91	52.00	817668.16	9206783.78	5.00
817147.92	9222744.88	51.00	797523.03	9203032.89	4.00
814575.36	9223198.59	50.00	803909.58	9204736.30	4.00
815982.44	9219032.58	49.00	800497.09	9204855.81	3.00
811375.72	9220638.15	48.00	785016.04	9201655.93	1.00
808985.59	9221600.51	48.00	782658.56	9200477.20	0.00
813846.89	9219637.89	48.00	808576.81	9203230.98	0.00
819215.59	9216493.71	48.00	816262.00	9204781.95	-1.00
806049.06	9222785.84	47.00	820249.77	9205878.21	-1.00
806110.77	9219976.21	47.00	785172.50	9199725.62	-3.00
802792.17	9222123.51	46.00	803228.70	9201600.75	-3.00
803115.65	9219445.29	46.00	788576.40	9199497.73	-4.00
800863.13	9218124.37	45.00	792013.32	9199158.57	-4.00
814036.66	9217213.31	45.00	796060.95	9200076.46	-4.00
824374.16	9214653.27	45.00	799845.32	9201348.24	-5.00
799752.49	9222374.91	43.00	806686.14	9201195.78	-6.00

Easting (metres)	Northing (metres)	Bouguer anomaly (mgals)	Easting (metres)	Northing (metres)	Bouguer anomaly (mgals)
822673.47	9203860.65	-6.00	822471.79	9189881.40	-47.00
798856.30	9198467.77	-8.00	829534.16	9176865.43	-46.00
808821.04	9201390.24	-8.00	827413.02	9171653.34	-46.00
802678.51	9199714.32	-10.00	824177.71	9170520.17	-48.00
813615.40	9201427.62	-11.00	830153.78	9181110.92	-48.00
819597.98	9202900.63	-11.00	817509.65	9190008.45	-48.00
816629.32	9202059.27	-11.00	828234.39	9183837.85	-47.00
825005.19	9201734.66	-13.00	827122.11	9175030.59	-49.00
805247.53	9198257.64	-14.00	823115.65	9180727.47	-49.00
807908.68	9198361.22	-16.00	821220.80	9182783.37	-49.00
811899.31	9198313.02	-20.00	825268.35	9184152.24	-49.00
825511.48	9199782.11	-21.00	800148.24	9173559.49	-49.00
777374.98	9197054.11	9.00	803115.70	9172693.09	-49.00
777673.83	9194227.80	3.00	819961.36	9170536.64	-50.00
780119.41	9171583.77	2.00	826691.38	9178630.62	-50.00
776993.15	9174843.66	2.00	819095.74	9180627.00	-50.00
776862.78	9191388.92	1.00	822248.68	9184694.45	-50.00
776530.71	9188428.59	-4.00	809394.98	9185486.13	-50.00
782501.29	9196525.12	-6.00	806316.45	9183312.42	-50.00
783244.90	9172162.30	-9.00	799518.21	9176328.42	-50.00
781769.52	9193321.70	-9.00	815968.40	9170398.63	-51.00
786363.72	9195636.80	-11.00	823216.65	9173176.00	-51.00
779205.20	9190374.07	-11.00	819283.23	9184745.53	-51.00
793308.10	9196345.12	-12.00	813138.59	9186827.13	-51.00
796589.58	9196172.92	-13.00	809134.24	9182157.76	-51.00
788845.77	9194366.36	-13.00	806426.21	9171396.26	-52.00
781957.14	9190545.87	-13.00	810235.87	9170423.17	-52.00
777004.27	9179734.62	-13.00	813128.69	9170447.59	-52.00
779035.49	9187413.64	-14.00	824407.22	9176208.44	-52.00
777415.19	9185412.42	-14.00	803522.50	9180452.91	-52.00
780767.48	9175363.91	-14.00	800913.07	9179479.04	-52.00
785582.33	9191694.36	-16.00	806440.95	9174954.90	-52.00
786994.98	9171812.00	-16.00	821655.12	9175728.14	-53.00
800512.62	9195661.56	-17.00	815491.15	9183591.85	-53.00
792738.35	9191878.51	-18.00	823700.92	9187278.90	-53.00
777501.22	9182581.05	-18.00	807561.27	9179887.67	-53.00
779236.62	9177821.24	-18.00	806154.96	9177923.88	-54.00
799146.95	9193766.01	-19.00	817964.88	9173924.20	-54.00
782350.54	9187286.69	-19.00	818408.61	9177997.05	-54.00
789173.04	9171608.91	-19.00	812660.00	9183615.09	-54.00
784801.53	9189513.17	-20.00	820227.71	9187902.06	-55.00
806446.91	9195618.31	-21.00	813402.66	9173302.74	-55.00
796128.60	9192136.38	-21.00	810004.98	9173609.95	-55.00
792404.82	9188983.47	-21.00	802666.19	9176684.51	-55.00
788458.89	9189075.00	-21.00	816742.75	9186664.66	-56.00
780033.32	9185394.31	-21.00	811878.20	9181294.13	-56.00
787036.54	9187311.39	-23.00	815290.71	9179407.67	-56.00
813760.26	9196663.43	-24.00	809806.34	9177254.83	-57.00
802599.66	9192750.91	-24.00	813676.04	9176471.78	-58.00
783447.92	9184730.83	-25.00	722835.33	9233442.47	3.21
794316.16	9170430.60	-25.00	726536.85	9233020.58	2.81
791233.03	9185503.98	-26.00	727422.60	9235742.83	1.38
787090.06	9184694.83	-27.00	729909.32	9233030.42	1.56
824913.64	9196761.88	-28.00	731888.88	9235401.64	2.17
822434.28	9197463.16	-28.00	723202.55	9230242.41	1.28
800277.79	9189645.69	-28.00	726303.53	9230619.43	1.37
793935.14	9185207.49	-28.00	732477.19	9231134.61	1.72
784162.55	9174796.22	-28.00	733532.73	9231805.76	0.84
818496.17	9196488.65	-29.00	735438.20	9232706.36	1.24
786923.71	9174413.39	-29.00	736291.28	9232762.98	1.32
796943.97	9188745.07	-30.00	737838.35	9233910.01	1.81
784435.97	9182640.53	-30.00	734326.29	9234363.26	1.43
780344.35	9180634.71	-30.00	736100.45	9236261.71	1.55
815364.16	9195207.91	-31.00	738803.08	9239221.96	0.32
810370.84	9193124.98	-31.00	735449.79	9229624.52	1.00
797048.79	9186130.76	-31.00	738610.65	9228231.47	1.00
792269.91	9172675.93	-31.00	737889.84	9231202.96	2.52
812572.88	9193114.72	-32.00	740227.00	9234167.37	2.65
807608.86	9193087.19	-32.00	742353.32	9230574.03	2.13
786134.74	9177321.13	-32.00	744881.30	9229253.17	1.33
792277.44	9172739.19	-32.00	741415.91	9237021.10	3.43
804761.68	9190733.56	-33.00	743457.31	9234333.33	5.08
790182.11	9173784.93	-33.00	743897.04	9233036.77	3.05
793550.02	9181011.67	-34.00	744447.87	9236420.41	4.32
790231.53	9179271.26	-34.00	749739.07	9225947.86	1.30
783193.84	9180226.74	-34.00	749341.59	9227117.16	1.35
793038.21	9178777.18	-36.00	748265.62	9228356.98	1.81
796992.14	9182972.35	-37.00	747918.82	9229515.31	3.05
797461.21	9171452.07	-37.00	747967.48	9230538.50	2.29
828313.15	9194696.00	-38.00	746364.29	9231236.75	2.89
825010.94	9193718.97	-38.00	745374.89	9231758.68	2.88
816858.15	9192937.25	-38.00	747075.95	9234900.43	3.90
802813.72	9188460.95	-38.00	749252.61	9234778.77	3.44
821917.33	9193552.07	-39.00	751120.56	9231874.01	3.04
810943.50	9190082.49	-39.00	753839.17	9233241.27	3.72
807685.03	9189781.61	-39.00	754441.92	9228595.16	6.31
827763.42	9192189.73	-41.00	750569.41	9229327.16	4.10
814227.25	9190380.87	-41.00	754446.78	9228547.57	6.31
796468.77	9180046.87	-41.00	756270.35	9228226.90	7.48
800673.95	9171114.51	-41.00	757399.61	9228158.38	8.84
800024.94	9185601.39	-42.00	759120.74	9229609.26	7.93
796492.41	9173618.70	-42.00	759707.31	9227487.32	8.01
793432.78	9175385.97	-43.00	759017.57	9227084.23	8.01
806334.01	9186704.01	-44.00	759742.78	9227474.07	8.95
795540.49	9176536.92	-44.00	762731.23	9227112.31	10.57
825079.27	9189967.22	-46.00	764332.46	9227336.04	11.40
800485.41	9182564.27	-46.00	765112.19	9227600.58	12.59
828038.62	9189015.05	-47.00	764970.62	9229819.50	11.35
826948.73	9187860.76	-47.00	766900.59	9231200.92	11.67

Easting (metres)	Northing (metres)	Bouguer anomaly (metres)	Easting (metres)	Northing (metres)	Bouguer anomaly (mgals)
768219.10	9228691.87	11.35	740745.87	9224335.71	-4.92
770055.45	9230293.09	11.37	738174.38	9225343.69	-4.53
776231.44	9235814.47	11.57	735865.92	9224150.48	-5.14
773940.34	9230861.67	10.81	733392.45	9223660.86	-6.33
776056.97	9228180.35	11.14	723275.81	9224162.13	-5.90
773233.01	9227346.21	11.09	727088.39	9223513.10	-12.56
770190.55	9226134.59	11.84	726673.54	9222762.58	-13.47
767621.66	9226631.89	13.74	723765.46	9221504.84	-12.31
765698.51	9225534.66	11.05	722198.77	9219512.21	-12.44
770784.63	9224893.86	11.98	725744.01	9220940.46	-15.35
772893.19	9224259.11	13.10	726859.92	9219871.35	-14.74
770655.93	9223839.64	12.78	726459.44	9218282.28	-15.65
774671.10	9221611.14	13.38	724397.27	9217084.89	-13.94
767642.52	9223018.42	9.80	721411.51	9217083.11	-13.04
771634.38	9220554.12	9.98	726305.64	9215696.10	-13.31
773318.51	9218880.07	12.03	727937.23	9217065.33	-12.37
776063.48	9218540.23	14.22	727781.84	9214839.93	-11.97
767116.41	9221520.96	8.98	729391.47	9213875.03	-7.97
764045.32	9222863.92	7.41	727747.99	9212074.10	-10.32
767329.59	9220133.81	4.69	725503.35	9214082.77	-11.46
769127.46	9218942.87	7.41	722106.44	9213838.32	-9.24
766608.64	9218702.84	6.28	723387.05	9211735.30	-6.78
766327.46	9217049.17	6.88	720974.96	9208195.73	-2.57
766239.34	9215956.17	7.31	727935.74	9208862.84	-3.26
766047.02	9214285.87	7.64	728067.23	9207090.24	-0.60
766405.64	9213325.58	8.34	728882.55	9209955.73	-5.81
772651.98	9212139.40	7.91	730262.61	9212820.01	-2.51
770734.17	9210754.92	8.74	735843.33	9214211.69	-0.41
773219.36	9207509.74	7.95	738422.96	9208177.31	-1.47
775117.34	9205807.29	6.61	739641.09	9213891.07	-1.98
774589.07	9202684.99	5.41	736978.73	9214333.75	-5.34
771846.29	9201269.87	13.74	738477.49	9216936.77	-9.09
772059.19	9204607.87	4.24	736500.26	9216601.79	-9.76
769940.59	9205034.10	2.30	732182.17	9218043.22	-7.53
768355.52	9207755.05	6.87	734193.49	9220338.60	-13.64
768624.37	9210196.01	6.94	729041.59	9221729.78	-9.91
766560.21	9206718.91	9.69	738919.09	9219126.94	-6.80
767733.11	9204514.63	6.96	741397.22	9216947.19	-7.39
768341.56	9200394.49	15.78	743804.06	9217029.09	-12.49
767200.77	9198070.98	17.16	744580.42	9219279.94	-13.99
767555.29	9202790.79	11.09	744303.29	9221928.18	-6.57
763764.15	9199230.82	14.00	749614.98	9219336.02	-10.96
761274.34	9200975.47	6.89	749302.71	9218533.29	-10.69
758366.97	9200476.77	3.41	745865.46	9215841.41	-7.66
756134.42	9202141.42	5.62	744969.84	9213394.31	-4.00
766085.50	9208308.13	12.74	747563.01	9211434.04	-0.84
765904.69	9209250.41	12.16	750656.94	9215451.96	-3.99
765400.54	9211322.55	13.72	753041.73	9218327.71	-5.81
764394.61	9213534.55	10.00	756558.73	9220113.99	-2.28
760696.35	9211839.86	23.31	758194.50	9220728.38	-2.90
759674.37	9206426.63	24.16	755196.95	9217986.85	-1.98
757555.31	9207475.11	30.20	753122.06	9220949.79	-9.29
755376.12	9204098.31	17.98	749670.78	9219322.45	-10.92
756593.17	9210217.32	26.10	747406.03	9220109.52	-10.96
759401.69	9214805.57	14.00	747917.31	9214090.13	-3.98
759901.77	9215539.28	12.14	727270.61	9204280.30	8.99
757224.27	9215154.30	12.30	727980.64	9205364.20	5.53
754392.78	9211333.23	17.21	749678.48	9200623.09	-0.68
752391.81	9209012.64	17.70	750295.09	9198494.86	0.34
751904.23	9207372.01	14.15	821629.76	9169449.46	-48.00
752277.83	9204651.46	12.16	818609.30	9168487.44	-48.00
753144.11	9199846.02	3.07	820163.36	9166880.82	-45.00
751835.51	9211560.81	9.00	814160.84	9167050.54	-44.00
762004.48	9215907.78	6.98	827303.35	9168823.40	-43.00
764010.57	9216661.19	3.36	823052.25	9166127.64	-42.00
764305.97	9219820.43	2.65	816645.26	9165804.57	-42.00
758166.90	9217722.19	3.51	810816.49	9166913.03	-42.00
760905.90	9218700.32	1.71	803228.40	9169849.37	-42.00
755461.71	9215951.16	4.73	806240.96	9168280.63	-41.00
752277.83	9213651.61	4.56	818636.89	9164464.51	-40.00
751304.01	9214073.07	1.98	830076.54	9168853.53	-36.00
749562.63	9209638.00	6.81	826604.25	9165844.43	-36.00
749150.23	9206815.23	5.17	821930.76	9163310.31	-36.00
745385.22	9209984.60	1.59	814057.42	9163607.16	-33.00
743033.48	9211496.66	2.46	807798.32	9166183.06	-33.00
745553.84	9206352.69	4.72	825234.83	9163001.57	-31.00
744093.73	9203154.80	3.65	811125.24	9164166.44	-31.00
742490.29	9200248.54	8.05	820145.61	9161133.40	-30.00
734932.22	9198993.13	17.22	804580.70	9166464.37	-28.00
735195.06	9201430.07	6.33	801378.22	9167814.91	-28.00
732523.12	9200536.43	16.11	822884.69	9159986.27	-26.00
730551.34	9201681.90	13.67	797702.42	9168498.81	-23.00
727218.61	9202449.56	18.04	829209.16	9162561.84	-22.00
724338.80	9200565.78	17.62	825793.13	9159933.21	-21.00
738668.48	9203992.76	2.52	811969.41	9161977.54	-20.00
735628.69	9204837.21	2.50	808821.26	9163018.47	-17.00
731195.15	9206320.49	3.75	828966.98	9160351.36	-16.00
732061.27	9210551.69	0.29	819827.98	9157173.19	-16.00
733312.07	9213859.84	0.37	817019.63	9157968.33	-16.00
758487.50	9224603.96	0.47	828181.99	9158204.37	-15.00
761613.61	9221129.53	-0.51	822951.12	9157170.44	-15.00
760163.77	9223150.62	-0.40	814413.51	9160287.96	-14.00
756198.01	9224863.28	-0.45	805111.24	9163384.24	-13.00
754248.82	9225488.05	-1.08	802430.74	9164292.11	-10.00
750182.43	9224655.28	-2.30	799049.20	9165577.33	-9.00
753114.12	9223009.47	-4.71	795806.90	9166230.01	-5.00
755555.78	9222730.04	-5.20	825846.84	9156482.98	-5.00
757942.65	9222349.90	-3.57	788563.04	9169614.41	-4.00
746326.92	9224187.39	-3.27	830308.70	9157433.00	-3.00

Easting (metres)	Northing (metres)	Bouguer anomaly (mgals)	Easting (metres)	Northing (metres)	Bouguer anomaly (mgals)
813454.12	9157470.24	0.00	777083.81	9148519.95	81.00
784372.37	9169504.05	1.00	785171.27	9149147.42	82.00
790139.23	9167209.82	2.00	779480.46	9146669.40	83.00
791914.47	9165959.95	3.00	787530.23	9148294.66	83.00
829296.39	9155018.93	4.00	775809.83	9145609.56	84.00
822748.71	9154171.20	4.00	808923.28	9145031.47	84.00
816336.30	9155578.41	6.00	795766.48	9144889.20	86.00
796752.15	9162994.11	7.00	798214.45	9143303.54	90.00
786352.42	9168070.66	7.00	778282.62	9142909.18	94.00
819543.89	9154012.91	9.00	781716.57	9145290.83	94.00
799669.74	9161744.96	10.00	785075.50	9146161.76	94.00
793545.53	9163201.86	12.00	802145.70	9144434.91	93.00
803432.91	9160743.22	12.00	789965.46	9146344.93	96.00
806690.67	9160069.91	13.00	805887.43	9143549.60	97.00
781374.11	9167311.39	13.00	792587.43	9144860.46	97.00
777720.94	9168649.21	15.00	808687.74	9142339.08	98.00
784269.31	9166879.46	15.00	784432.56	9142967.00	106.00
810879.43	9157786.37	15.00	787579.03	9143372.26	107.00
824938.20	9153232.28	15.00	794356.87	9142608.52	110.00
810864.30	9157781.13	15.00	790552.94	9142530.44	120.00
830081.50	9152685.94	17.00	779122.76	9152088.30	67.00
789575.23	9164155.40	20.00	795460.63	9150222.55	67.00
827387.13	9151990.16	21.00	787203.92	9140219.28	120.00
781064.15	9164832.49	21.00	790420.11	9138440.79	119.00
778024.94	9165446.30	22.00	794052.02	9139279.30	119.00
783644.34	9164478.75	22.00	788217.89	9137190.75	115.00
795216.54	9159639.70	22.00	785371.25	9136515.75	109.00
811825.91	9154875.30	23.00	783697.67	9139293.47	109.00
808795.72	9157923.94	24.00	797008.91	9136709.94	105.00
792276.83	9159980.06	25.00	781578.42	9141887.18	104.00
783213.29	9162171.61	26.00	779253.51	9138618.12	99.00
786659.80	9162666.00	28.00	777605.51	9135485.53	90.00
798231.95	9159536.77	28.00	782282.04	9134463.67	90.00
780784.75	9161486.24	29.00	785494.56	9132563.58	90.00
777237.63	9161998.57	30.00	790219.75	9134240.74	86.00
825221.28	9151154.39	31.00	794595.59	9132165.62	86.00
818992.41	9151611.45	32.00	797888.21	9132618.83	86.00
829107.57	9149813.89	32.00	788724.80	9128127.09	84.00
795078.21	9157212.77	33.00	791906.29	9130239.32	84.00
785797.16	9160016.07	34.00	784655.51	9130046.33	84.00
815548.21	9152413.49	34.00	779624.17	9132239.36	80.00
778649.95	9159529.05	35.00	775886.16	9128413.29	80.00
789117.98	9160430.22	35.00	778724.14	9128743.70	88.00
788037.36	9157793.36	36.00	780652.89	9127025.58	88.00
802054.31	9158031.46	36.00	783612.58	9127177.40	87.00
805799.33	9156853.59	36.00	785976.27	9127734.57	86.00
807873.84	9154719.96	36.00	800127.62	9135228.70	93.00
781433.09	9158296.62	37.00	792133.91	9119681.11	93.00
784207.11	9158257.44	37.00	798929.75	9121839.95	94.00
776316.73	9159348.56	38.00	799421.11	9124711.23	91.00
790389.27	9156187.42	38.00	796079.69	9122962.44	86.00
812940.90	9151425.98	40.00	792870.00	9125988.63	85.00
793373.04	9155124.48	41.00	797051.13	9129211.18	84.00
829733.86	9147204.25	41.00	799542.46	9127960.46	81.00
810357.11	9152080.92	42.00	796511.50	9126371.96	78.00
827011.84	9147980.52	42.00	792635.86	9122601.86	71.00
797485.29	9156294.37	45.00	798121.77	9118531.61	96.00
777272.80	9157118.84	47.00	799691.94	9138172.34	103.00
784505.71	9155937.03	47.00	800150.23	9135239.20	93.00
803624.92	9155032.73	47.00	805255.69	9130061.33	122.00
830620.72	9144622.49	47.00	806012.19	9136222.46	114.00
786785.86	9155254.19	48.00	806059.04	9139134.19	111.00
818820.10	9149913.93	48.00	809127.39	9137949.64	109.00
813567.09	9149675.18	49.00	801921.07	9126449.18	105.00
780007.74	9155679.75	50.00	804308.70	9141349.31	104.00
790097.06	9153494.55	50.00	803574.59	9134088.14	104.00
796027.11	9153457.55	52.00	801927.44	9123087.97	100.00
822005.57	9149570.12	52.00	802082.75	9120397.26	99.00
824412.44	9147392.89	52.00	815760.00	9135675.24	114.00
829210.61	9142431.55	52.00	818961.80	9134445.51	103.00
816649.92	9148803.34	53.00	815118.07	9138029.63	104.00
800117.53	9155184.62	55.00	811863.83	9137268.46	102.00
794122.79	9151927.36	56.00	810422.60	9141905.02	96.00
827563.00	9144873.62	56.00	819688.03	9137626.79	96.00
777014.34	9154355.72	57.00	813239.17	9139954.86	97.00
810255.81	9149948.99	57.00	829552.31	9116491.45	97.00
815344.69	9146524.75	58.00	818433.52	9140007.43	91.00
820449.67	9147922.95	60.00	807816.32	9120155.96	91.00
819383.77	9144902.95	60.00	817584.01	9115115.74	91.00
792692.07	9150829.40	61.00	821992.58	9133107.02	89.00
824005.75	9144531.72	63.00	815787.67	9131527.01	89.00
822174.38	9142619.74	63.00	812883.53	9130960.52	89.00
802382.08	9152406.41	63.00	811149.38	9129489.57	89.00
798875.71	9151833.05	65.00	808473.36	9126003.42	90.00
783041.55	9152749.69	66.00	810026.38	9121674.80	90.00
786273.96	9151864.67	66.00	813389.71	9118709.96	90.00
798433.77	9150363.70	69.00	825852.79	9117122.04	90.00
779518.38	9151235.67	70.00	822358.95	9135955.52	85.00
782812.73	9151627.41	70.00	819703.14	9117684.82	85.00
804780.99	9150362.92	70.00	804247.18	9125244.23	98.00
790564.17	9149475.82	72.00	807909.21	9117033.92	98.00
776420.93	9150705.86	73.00	813427.81	9134399.23	98.00
817216.00	9142889.02	70.00	804765.89	9122341.60	92.00
810954.45	9147114.93	76.00	804521.14	9119409.66	92.00
781373.66	9148697.31	78.00	809032.02	9133999.93	101.00
793326.22	9147519.10	78.00	808125.13	9130429.19	99.00
812579.64	9144973.22	78.00	812511.21	9115088.99	100.00
802143.64	9147692.78	79.00	823168.35	9116875.25	88.00
805181.45	9147470.60	81.00	824125.40	9129896.50	84.00

Easting (metres)	Northing (metres)	Bouguer anomaly (mgals)	Easting (metres)	Northing (metres)	Bouguer anomaly (mgals)
816694.78	9118174.21	84.00	620127.79	9236789.36	23.00
830195.95	9127624.54	83.00	621095.36	9233330.15	23.00
827124.16	9129136.57	83.00	618242.11	9226413.60	23.00
820604.77	9129951.04	83.00	626171.70	9227479.31	23.00
813586.90	9127895.09	83.00	625205.46	9238839.71	24.00
811399.31	9124503.61	83.00	624922.14	9236298.69	24.00
814508.31	9121661.57	83.00	621582.94	9229365.54	25.00
823107.97	9119244.32	83.00	627977.74	9238735.72	25.00
828986.24	9121797.27	82.00	619470.67	9229471.56	25.00
825786.94	9121038.40	81.00	621265.75	9227128.29	28.00
817904.88	9128144.62	81.00	623379.66	9226638.53	30.00
828604.96	9125518.12	79.00	635177.30	9228380.98	14.00
825717.99	9123133.06	79.00	638578.21	9232878.97	14.00
822892.79	9121466.43	79.00	660363.92	9242700.33	14.00
825478.15	9125143.99	78.00	659700.32	9242953.93	13.00
823683.72	9126494.90	77.00	642700.41	9235625.01	13.00
822627.88	9123804.56	76.00	655243.07	9238992.12	12.00
829579.86	9130745.70	79.00	646393.72	9236408.25	12.00
826580.77	9132822.52	77.00	659171.02	9240186.36	11.00
824856.24	9135486.80	74.00	652589.30	9236698.71	11.00
824013.53	9139344.10	71.00	661931.81	9240409.58	9.00
827288.24	9134969.04	70.00	658300.05	9237977.69	9.00
826346.43	9137779.17	66.00	648751.27	9235646.72	9.00
828747.18	9134898.92	65.00	641107.07	9232939.38	9.00
830697.61	9134985.62	64.00	639079.17	9229744.04	9.00
828388.70	9137273.31	61.00	645848.89	9233072.15	8.00
827292.39	9140276.54	61.00	655883.18	9235957.37	8.00
828959.62	9140003.56	55.00	661718.38	9237509.84	7.00
815768.53	9124642.93	81.00	659504.79	9235130.14	7.00
776521.91	9125539.11	88.05	647242.61	9233267.24	7.00
779136.85	9124197.77	88.47	660253.58	9232194.74	6.00
777100.52	9122211.55	93.48	642027.87	9228571.59	6.00
780892.58	9121231.83	94.02	644674.04	9227682.57	5.00
780695.73	9120430.50	96.10	663200.77	9236253.57	4.00
775942.24	9118239.56	101.17	657236.75	9234230.49	4.00
778068.11	9119818.25	97.00	654714.98	9232463.94	3.00
781741.59	9123926.93	87.62	650356.89	9231535.08	3.00
785068.16	9124066.15	85.29	662263.18	9234089.73	3.00
787674.03	9124832.39	85.47	652140.33	9226818.03	3.00
784633.80	9120714.32	93.18	652311.78	9229494.62	2.00
787094.21	9121369.48	92.00	648293.07	9229707.95	2.00
782989.21	9118569.05	100.00	664954.63	9231165.42	1.00
786993.40	9118328.05	98.09	654750.00	9229261.74	6.00
779683.57	9116135.90	104.65	655207.19	9226223.57	6.00
783459.08	9115774.84	101.31	658377.63	9227148.05	4.00
785804.26	9115206.19	99.04	659133.93	9229265.09	-1.00
789800.65	9116210.99	98.47	661158.49	9227525.39	-1.00
792408.78	9114983.30	100.73	650437.09	9228175.03	-2.00
796095.40	9115439.34	100.36	663428.88	9228870.26	-2.00
789657.37	9119047.52	95.67	665097.46	9226747.88	-2.00
801612.32	9116594.05	98.44	727125.29	9168170.76	52.00
805625.27	9115543.61	100.63	724142.70	9169562.19	52.00
611392.24	9247214.09	16.00	731408.20	9169991.12	54.00
612442.54	9243154.80	16.00	721120.80	9169388.69	54.00
610508.27	9241119.94	16.00	730888.84	9167121.94	55.00
611562.16	9226776.25	16.00	728567.93	9165984.22	55.00
652288.54	9241218.57	16.00	724461.18	9166254.26	55.00
615590.31	9246394.56	17.00	721271.90	9167199.27	55.50
613667.21	9240657.23	17.00	725716.80	9164263.44	56.00
612832.04	9238609.74	17.00	721629.03	9164084.23	57.00
612363.30	9236059.89	17.00	735372.96	9168843.08	58.00
613363.76	9229914.24	17.00	726957.84	9161933.48	58.00
650098.64	9240248.81	17.00	723917.69	9162314.62	59.00
646133.14	9239255.91	17.00	721356.51	9161317.51	61.00
634768.22	9233746.21	17.00	724796.70	9158462.79	67.00
632033.07	9230000.11	17.00	721897.34	9158095.17	70.00
610646.86	9230763.78	15.00	722996.38	9155175.31	79.00
662302.83	9242785.30	15.00	726213.43	9154943.47	88.00
640529.94	9236187.97	15.00	730713.15	9159065.41	86.00
635228.15	9232035.53	15.00	729035.39	9155476.88	92.00
613734.69	9233498.62	18.00	734947.88	9161260.28	92.00
615153.65	9226708.42	18.00	736936.18	9162437.96	91.00
646602.08	9240323.87	18.00	732508.50	9157221.87	94.00
643347.29	9239971.09	18.00	724749.04	9152401.77	96.00
640995.95	9240016.48	18.00	721310.03	9150431.42	97.00
630820.67	9233756.33	18.00	731883.51	9154797.04	98.00
638547.60	9240226.35	19.00	728811.72	9152699.35	104.00
637763.63	9237364.02	19.00	724237.07	9150039.75	106.00
627880.81	9232268.13	19.00	731555.99	9152301.41	107.00
627787.57	9230252.70	19.00	722962.29	9147543.17	111.00
629351.32	9226318.83	19.00	721209.23	9146304.28	98.00
615254.27	9233808.71	20.00	720833.46	9143425.95	113.00
616448.12	9229826.54	20.00	737160.25	9157679.89	108.00
628539.78	9226874.09	20.00	737351.60	9155369.74	108.00
615279.41	9234945.33	21.00	733649.15	9151238.22	117.00
634727.34	9237706.08	21.00	736780.56	9145483.66	117.00
618374.00	9243752.26	22.00	735816.43	9148475.85	118.00
617020.91	9239801.57	22.00	723841.79	9145386.55	119.00
618222.85	9235632.76	22.00	728216.37	9148068.59	123.00
624767.50	9230303.24	22.00	725809.78	9144147.64	130.00
625314.52	9232608.72	22.00	728138.90	9144261.00	139.00
631002.93	9237234.37	22.00	731353.85	9144316.22	141.00
635505.83	9240627.21	22.00	734181.94	9146026.45	130.00
622519.74	9242957.48	23.00	734788.56	9143125.04	124.00
625593.67	9242557.14	23.00	740857.35	9143774.36	116.00
627469.06	9241597.00	23.00	747590.21	9144182.92	113.00
631066.02	9240981.37	23.00	738921.00	9147852.38	112.00
627536.10	9235805.41	23.00	745217.61	9146266.63	110.00
620265.67	9239568.26	23.00	749804.03	9145063.26	111.00

Easting (metres)	Northing (metres)	Bouguer anomaly (metres)	Easting (metres)	Northing (metres)	Bouguer anomaly (mgals)
742661.74	9148156.09	108.00	727463.05	9140871.50	143.00
740836.46	9149475.48	107.00	732478.88	9135996.54	143.00
738838.33	9151692.92	107.00	731307.98	9144339.37	141.00
740869.83	9157156.33	106.00	732118.65	9141350.42	141.00
744759.34	9150307.23	107.00	731892.08	9132891.21	140.00
748235.19	9147929.54	102.00	729623.63	9130992.08	139.00
754344.23	9145429.98	108.00	723868.73	9142092.56	126.00
752379.44	9147934.30	95.00	721092.56	9140578.35	114.00
749334.63	9150611.99	95.00	720933.61	9137806.63	114.00
744240.41	9152928.34	93.00	723525.74	9139068.37	131.00
744771.53	9156160.41	92.00	725732.02	9129742.23	131.00
742674.17	9159077.25	99.00	735074.36	9134599.87	131.00
738825.52	9160118.72	103.00	722306.69	9135666.36	128.00
739983.97	9163026.52	89.00	723130.82	9132176.94	134.00
738275.32	9164814.31	79.00	724404.69	9126800.66	116.00
732501.59	9163571.20	78.00	721852.29	9128239.73	117.00
728434.34	9160452.78	76.00	734321.27	9130614.14	120.00
734299.55	9165924.65	69.00	751063.78	9138004.03	120.00
729692.86	9163281.96	69.00	729769.53	9125135.51	110.00
742334.98	9163144.94	77.00	736986.50	9132687.37	110.00
751509.33	9152814.58	77.00	731900.13	9127251.36	113.00
745802.66	9158546.07	78.00	741879.84	9137681.41	111.00
748648.89	9153966.42	81.00	745537.78	9137086.33	111.00
753457.76	9150687.86	80.00	738626.32	9136752.76	112.00
744827.14	9162259.52	67.00	756954.52	9139570.92	113.00
751009.79	9155509.84	67.00	752343.90	9140793.40	124.00
748760.24	9157018.33	69.00	754856.38	9140122.64	119.00
753618.91	9155184.11	69.00	746636.91	9140088.82	119.00
747404.42	9160954.37	61.00	743643.11	9140115.29	119.00
750541.42	9158952.23	64.00	752732.78	9136348.67	115.00
752375.02	9160423.40	65.00	755350.47	9136933.09	114.00
753870.26	9158166.78	71.00	748812.05	9141512.92	120.00
749023.71	9162828.82	46.00	747823.70	9138338.41	117.00
753979.87	9163017.22	44.00	749420.91	9135613.42	107.00
743126.71	9169503.00	41.00	740823.15	9135717.59	105.00
746465.56	9165916.39	39.00	737633.23	9130228.17	106.00
759720.22	9160484.35	39.00	734947.22	9126891.83	106.00
763554.30	9158596.01	39.00	733391.78	9123620.72	104.00
762090.17	9160481.24	38.00	740036.24	9133132.73	103.00
745426.95	9168773.42	35.00	740472.23	9129476.54	101.00
769195.66	9160398.37	35.00	758558.78	9133811.39	101.00
752373.50	9164956.13	32.00	738584.72	9126169.43	100.00
766407.44	9160626.03	32.00	737483.76	9121886.83	96.50
772481.89	9160367.39	33.00	743175.60	9128764.64	95.50
758192.65	9163467.93	29.00	745292.96	9134233.51	95.00
749892.22	9166859.51	27.00	748091.39	9132483.88	95.00
755698.20	9166488.55	26.00	740803.25	9123664.36	94.00
771937.22	9161868.03	25.00	763501.63	9124429.10	94.00
764412.24	9162053.43	24.00	758169.59	9122213.18	94.00
762595.90	9162549.94	23.00	742896.14	9125685.85	93.00
773809.77	9165309.79	20.00	744658.41	9131735.74	93.00
749126.81	9169240.65	18.00	763950.00	9134022.19	93.00
758870.74	9167186.74	14.00	767297.22	9131199.66	93.00
765694.24	9167341.23	13.00	752159.57	9119133.42	93.00
763027.54	9166550.91	13.00	740451.13	9120457.37	92.00
773891.98	9169172.47	12.00	761500.19	9132512.97	92.00
752901.26	9169047.72	12.00	758057.71	9131121.67	91.00
755566.71	9169974.73	7.00	764749.38	9131892.61	91.00
770758.14	9169761.23	8.00	765011.94	9129709.60	91.00
761771.62	9170053.58	-2.00	754678.84	9122273.74	91.00
768471.37	9158117.14	45.00	747223.43	9116264.41	91.00
774782.15	9157581.14	44.00	761277.65	9126190.41	90.00
765896.41	9158323.97	44.00	743479.24	9117829.82	89.00
772110.40	9155965.34	51.00	743732.04	9122555.37	89.00
760741.52	9156842.80	54.00	748922.01	9130254.10	89.00
758350.81	9157423.52	56.00	746267.13	9129155.25	88.00
764760.59	9155540.62	56.00	753292.18	9130473.06	88.00
768229.04	9154783.42	56.00	761540.71	9129168.05	88.00
774536.44	9154039.70	57.00	759039.59	9124861.10	88.00
759323.56	9154896.10	61.00	748312.95	9119028.65	88.00
764111.60	9152523.27	62.00	750913.74	9126966.51	87.00
761331.70	9153453.36	62.00	747034.45	9121817.15	87.00
774551.54	9154112.49	57.00	746114.73	9126160.41	87.00
770829.99	9152932.00	63.00	758186.77	9127799.22	87.00
756043.74	9154487.08	66.00	755101.47	9128370.45	87.00
766541.24	9151873.95	63.00	753368.52	9125028.69	87.00
766702.05	9149904.17	69.00	755790.61	9125390.52	86.00
760302.31	9150929.84	71.00	748998.64	9124921.29	85.00
771233.54	9150003.54	72.00	750533.83	9122718.46	85.00
757034.69	9151638.25	72.00	751109.75	9133171.47	97.00
763341.27	9149449.36	73.00	760931.76	9135346.59	97.00
769843.14	9147843.83	77.00	766551.05	9141596.96	97.00
766080.58	9147733.13	77.00	755601.75	9132596.27	99.00
758309.15	9149146.06	79.00	757711.58	9141874.55	107.00
774340.89	9148563.50	82.00	758189.54	9136993.92	108.00
763126.78	9147170.31	83.00	760186.28	9139975.38	109.00
768519.48	9145330.14	88.00	773836.95	9141615.96	90.00
772496.66	9146098.54	88.00	768246.29	9138765.12	90.00
773527.30	9143955.15	88.00	771546.12	9139702.78	89.00
759768.17	9146738.68	89.00	773615.41	9135586.36	89.00
764389.01	9144928.11	92.00	774296.95	9138412.43	88.00
760387.60	9143481.07	101.00	767989.99	9136412.63	92.00
756890.69	9144517.79	102.00	765636.88	9138752.80	95.00
743754.98	9142775.54	119.00	766208.17	9134977.62	96.00
726784.49	9138557.87	146.00	769121.78	9133974.61	94.00
726381.50	9134800.97	145.00	771736.12	9122913.13	94.00
729542.98	9135159.82	145.00	769315.28	9124852.10	93.00
730597.32	9138241.44	144.00	769093.61	9141445.74	93.00
726592.58	9131921.53	144.00	765687.18	9138771.73	95.00

Easting (metres)	Northing (metres)	Bouguer anomaly (mgals)	Easting (metres)	Northing (metres)	Bouguer anomaly (mgals)
775372.00	9130753.53	80.00			
771780.89	9129406.63	83.00			
770118.28	9127572.09	84.00			
771908.64	9125580.05	87.00			
766370.56	9125601.48	96.00			
768037.45	9123067.39	97.00			
756849.35	9121128.69	97.00			
750372.67	9115641.28	98.00			
765599.49	9122935.51	99.00			
771255.20	9120712.15	101.00			
761354.46	9122003.55	101.00			
756005.09	9119686.13	104.00			
772028.09	9118191.91	106.00			
766034.07	9119954.25	107.00			
763170.62	9120204.54	109.00			
768130.22	9117291.15	110.00			
766080.85	9117667.31	110.00			
770116.20	9116604.67	112.00			
759873.53	9119733.25	112.00			
766239.95	9114945.19	118.00			
774086.26	9110677.94	120.00			
762210.00	9117825.21	124.00			
771263.85	9114523.69	125.00			
762368.25	9114842.46	125.00			
761669.75	9111930.35	128.00			
773602.84	9104778.81	129.00			
766852.21	9113076.72	129.00			
764959.45	9111452.13	132.00			
755159.49	9116887.05	131.00			
771333.31	9107005.29	134.00			
771482.89	9110800.53	134.00			
758204.01	9112444.84	134.00			
758802.88	9115273.49	133.00			
768777.53	9106956.98	139.00			
767119.19	9108461.38	139.00			
738604.60	9141572.74	117.00			
740941.01	9140151.32	122.00			
737409.72	9137968.42	125.00			
734675.14	9139671.23	129.00			

REFERENCES

ALMOND, R. A., **1986**, Operating Instruction for GRIN program: *Unpublished Internal Report, the Geological Research and Development Centre of Indonesia.*

ASIKIN, S., **1974**, Evolusi Geologi Jawa Tengah dan sekitarnya, ditinjau dari segi teori tektonik - dunia yang baru: *Unpublished Ph.D. thesis, Geol. Dept., Bandung Institute. of Technology.*

AUDLEY-CHARLES, M. G., **1975**, The Sumba Fracture: A Major Discontinuity Between Eastern and Western Indonesia: *Tectonophysics Vol.26* pp 213-228.

AUDLEY-CHARLES, M. G and MILSOM, J., **1974**, Comment on 'Plate Convergence, Transcurrent Faults and Internal Deformation Adjacent to South East Asia and the Western Pacific' by Fitch, T, J.: *Journal of Geophysical Research Vol.79* pp 4980-4981.

BAHAR, I. and GIROD, M., **1983**, Controle Structural du Volcanisme Indonesien (Sumatra, Java-Bali); Application et Critique de La Methode de Nakamura: *Bull. Soc. Geol. France Vol.XXV, No.4* pp 609-614.

BANCROFT, A. M., **1960**, Gravity Anomalies Over A Buried Step : *Journal of Geophysical Research, Vol.65,* pp 1630-1631.

BARDINTZEFF, J. M., **1984**, Merapi Volcano (Java, Indonesia) and Merapi-Type Nuee Ardente: *Bull. Volcanol. Vol.47, No.3* pp 433-435.

BEN-AVRAHAM, Z. and K. O. EMERY., **1973**, Structural Framework of Sunda Shelf: *Bull. of A. A. P. G., v.7, part II.*

BOSTROM, R. C. SAAR, K. K. and TERRY, D. A., **1983**, Basin Formation; The Mass Anomaly at the West Pacific Margin: *In Hilde, W. C. and Uyeda, S. (ed.) Geodynamics of the Western Pacific-Indonesian Region* pp 51-62.

BOTT, M. H. P. and SMITH, R. A., **1958**, The Estimation of the Limiting Depth of Gravitational Bodies: *Geophys. Prosp. Vol.6,* pp 1-10.

BOYD, D. M., **1967**, The Contribution to Airborne Magnetic Surveys to Geological Mapping: *In Morley, L. W. (ed.) Mining and Ground Water Geophysics 1967. Geological Survey of Canada Economic Geology Report 26* pp 213-227.

BUYUNG, N., **in prep.**, Geophysics Along Transect VII: *In Untung, M. (ed.) The Jawa-Kalimantan Transect (Transect VII)* pp 42-65.

CADY, J. W., **1980**, Calculation of Gravity and Magnetic Anomalies of Finite Length Right Polygonal Prisms: *Geophysics Vol.45 No.10* pp 1507-1512.

CADY, J. W., 1981, Erratum to paper " Calculation of Gravity and Magnetic Anomalies of Finite Length Right Polygonal Prisms. ": *Geophysics Vol.46* pp 958-958.

CAS, R. A. F. and WRIGHT, J. V., 1987, Volcanic Successions Modern and Ancient: London, *Allen & Unwin* 528 p.

CHOTIN, P., GIRET, A., RAMPNOUX, J. P., SUMARSO and SUMINTA, 1980, L'ile de Java, un Enregistreur Des Mouvements Tectoniques A L'aplomb D'une Zone de Subduction: *C. R. Somm. Soc. Geol. France, Vol.5* pp 175-177.

COLLETTE, B. J., 1954, On the Gravity Field of the Sunda Region (West Indonesia): *Geol. en Mijnb. Vol.16, No.7* pp 271-300.

CONDON, W. H., PARDYANTO, L. and KETNER, K. B., 1975, Geologic Map of the Banjarnegara and Pekalongan Quadrangles, Java 1:100000 sheet: *Geological Survey of Indonesia.*

CORBATO, C. E., 1965, A Least-Squares Procedure for Gravity Interpretation: *Geophysics Vol.30 No.02* pp 228-233.

DE BRUYN, J. W., 1951, Isogam Map of Caribbean Sea and Surroundings and of Southeast Asia: *Third Petroleum Congr. Proc., The Hague* pp 598-612.

DEWEY, J. F. and BIRD. J. M., 1970, Mountain Belts and the New Global Tectonics: *Jour. Geophys. Research Vol.75, No.14,* pp 2625-2647.

DJURI, M., 1975, Geologic Map of the Purwokerto and Tegal Quadrangles, Java 1:100000 sheet: *Geological Survey of Indonesia.*

DOBRIN, M. B. and SAVIT, C. H., 1989, Introduction to Geophysical Prospecting: *McGraw-Hill Inc.* 867 p.

EWING, M. and WORZEL, J. L., 1954, Gravity Anomalies and Structure of the West Indies Part I: *Bull. of the Geol. Society of America, Vol.65* pp 165-174.

FITCH, T. J., 1970, Earthquake Mechanisms and Island Arc Tectonics in the Indonesian-Philipphines Region: *Seismol. Soc. America Bull. Vol.60,* pp 565-591.

FITCH, T. J., 1972, Plate Convergence, Transcurrent Faults, and Internal Deformation Adjacent to Southeast Asia and the Western Pacific: *Journal of Geophysical Research Vol.77, NO.23,* pp 4432-4460.

FITCH, T. J. and HAMILTON, W., 1974, Reply to Comments by M. G. Audley-Charles and J. S. Milsom on Paper 'Plate Convergence, Transcurrent Faults and Internal Deformation Adjacent to South East Asia and the Western Pacific': *Journal of Geophysical Research Vol.19* pp 4982-4985.

FORD, M., BROWN, C. and READMAN, P., 1991, Analysis and Tectonic Interpretation of Gravity Data Over the Variscides of Southwest Ireland: *Jour. of the Geol. Soc. London, Vol.148* pp 137-148.

GAFOER, S., SUPRIATNA, S., MARGONO, U. and ANDI MANGGA, S., in prep., Geology Along Transect VII: *In Untung, M. (ed.) The Jawa-Kalimantan Transect (Transect VII)* pp 8-25.

GAFOER, S., SUWARNA, S. and BAHARUDIN, A., in prep., Tectonics Along Transect VII: *In Untung, M. (ed.) The Jawa-Kalimantan Transect (Transect VII)* pp 26-41.

GEOLOGICAL SURVEY of INDONESIA, 1977, Geological Map of Java and Madura Sheet : Central Java 1:500000 sheet: *Geological Survey of Indonesia.*

GELDART, L. P., GILL, D. E. and SHARMA, B., 1966, Gravity Anomalies of Two-Dimensional Faults: *Geophysics Vol.31 No.02* pp 372-397.
GETTINGS, M. E., Gravity Model Studies of Newberry Volcano, Oregon: *Jour. of Geophys. Research Vol.93, No.B9* pp 10109-10118.

GIBB, R. A. and THOMAS, M. D., 1980, Density Determinations of Basic Volcanic Rocks of the Yellowknife Supergroup by Gravity Measurements in Mine Shafts-Yellowknife, Northwest Territories: *Geophysics Vol.45, No.1,* pp 18-31.

GOODACRE, A. K., 1980, Estimation of the Minimum Density Contrast of A Homogeneous Body As An Aid to the Interpretation of Gravity Anomalies: *Geophysical Prospecting Vol.28,* pp 408-414.

GRANT, F. S. and ELSAHARTY, A. F., 1962, Bouguer Gravity Corrections Using A Variable Density: *Geophysics Vol.27, NO.5,* pp 616-626.

GRANT, F. S. and WEST, G. F., 1965, Interpretation Theory in Applied Geophysics: *New York, McGraw Hill.*

GUINNESS, E. A., ARVIDSON, R. E., LEFF, C. E., EDWARDS, M. H. and BINDSCHADLER, D. L., 1983, Digital Image Processing Applied to Analysis of Geophysical and Geochemical Data for Southern Missouri: *Economic Geology, Vol.78,* pp 654-663.

HAMILTON, B. W., 1971, Plate Tectonic Evolution of Indonesia (abs.): *Geol. Soc. America Abs. Vol3, No.7* pp 589-590.

HAMILTON, B, W., 1977, Subduction in the Indonesian Region, in Island Arcs, Deepsea Trenches and Back-Arc Basins, Maurice Ewing Series: *American Geophysical Union, Vol.1,* pp 15-31.

HAMILTON, B. W., 1979, Tectonics of the Indonesian region: *U. S. Geol. Surv., Prof. paper, Vol.1078,* 345p.

HAMILTON, B. W., 1988, Plate Tectonics and Island Arcs: *Geological Society of America Bulletin, Vol.100* pp 1503-1527.

HASEGAWA, H. and UNTUNG, M., 1978, Interpretation of Results: *In Untung, M. and Sato, Y. (ed.) Gravity and Geological Studies in Jawa, Indonesia* pp 46-70.

HENDERSON, G. C., 1963, Preliminary Study of the Crustal Structure Across the Campeche Escarpment from Gravity Data: *Geophysics Vol.28 No.05 Part I* pp 736-744.

HORD, M. R., 1982, Digital Image Processing of Remotely Sensed Data: *Academic Press, New York.*

HOSHINO, K. and SUNOTO, W., 1978, Geologic Structure: *In Untung, M and Sato, Y. (ed.) Gravity and Geological Studies in Jawa, Indonesia* pp 136-144.

HOSHINO, K., SUNOTO, W. and INAMI, K., 1978, Density and Porosity: *In Untung, M. and Sato, Y. (ed.) Gravity and Geological Studies in Jawa, Indonesia* pp 147-158.

KANE, M. F., MABEY, D. R. and BRACE, R. L., 1976, A gravity and Magnetic Investigation of the Long Valley Caldera, Mono County, California: *Jour. of Geophys. Research Vol.81 No.5* pp 754-762.

KATILI, J. A., 1970, Large Transcurrent Faults in Southeast Asia With Special Reference to Indonesia: *Geol. Rundschau, Vol.59*, pp 581-600.

KATILI, J. A., 1971, A Review of the Geotectonic Theories and Tectonic Maps of Indonesia: *Earth Science Reviews Vol.7*, pp 195-212.

KATILI, J. A., 1973, Plate Tectonics of Indonesia With Special Reference to the Sundaland Area: *Proc. Indon. Petrol. Assoc. 1st Ann. Conv., June, Jakarta, 57-61.*

KATILI, J. A., 1975, Volcanism and Plate Tectonics in the Indonesian Island Arc: *Tectonophysics, Vol.26, pp 165-188.*

KATILI, J. A. and HARTONO, H. M. S., 1981, Complications of Cenozoic Tectonic Development in Eastern Indonesia: *In Hilde, T. W. C. and Uyeda. S. (ed.) Geodynamics of the Western Pacific-Indonesian Region*, pp 387-399.

KATILI, J. A. and REINEMUND, J. A., 1984, Southeast Asia: Tectonic Framework, Earth Resources and Regional Geological Programs: *International Union of Geological Sciences publication No.13*

KEINKOPF, M. D., PETERSON, D. L. and MATTICK, R. E., 1979, Gravity , Magnetic and Seismic Studies of the Silver Cliff and Rosita Hills Volcanic Area, Colorado: *Geological Survey Professional Paper 726-F* pp F1-F17.

KOWALIK, W. S. and Glenn, W. E., 1987, Image Processing of Aeromagnetic Data and Integration With Landsat Images for Improved Structural Interpretation: *Geophysics Vol.52, No.7* pp 875-884.

LA FEHR, T. R., 1980, Gravity Method: *Geophysics Vol.45, No.11* pp1634-1639.

LE PICHON, X., 1968, Sea-Floor Spreading and Continental Drift: *Jour. Geophys. Research Vol.73*, pp 3661-3705.

LE PICHON, X. and TALWANI. M., 1969, Regional Gravity Anomalies in the Indian Ocean: *Deep-Sea Research Vol.16*, pp 263-274.

LITINSKY, V. A., 1989, Concept of Effective Density: Key to Gravity Depth Determinations for Sedimentary Basins: *Geophysics, Vol.54, No.11* pp 1474-1482.

LODDO, M., PATELLA, D., QUARTO, R., RUINA, G., TRAMACERE, A. and ZITO, G., 1989, Application of Gravity and Deep Dipole Geoelectrics in the Volcanic Area of Mt. Etna (Sicily): *Jour. of Volcanol. and Geotherm. Research Vol.39* pp 17-39.

MILSOM, J., AUDLEY-CHARLES, M. G., BARBER, A. J. and CARTER, D. J., 1981, Geological-Geophysical Paradoxes of the Eastern Indonesia Collision Zone: *In Hilde, T. W. C. and Uyeda, S. (ed.) Geodynamics of the Western Pacific-Indonesian Region*, pp 401-411.

MOORE, D. G., CURRAY, J. R. and EMMEL, F. J., 1976, Large Submarine Slide (Olistostrome) Associated With Sunda Arc Subduction Zone, Northeast Indian Ocean: *Mar. Geol., Vol.21*, pp 211-226.

MUKHOPADHYAY, M., VERMA, R. K. and ASHRAF, M. H., 1986, Gravity Field and Structure of the Rajmahal Hills: Example of the Paleo-Mesozoic Continental Margin in eastern India: *Tectonophysics Vol.131* pp 353-367.

NETLLETON, L. L., **1939,** Determination of Density for Reduction of Gravimeter Observations: *Geophysics Vol.4* pp 176-183.

NETLLETON, L. L., **1940,** Geophysical Prospecting for Oil: *McGraw-Hill Book Company, New York,* 444 p.

NETLLETON, L. L., **1942,** Gravity and Magnetic Calculations: *Geophysics Vol.7* pp 293-309.

NETLLETON, L. L., **1976,** Gravity and Magnetics in Oil Prospecting: *McGraw-Hill Book Company, New York,* 464 p.

PARASNIS, D. S., **1952,** A Study of Rock Densities in the English Midlands: *Jour. of Royal Astronomical Society, Supple. edition Vol.6,* pp 252-271.

PARASNIS, D. S., **1961,** Principles of Applied Geophysics: *London: Methuen & Co Ltd* 176pp.

PARASNIS, D. S., **1966,** Mining Geophysics: *Elsevier Publishing Company* 356pp.

RAO, B. S. R., MURTHY, I. V. R. and RAO, C. V., **1974,** Gravity Interpretation by Characteristic Curves: *Andhra University Press & Publications* 44 p.

RAHARDJO, W., SUKANDARRUMIDI and ROSIDI, H. M. D., **1977,** Geologic Map of the Yogyakarta Quadrangle Jawa 1:100000 sheet: *Geological Survey of Indonesia.*

ROUSSET, D., LESQUER, A., BONNEVILLE, A. and LENAT, J. F., **1989,** Complete Gravity Study of Piton De La Fournaise Volcano, Reunion Island: *Jour. of Volcanol. and Geotherm. Research Vol.36* pp 37-52.

ROBERTSON, E. I., **1967a,** Gravity Effects of Volcanic Islands: *New Zealand Jour. of Geol. and Geophys. Vol.10 No.6* pp 1466-1483.

ROBERTSON, E. I., **1967b,** Gravity Survey in the Cook Islands: *New Zealand Jour. of Geol. and Geophys. Vol.10* pp 1484-1497.

ROBERTSON, E. I., **1970,** Additional Gravity Survey in the Cook Islands: *New Zealand Jour. of Geol. and Geophys. Vol13* pp 184-198.

ROY, A., **1962,** Ambiguity in Geophysical Interpretation: *Geophysics Vol.27* pp 90-99.

RYMER, H. and BROWN, G. C., **1986,** Gravity Fields and the Interpretation of Volcanic Structures: Geological Discrimination and Temporal Evolution: *Jour. of Volcanol. and Geotherm. Research Vol.27* pp 229-254.

SANO, S., UNTUNG, M. and FUJII, K., **1978,** Epilogue: *In Untung, M. and Sato, Y. (ed.) Gravity and Geological Studies in Jawa, Indonesia* pp 183-207.

SISSONS, A., **1981,** Densities Determined From Surface and Subsurface Gravity Measurements: *Geophysics Vol.46, No.11* pp 1568-1571.

SKEELS, D. C., **1947,** Ambiguity in Gravity Interpretation: *Geophysics Vol.05* pp 43-56.

SPECTOR, A. and GRANT, F. S., **1970,** Statistical Models for Interpreting Aeromagnetic Data: *Geophysics, Vol.35, NO.2* pp 293-302.

TALWANI, M. and EWING, M., **1960,** Rapid Computation of Gravitational Attraction of Three-Dimensional Bodies of Arbitrary Shape: *Geophysics Vol.25* pp 203-225.

TALWANI, M., SUTTON, G. H. and WORZEL, J. L., 1959, A Crustal Section Across the Puerto Rico Trench: *Jour. of Geoph. Res. Vol.64* pp 1545-1555.

TELFORD, W. M., GELDART, L. P., SHERIFF, R. E. and KEYS, D. A., 1989, Applied Geophysics: *Cambridge University Press* 860 p

THADEN, R. E., SUMADIRDJA, H. and RICHARDS, R. W., 1975, Geologic Map of the Magelang and Semarang Quadrangles, Java 1:100000 sheet: *Geological Survey of Indonesia.*

TJIA, H. D., 1966, Structural Analysis of the pre-Tertiary of the Lukulo Area, Central Jawa: *Unpublished Ph.D. thesis Geol. Dept. Bandung Institute Technology* 110 p.

TSUBOI. C., 1983, Gravity: *George Allen and Unwin Ltd* 254 p.

UMBGROVE, J. H. F., 1949, Structural History of the East Indies: *Cambridge University Press,* 64p.

UNTUNG, M., 1978, Gravity: *In Untung, M. and Sato, Y. (ed.) Gravity and Geological Studies in Jawa, Indonesia* pp 7-14.

UNTUNG, M. and WIRIOSUDARMO, G., 1975, Structural Pattern of Jawa and Madura as a result of Preliminary Interpretation of Gravity Data: *Geol. Indonesia Vol.2, No.1* pp15-24.

VAN BEMELLEN, R. W., 1949, The Geology of Indonesia, Vol.1A: *Govt. Print. Office, The Hague* 732 p.

VAN BEMELLEN, R. W., 1957, Mountain Building: *Martinus Nijhoff The Hague Holland* 177 p.

VENING MEINESZ, F. A., 1948, Gravity Expeditions at Sea 1923-1938: *Delftsche Uitgevers Maatschappil-Delft, Vol.IV,* 233 p.

VENING MEINESZ, F. A., 1954, Indonesian Archipelago: A Geophysical Study: *Bullettin of The Geological Society of America, Vol.65,* pp 143-164.

VENING MEINESZ, F. A., UMBGROVE, J. H. F. and KUENEN, Ph. H., 1934, Gravity Expeditions at Sea, Vol.II: *Pub. Neth. Geod. Comm., Delft.*

VREUGDE, L. M. H., 1935, Quelques Anomalies de Pesanteur Dans le Nord de Java (Ind. Ne'erlandaises): *Congr. Internat. des Mines, etc. VIIe Session Paris,* pp 919-1001.

WALKER, G. P. L., 1989, Gravitational (Density) Controls on Volcanism, Magma Chambers and Intrusions: *Australian Jour. of Earth Sciences Vol36* pp 149-165.

WILLIAMS, D. L. and FINN, C., 1985, Analysis of Gravity Data in Volcanic Terrain and Gravity Anomalies and Subvolcanic Intrusions in the Cascade Range, U.S.A., and at Other Selected Volcanoes: *In Hinze. W. J. (ed.) The Utility of Regional Gravity and Magnetic Anomaly Maps* pp 361-374.

WORZEL, J. L., 1976, Gravity Investigations of the Subduction Zone: *In Sutton, G. H. Manghnani, M. H. and Moberley, R. (ed.) The Geophysics of the Pacific Ocean Basin and its Margin: American Geophysics Union, Washington, D. C.* pp 1-15.

YOKOYAMA, I., 1958, Gravity Survey on Kuttyaro Caldera Lake: *Jour. Phys. Earth, Vol.6 No.2* pp 75-79.

YOKOYAMA, I., 1961, Gravity Survey on the Aira Caldera, Kyushu, Japan: *Nature, Vol.191 No.4792* pp 966-967.

YOKOYAMA, I., 1963a, Structure of Caldera and Gravity Anomaly: *Bull. Volcanol., Vol.26* pp 67-72.

YOKOYAMA, I., 1963b, Gravity Survey on the Aso Caldera: *Geophys. Pap. Dedicated to Prof. K. Sassa* pp 687-692.

YOKOYAMA, I., 1969, The Subsurface Structure of Oosima Volcano, Izu: *J. Phys. Earth Vol.17* pp 55-68.

YOKOYAMA, I. and HADIKUSUMO, D., 1969, A Gravity Survey on the Krakatau Islands, Indonesia: *Bulletin Earthquake Research Institute, Vol.47,* pp 991-1001.

YOKOYAMA, I., SURYO, I. and BUYUNG, N., 1970, A Gravity Survey in Central Java: *Earthquake Research Inst. Bull. Vol.48,* pp 303-315.

YOKOYAMA, I., 1983, Gravimetric Studies and Drilling Results at the Four Calderas in Japan: *In Shimozuru, D. and Yokoyama, I. (ed.) Arc Volcanism: Physics and Tectonics* pp 29-41.